

E-ISSN 1309 - 2251

KAFKAS ÜNİVERSİTESİ VETERİNER FAKÜLTESİ DERGİSİ

Journal of the Faculty of Veterinary Medicine, Kafkas University

Published Bi-monthly

Volume: 31
Issue: 5 (September - November)
Year: 2025

E-ISSN: 1309-2251

This journal is published bi-monthly, by the Faculty of Veterinary Medicine, University of
Kafkas, Kars - Turkey

This journal is indexed and abstracted in:

- Web of Science Core Collection: Science Citation Index Expanded (since 2007)
- Additional Web of Science Indexes: Essential Science Indicators - Zoological Record
- CABI - Veterinary Science Database
- DOAJ
- EBSCO - Academic Search Premier
- Elsevier - SCOPUS
- Elsevier - EMBASE
- SOBİAD Atıf Dizini
- TÜBİTAK/ULAKBİM TR-Dizin
- Türkiye Atıf Dizini

ADDRESS FOR CORRESPONDENCE

Kafkas Üniversitesi Veteriner Fakültesi Dergisi Editörlüğü 36040, Kars - TÜRKİYE
Phone: +90 474 2426807-2426836/5228 Fax: +90 474 2426853 E-mail: vetdergi@kafkas.edu.tr

ELECTRONIC EDITION <http://vetdergikafkas.org>

ONLINE SUBMISSION <http://submit.vetdergikafkas.org>

OFFICIAL OWNER

Prof. Dr. Mete CİHAN
Dean of the Faculty of Veterinary Medicine, Kafkas University
E-mail: vetfak@kafkas.edu.tr; ORCID: 0000-0001-9883-2347

EDITOR-IN-CHIEF

Prof. Dr. İsa ÖZAYDIN
Kafkas University, Faculty of Veterinary Medicine
E-mail: iozaydin@kafkas.edu.tr; aras_isa@hotmail.com; ORCID: 0000-0003-4652-6377

MANAGING EDITOR

Prof. Dr. Özgür AKSOY
Kafkas University, Faculty of Veterinary Medicine
E-mail: drozguraksoy@hotmail.com; ORCID: 0000-0002-4800-6079

LANGUAGE EDITOR

Prof. Dr. Hasan ÖZEN
Balıkesir University, Faculty of Veterinary Medicine
E-mail: hasanozen@hotmail.com; ORCID: 0000-0002-6820-2536
Assist. Prof. Dr. Nüvit COŞKUN
Kafkas University, Faculty of Veterinary Medicine
E-mail: nuvitcoskun@gmail.com; ORCID: 0000-0001-7642-6460

STATISTICS EDITOR

Prof. Dr. İ. Safa GÜRCAN
Ankara University, Faculty of Veterinary Medicine
E-mail: sgurcan@ankara.edu.tr; ORCID: 0000-0002-0738-1518

ASSOCIATE EDITORS

Prof. Dr. Fatih BÜYÜK
Kafkas University, Faculty of Veterinary Medicine
E-mail: fatihbyk08@hotmail.com; ORCID: 0000-0003-3278-4834

Prof. Dr. Erol AYDIN
Kafkas University, Faculty of Veterinary Medicine
E-mail: dr-erolaydin@hotmail.com; ORCID: 0000-0001-8427-5658

Prof. Dr. Ali YİĞİT
Dokuz Eylül University, Faculty of Veterinary Medicine
E-mail: aliyig@gmail.com; ORCID: 0000-0002-1180-3517

Prof. Dr. Serap KORAL TAŞÇI
Kafkas University, Faculty of Veterinary Medicine
E-mail: serapkoralt@hotmail.com; ORCID: 0000-0001-8025-7137

Prof. Dr. Ekin Emre ERKİLİÇ
Kafkas University, Faculty of Veterinary Medicine
E-mail: ekin_emre_24@hotmail.com; ORCID: 0000-0003-2461-5598

Assist. Prof. Dr. Seda ÇAVUŞ ALAN
Kafkas University, Faculty of Veterinary Medicine
E-mail: sedacavusss@gmail.com; ORCID: 0000-0002-4989-4813

ASSOCIATE MANAGING EDITOR

Assoc. Prof. Dr. Semine DALGA
Kafkas University, Faculty of Veterinary Medicine
E-mail: sdalga91@gmail.com; ORCID: 0000-0001-7227-2513

Assoc. Prof. Dr. Emin KARAKURT
Kafkas University, Faculty of Veterinary Medicine
E-mail: eminkarakurt@kafkas.edu.tr; ORCID: 0000-0003-2019-3690

EDITORIAL BOARD

- Prof. Dr. Harun AKSU, İstanbul University-Cerrahpaşa, TÜRKİYE – h.aksu@iuc.edu.tr
- Prof. Dr. M. Sinan AKTAŞ, Atatürk University, TÜRKİYE – sinanaktas@atauni.edu.tr
- Prof. Dr. Feray ALKAN, Ankara University, TÜRKİYE – falkan@ankara.edu.tr
- Prof. Dr. Kemal ALTUNATMAZ, VetAmerican Animal Hospital, TÜRKİYE – altunatmaz@hotmail.com
- Prof. Dr. Divakar AMBROSE, University of Alberta, CANADA – dambrose@ualberta.ca
- Prof. Dr. Mustafa ARICAN, Selçuk University, TÜRKİYE – marican@selcuk.edu.tr
- Prof. Dr. Selim ASLAN, Near East University, NORTHERN CYPRUS – selim.aslan@gmail.com
- Prof. Dr. Sevil ATALAY VURAL, Ankara University, TÜRKİYE – [sevilvural\[at\]yahoo.com](mailto:sevilvural[at]yahoo.com)
- Prof. Dr. Tamer ATAÖĞLU, İstinye University, TÜRKİYE – tamer.ataoglu@istinye.edu.tr
- Prof. Dr. Levent AYDIN, Bursa Uludağ University, TÜRKİYE – laydin09@gmail.com
- Prof. Dr. Les BAILLIE, Cardiff School of Pharmacy & Pharmaceutical Sciences, UK – bailliel@cf.ac.uk
- Prof. Dr. Urban BESENFELDER, University of Veterinary Sciences, AUSTRIA – urban.besenfelder@vetmeduni.ac.at
- Prof. Dr. Kemal BÜYÜKGÜZEL, Zonguldak Bülent Ecevit University, TÜRKİYE – buyukguzelk@hotmail.com
- Prof. Dr. K. Paige CARMICHAEL, The University of Georgia, USA – kpc@uga.edu
- Assoc. Prof. Dr. Om Prakash CHOUDHARY, Guru Angad Dev Veterinary and Animal Sciences University, INDIA – dr.om.choudhary@gmail.com
- Prof. Dr. Burhan ÇETİNKAYA, Fırat University, TÜRKİYE – bctinkaya@firat.edu.tr
- Prof. Dr. Recep ÇİBIK, Bursa Uludağ University, TÜRKİYE – rcibik@uludag.edu.tr
- Prof. Dr. Ali DAŞKIN, Ankara University, TÜRKİYE – daskin@ankara.edu.tr
- Prof. Dr. Ömer Orkun DEMİRAL, Erciyes University, TÜRKİYE – orkun.erciyes@gmail.com
- Prof. Dr. İbrahim DEMİRKAN, Afyon Kocatepe University, TÜRKİYE – demirkan007@hotmail.com
- Prof. Dr. Hasan Hüseyin DÖNMEZ, Selçuk University, TÜRKİYE – donmez68@hotmail.com
- Prof. Dr. Emrullah EKEN, Selçuk University, TÜRKİYE – eeken@selcuk.edu.tr
- Prof. Dr. Mohamed Ibrahim EL SABRY, Cairo University, EGYPT – m.elsabry@gmail.com
- Prof. Dr. Marcia I. ENDRES, University of Minnesota, St. Paul, MN, USA – miendres@umn.edu
- Prof. Dr. Ayhan FİLAZİ, Ankara University, TÜRKİYE – afilazi@gmail.com
- Prof. Dr. Bahadır GÖNENÇ, Ankara University, TÜRKİYE – bahago@gmail.com
- Prof. Dr. Aytekin GÜNLÜ, Selçuk University, TÜRKİYE – agunlu@selcuk.edu.tr
- Prof. Dr. İ. Safa GÜRCAN, Ankara University, TÜRKİYE – sgurcan@ankara.edu.tr
- Prof. Dr. Hasan Hüseyin HADİMLİ, Selçuk Üniversitesi, KONYA – hhadimli@selcuk.edu.tr
- Prof. Dr. Johannes HANDLER, Freie Universität Berlin, GERMANY – johannes.handler@fu-berlin.de
- Prof. Dr. Riaz HUSSAIN, Islamia University of Bahawalpur, PAKISTAN – dr.riaz.hussain@iub.edu.pk
- Prof. Dr. Ali İŞMEN, Çanakkale Onsekiz Mart University, TÜRKİYE – alismen@yahoo.com
- Prof. Dr. Fatih Mehmet KANDEMİR, Aksaray University, TÜRKİYE – fkandemir03@gmail.com
- Prof. Dr. Kanber KARA, Erciyes University, TÜRKİYE – karananber@hotmail.com
- Prof. Dr. Mehmet Çağrı KARAKURUM, Burdur Mehmet Akif Ersoy University, TÜRKİYE – mckarakurum@yahoo.com
- Prof. Dr. Muhamed KATICA, University of Sarajevo, BOSNIA and HERZEGOWINA – muhamed.katica@vfs.unsa.ba
- Prof. Dr. Mükerrerem KAYA, Atatürk University, TÜRKİYE – mukerremkaya@hotmail.com
- Prof. Dr. Servet KILIÇ, Tekirdağ Namık Kemal University, TÜRKİYE – skilic@nku.edu.tr
- Prof. Dr. Ömür KOÇAK, İstanbul University-Cerrahpaşa, TÜRKİYE – okocak@iuc.edu.tr
- Prof. Dr. Marycz KRZYSZTOF, European Institute of Technology, POLAND – krzysztof.marycz@upwr.edu.pl
- Prof. Dr. Ercan KURAR, Necmettin Erbakan University, TÜRKİYE – ercankurar@gmail.com
- Prof. Dr. Hasan Rüştü KUTLU, Çukurova University, TÜRKİYE – hrc@cu.edu.tr
- Prof. Dr. Erdoğan KÜÇÜKÖNER, Süleyman Demirel University, TÜRKİYE – erdogankucukoner@sdu.edu.tr
- Prof. Dr. Levan MAKARADZE, Georgian State Agrarian University, GEORGIA – lmakaradze@yahoo.com
- Prof. Dr. Erdal MATUR, İstanbul University-Cerrahpaşa, TÜRKİYE – mature@iuc.edu.tr
- Prof. Dr. Muhammad Aamer MEHMOOD, Government College University Faisalabad, PAKISTAN – draamer@gcuf.edu.pk

EDITORIAL BOARD

- Prof. Dr. Erdoğan MEMİLİ, Prairie View A&M University, USA – ermemili@pvamu.edu
- Prof. Dr. Nora MIMOUNE, National High School of Veterinary Medicine, ALGERIA – n.mimoune@ensv.dz
- Prof. Dr. Cevat NİSBET, Ondokuz Mayıs University, TÜRKİYE – cnisbet@omu.edu.tr
- Prof. Dr. Vedat ONAR, Muğla Sıtkı Koçman University-Cerrahpaşa, TÜRKİYE – vedatonar@mu.edu.tr
- Prof. Dr. Abdullah ÖZEN, Fırat University, TÜRKİYE – abdulloazen@hotmail.com
- Prof. Dr. Zeynep PEKCAN, Kırıkkale University, TÜRKİYE – vetzeynep@yahoo.com
- Prof. Dr. Alessandra PELAGALLI, University of Naples Federico II, ITALY – alpelaga@unina.it
- Prof. Dr. Abdul Qayyum RAO, Centre of Excellence in Molecular Biology University of the Punjab, PAKISTAN – qayyum.cemb@pu.edu.pk
- Prof. Dr. Muhammad Asif RAZA, MNS University of Agriculture, PAKISTAN – asif.raza@mnsuam.edu.pk
- Prof. Dr. Michael RÖCKEN, Justus-Liebig University, GERMANY – michael.roecken@vetmed.uni-giessen.de
- Prof. Dr. Sabine SCHÄFER-SOMI, University of Veterinary Medicine Vienna, AUSTRIA – sabine.schaefer@vetmeduni.ac.at
- Prof. Dr. Çiğdem TAKMA, Ege University, TÜRKİYE – cigdem.takma@ege.edu.tr
- Prof. Dr. Fotina TAYANA, Sumy National Agrarian University, UKRAINE – tif_ua@meta.ua
- Prof. Dr. Zafer ULUTAŞ, Ondokuz Mayıs University, TÜRKİYE – zulutas@hotmail.com
- Prof. Dr. Cemal ÜN, Ege University, TÜRKİYE – cemaluen@gmail.com
- Prof. Dr. Oya ÜSTÜNER AYDAL, İstanbul University-Cerrahpaşa, TÜRKİYE – oyaustuner@gmail.com
- Prof. Dr. Axel WEHRND, İstanbul University-Cerrahpaşa, TÜRKİYE – axel.wehrend@vetmed.uni-giessen.de
- Prof. Dr. Thomas WITTEK, Justus-Liebig-Universität Gießen, GERMANY – thomas.wittek@vetmeduni.ac.at
- Prof. Dr. Rifat VURAL, Ankara University, TÜRKİYE – vural@ankara.edu.tr
- Prof. Dr. Cenk YARDIMCI, Ondokuz Mayıs University, TÜRKİYE – cenkyardimci@yahoo.com
- Prof. Dr. Alparslan YILDIRIM, Erciyes University, TÜRKİYE – yildirima@erciyes.edu.tr
- Prof. Dr. Serkan YILDIRIM, Atatürk University, TÜRKİYE – syildirim@atauni.edu.tr
- Prof. Dr. Tülay YILDIRIM, Yıldız Technical University, TÜRKİYE – tulay@yildiz.edu.tr
- Prof. Dr. Hüseyin YILMAZ, İstanbul University-Cerrahpaşa, TÜRKİYE – hyilmaz@istanbul.edu.tr
- Prof. Dr. Zeki YILMAZ, Bursa Uludag University, TÜRKİYE – zyilmaz@uludag.edu.tr

THE REFEREES LIST OF THIS ISSUE (in alphabetical order)

Ahmet ALTINDAĞ	Ankara Üniversitesi Fen Fakültesi
Aliye GÜLMEZ SAĞLAM	Kafkas Üniversitesi Veteriner Fakültesi
Arda Onur ÖZKÖK	Amasya Üniversitesi, Suluova Meslek Yüksekokulu
Ayesha SADIQA	University of Engineering and Technology, Pakistan
Cafer TEPELİ	Selçuk Üniversitesi Veteriner Fakültesi
Caner ÖZTÜRK	Aksaray Üniversitesi Veteriner Fakültesi
Celal Şahin ERMUTLU	Kafkas Üniversitesi Veteriner Fakültesi
Çağatay ESİN	Ondokuz Mayıs Üniversitesi Veteriner Fakültesi
Diana A. AL-QUWAIE	King Abdulaziz University, College of Science & Arts, Saudi Arabia
Eser AKAL	Ondokuz Mayıs Üniversitesi Veteriner Fakültesi
Fatih BÜYÜK	Kafkas Üniversitesi Veteriner Fakültesi
Gökçenur SANIOĞLU GÖLEN	Aksaray Üniversitesi Veteriner Fakültesi
Gülseren KIRBAŞ DOĞAN	Kafkas Üniversitesi Veteriner Fakültesi
Hüseyin YILDIZ	Bursa Uludağ Üniversitesi Veteriner Fakültesi
Kadir ÖNK	Kafkas Üniversitesi Veteriner Fakültesi
Kemal KIRIKÇI	Selçuk Üniversitesi Veteriner Fakültesi
Mahir MAHARRAMOV	Nakhchivan State University, Nakhchivan - Azerbaijan
Mahmoud Mahrous M. ABBAS	Al-Azhar University, Science Faculty, Egypt
Mohamed A. FAHMY	Zagazig University, Faculty of Agriculture, Egypt
Muazzez GÜRGAN ESER	Tekirdağ Namık Kemal Üniversitesi Fen Edebiyat Fakültesi
Nuray ŞAHİNLER	Uşak Üniversitesi Ziraat Fakültesi
Osman SERDAR	Munzur Üniversitesi Su Ürünleri Fakültesi
Pınar CİHAN	Tekirdağ Namık Kemal Üniversitesi Mühendislik Fakültesi
Rao Zahid ABBAS	Faculty of Veterinary Science University of Agriculture, Pakistan
Sadık YAYLA	Dicle Üniversitesi Veteriner Fakültesi
Serap İLHAN AKSU	Kafkas Üniversitesi Veteriner Fakültesi
Serdar GENÇ	Kırşehir Ahi Evran Üniversitesi Ziraat Fakültesi
Sevdan YILMAZ	ÇOMÜ Deniz Bilimleri ve Teknolojisi Fakültesi
Sibel ÇİMEN	Yıldız Teknik Üniversitesi Elektrik-Elektronik Fakültesi
Sobia NASEEM	University of Engineering and Technology, Pakistan
Suna AKKOL	Van Yüzüncü Yıl Üniversitesi Ziraat Fakültesi

CONTENTS

REVIEW

Managing Mycotoxins in Animal/Poultry Feed Through Innovative Control Strategies: A Review

KHATOON A, ABİDİN ZU, ALİ A, SALEEMİ MK, ABBAS RZ, IJAZ MU, REHMAN MU, MURTAZA B

(DOI: 10.9775/kvfd.2025.34700)

581

RESEARCH ARTICLES

Hybrid Ensemble Model for Lactation Milk Yield Prediction of Holstein Cows

TOPUZ D, TEKGÖZ S

(DOI: 10.9775/kvfd.2025.34031)

603

Effects of Different Time Schedules for Regrouping on Socio-Positive Behaviors in Group-Housed Rabbit Does

PETEK M, GEBHARDT-HENRİCH SG

(DOI: 10.9775/kvfd.2025.34134)

613

Evaluating the Multifunctional Therapeutic Potential of Phycocyanin: Antidiabetic, Antioxidant, Anticancer and Antimicrobial Effects on Metabolic, Oxidative, and Histopathological Parameters in Dithizone-Induced Diabetic Rats

ALDUWİSH MA, ALHARTHİ NS, ALHARBİ AA, ALBALAWİ M, OBİDAN A, BEYARİ EA, AL-GHEFFARİ HK, SHAKAK AO, ALLOHİBİ A, ALMUTAİRİ LA, ALMASOUDİ SH, ALSULAMİ RN, AL-DOAİSS AA, ABU-ELSAOUD AM

(DOI: 10.9775/kvfd.2025.34347)

619

Assessment of Testicular Artery Blood Flow Using Doppler Ultrasonography and Its Correlation with Spermatological Parameters in Kangal Shepherd Dogs

EŞİN B, KAYA C, EŞİN Ç

(DOI: 10.9775/kvfd.2025.34432)

635

How Light and Stocking Density Affect the Morphometric and Mechanical Traits of Quail Tibiotarsus?

YILDIRIM İG, SEVİL KİLİMCİ F, KHAN K, TÜRKER YAVAŞ F, KOÇ YILDIRIM E, RAZA S

(DOI: 10.9775/kvfd.2025.34495)

645

Comparative Performance of Convolutional Neural Network Models in Wing Morphometric Classification of Honey Bee Populations Across Europe

YILDIZ Bİ

(DOI: 10.9775/kvfd.2025.34544)

653

Component Identification of Buyang Huanwu Decoction and the Effect of Main Components on Preventing Muscle Atrophy

ZHOU L, LUO S, MENG L, WANG G, ZHANG L, WU H

(DOI: 10.9775/kvfd.2025.34593)

661

First Report of Gastroenteritis Caused by *Citrobacter braakii* in a Yellow-margined Box Turtle (*Cuora flavomarginata*)

CHEN M, SONG Y, LIU C, CHEN N, XUE J

(DOI: 10.9775/kvfd.2025.34626)

669

Evaluation of Microbiological Properties in Kefir Production with Fuzzy Logic-Based Decision Support System

AKILLI A, KEZER G, KUL E

(DOI: 10.9775/kvfd.2025.34643)

679

Acute and Chronic Toxicity of the Coccidiostat Amprolium to *Daphnia magna* and Its Implications for Aquatic Contamination from Livestock Waste

YARDIMCI M, YAĞCILAR Ç, POLAT C

(DOI: 10.9775/kvfd.2025.34670)

689

Ecotoxicological Consequences of Heavy Metals on Emperor Fish (*Lethrinus*) species in the Red Sea: Histopathology and Biochemistry

ALSOLMY SA, MOMİNKHAN R, MELEBARY SJ

(DOI: 10.9775/kvfd.2025.34770)

697

REVIEW ARTICLE

Managing Mycotoxins in Animal/Poultry Feed Through Innovative Control Strategies: A Review

Aisha KHATOON ¹ (*)  Zain ul ABIDIN ²  Ashiq ALI ³  Muhammad Kashif SALEEMI ¹ 
Rao Zahid ABBAS ⁴  Muhammad Umar IJAZ ⁵  Mujeeb ur REHMAN ⁶  Bilal MURTAZA ⁷ 

¹ Department of Pathology, Faculty of Veterinary Science University of Agriculture Faisalabad 38040 PAKISTAN

² Veterinary Research Institute, Zarrar Shaheed Road Lahore Cantt-13 PAKISTAN

³ Department of Histology and Embryology Shantou Medical University, Shantou, 515041 CHINA

⁴ Department of Parasitology, Faculty of Veterinary Science University of Agriculture Faisalabad, 38040 PAKISTAN

⁵ Department of Zoology, Wildlife and Fisheries, University of Agriculture Faisalabad-38040 PAKISTAN

⁶ Single Cell Bioengineering Group (SCBEG), State Key Laboratory of Marine Resource Utilization in South China Sea, College of Oceanology, Hainan University, Haikou 570228, Hainan, CHINA

⁷ School of Bioengineering, Dalian University of Technology, No. 2 Linggong Road, Dalian, 116024, CHINA



(*) Corresponding author:

Aisha Khatoon

Phone: +92 92-42-9200161

E-mail: aisha.khatoon@uaf.edu.pk;

aishavp@yahoo.com

How to cite this article?

Khatoon A, Abidin ZU, Ali A, Saleemi MK, Abbas RZ, Ijaz MU, Rehman MU, Murtaza B:

Managing mycotoxins in animal/poultry feed through innovative control strategies: A review. *Kafkas Univ Vet Fak Derg*, 31 (5):

581-602, 2025.

DOI: 10.9775/kvfd.2025.34700

Article ID: KVFD-2025-34700

Received: 30.06.2025

Accepted: 12.09.2025

Published Online: 17.09.2025

Abstract

Mycotoxins are the secondary metabolites of certain toxigenic fungi that have deleterious effects upon the health of humans, animals, and poultry. More than 300 chemically different mycotoxins have been identified to date, among which the most important are aflatoxins, ochratoxins, fumonisins, trichothecenes, and patulins. Approximately 25% of global food crops are significantly affected by mycotoxins every year. Animals become exposed to the adverse effects of mycotoxins when fed mycotoxin-contaminated feed, and animal byproducts containing mycotoxin residues become a constant source of exposure to the human population. Once mycotoxins enter the food chain, their complete removal is inevitable; therefore, different control strategies are being adopted to minimize the adverse effects associated with them. This review encompasses various control strategies adapted to minimize mycotoxicosis.

Keywords: Mycotoxins, Animal feed, Poultry feed, Mycotoxicosis, Control strategies

INTRODUCTION

Certain toxic fungal species are ubiquitous in nature and have strong ecological link with human and animal food supplies. These fungi often produce certain chemical ingredients which are not necessarily required for their growth but play a crucial role in their survival and these chemical compounds are often termed as 'secondary fungal metabolites'. Mycotoxins are a diverse group of chemically different compounds originally produced as secondary metabolites by several toxigenic fungal species. Many fungal genera are predominantly involved in the production of these hazardous chemical compounds, but the most important among them are *Aspergillus*, *Fusarium*, *Penicillium*, *Alternaria* and *Claviceps* ^[1]. To date, about 400

chemically diverse mycotoxins have been identified which pose severe toxic effects in different animal species and human population in one way or another. Mycotoxin-associated toxicities and/or adverse effects are directly related to the dose, duration, mycotoxin type, and route of exposure to a specific mycotoxin ^[2]. Mycotoxins generally exhibit hepatotoxic, nephrotoxic, carcinogenic, and immunosuppressive effects in certain animal species, ultimately compromising the overall health of animals. When produced within the feed, mycotoxins form 'mycotoxin pockets' within the feed, which are generally rich in their concentration and are considered hotspots for mycotoxins, thereby ensuring an uneven distribution of mycotoxins within the feed.



The route of mycotoxin entry into the animal food/feed chain involves the use of contaminated agricultural byproducts during the formation of feed or production of different mycotoxins within the feed by storage fungi descending either from pre-harvest, harvest, or post-harvest durations of crops [3]. Contamination by different agricultural products also limits international trade, as certain countries have different regulatory measures regarding the levels of mycotoxins [4]. Entry of mycotoxins

into the human food chain occurs either through the consumption of mycotoxin-contaminated agricultural products or through animal byproducts derived from animals fed mycotoxin-contaminated rations. The mycotoxin residues exhibit certain anomalies in humans, the details of which have been presented and elaborated in *Table 1* and *Fig. 1*.

Discussing about the classification of mycotoxins, some of the significant mycotoxins from the vast list are aflatoxins,

Table 1. Mycotoxins associated diseases in human population along with details of specific mycotoxins involved in disease production

Fungi Involved	Source of Contamination	Disease Production	Specific Mycotoxin Involved	Reference
<i>Fusarium verticillioides</i> , <i>Fusarium proliferatum</i>	Corn/maize	Oesophageal tumors	Fumonisin B2	[5]
<i>Fusarium</i> species	Toxic bread (cereal grains)	Alimentary toxic aleukemia	Trichothecene, Fumonisin B1	[6]
<i>Stachybotrys atra</i>	Contaminated dust from ventilation slits, ceilings and walls	Sick-building syndrome	T-2, Diacetoxyscirpenol, Verrucarol	[7]
<i>Fusarium</i> species	Wheat, oats, barley, rice	Akakabio-byo	Fusarium toxins	[8]
<i>Aspergillus flavus</i> and <i>Aspergillus parasiticus</i>	Cereal grains	Kwashiorkor	Aflatoxin M1, AFM2	[9]
<i>Aspergillus ochraceus</i> , <i>Penicillium</i> species	Cereal grains	Balkan endemic nephropathy	Ochratoxin A	[10]
<i>Penicillium</i> and <i>Aspergillus</i> species	Rice	Cardiac beriberi	Aflatoxins	[11]
<i>Fusarium proliferatum</i> , <i>Fusarium verticillioides</i>	Maize/corn	Neural tube defect	Fumonisin B1 and B2	[12]
<i>Claviceps purpurea</i> , <i>Claviceps fusiformis</i>	Cereal grains, rye	Ergotism	Ergotamine-ergocristine Alkaloids	[12]
<i>Aspergillus flavus</i> and <i>Aspergillus parasiticus</i>	Peanuts, cereal grains	Hepatocellular carcinoma	Aflatoxin B1	[13]
<i>Stachybotrys atra</i>	Grain dust	Stachybotryotoxicosis	Satratoxins, Trichothecene	[14]
<i>Aspergillus</i> species	Grain dust	Reye's syndrome	Aflatoxin B1, B2 and M1	[15]
<i>Fusarium</i> species	Wheat, rice, corn	Scabby grain toxicosis	Zearalenone, deoxynivalenol	

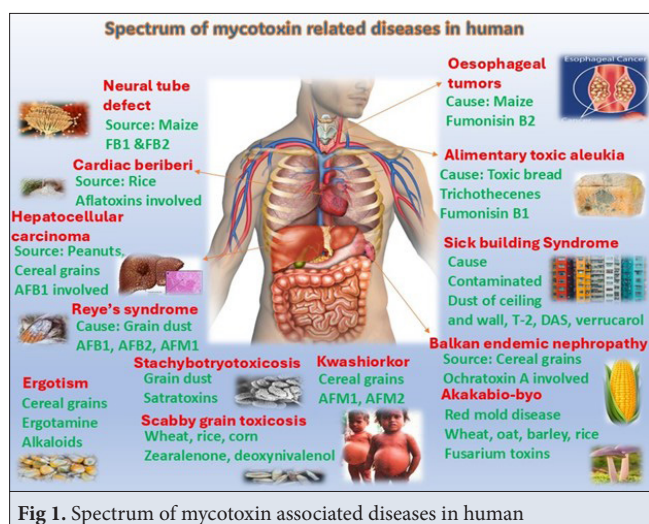


Fig 1. Spectrum of mycotoxin associated diseases in human

ochratoxins, zearalenone, trichothecenes, fumonisins, patulin, ergot toxins etc. However, keeping in view the one health perspectives, the most significant among all the mycotoxins are aflatoxins and ochratoxins. This review emphasizes the existence and after-effects of mycotoxins and control strategies adapted for these mycotoxins (in particular), along with the strategies adapted for the control of other mycotoxins in different livestock species.

EXISTENCE OF DIFFERENT MYCOTOXINS IN ANIMAL/POULTRY FEED AND THEIR EFFECTS

Aflatoxins

Contamination of food with aflatoxins has remained a

persistent issue for livestock and poultry feed, along with all processed food products. These chemical compounds were discovered accidentally in 1961 when many turkey poult s suddenly died in England due to an unrecognized disorder named as “Turkey-X disease.” When investigated, it was revealed that a similar syndrome also appeared in farms where Brazil imported moldy peanut meal during feed formulation. Extraction using chloroform and detailed chemical analysis linked the extracted compound with “*Aspergillus flavus*.” Scientists then gave the name “Aflatoxin” to this chemical compound by joining first three letters of both “*Aspergillus*” and “*flavus*.” In the same year, this compound was also isolated in crystalline form in Netherlands and further fragmented as Aflatoxin B and G in United Kingdom based on color, they fluoresced under ultraviolet (UV) light. However, further investigations subdivided it into aflatoxins B1, B2, G1, and G2 based on minor differences in their chemical structures [16,17]. Furthermore, many other derivatives are linked to it from time to time, such as aflatoxin M1, aflatoxicol, AFP1, and AFQ1. There are approximately 20 different types of aflatoxins, but aflatoxin B1 (AFB1) (Fig. 2) is considered to be the most important and toxic among all types due to its toxicity [18].

Aflatoxins, belonging to the difuranocoumarin group, are secondary metabolites produced by a variety of toxigenic fungal species belonging to two important genera, *Aspergillus* and *Penicillium* [19] with *Aspergillus flavus* and *Aspergillus parasiticus* are considered major producers of aflatoxins [20,21]. Among all aflatoxins, aflatoxin B1 (AFB1) is the most toxic to animals, humans, and poultry, followed by AFB2, AFG1, and AFG2. Based on its extent of toxicity, the International Agency for Research on Cancer (IARC) has classified it as a group 1 carcinogen in humans and animals. Along with cancer, it causes hepatic disorders, metabolic diseases, vomiting, stunted growth, and diarrhea in human population.

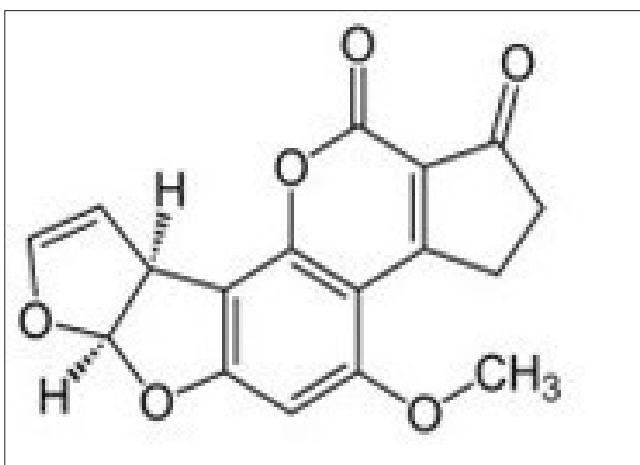


Fig 2. Structural presentation of Aflatoxin B1

Cereal crops, such as corn, wheat, sorghum, and rice, along with other feed ingredients, are readily contaminated with aflatoxins during their storage period when anaerobic conditions coupled with high humidity develop within the stored ingredients [6,22]. Aflatoxins have a tendency to easily infiltrate body tissues, muscles, and fatty tissues as residues, and when consumed, they become a potent source of contamination in the human population consuming such meat [23]. Table 2 illustrates some studies on mycotoxins reporting the existence of tissue residues in animals. The problem of aflatoxins occasionally occurs in crops prior to harvesting, but they are also produced in the stored ingredients whenever the storage fungi get a favorable environment for their growth, ultimately producing them as their secondary metabolites [24]. There are different legislations for the maximum tolerable levels (MTL) for all foods, including feed/feed ingredients for poultry and large animals (sheep, cattle, and buffalo). The United States Food and Drug Administration (US FDA) recommends 20 µg/kg of feed as a worldwide range for maximum permissible and tolerable levels for the poultry sector, whereas the maximum tolerable level for cattle and buffalo is 100 µg/kg of feed [25,26]. However, many studies are available, particularly in developing countries, which report much higher levels in feed/feed ingredients than in the recommended MTL [23,27-32].

Table 2. Occurrence of tissue residues of different mycotoxins in various animal species

Mycotoxin	Specie	Level Used	Residues Detected	Reference
Aflatoxins	Broiler	100 µg/kg	0.32 µg/kg 0.08 µg/kg (Muscles)	[33]
	Broiler	1 mg/kg	0.166 µg/kg	[34]
	Broiler	1600-6400 µg/kg	6.97 ng/g 0.49-2.18 ng/g (Muscles)	[35]
	Broiler	Field Study	0.78-10.41 ng/g 0.23-5.67 ng/g (Kidney) 0.01-0.97 ng/g (Muscles)	[36]
	Broiler	600-1800 µg/kg	0.53-2.05 µg/kg	[37]
	Cattle	Field Study	0.36 µg/kg 1.37 µg/kg (Kidney)	[38]
Ochratoxins	Broiler	Field Study	0.58 µg/kg 0.51 µg/kg (Kidney)	[39]
	Broiler	100 µg/kg	1.92 ng/g 3.58 ng/g (Kidney)	[40]
	Broiler	2 mg/kg	1.79 ng/g 4.42 ng/g (Kidney)	[41]
	Beef sausages	Field Study	4.1-7.1 ppm	[42]

Table 3. Health impacts associated with aflatoxins in ruminants and poultry				
Specie	Dose Tested	Duration	Effects	Reference
Cattle	300 µg/kg	133 days	No effects	[48]
Cattle	200-500 µg/kg	14 days	Severe pathological effects	[49]
Cattle	350-455 µg/kg	15-17.5 weeks	No effects	[50]
Cattle	60-300 µg/kg	155 days	No effects	[51]
Beef calves	1400 µg/kg	FS	Neurological signs, ataxia, depression	[52]
Lambs	2 mg/kg	37 days	Decreased body weight and immune responses	[53]
Lambs	350 µg/kg	150 days	Decreased serum parameters	[54]
Lambs	5.9-23.5 µg/kg	91 days	Decreased cellular immunity	[55]
Lactating dairy cows	96 µg/kg	7-12 days	Slight increase in serum proteins	[56]
Broilers	40 µg/kg	42 days	Reduced growth performance	[57]
White Leghorn cockerels	400 µg/kg	60 days	Hematological alterations	[58]
Broiler chicks	100-600 µg/kg	42 days	Immunosuppression	[16]
Broiler chicks	200 µg/kg	42 days	Serum biochemical and immunological alterations	[59]

Ruminants: Ruminants have a complex ecosystem of microflora and microfauna within the rumen [43,44] and nature has provided ruminants with diverse properties for detoxifying mycotoxins into their less toxic products through a diversified range of microflora and microfauna existing within their ruminal fluid [45]. As far as cattle are concerned, mature animals are less prone to the adverse effects of aflatoxins compared to growing, young, and pregnant animals. Aflatoxins are degraded in the rumen and converted to less toxic aflatoxicol [46]. Aflatoxins in feed bind with ruminal contents, and a lower quantity (only 2-5%) of ingested aflatoxin reaches the intestine. Feed levels of approximately 100 µg/kg are toxic to ruminants [47]. The health effects of aflatoxins in different species are listed in Table 3.

Aflatoxin B1 (AFB1), which escapes ruminal degradation, enters the liver and is converted into aflatoxin (AFM1), which is released in milk. The maximum tolerable level of AFM1 in milk is 0.5 µg/kg. This metabolite can be detected in milk 6 h after the ingestion of AFB1, whereas its peak level can be noticed 24-48 hours after continuous AFB1 ingestion. Its clearance from milk can be observed 3 days after withdrawal of a controlled diet [60]. It has been reported that AFM1 can cause pronounced aflatoxicosis in weaning calves often characterized by development of histopathological lesions in liver and kidney along with disturbance of hepatic enzymes [61]. About 1-2% of the total ingested AFB1 is released as AFM1 in milk [62]. The average transfer of aflatoxin from feed to milk is 1.7% while the maximum permissible level of aflatoxin for milk is 0.05 µg/liter in Asia [63]. Therefore, to avoid its residues in milk, dietary aflatoxin levels for ruminants must be as low as 25 µg/kg [64].

Poultry: In the poultry industry, chicks of all age groups are prone to adverse effects caused by aflatoxins, particularly AFB1. Apart from adversely affecting all organs of chicks, their residues infiltrate muscles and organs, making them a direct source of contamination for the human population consuming such meat. Aflatoxins in feed result in reduced feed intake and body weight gain, along with suppressed relative organ weights, and birds become dull and less attractive towards feed. Similarly, hematological and serum biochemical parameters are adversely affected, leading to anemic conditions, along with permanent damage to the kidney and liver [65,66]. In addition, the most prominent anomaly expressed by AFB1 in feed is immunosuppression, which makes birds susceptible to secondary bacterial infections [67,68]. Moreover, AFB1 forms DNA adducts, ultimately affecting the overall genome of organisms.

Ochratoxins

Ochratoxins are produced as secondary metabolites of certain species of *Aspergillus* and *Penicillium* with *Aspergillus ochraceus* being the major producer [30]. Based on minor structural differences, it has been further subdivided into ochratoxin A (OTA), ochratoxin B (Mohamed, #123), and OTC, with OTA being the most important and toxic among all. OTA is highly carcinogenic, and the International Agency for Research on Cancer has classified it as Group 2B [69]. *Penicillium verrucosum* is considered a major OTA producer in cold and temperate climatic zones, *Penicillium verrucosum* whereas *Aspergillus carbonarius*, *A. ochraceus*, *A. niger*, and *A. melleus* are considered major OTA producers.

Ochratoxins contaminate different crops, including corn, maize, sorghum, barley, and rice, resulting in a

high chance of contamination in animal/poultry feed. Different regulatory levels are recommended for different raw materials and animal byproducts. According to the European Commission Recommendations (2006, 576), the MTL for complete feedstuff is 100 µg/kg feed [70]. Certain predisposing factors, such as hot and humid environments, poor pre-harvest/harvest conditions, and poor storage environments, enhance the production of OTA in feed.

Ruminants: OTA administered to young ruminants causes severe signs of depression, degeneration of the kidney, and polyuria, ultimately leading to the death of animals [71]. Ruminal microflora causes the degradation of amide bonds between ochratoxin-α and phenylalanine (Fig. 3), ultimately producing less toxic compounds [72]. In the rumen, 50% of the total OTA is degraded within the first 15 min, while 95% of the total OTA is degraded into less toxic ochratoxin-α and phenylalanine moieties by ruminal microflora within 4 h of ingestion. Owing to this phenomenon, OTA does not affect or penetrate vital organs of the body [45].

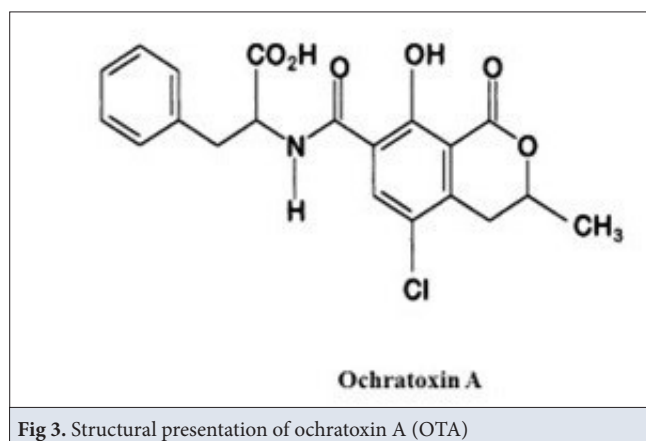


Fig 3. Structural presentation of ochratoxin A (OTA)

Poultry: Poultry chicks are highly sensitive to the effects of OTA, which affects almost all vital organs of the body. Toxicopathological effects include reduced feed intake, body weight gain, dullness, and reduced attraction to feed. Serum biochemical parameters and hematological indices are also severely affected by exposure to OTA [73,74]. Immunosuppression has been extensively observed in this regard. In this regard, our recent reviews elaborate on experimental ochratoxicosis in poultry [24,69].

Fumonisin

Fumonisin are secondary metabolites of *Fusarium proliferatum* and *Fusarium moniliformis*. Apart from these two species, some *Alternaria*, especially *A. alternata* have been found to produce fumonisins [75]. There are twenty-eight (28) chemically different types of fumonisins (FA1, FA2, FB1, FB2, FB3, and FB4), among which fumonisins

B1 (FB1) is the most important and toxic form of fumonisins [76].

Ruminants: Regarding ruminants, fumonisins are tolerant to ruminal biodegradation; however, due to their low oral bioavailability, acute or chronic intoxication does not occur at the farm level [77]. However, the presence of very high levels in the feed can cause histopathological lesions in the kidneys and liver [78].

Poultry: The mechanism by which fumonisins cause toxicity in animals is thought to be the disruption of sphingolipid metabolism. It has been observed that fumonisins are the specific inhibitors of ceramide synthase enzyme which is needed for ceramide and complex sphingolipids synthesis. Because of this inhibition, a change in the sphingosine [7] to sphinganine [1] ratio occurs, and such an increased ratio has been observed in the tissues of turkeys, ducklings, and broilers exposed to FB1 in feed [79,80]. Turkeys and chicks were relatively resistant to the adverse effects of FB1, but mild to moderate toxicity was observed in turkeys and ducks fed FB1 at 75-400 mg/kg feed for 21 days. The observed changes included reduced body weight gain and hepatic damage, such as hepatic necrosis and biliary hyperplasia [81].

Trichothecenes

Trichothecenes are a diverse group of mycotoxins, the most important of which is deoxynivalenol [20] also known as vomitoxin. Other important members of this group are T-2 toxins, diacetoxyscirpenol (DAS), and scirpenol. They are produced by a variety of *Fusarium* species, while DON is produced primarily by *Fusarium roseum* and T-2 toxins are produced by *F. poae* and *F. sporotrichioides* under storage conditions [82].

Ruminants: Discussing about ruminants, microorganisms present within the ruminal fluid have distinct property of deacetylation and DAS is de-acetylated into monoacetoxyscirpenol [7] and scirpenetriol; and these products are less toxic as compared to their parent compounds [83]. DON occurs in excessive quantities within the concentrates, and it is also readily degraded within the rumen, but in animals suffering from ruminal acidosis, such degradation becomes incomplete, ultimately producing trichothecene-associated adverse effects in the animals [84]. However, in general, ruminants can easily tolerate 8.5 mg/g DON within the feed and is readily degraded within 6-24 h of its ingestion by the ruminants [85]. Furthermore, DON-associated lesions in animals include lesions within the gastrointestinal tract, vomiting, severe dermatitis, hemorrhage, and bloody diarrhea [86].

Poultry: Poultry chicks are also resistant to the adverse effects of DON to some extent, but the associated adverse effects include decreased feed efficiency, reduced body

weight gain, and poor efficiency when fed extremely high doses ^[87].

APPROACHES/STRATEGIES FOR DETOXIFICATION/REDUCTION OF MYCOTOXINS

Three main approaches and strategies are generally adopted for the control and prevention of mycotoxins in animal and poultry feedstuff, which include physical, chemical, and biological methods.

Physical Methods

There are different physical methods for the control of mycotoxins, which unfortunately become impractical at a large scale, but such methods can efficiently help detoxify mycotoxins on a small scale. These methods include adsorption, irradiation, heating, solvent extraction, washing and separation.

Sorting and Separation

Grains are the major part of animal/poultry feed formulations ^[88] and when these grains are significantly contaminated with mycotoxins, they appear as moldy, broken, discolored and not distributed uniformly in the contaminated cereals rather they cluster together forming 'mycotoxin pockets' ^[89,90]. The separation and sorting of mycotoxin-contaminated grains are performed using sieving, aspiration, photoelectric separation, and image separation techniques ^[91]. Hand sorting, dehulling, and flotation alone can remove 93%, 63%, and 51% of mycotoxins from white-shelled maize, respectively, whereas using these three methods in combination can remove nearly 98% of mycotoxins ^[92]. Similarly, gravity separation and aspiration can reduce mycotoxins by 80%, but this also reduces wheat crop ^[93]. Moreover, visual sorting strategies (optical viscosity and near-infrared spectroscopy) have been used to remove mycotoxins from maize and wheat ^[90,94-96]. The limitations of these methods are that they are costly and limited to small-scale use.

Washing and Solvent Extraction

Mycotoxins can be easily removed by washing and solvent extraction because of their distinct fat-soluble and water-soluble properties. The floating method has the potential to decrease the concentrations of zearalenone, fumonisins, aflatoxins, and trichothecenes by 61%, 73%, 72%, and 69%, respectively ^[92,96,97]. The best results obtained by the floating method can be achieved by adding NaCl and sucrose to water to attain the maximum output ^[98]. When these physical techniques are used in combination to control mycotoxins, they provide better results than the individual techniques ^[99]. Commonly used solvents for mycotoxin extraction include hexane, methanol, ethanol, and aqueous acetone ^[100]. However, the

major disadvantages associated with washing and solvent extraction are that they cause the loss of nutrients and are costly, which limits their application at larger scales.

Heating

This method for the control of mycotoxins has been extensively used for the removal of different mycotoxins; however, AFB1 and FB1 can tolerate heat and require high temperatures (probably more than 150°C) for their decomposition ^[101-104] ultimately making their decomposition difficult. Some studies have shown that thermal treatment up to 160°C for 20 min under a pressure of 10 MPa can reduce aflatoxins in rice by 80% from rice ^[105] while heating barley at 220°C can destroy 90% of zearalenone (ZEN) and DON ^[101]. Similarly, 150-200°C temperature can cause a 70% reduction in the concentration of FB1 in rice ^[106]. However, the disadvantage of this method is the production of the Maillard reaction, formation of certain carcinogens such as acrylamide, and reduction of the nutritive value, thereby limiting the use of this method at larger scales ^[105].

Decontamination by Irradiation

The irradiation process is usually divided into two forms: non-ionizing and ionizing. Non-ionizing processes involve microwaves, radio waves, visible light waves, and infrared waves, whereas the ionizing form includes ultraviolet rays, X-rays, electron beams, and gamma rays ^[107]. Extensive research has been performed by many scientists to evaluate the degradation of different mycotoxins using different irradiation technologies. *Table 4* presents different studies reporting the use of irradiation technologies for the degradation of mycotoxins in animal/poultry feed and their ingredients.

Using gamma irradiation: Gamma rays are electromagnetic waves produced as a result of decaying an unstable source such as radioactive isotopes. Gamma rays are preferred in the food industry because of their high reactivity and penetration power. However, certain factors are important in this regard as far as the usage of gamma rays for degradation of mycotoxin is concerned such as dose of radiation used, level of mycotoxin contamination, water content within feed and composition of matrix. Many studies have reported possible degradation of aflatoxins within feed at 5-10 KGy exposure to gamma rays ^[112,122,123].

Gamma irradiation is undoubtedly gaining popularity due to its excellent results in finished food products, whereas Di Stefano et al. ^[110] reported only up to 21% aflatoxin reduction from finished poultry feed, which suggests that this technique is not suitable for products containing high lipid and vitamin contents ^[107].

Using electron beam: Irradiation through electron beams has shown promising results in the degradation of certain mycotoxins because of their short processing time,

Table 4. Degradation of mycotoxins by different irradiation techniques in animal/poultry feed and its ingredients

Technique used	Feed type	Mycotoxin	Treatment Condition	Degradation Percentage	Reference
Gamma irradiation	Soybean	AFB1	10 kGy	62.20%	[108]
	Wheat	OTA	30.5 kGy	24%	[109]
	Commercial poultry feed	OTA	15 kGy	23.9%	[110]
	Commercial poultry feed	AFB1	15 kGy	18.2%	[110]
	Poultry feed	Aflatoxins	25 kGy	42.7%	[111]
	Maize feed	AFB1	10 kGy	94.5%	[112]
	Broiler feed	AFB1	6 kGy	89.53%	[113]
	Chicken liver	AFB1	10 kGy	25%	[114]
	Chicken liver	OTA	10 kGy	60%	[114]
	Poultry feed	OTA	4 kGy	100%	[115]
	Poultry feed	AFB1	6 kGy	100%	[116]
Electron beam	Corn	Zearalenone	50 kGy	71.1%	[117]
	Barley	Fusarium species	10 kGy	50-98%	[118]
	Wheat	DON	55.8 kGy	78.4%	[119]
Pulsed light	Rice bran	AFB1	0.52 J/cm per pulse for 15 sec	90.3%	[120]
Ultraviolet irradiation	Wheat	254 nm for 160 min	Aflatoxins	65-90%	[121]

dosage control, and low equipment costs. In the case of aflatoxins, this technology breaks down toxins into less toxic products, thereby reducing their toxicity potential of aflatoxins [124,125].

However, this technique has a lower degradation capacity than gamma irradiation. Moreover, Liu et al. [126] reported that this technique was not very efficient in degrading AFB1 from peanut meals, as this technique cannot be declared as a complete solution for degradation/decontamination purposes as far as mycotoxins are concerned.

Using ultraviolet irradiation: Over the past several decades, UV irradiation has been considered an effective technique for the destruction of several mycotoxins, particularly aflatoxins, owing to their photosensitivity. Being a non-thermal technique, UV irradiation depicts the benefits of being practical, cost-efficient and eco-friendly and it does not result in any toxic and/or waste product generation [127].

Ultraviolet (UV) irradiation has a strong penetration capacity through transparent and/or clear liquids, whereas its penetration capacity through solid materials is very limited, leading to its low decontamination ability for compact food products [128]. The disadvantage of this technique is that granular or opaque items should be presented in the form of a thin layer to achieve decontamination of mycotoxins by UV irradiation, thereby limiting its application at the field level for the degradation of mycotoxins in feed.

By photocatalysis: Recent advancements in the field have revealed that UV-visible irradiation, along with semiconducting photocatalysis, can efficiently degrade aflatoxins in a liquid matrix [129,130]. The most commonly used photocatalyst is titanium oxide (TiO₂), which is highly active under UV irradiation. Sun et al. [129] reported that AFB1 in methanol was efficiently degraded up to 95% within 120 min using this technique, while Xu et al. [130] reported up to 60.4% removal of AFB1 within 120 min through UV-vis irradiation. Similarly, DON degradation can also be achieved through photocatalytic techniques [131]. Although this is an efficient technique, less information is available on the safety and stability of photocatalysts.

By pulsed light: Pulsed light is an emerging non-thermal technique for decontaminating mycotoxins from food and feed. Pulsed light is an FDA-approved technique for efficient and rapid decontamination of different food products. In this advanced technique, short- and high-intensity broadband emission light is produced, which includes ultraviolet, visible, and infrared rays [132]. Moreau et al. [133] reported a 92.7% reduction in AFB1 in water using eight flashes of pulsed light, while Wang et al. [120] reported 75% AFB1 and 39.2% AFB2 reductions from raw rice samples using this technique. Pulsed light technology can also be used for the efficient degradation of OTA, ZEN, and DON [133].

Despite the great outcomes of this technology, further studies are needed to investigate the breakdown products

of pulsed light treatments. The design of cost-effective PL equipment is still needed, which can produce high UV output, so that this emerging technique can be effectively used at the industrial level.

By microwave heating: Electromagnetic waves with wavelengths ranging from 1m to 1 mm and frequencies of 300 MHz to 3000 MHz are used in microwave heating. It is a unique volumetric heating technology that efficiently converts electromagnetic field energy into thermal energy via the polarization effect of electromagnetic radiation^[134]. Microwave heating is extensively used for heating, drying, extraction, and cooling of certain food products. Various studies have reported the use of this technology for non-thermal degradation of different mycotoxins. Flores et al.^[135] studied the effects of microwave heating during alkaline cooling of aflatoxin-contaminated maize grains. They reported 36% AFB1 and 58% AFB2 reduction using microwave heating at 1650 W for 5.5 min.

Microwave manufacturers can customize equipment according to the needs of industrial and food product types. However, the non-uniform distribution of temperature during microwave heating is a challenge that could lead to hot/cold spot formation within food^[136]. The presence of mycotoxins within the cold spot cannot be properly detoxified, whereas hot spots may lead to nutritional degradation of the feed. Further studies in this regard are required to ensure the proper distribution of temperature at all spots so that efficient degradation of mycotoxins can be achieved without disturbing the nutritional values of food and feed products.

By cold plasma: Plasma, often referred to as the fourth state of matter, is a highly energetic ionized gas that usually consists of ions, UV irradiation, electrons, and reactive nitrogen and oxygen species (RNS and ROS)^[137]. Plasma is further categorized as cold or thermal. Additionally, it can be explained by the type of system generating it, such as dielectric barrier discharge (DBD), corona discharge (CD), and radio frequency plasma (RFP) and many others^[138].

This latest technology has been used for the decontamination of different mycotoxins under ambient pressure and temperature conditions^[139]. Aflatoxins were degraded using the DBD N2-plasma technique in hazelnuts, where 70% of AFB1 was detoxified under 1150 W plasma treatment within 12 min^[140]. Similarly, cold plasma technology has been reported to efficiently degrade various mycotoxins including OTA^[141], DON^[142,143], T2^[144], fumonisins^[145] and citrinin^[140]. Cold plasma technology has been proven to be an efficient technique for the decontamination of mycotoxins. However, this technique is still in the early stages of development, and further advanced research is required to optimize various food

products. Furthermore, the negative impact of plasma treatment on the nutritive value of different food materials needs to be addressed before the commercialization of this technology.

Adsorption

Some adsorbing substances have the potential to bind to mycotoxins and remove them from the gastrointestinal tract^[146]. This technique is widely used and well understood, as it has fewer disadvantages than other available methods. The adsorbing agent used for the detoxification of mycotoxins should have some specific properties, including a high adsorption capacity for multiple mycotoxins, low binding efficacy for nutrients, and high safety and palatability^[102].

The most commonly used adsorbents for mycotoxin detoxification are aluminosilicate minerals, including montmorillonites and aluminosilicates^[146]. The adsorption ability depends on the structures of both the binding agent and the targeted mycotoxin^[102]. Some studies have indicated that zeolite and bentonite clay can reduce AFB1 residues in the liver by 87%^[147-150]. Similarly, Bentonite clay can decrease the bioavailability of AFB1 in the rumens of lactating animals^[151,152]. Many studies have revealed that polar toxins, such as AFB1 and FB1, can be easily adsorbed by many aluminosilicates, which become ineffective against different non-polar mycotoxins^[153,154]. Bentonites are considered good agents for the adsorption of mycotoxins because they are bioenvironment-friendly, have high adsorption efficiency, and are generally more economical than other agents^[155-157]. Details of some of the adsorbing agents that are effective against mycotoxins are shown in [Table 5](#).

Chemical Methods

Different chemical agents can be used to efficiently convert mycotoxins to less toxic or non-toxic compounds by destroying their structural makeup. Certain alkalines and ozone treatments are chemical methods that have proven beneficial in this regard^[225,226]. [Fig. 4](#) shows a schematic flow of different chemical methods used for the control of mycotoxicosis.

Alkaline Treatment

Commonly used alkaline chemicals for the control of mycotoxins in moldy feed include sodium carbonate, potassium hydroxide, sodium hydroxide, and ammonia^[226]. Base hydrolysis can open the lactone ring structure of AFB1, and the hydrolyzed product can then be removed by washing with water^[227]. Treatment of various cereals with ammonia and hydroxide salts can remove almost 95% of the mycotoxins^[228]. Although these treatments can nearly reduce the complete concentration of mycotoxins, the possible transformation of mycotoxins to other

Table 5. Details of different *In vitro* and *in vivo* studies reporting the use of different adsorbents (binders) against mycotoxicosis

Mycotoxin	Agent (Adsorbent)	Type of Study (and Efficacy)	Reference	Mycotoxin	Agent (Adsorbent)	Type of Study (and Efficacy)	Reference
Aflatoxins	Bentonite	<i>In Vitro</i>	[158]	Ochratoxins	Activated charcoal	Leghorn Chicks	[199]
	Activated charcoal	<i>In Vitro</i> Study	[159]		HSCAS	Chickens (Partial)	[200]
	Activated charcoal	Goats	[160]		Activated charcoal	<i>In Vitro</i>	[201]
	Activated charcoal	White Rock Chicks	[161]		Activated Charcoal	Pigs	[201]
	Activated charcoal	Broiler Chicks	[162]		HSCAS, Bento	Pigs	[201]
	HSCAS	Chickens	[163]		Cholestyramine	Pigs	[201]
	HSCAS	Broiler Chicks	[164]		Activated carbon	<i>In Vitro</i>	[202]
	Activated charcoal	Chickens	[165]		Diatomaceous earth	<i>In Vitro</i>	[189]
	HSCAS	Chickens	[166]		Bentonite	<i>In Vitro</i>	[195]
	HSCAS	Pigs	[167]		Bentonite	Broiler (Partial)	[203]
	HSCAS	Pigs	[168]	Fumonisin	Activated charcoal	<i>In Vitro</i>	[204]
	Zeolite	<i>In Vitro</i>	[169]		Activated carbon	Rats	[205]
	HSCAS	Pigs	[170]		Bentonite	<i>In Vitro</i>	[206]
	Zeolite	Broiler Chicks	[171]	Zearalenone	Divinylbenzene-styrene polymer	Rats	[207]
	HSCAS	<i>In Vitro</i> Study	[173]		HSCAS	Minks	[208]
	HSCAS	Turkey Poults	[174]		Cholestyramine	<i>In Vitro</i>	[209]
	Activated charcoal	Rabbits (Partial)	[175]		Bentonite	Pigs	[210]
	Zeolite	Domestic Fowls	[176]		Maifanite	Pigs	[211]
	Bentonite, HSCAS	Broilers	[177]		Montmorillonite	Goat	[151]
	HSCAS	Turkey Poults	[178]		Activated charcoal	<i>In Vitro</i>	[212]
	Activated charcoal	Minks	[179]		Cholestyramine	<i>In Vitro</i>	[212]
	HSCAS	Dairy Cows	[180]		Montmorillonite, Magnesium trisilicate, cholestyramine	<i>In Vitro</i>	[185]
	Aluminosilicate	Chicks	[181]		Organophilic montmorillonite	<i>In Vitro</i>	[213]
	HSCAS	Wethers	[179]	DON	Polyvinylpyrrolidone	Pigs	[214]
	HSCAS	Pigs	[182]		Activated carbon	<i>In Vitro</i>	[202]
	Zeolite	Chickens	[181]		Activated carbon	<i>In Vitro</i>	[215]
	Zeolite	Broiler Chicks	[183]	Trichothecenes	HSCAS	Turkey Poults	[174]
	Calcium Bentonite	Pigs	[182]		HSCAS	Chicks	[153]
	HSCAS, Bentonite	Pigs	[184]		HSCAS	Pigs	[216]
	Montmorillonite	<i>In Vitro</i>	[185]		Super-activated charcoal	Turkey Poults	[187]
	Activated Charcoal	Turkey Poults	[186]		HSCAS	Broiler Chicks	[217]
	HSCAS	Turkey Poults	[186]	T-2 toxins	Inorganic clay	Broiler Chicks (Partial)	[188]
	Super-activated charcoal	Broiler Chicks	[187]		Bentonite	Rats	[218]
	Inorganic clay	Broiler Chicks	[188]		Divinylbenzene-styrene polymer	Rats	[218]
	Diatomaceous earth	<i>In Vitro</i>	[189]		Super-activated charcoal	Rats	[219]
	Clinoptilolite	Quail Chicks	[190]		Super-activated charcoal	Rats	[220]
	Aluminosilicate	<i>In Vitro</i>	[191]	Cyclopiazonic Acid	Activated charcoal	Swine	[221]
	HSCAS, bentonite	Rats	[192]		Acidic clay, neutral clay, clinoptilolite	<i>In Vitro</i>	[222]
	HSCAS	<i>In Vitro</i>	[193]	Ergotamine	Acidic clay, neutral clay, clinoptilolite	Broilers	[222]
	HSCAS	Broilers	[193]		Montmorillonite	<i>In Vitro</i>	[223]
	Zeolite	Broiler Chicks	[194]	Patulin	Activated charcoal	<i>In Vitro</i>	[224]
	Bentonite	<i>In Vitro</i> Study	[195]				
	Bentonite	Broiler Chicks	[196]				
	Alumino silicate	<i>In Vitro</i>	[197]				
	Sodium bentonite	Poultry Chicks	[147]				
	Bentonite clay	Broilers	[149]				
	Zeolite	Poultry Chicks	[198]				
	Organo-clay composites	Broilers	[152]				

forms, such as masked mycotoxins, along with harmful side effects on the environment and food (changes in nutritional quality, texture, or flavor) are some of the disadvantages that make this method less desirable at larger scales [225].

Ozone Treatment

Oxidizing agents, such as sodium and ozone, play a role in detoxifying mycotoxins by modulating the structures of these secondary metabolites [229,230]. Ozone can degrade the

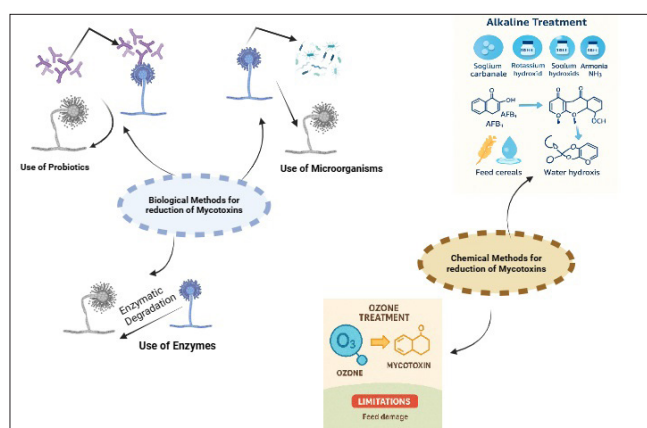


Fig 4. Flow diagram showing different chemical and biological methods used for the control of mycotoxicosis

FB1, AFs, ZEN and DON in various feeds of animals [231-234]. AFs can be reduced in corn and peanuts through ozone treatment [235-237]. Similarly, DON can be decomposed in corn and wheat using ozone [216,238-240]. Similarly, zearalenone can also be decomposed by treatment with varying concentrations of ozone [241]. Mycotoxins can also be degraded using other oxidizing agents, such as sodium hypochlorite [242,243]. However, the use of oxidizing agents for the detoxification of mycotoxins has some limitations, as these agents can change the physical and chemical composition of the feed, such as protein denaturation and lipid oxidation. Another disadvantage of using oxidizing agents is that they produce harmful chemicals during mycotoxin detoxification, making this method unsuitable for commercial use [230,235,236].

Biological Methods

Many physical and chemical techniques used to reduce the concentration of mycotoxins in feed have various limitations, as discussed above. However, the use of different biological methods for mycotoxin detoxification is necessary, as these methods have shown promising results in various studies [243,244]. Fig. 4 shows a schematic flow of different biological methods used for the control of mycotoxicosis.

Microorganisms with Detoxification Activities

The use of different probiotics in animals promotes their development and growth and also improves the host's resistance against different diseases and metabolic disorders [245-249]. Certain beneficial microorganisms belonging to the category of probiotics are extensively used for the control of mycotoxicosis. These microorganisms play a significant role in maintaining normal bacterial balance within the GIT and are often used to tackle certain pathological abnormalities, including fungal modifications [250,251]. These beneficial organisms can bind mycotoxins and eliminate them from the gastrointestinal tract [252]. In addition, they also possess

Table 6. Details of different In vitro studies reporting the biological degradation/detoxification of certain mycotoxins

Mycotoxin	Biological Strain/Type	Detoxification Rate [18]	Reference
AFB1	<i>Bacillus subtilis</i>	93.00%	[257]
	<i>Pseudomonas putida</i>	92.00%	[258]
	<i>Bacillus licheniformis</i>	95.70%	[259]
	<i>Bacillus shackletonii</i>	93.10%	[260]
	<i>Bacillus subtilis</i>	66.20%	[13]
	<i>Bacillus velezensis</i>	92.50%	[261]
	<i>Escherichia coli</i>	93.70%	[262]
	<i>S. cerevisiae</i>	68.00%	[244]
	<i>Aspergillus niger</i> RAF105	87.59%	[263]
	<i>Stenotrophomonas</i> sDOI:	99.00%	[264]
DON	<i>Aspergillus niger</i> FS11	97.64%	[265]
	Bacterial strain	100%	[266]
	Bacterial isolates	100.00%	[267]
	<i>Aspergillus</i> (NJA-1)	98.40%	[268]
	<i>Eggerthella</i> sDOI:	100.00%	[269]
	<i>Pseudomonas</i> sDOI: and <i>Lysobacter</i> sDOI:	100.00%	[270]
	<i>Devosia insulae</i>	85.00%	[271]
	Strain E3-39	100.00%	[272]
	<i>Bacterial consortium</i> C20	73.29%	[273]
	<i>Bacillus subtilis</i>	83.10%	[274]
ZEN	<i>Bacillus pumilus</i>	96.70%	[275]
	<i>Bacillus natto/ pumilus</i>	97.70%	[276]
	<i>Bacillus subtilis</i>	88.00%	[272]
FB1	<i>Bacillus</i> spDOI:	22%-50%	[277]
	<i>Saccharomyces cerevisiae</i>	100.00%	[278]
	Bacterial consortium	89.65%	[279]
	Strain NCB/ Bacterial consortium	100.00%	[280]

the ability to biologically degrade mycotoxins, ultimately converting them into less toxic metabolites, thereby protecting animals/chicks from mycotoxin-associated lethal damage [253]. Microorganisms, including various species of *Lactobacillus*, *Lactococcus*, *Streptococcus* and *Bifidobacterium* possess antimutagenic, antifungal, and immunomodulatory effects in this regard [254-256]. Many studies have been conducted in this regard, and Table 6 and Table 7 summarize some probiotics associated with different types of mycotoxins *in vitro* and *in vivo*.

Biodegradation/Biotransformation by Degrading Enzymes

In addition to the use of different bacteria, fungi, and their byproducts for the degradation of mycotoxins, the use of certain biological enzymes is also gaining popularity.

Table 7. Details of different in vivo studies reporting biological degradation/transformation of certain mycotoxins

Mycotoxin	Biological Specie Used	Animal Model Used	Reference
Aflatoxins	<i>Sacchromyces cerevisiae</i>	Broilers	[281]
	Esterified glucomannan	Cows	[282]
	Manno-oligosaccharides	Wistar rats	[283]
	<i>Nocardia corynebacteroides</i>	Chicks	[284]
	Modified yeast extract	Cows	[285]
	Dried yeast culture	Sheep	[286]
	<i>Lactobacillus casei Shirota</i>	Wistar rats	[287]
	Modified yeast cell wall	Sheep	[288]
	<i>Lactobacillus rhamnosus</i> GAF01	Mice	[289]
	<i>Lactobacillus plantarum</i> MON03	Mice	[290]
	Yeast cell wall	Broilers	[291]
	<i>Pichia kudriavzevii</i>	Broilers	[292]
	<i>Lactobacillus plantarum</i>	Broilers	[293]
	Esterified glucomannan	Broilers	[293]
Ochratoxins	Yeast cell wall preparation (YCW)	Rats	[294]
	<i>Saccharomyces cerevisiae</i>	Ross male broilers	[295]
	<i>Lactobacillus paracasei</i>	Ross Broilers	[296]
	<i>Saccharomyces cerevisiae</i>	Ross Broilers	[296]
	Yeast sludge	Broilers	[297]
	<i>Lactobacillus kunkeei</i>	Male Rats	[298]
	<i>Lactobacillus plantrum</i>	Male Rats	[298]
T-2	<i>Saccharomyces cerevisiae</i> lysate (Masclaux-Daubresse, #1128)	Laying hens	[299]

These enzymes have been isolated from a wide range of microorganisms. These enzymes are also obtained from certain fungal species, but the isolation processes involving crushing of fungal mycelia are quite complicated, and their use on a larger scale is restricted. However, the use of enzymes isolated from different bacteria is promising for mycotoxin biodegradation [260]. Table 8 shows the details of different degrading enzymes, along with the types of mycotoxins against which their efficacy has been reported.

Table 8. Different experimental studies reporting the use of various degrading enzymes for the detoxification of mycotoxins

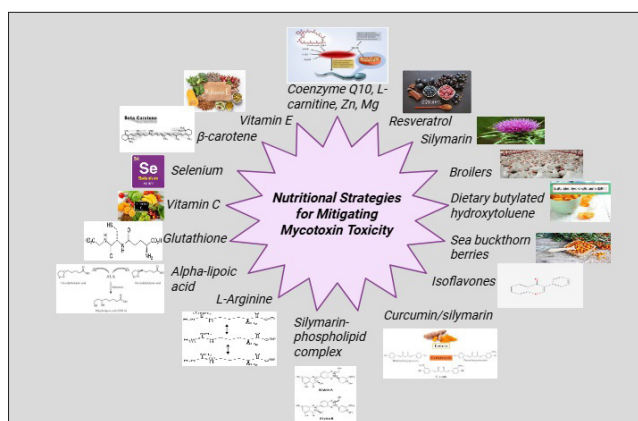
Mycotoxin	Degrading Enzyme	Source	Reference
AFB ₁	<i>Trametes versicolor</i> Laccase enzyme	<i>Aspergillus niger</i>	[300]
	F42H2-dependent reductase enzyme	<i>Mycobacterium smegmatis</i>	[301]
	Aflatoxin-Oxidase	<i>Aspergillus tabescens</i>	[302]
	Myxobacteria aflatoxin degradation enzyme	<i>Myxococcus fulvus</i>	[303]
	Manganese peroxidase	<i>Phanerochaete sordida</i> YK 624	[304]
	Manganese peroxidase	<i>Pleurotus ostreatus</i>	[305]
	<i>Bacillus</i> aflatoxin-degrading enzyme	<i>Bacillus shackletonii</i> L7	[260]
	Cytochrome P450 system	<i>Sphingomonas</i> sDOI: strain KSM1	[306]
DON	Peroxidase	Extract of rice bran	[307]
	Aldo-keto reductase DepA/DepB	<i>Devosia mutans</i> 17-2-E-8	[308]
	Quinone-dependent dehydrogenase, NADPH-dependent aldo/ keto reductases	<i>Devosia</i> strain D6-9	[309]
	Manganese peroxidase and Lignin peroxidase	<i>Flammulina velutipes</i>	[310]
	ZEN-specific lactonohydrolase	<i>Penicillium canescens</i> strain PCA-10	[311]
	Recombinant fusion enzyme (ZHDCP)	Zearalenone hydrolase (ZHD) and carboxypeptidase (CP)	[312]
FB ₁	<i>Fumonisin carboxylesterase</i> FumD	<i>Sphingopyxis</i> sDOI: MTA144	[313]

Nutritional Strategies

Certain nutritional strategies have also been adapted to nullify the adverse effects of mycotoxins in animals. Similarly, the use of certain plants and their extracts has been practiced since ancient times for the rectification of different ailments in both humans and animals [314-317]. These plants contain a variety of flavonoids, alkaloids, essential oils, and tannins, which enhance the body's defense system by mitigating several pathological and management issues in animals and humans [318,319]. The mycotoxin detoxification system can be modulated by nutritional measures. In animals, detoxification systems include ketoreductase, CYP450s and α -glutathione transferase, which can efficiently degrade mycotoxins [239]. Therefore, nutritional regulators may enhance the detoxification potential of the body [320]. Cysteine, glycine, and glutamate synthesize glutathione and help detoxify mycotoxins by forming glutathione. The addition of

Table 9. Details of different experimental studies showing different nutritional strategies against the toxic effects of mycotoxins

Mycotoxins	Nutritional strategy	Animal Model	Reference
AFB1	β -carotene, canthaxanthin, lycopene	Rats	[328]
	Dietary butylated hydroxytoluene	White Turkey poults	[329]
	Vitamin C	<i>Labeo rohita</i>	[330]
	Silymarin-phospholipid complex	Broiler	[331]
	Vitamin C & E	Rabbits	[332]
	Sea buckthorn berries	Broiler	[333]
	Alpha-lipoic acid	Broilers	[334]
	Resveratrol	Broilers	[335]
	Curcumin, quercetin, resveratrol	<i>In vitro</i>	[336]
	Selenium	Cobb male broilers	[280]
	Curcumin	Chickens	[337]
	Vitamin E	Leghorn cockerels	[58]
DON	Vitamin E & C, selenium	Wistar rats	[338]
	L-Arginine	Pig	[339]
	Selenium	<i>In vitro</i>	[276]
FB1	Isoflavones	Rats	[340]
	Vitamin E	rabbits	[341]
	Curcumin/silymarin	<i>In vitro</i>	[342]
OTA	Vitamin C	Mice	[343]
	Vitamin E & C	Broilers	[344]
	Retinol, ascorbic acid, α -tocopherol	Mice	[345]
	Coenzyme Q10, L-carnitine, Zn, Mg	Mice	[346]
	Vitamin C	Nile Tilapia	[347]
	L-carnitine	Leghorn cockerels	[66]
	Silymarin	Leghorn cockerels	[67]
	Curcumin	<i>In vitro</i>	[342]
	Ducks	Curcumin	[348]
T-2 toxin	Vitamin C & E, selenium	Wistar rats	[338]
	Vitamin E & C	Broiler	[344]
	Broilers	Lycopene	[349]
Zearalenone	Retinol, ascorbic acid, α -tocopherol	Mice	[345]
	Vitamin E	<i>In vitro</i>	[350]
	Vitamin C	Weaning piglets	[351]
	Silymarin	Rats	[352]
	Vitamin C	piglets	[353]

**Fig 5.** Schematic flow showing different nutritional strategies used for the control of mycotoxicosis

specific nutrients and prebiotics to mitigate the damaging effects of pathogens and toxins is another benefit [321-324]. Cytotoxicity occurs due to oxidants produced within the body by mycotoxins, and adding antioxidants can improve the ability of organisms to fight against mycotoxin toxicity. In this regard, selenium and vitamins (C and E) have proven beneficial as they act as superoxide anion scavengers [325-327]. Table 9 describes some nutritional strategies reported in this regard while Fig. 5 shows the schematic flow of use of different nutritional strategies used for the control of mycotoxicosis.

CONCLUSION

The presence of mycotoxins in feed is an unavoidable problem worldwide. This review summarizes a number of strategies to reduce mycotoxicosis, including physical methods (separation, washing, adsorption, heating, and irradiation), chemical strategies (oxidizing agents and basis), biological methods (enzymes and probiotics), and nutritional regulation strategies. Each of these approaches can be used practically, along with its own advantages and disadvantages. However, with the growing awareness of environmental protection, as well as feed and food safety, there is a growing expectation for more green and innovative technologies to control mycotoxin contamination.

FUTURE PERSPECTIVES

More advanced techniques should be adapted for the control of mycotoxicosis in poultry. As there is a paradigm shift to the use of natural ingredients for the treatment globally, measures should be taken for the large-scale implementation of biological strategies to avoid physical and chemical strategies-associated disadvantages at farm levels. Widescale commercialization should be done to mitigate mycotoxicosis at farm (both dairy and poultry) levels.

DECLARATIONS

Availability of Data and Materials: All the generated data are included in the manuscript.

Acknowledgements: None

Competing Interests: The authors declared that there is no competing interest.

Declaration of Generative Artificial Intelligence (AI): The article and/or tables and figures were not written/created by AI and AI assisted technologies.

Author Contributions: AK, ZA, and AA: Conceptualization, methodology, and data curation; MKS and RZA: Data extraction and editing. MUI: Editing; MUR and BM: Revised and proof-read. All authors read and approved the final manuscript.

REFERENCES

1. Gurikar C, Shivaprasad D, Sabillón L, Gowda N N, Siliveru K: Impact of mycotoxins and their metabolites associated with food grains. *Grain Oil Sci Technol*, 6 (1): 1-9, 2023. DOI: 10.1016/j.gaost.2022.10.001
2. Furian AF, Figuera MR, Royes LFF, Oliveira MS: Recent advances in assessing the effects of mycotoxins using animal models. *Cur Opin Food Sci*, 47:100874, 2022. DOI: 10.1016/j.cofs.2022.100874
3. Fumagalli F, Ottoboni M, Pinotti L, Cheli F: Integrated mycotoxin management system in the feed supply chain: Innovative approaches. *Toxins (Basel)*, 13 (8): 572, 2021. DOI: 10.3390/toxins13080572
4. Luo S, Du H, Kebede H, Liu Y, Xing F: Contamination status of major mycotoxins in agricultural product and food stuff in Europe. *Food Cont*, 127:108120, 2021. DOI: 10.1016/j.foodcont.2021.108120
5. Marlière CA, Pimenta RCJ, Cunha AC: Fumonisin as a risk factor to esophageal cancer: A review. *Appl Cancer Res*, 29, 102-105, 2009.
6. Benkerroum N: Aflatoxins: Producing-molds, structure, health issues and incidence in Southeast Asian and Sub-Saharan African countries. *Int J Environ Res Public Health*, 17 (4):1215, 2020. DOI: 10.3390/ijerph17041215
7. Wang M, Li L, Hou C, Guo X, Fu H: Building and health: Mapping the knowledge development of sick building syndrome. *Buildings*, 12:287, 2022. DOI: 10.3390/buildings12030287
8. Goudarzi G, Reshadatian N: The study of effective factors in sick building syndrome related to fungi and its control methods. *Res Eng*, 23:102703, 2024. DOI: 10.1016/j.rineng.2024.102703
9. Soriano JM, Rubini A, Morales-Suarez-Varela M, Merino-Torres JF, Silvestre D: Aflatoxins in organs and biological samples from children affected by kwashiorkor, marasmus and marasmic-kwashiorkor: A scoping review. *Toxicon*, 185, 174-183, 2020. DOI: 10.1016/j.toxicon.2020.07.010
10. Stoyanov GS, Kobakova I, Petkova L, Dzhakov DL, Popov H: Balkan endemic nephropathy: An autopsy case report. *Cureus*, 13 (1):e12415, 2021 DOI: 10.7759/cureus.12415
11. Sadashivanavar V, Madalageri M, Pai KSR, Sharma H, Halagali P, Seenivasan R, Tippavajhala VK, Somanna P, Noman AI: Cardiovascular impacts of foodborne toxins. In, *Physiological Perspectives on Food Safety: Exploring the Intersection of Health and Nutrition*. 351-375, Cham: Springer Nature Switzerland, 2025.
12. Lumsangkul C, Tso KH, Fan YK, Chiang HI, Ju JC: Mycotoxin fumonisin B1 interferes sphingolipid metabolisms and neural tube closure during early embryogenesis in brown tsaiya ducks. *Toxins*, 13 (11):743, 2021. DOI: 10.3390/toxins13110743
13. Cai P, Zheng H, She J, Feng N, Zou H, Gu J, Yuan Y, Liu X, Liu Z, Bian J: Molecular mechanism of aflatoxin-induced hepatocellular carcinoma derived from a bioinformatics analysis. *Toxins*, 12:203, 2020. DOI: 10.3390/toxins12030203
14. Jagels A, Stephan F, Ernst S, Lindemann V, Cramer B, Hübner F, Humpf HU: Artificial vs natural Stachybotrys infestation - Comparison of mycotoxin production on various building materials. *Indoor Air*, 30 (6): 1268-1282, 2020. DOI: 10.1111/ina.12705
15. Leslie JF, Moretti A, Mesterházy Á, Ameye M, Audenaert K, Singh PK, Richard-Forget F, Chulze SN, Ponte EMD, Chala A, Battilani P: Key global actions for mycotoxin management in wheat and other small grains. *Toxins*, 13 (10):725, 2021. DOI: 10.3390/toxins13100725
16. Khattoon A, Khan MZ, Abidin Z, Saleemi MK, Oguz H, Gul S T, Abbas RZ, Ali A, Bhatti SA: Aflatoxin B1-associated oxidative stress along with toxicopathological and immunological alterations is efficiently counteracted by dietary supplementation of distillery yeast sludge in broilers. *Mycotox Res*, 40 (4): 615-629, 2024. DOI: 10.1007/s12550-024-00549-y
17. Sarwar MK, Ijaz S, Javed N, Akbar N: Molecular and analytical approaches based characterization of aflatoxins producing *Aspergillus* species affecting groundnut. *Pak J Agric Sci*, 61 (3): 931-940, 2024. DOI: 10.3390/toxins14050307
18. Shabeer S, Asad S, Jamal A, Ali A: Aflatoxin contamination, its impact and management strategies: An updated review. *Toxins*, 14 (5):307, 2022. DOI: 10.3390/toxins14050307
19. Abidin Z, Khattoon A, Numan MJ: Mycotoxins in broilers: Pathological alterations induced by aflatoxins and ochratoxins, diagnosis and determination, treatment and control of mycotoxicosis. *World Poult Sci J*, 67 (3): 485-496, 2011. DOI: 10.1017/S0043933911000535
20. Cui R, Pan A, Wang T, Liang Y, Yu HF: Aflatoxin B1 in animals: metabolism and immunotoxicity. *Pak Vet J*, 2025 (Early Online). DOI: 10.29261/pakvetj/2025.207
21. El-Hamaky AM, Hassan AA, Wahba AK, El-Mosalamy MM: Influence of copper and zinc nanoparticles on genotyping characterizations of multi-drug resistance genes for some calf pathogens. *Int J Vet Sci*, 12: 309-317, 2023. DOI: 10.47278/journal.ijvs/2022.195
22. Khashan SA, Khashan BA, Thalij KM, Konca Y: The effect of nano-chitosan in reducing the toxicity of aflatoxin B1 and fumonisin B1 in broilers. *Pak Vet J*, 45 (1): 268-276, 2025. DOI: 10.29261/pakvetj/2025.116
23. Khan MA, Khan IA, Tahir AH, Shahid MA, Nazish N, Zafar MA, Bhatti SA, Pasha RH, Abbas Y, Sadiq S, Jamil B: Isolation and identification of deleterious fungi associated with stored grains and cattle feedstuff of Potohar region of Pakistan. *Pak Vet J*, 44 (3): 861-867, 2024. DOI: 10.29261/pakvetj/2024.189
24. Khattoon A, Abidin Z: Mycotoxicosis - diagnosis, prevention and control: Past practices and future perspectives. *Toxin Rev*, 39, 99-114, 2020. DOI: 10.1080/15569543.2018.1485701
25. Mengesha G, Bekele T, Ashagrie H, Woldegiorgis AZ: Level of aflatoxins in dairy feeds, poultry feeds, and feed ingredients produced by feed factories in Addis Ababa, Ethiopia. *Mycotox Res*, 40: 309-318, 2024. DOI: 10.1007/s12550-024-00531-8
26. Aboagye-Nuamah F, Kwoseh CK, Maier DE: Toxigenic mycoflora, aflatoxin and fumonisin contamination of poultry feeds in Ghana. *Toxicon*, 198, 164-170, 2021. DOI: 10.1016/j.toxicon.2021.05.006
27. Meijer N, Kleter G, de Nijs M, Rau ML, Derckx R, van der Fels-Klerx HJ: The aflatoxin situation in Africa: Systematic literature review. *Comp Rev Food Sci Food Saf*, 20, 2286-2304, 2021. DOI: 10.1111/1541-4337.12731
28. Priya MS, Jagadeeswaran A, Natarajan A: Detection of aflatoxin B1 (AFB1) in common ingredients of poultry and broiler feed under different seasons. *J Livest Sci*, 14, 163-168, 2023. DOI: 10.33259/JLivestSci.2023.163-168
29. Negash D: Animal feed safety: Cases and approaches to identify the contaminants and toxins. *Safety*, 4, 1-8, 2020.
30. Abidin Z, Khattoon A, Numan M: Mycotoxins in broilers: Pathological alterations induced by aflatoxins and ochratoxins, diagnosis and determination, treatment and control of mycotoxicosis. *World Poult Sci J*, 67 (3): 485-496, 2011. DOI: 10.1017/S0043933911000535
31. Olatoye O, Aiyedun J, Oludairo O: Incidence of aflatoxin B1 in commercial poultry feed and tissues of broiler chickens in ibadan, Nigeria. *Sahel J Vet Sci*, 17 (2): 13-18, 2020
32. Kassaw TS, Megerssa YC, Woldemariam FT: Occurrence of aflatoxins in poultry feed in selected chicken rearing villages of bishoftu Ethiopia. *Vet Med (Auckl)*, 13: 277-286, 2022. DOI: 10.2147/VMRR.S384148
33. Bintvihok A, Kositcharoenkul S: Effect of dietary calcium propionate on performance, hepatic enzyme activities and aflatoxin residues in broilers fed a diet containing low levels of aflatoxin B1. *Toxicon*, 47 (1): 41-6, 2006. DOI: 10.1016/j.toxicon.2005.09.009
34. Denli M, Blandon JC, Guynot ME, Salado S, Perez JF: Effects of dietary

- AflaDetox on performance, serum biochemistry, histopathological changes, and aflatoxin residues in broilers exposed to aflatoxin B (1). *Poult Sci*, 88 (7): 1444-1451, 2009. DOI: 10.3382/ps.2008-00341
35. Hussain Z, Khan MZ, Khan A, Javed I, Saleemi MK, Mahmood S, Asi MR: Residues of aflatoxin B1 in broiler meat: Effect of age and dietary aflatoxin B1 levels. *Food Chem Toxicol*, 48 (12): 3304-3307, 2010. DOI: 10.1016/j.fct.2010.08.016
36. Khan MZ, Hameed MR, Hussain T, Khan A, Javed I, Ahmad I, Hussain A, Saleemi MK, Islam NU: Aflatoxin residues in tissues of healthy and sick broiler birds at market age in Pakistan: A one year study. *Pak Vet J*, 33 (4): 423-427, 2013.
37. Fowler J, Li W, Bailey C: Effects of a calcium bentonite clay in diets containing aflatoxin when measuring liver residues of aflatoxin B1 in starter broiler chicks. *Toxins*, 7 (9): 3455-3464, 2015. DOI: 10.3390/toxins7093455
38. Aljazzar A, El-Ghareeb WR, Darwish WS, Abdel-Raheem SM, Ibrahim AM: Content of total aflatoxin, lead, and cadmium in the bovine meat and edible offal: Study of their human dietary intake, health risk assessment, and molecular biomarkers. *Environ Sci Poll Res*, 28 (43): 61225-61234, 2021. DOI: 10.1007/s11356-021-12641-2
39. Milicevic D, Jovanovic M, Matekalo-Sverak V, Radicevic T, Petrovic MM, Lilic S: A survey of spontaneous occurrence of ochratoxin A residues in chicken tissues and concurrence with histopathological changes in liver and kidneys. *J Environ Sci Health C Environ Carcinog Ecotoxicol Rev*, 29 (2): 159-175, 2011. DOI: 10.1080/10590501.2011.577687
40. Pozzo L, Cavallarin L, Antoniazzi S, Guerre P, Biasibetti E, Capucchio MT, Schiavone A: Feeding a diet contaminated with ochratoxin A for broiler chickens at the maximum level recommended by the EU for poultry feeds (0.1 mg/kg). 2. Effects on meat quality, oxidative stress, residues and histological traits. *J Anim Physiol Anim Nutr*, 97, 23-31, 2013. DOI: 10.1111/jpn.12051
41. Qu D, Huang X, Han J, Man N: Efficacy of mixed adsorbent in ameliorating ochratoxicosis in broilers fed ochratoxin A contaminated diets. *It J Anim Sci*, 16 (4): 573-579, 2017. DOI: 10.1080/1828051X.2017.1302822
42. Hussein MA, Gherbawy Y: Genotypic identification of ochratoxigenic *Aspergilli* that contaminated beef luncheon and their protease activity. *Rendiconti Lincei. Scienze Fisiche e Naturali*, 30 (4): 767-773, 2019. DOI: 10.1007/s12210-019-00845-1
43. Yue S, Li X, Qian J, Du J, Liu X, Xu H, Liu H, Chen X: Impact of enzymatic hydrolyzed protein feeding on rumen microbial population, blood metabolites and performance parameters of lactating dairy cows. *Pak Vet J*, 43 (4): 804-808, 2023. DOI: 10.29261/pakvetj/2023.081
44. Agustin F, Pazla R, Jamarun N, Suryadi H: Exploring the impact of processed cassava peel on microbial dynamics and *in vitro* nutrient digestibility in ruminant diets. *Int J Vet Sci*, 13 (4): 463-470, 2024. DOI: 10.47278/journal.ijvs/2023.119
45. Abidin Z, Khatoon A: Ruminal microflora, mycotoxin inactivation by ruminal microflora and conditions favouring mycotoxicosis in ruminants: A review. *Int J Vet Sci*, 1, 36-43, 2012.
46. Min L, Fink-Gremmels J, Li D, Tong X, Tang J, Nan X, Yu Z, Chen W, Wang G: An overview of aflatoxin B1 biotransformation and aflatoxin M1 secretion in lactating dairy cows. *Anim Nutr*, 7 (1): 42-48, 2021. DOI: 10.1016/j.aninu.2020.11.002
47. Jiang, Y, Ogunade IM, Vyas D, Adesogan AT: Aflatoxin in dairy cows: toxicity, occurrence in feedstuffs and milk and dietary mitigation strategies. *Toxins*, 13:283, 2021
48. Keyl AC, Booth AN: Aflatoxin effects in livestock. *J Am Oil Chem Soc*, 48 (10): 599-604, 1971. DOI: 10.1007/BF02544571
49. Pier A, Richard J, Thurston J: Effects of mycotoxins on immunity and resistance of animals. *Nat Toxins*, 691-699, 1980. DOI: 10.1016/B978-0-08-024952-0.50087-9
50. Richard JL, Pier AC, Stubblefield RD, Shotwell OL, Lyon RL, Cutlip RC: Effect of feeding corn naturally contaminated with aflatoxin on feed efficiency, on physiologic, immunologic, and pathologic changes, and on tissue residues in steers. *Am J Vet Res*, 44 (7): 1294-1299, 1983.
51. Helferich WG, Baldwin RL, Hsieh DP: [14C]-aflatoxin B1 metabolism in lactating goats and rats. *J Anim Sci*, 62 (3): 697-705, 1986. DOI: 10.2527/jas1986.623697x
52. D'Angelo A, Bellino C, Alborali GL, Biancardi A, Borrelli A, Capucchio MT, Catalano D, Dellafrera G, Maurella C, Cagnasso A: Neurological signs associated with aflatoxicosis in Piedmontese calves. *Vet Rec*, 160 (20): 698-700, 2007. DOI: 10.1136/vr.160.20.698
53. Fernandez A, Hernandez M, Verde MT, Sanz M: Effect of aflatoxin on performance, hematology, and clinical immunology in lambs. *Can J Vet Res*, 64 (1): 53-58, 2000.
54. Gowda N, Suganthi R, Malathi V, Raghavendra A: Efficacy of heat treatment and sun drying of aflatoxin-contaminated feed for reducing the harmful biological effects in sheep. *Anim Feed Sci Technol*, 133 (1-2): 167-175, 2007. DOI: 10.1016/j.anifeedsci.2006.08.009
55. Tripathi M, Mondal D, Karim S: Growth, haematology, blood constituents and immunological status of lambs fed graded levels of animal feed grade damaged wheat as substitute of maize. *J Anim Physiol Anim Nutr*, 92 (1): 75-85, 2008. DOI: 10.1111/j.1439-0396.2007.00712.x
56. Masoero F, Moschini M, Gallo A, Diaz D: *In vivo* release of aflatoxin B1 bound to different sequestering agents in dairy cows. *It J Anim Sci*, 6 (Suppl.-1): 315-317, 2007. DOI: 10.4081/ijas.2007.1s.315
57. Guo H, Wang P, Liu C, Chang J, Yin Q, Wang L, Jin S, Zhu Q, Lu F: Compound mycotoxin detoxifier alleviating aflatoxin B(1) toxic effects on broiler growth performance, organ damage and gut microbiota. *Poult Sci*, 102 (3):102434, 2023. DOI: 10.1016/j.psj.2022.102434
58. Saleemi MK, Raza A, Khatoon A, Zubair M, Murtaza B, Jamil M, Imran M, Muhammad F, Zubair K, Bhatti SA: Toxic effects of aflatoxin B1 on hematobiochemical and histopathological parameters of juvenile white Leghorn male birds and their amelioration with mitamin E and *Moringa oleifera*. *Pak Vet J*, 43 (3): 405-411, 2023. DOI: 10.29261/pakvetj/2023.053
59. Khatoon A, Amin A, Majeed S, Gul ST, Arshad MI, Saleemi MK, Ali A, Abbas RZ, Bhatti SA: Dietary *Chlorella vulgaris* mitigates aflatoxin B1 toxicity in broiler chicken: Toxicopathological, hematobiochemical and immunological perspectives. *Toxicon*, 251:108127, 2024. DOI: 10.1016/j.toxicon.2024.108127
60. Zentai A, Jozwiak A, Süth M, Farkas Z: Carry-over of aflatoxin B1 from feed to cow milk - A review. *Toxins*, 15:195, 2023. DOI: 10.3390/toxins15030195
61. Alnuimy A: Toxopathological and histopathological effects of aflatoxins. *Mag Al-Kufa Univ Biol*, 16, 25-43, 2024. DOI: 10.36320/ajb/v16.i1.13241
62. Muaz K, Riaz M, Oliveira CAFD, Akhtar S, Ali SW, Nadeem H, Park S, Balasubramanian B: Aflatoxin M1 in milk and dairy products: Global occurrence and potential decontamination strategies. *Toxin Rev*, 41, 588-605, 2022. DOI: 10.1080/15569543.2021.1873387
63. Abedullah A, Kouser S, Badar H, Ibrahim MNM: Consumer demand for aflatoxin-free raw milk in Pakistan. *J Anim Plant Sci*, 33, 125-134, 2023. DOI: 10.36899/JAPS.2023.1.0602
64. Bervis N, Loran S, Juan T, Carramiñana JJ, Herrera A, Arino A, Herrera M: Field monitoring of aflatoxins in feed and milk of high-yielding dairy cows under two feeding systems. *Toxins*, 13:201, 2021. DOI: 10.3390/toxins13030201
65. Abidin Z, Khan MZ, Khatoon A, Saleemi MK, Khan A: Protective effects of L-carnitine upon toxicopathological alterations induced by ochratoxin A in white Leghorn cockerels. *Toxin Rev*, 35 (3-4): 157-164, 2016. DOI: 10.1080/15569543.2016.1219374
66. Abidin Z, Khan MZ, Khatoon A, Saleemi MK, Khan A, Javed I: Ameliorative effects of L-carnitine and vitamin E (alpha-tocopherol) on hematological and serum biochemical parameters in white Leghorn cockerels given ochratoxin A contaminated feed. *Br Poult Sci*, 54 (4): 471-477, 2013. DOI: 10.1080/00071668.2013.796509
67. Khatoon A, Khan MZ, Khan A, Saleemi MK, Javed I: Amelioration of ochratoxin A-induced immunotoxic effects by silymarin and vitamin E in white Leghorn cockerels. *J Immunotoxicol*, 10 (1): 25-31, 2013. DOI: 10.3109/1547691X.2012.686533
68. Khatoon A, Khan MZ, Abidin Z, Khan A, Saleemi M: Mitigation potential of distillery sludge against ochratoxin A induced immunological alterations in broiler chicks. *World Mycotox J*, 10 (3): 255-262, 2017.

69. Khatoon A, Abidin Z: An extensive review of experimental ochratoxycosis in poultry: I. Growth and production parameters along with histopathological alterations. *World Poult Sci J*, 74 (4): 627-646, 2018. DOI: 10.1017/S0043933918000685
70. Abidin Z, Khatoon A, Arooj N, Hussain S, Ali S, Manzoor AW, Saleemi MK: Estimation of ochratoxin A in poultry feed and its ingredients with special reference to temperature conditions. *Br Poult Sci*, 58 (3): 251-255, 2017. DOI: 10.1080/00071668.2017.1293797
71. Longobardi C, Ferrara G, Andretta E, Montagnaro S, Damiano S, Ciarcia R: Ochratoxin A and kidney oxidative stress: The role of nutraceuticals in veterinary medicine - A review. *Toxins*, 14:398, 2022. DOI: 10.3390/toxins14060398
72. Xu H, Wang L, Sun J, Wang L, Guo H, Ye Y, Sun X: Microbial detoxification of mycotoxins in food and feed. *Crit Rev Food Sci Nutr*, 62, 4951-4969, 2022. DOI: 10.1080/10408398.2021.1879730
73. Khatoon A, Khan MZ, Khan A, Javed I: Toxicopathological and serum biochemical alterations induced by ochratoxin A in broiler chicks and their amelioration by locally available bentonite clay. *Pak J Agric Sci*, 53 (4): 977-984, 2016.
74. Khatoon A, Nawaz MY, Mehboob G, Saleemi MK, Gul ST, Abbas RZ, Ijaz MU, Murtaza B, Bhatti SA, Abidin Z: Unraveling the combined deleterious effects of ochratoxin A and atrazine upon broiler's health: Toxicopathological, serum biochemical and immunological perspectives. *Toxicon*, 236:107327, 2023. DOI: 10.1016/j.toxicon.2023.107327
75. Meng J, Li R, Huang Q, Guo D, Fan K, Zhang J, Zhu X, Wang M, Chen X, Nie D, Cao C: Survey and toxigenic abilities of *Aspergillus*, *Fusarium*, and *Alternaria* fungi from wheat and paddy grains in Shanghai, China. *Front Plant Sci*, 14:1202738, 2023. DOI: 10.3389/fpls.2023.1202738
76. Chen J, Wen J, Tang Y, Shi J, Mu G, Yan R, Cai J, Long M: Research progress on fumonisin B1 contamination and toxicity: A review. *Molecules*, 26 (17):5238, 2021. DOI: 10.3390/molecules26175238
77. Mostrom MS, Jacobsen BJ: Ruminant mycotoxicosis: An update. *Vet Clin North Am Food Anim Pract*, 36 (3): 745-774, 2020. DOI: 10.1016/j.cvfa.2020.08.011
78. Loh ZH, Ouwerkerk D, Klieve AV, Hungerford NL, Fletcher MT: Toxin degradation by rumen microorganisms: A Review. *Toxins (Basel)*. 12 (10):664, 2020. DOI: 10.3390/toxins12100664
79. Guerre P, Gilleron C, Matard-Mann M, Nyvall Collen P: Targeted sphingolipid analysis in heart, gizzard, and breast muscle in chickens reveals possible new target organs of fumonisins. *Toxins*, 14:828, 2022. DOI: 10.3390/toxins14120828
80. Guerre P, Travel A, Tardieu D: Targeted analysis of sphingolipids in turkeys fed fusariotoxins: First evidence of key changes that could help explain their relative resistance to Fumonisin toxicity. *Int J Mol Sci*, 23 (5):2512, 2022. DOI: 10.3390/ijms23052512
81. Galli GM, Griss LG, Fortuoso BF, Silva AD, Fracasso M, Lopes TF, Schetinger MRS, Gundel S, Ourique AE, Carneiro C, Mendes RE: Feed contaminated by fumonisin (*Fusarium* spp.) in chicks has a negative influence on oxidative stress and performance, and the inclusion of curcumin-loaded nanocapsules minimizes these effects. *Microb Pathog*, 148:104496, 2020. DOI: 10.1016/j.micpath.2020.104496
82. Wang J, Zhang M, Yang J, Yang X, Zhang J, Zhao Z: Type A trichothecene metabolic profile differentiation, mechanisms, biosynthetic pathways, and evolution in *Fusarium* species - A mini review. *Toxins*, 15:446, 2023. DOI: 10.3390/toxins15070446
83. Kibugu J, Munga L, Mburu D, Maloba F, Auma JE, Grace D, Lindahl JF: Dietary mycotoxins: An overview on toxicokinetics, toxicodynamics, toxicity, epidemiology, detection, and their mitigation with special emphasis on aflatoxicosis in humans and animals. *Toxins*, 16:483, 2024. DOI: 10.3390/toxins16110483
84. Dong JN, Zhao ZK, Wang ZQ, Li SZ, Zhang YP, Sun Z, Qin GX, Zhang XF, Zhao W, Aschalew ND, Wang T: Impact of deoxynivalenol on rumen function, production, and health of dairy cows: Insights from metabolomics and microbiota analysis. *J Hazard Mater*, 465:133376, 2024. DOI: 10.1016/j.jhazmat.2023.133376
85. Zhang F, Wu Q, Wang W, Guo S, Li W, Lv L, Chen H, Xiong F, Liu Y, Chen Y, Li S: Inhibitory effect mediated by deoxynivalenol on rumen fermentation under high-forage substrate. *Ferment*, 8:369, 2022. DOI: 10.3390/fermentation8080369
86. Cope RB: Trichothecenes. In, *Veterinary Toxicology*. Academic Press, pp. 1083-1093, 2025.
87. Riahi I, Marquis V, Ramos AJ, Brufau J, Esteve-Garcia E, Perez-Vendrell AM: Effects of deoxynivalenol-contaminated diets on productive, morphological, and physiological indicators in broiler chickens. *Animals*, 10:1795, 2020. DOI: 10.3390/ani10101795
88. Anwar U, Yousaf M, Mirza MA, Aziz-ur-Rahman M: Impact of stored wheat-based feed on gut morphology, digesta viscosity and blood metabolites of broiler chickens. *Pak Vet J*, 43 (1): 179-183, 2023.
89. Yu J, Pedroso IR: Mycotoxins in cereal-based products and their impacts on the health of humans, livestock animals and pets. *Toxins*, 15:480, 2023. DOI: 10.3390/toxins15080480
90. Wenndt AJ, Sudini HK, Mehta R, Pingali P, Nelson R: Spatiotemporal assessment of post-harvest mycotoxin contamination in rural North Indian food systems. *Food Cont*, 126:108071, 2021. DOI: 10.1016/j.foodcont.2021.108071
91. Wasti S, Sah N, Singh AK, Lee CN, Jha R, Mishra B: Dietary supplementation of dried plum: A novel strategy to mitigate heat stress in broiler chickens. *J Anim Sci Biotechnol*, 12:58, 2021. DOI: 10.1186/s40104-021-00571-5
92. Liu M, Zhao L, Gong G, Zhang L, Shi L, Dai J, Han Y, Wu Y, Khalil MM, Sun L: Remediation strategies for mycotoxin control in feed. *J Anim Sci Biotechnol*, 13:19, 2022. DOI: 10.1186/s40104-021-00661-4
93. Ismail AM, Raza MH, Zahra N, Ahmad R, Sajjad Y, Khan SA: Aflatoxins in wheat grains: Detection and detoxification through chemical, physical, and biological means. *Life*, 14:535, 2024. DOI: 10.3390/life14040535
94. Pascale M, Logrieco AF, Lippolis V, De Girolamo A, Cervellieri S, Lattanzio VM, Ciasca B, Vega A, Reichel M, Graeber M, Slettengren K: Industrial-scale cleaning solutions for the reduction of *Fusarium* toxins in maize. *Toxins*, 14:728, 2022. DOI: 10.3390/toxins14110728
95. Cujbescu, D, Nenciu F, Persu C, Găgeanu I, Gabriel G, Vlăduț NV, Mătache M, Voica I, Pruteanu A, Bularda M, Paraschiv G: Evaluation of an optical sorter effectiveness in separating maize seeds intended for sowing. *Appl Sci*, 13:8892, 2023. DOI: 10.3390/app13158892
96. Bailly S, Orlando B, Brustel J, Bailly JD, Levasseur-Garcia C: Rapid detection of aflatoxins in ground maize using near infrared spectroscopy. *Toxins*, 16:385, 2024. DOI: 10.3390/toxins16090385
97. Conte G, Fontanelli M, Galli F, Cotrozzi L, Pagni L, Pellegrini E: Mycotoxins in feed and food and the role of ozone in their detoxification and degradation: An update. *Toxins*, 12:486, 2020. DOI: 10.3390/toxins12080486
98. Shetty PH, Bhat RV: A physical method for segregation of fumonisin-contaminated maize. *Food Chem*, 66 (3): 371-374, 1999. DOI: 10.1016/S0308-8146(99)00052-7
99. Van der Westhuizen L, Shephard GS, Rheeder J, Burger HM, Gelderblom W, Wild C, Gong Y: Optimising sorting and washing of home-grown maize to reduce fumonisin contamination under laboratory-controlled conditions. *Food Cont*, 22 (3-4): 396-400, 2011. DOI: 10.1016/j.foodcont.2010.09.009
100. Bian Y, Zhang Y, Zhou Y, Wei B, Feng X: Recent insights into sample pretreatment methods for mycotoxins in different food matrices: A critical review on novel materials. *Toxins*, 15:215, 2023. DOI: 10.3390/toxins15030215
101. Yumbe-Guevara BE, Imoto T, Yoshizawa T: Effects of heating procedures on deoxynivalenol, nivalenol and zearalenone levels in naturally contaminated barley and wheat. *Food Addit Contam*, 20 (12): 1132-1140, 2003. DOI: 10.1080/02652030310001620432
102. Kabak B, Dobson AD, Var I: Strategies to prevent mycotoxin contamination of food and animal feed: A review. *Crit Rev Food Sci Nutr*, 46 (8): 593-619, 2006. DOI: 10.1080/10408390500436185
103. Ryu D, Hanna MA, Eskridge KM, Bullerman LB: Heat stability of zearalenone in an aqueous buffered model system. *J Agric Food Chem*, 51 (6): 1746-1748, 2003. DOI: 10.1021/jf0210021

104. Colovic R, Puvaca N, Cheli F, Avantaggiato G, Greco D, Duragic O, Kos J, Pinotti L: Decontamination of mycotoxin-contaminated feedstuffs and compound feed. *Toxins (Basel)*, 11 (11):617, 2019. DOI: 10.3390/toxins11110617
105. Park JW, Kim YB: Effect of pressure cooking on aflatoxin B1 in rice. *J Agric Food Chem*, 54 (6): 2431-2435, 2006. DOI: 10.1021/jf053007e
106. Becker-Algeri TA, Heidtmann-Bemvenuti R, dos Santos Hackbart HC, Badiale-Furlong E: Thermal treatments and their effects on the fumonisin B1 level in rice. *Food Cont*, 34 (2): 488-493, 2013. DOI: 10.1016/j.foodcont.2013.05.016
107. Guo Y, Zhao L, Ma Q, Ji C: Novel strategies for degradation of aflatoxins in food and feed: A review. *Food Res Int*, 140:109878, 2021. DOI: 10.1016/j.foodres.2020.109878
108. Zhang X, Chen Z, Gu W, Ji W, Wang Y, Hao C, He Y, Huang L, Wang M, Shao X, Yan Y: Viral and bacterial co-infection in hospitalised children with refractory Mycoplasma pneumoniae pneumonia. *Epidemiol Infect*, 146 (11): 1384-1388, 2018. DOI: 10.1017/S0950268818000778
109. Calado T, Venâncio A, Abrunhosa L: Irradiation for mold and mycotoxin control: A review. *Comp Rev Food Sci Food Saf*, 13 (5): 1049-1061, 2014. DOI: 10.1111/1541-4337.12095
110. Di Stefano V, Pitonzo R, Cicero N, D'Oca MC: Mycotoxin contamination of animal feedingstuff: Detoxification by gamma-irradiation and reduction of aflatoxins and ochratoxin A concentrations. *Food Addit Contam*, 31 (12): 2034-2039, 2014. DOI: 10.1080/19440049.2014.968882
111. Herzallah S, Alshawabkeh K, Fataftah AA: Aflatoxin decontamination of artificially contaminated feeds by sunlight, γ -radiation, and microwave heating. *J Appl Poult Res*, 17 (4): 515-521, 2008. DOI: 10.3382/japr.2007-00107
112. Markov K, Mihaljević B, Domijan AM, Pleadin J, Delaš F, Frece J: Inactivation of aflatoxigenic fungi and the reduction of aflatoxin B1 *in vitro* and *in situ* using gamma irradiation. *Food Cont*, 54, 79-85, 2015. DOI: 10.1016/j.foodcont.2015.01.036
113. Serra MS, Pulles MB, Mayanquer FT, Vallejo MC, Rosero MI, Ortega JM, Naranjo LN: Evaluation of the use of gamma radiation for reduction of aflatoxin B1 in corn (*Zea mays*) used in the production of feed for broiler chickens. *J Agric Chem Environ*, 7 (1): 21-33, 2018. DOI: 10.4236/jacen.2018.71003
114. Abd El-Tawaab AA, El-Hofy FI, Mahmoud AH, Rashed DM: Mycotoxin residues in different chicken products by HPLC and their inactivation using Gamma radiation. *Int J Pharma Res All Sci*, 8 (4-2019): 71-81, 2019.
115. Refai M, Aziz N, El-Far F, Hassan A: Detection of ochratoxin produced by *A. ochraceus* in feedstuffs and its control by γ radiation. *Appl Rad Iso*, 47 (7): 617-621, 1996. DOI: 10.1016/0969-8043(96)00022-X
116. El-Far F, Aziz N, Hegazy S: Inhibition by gamma-irradiation and antimicrobial food additives of aflatoxin B1 production by *Aspergillus flavus* in poultry diet. *Food/Nahrung*, 36 (2): 143-149, 1992. DOI: 10.1002/food.19920360207
117. Luo X, Zhai Y, Qi L, Pan L, Wang J, Xing J, Wang R, Wang L, Zhang Q, Yang K, Chen Z: Influences of electron beam irradiation on the physical and chemical properties of zearalenone- and ochratoxin A-contaminated corn and *in vivo* toxicity assessment. *Foods*, 9 (3):376, 2020. DOI: 10.3390/foods9030376
118. Kottapalli B, Wolf-Hall CE, Schwarz P: Effect of electron-beam irradiation on the safety and quality of *Fusarium*-infected malting barley. *Int J Food Microbiol*, 110 (3): 224-31, 2006. DOI: 10.1016/j.ijfoodmicro.2006.04.007
119. Stepanik T, Kost D, Nowicki T, Gaba D: Effects of electron beam irradiation on deoxynivalenol levels in distillers dried grain and solubles and in production intermediates. *Food Addit Contam*, 24 (9): 1001-1006, 2007. DOI: 10.1080/02652030701329629
120. Wang B, Mahoney NE, Pan Z, Khir R, Wu B, Ma H, Zhao L: Effectiveness of pulsed light treatment for degradation and detoxification of aflatoxin B1 and B2 in rough rice and rice bran. *Food Cont*, 59, 461-467, 2016. DOI: 10.1016/j.foodcont.2015.06.030
121. Ghanghro AB, Channa MJ, Sheikh SA, Nizamani SM, Ghanghro IH: Assessment of aflatoxin level in stored wheat of godowns of Hyderabad division and decontamination by uv radiation. *Int J Biosci*, 8 (1): 8-16, 2016. DOI: 10.12692/ijb/8.1.8-16
122. Alkadi H, Altal J: Effect of microwave oven processing treatments on reduction of aflatoxin B1 and ochratoxin A in maize flour. *Europ J Chem*, 10 (3): 224-227, 2019. DOI: 10.5155/eurjchem.10.3.224-227.1840
123. Mohamed NF, El-Dine RS, Kotb MAM, Saber A: Assessing the possible effect of gamma irradiation on the reduction of aflatoxin B1, and on the moisture content in some cereal grains. *Am J Biomed Sci*, 7 (1): 33-39, 2015. DOI: 10.5099/ajl150100033
124. Wang SQ, Huang GQ, Li YP, Xiao JX, Zhang Y, Jiang WL: Degradation of aflatoxin B1 by low-temperature radio frequency plasma and degradation product elucidation. *Europ Food Res Technol*, 241 (1): 103-113, 2015. DOI: 10.1007/s00217-015-2439-5
125. Liu R, Wang R, Lu J, Chang M, Jin Q, Du Z, Wang S, Li Q, Wang X: Degradation of AFB1 in aqueous medium by electron beam irradiation: Kinetics, pathway and toxicology. *Food Cont*, 66, 151-157, 2016. DOI: 10.1016/j.foodcont.2016.02.002
126. Liu R, Lu M, Wang R, Wang S, Chang M, Jin Q, Wang X: Degradation of aflatoxin B1 in peanut meal by electron beam irradiation. *Int J Food Prop*, 21 (1): 892-901, 2018. DOI: 10.1080/10942912.2018.1466321
127. Gayán E, Condón S, Álvarez I: Biological aspects in food preservation by ultraviolet light: A review. *Food Bioproc Technol*, 7 (1): 1-20, 2014. DOI: 10.1007/s11947-013-1168-7
128. Fan X, Huang R, Chen H: Application of ultraviolet C technology for surface decontamination of fresh produce. *Trends Food Sci Technol*, 70, 9-19, 2017. DOI: 10.1016/j.tifs.2017.10.004
129. Sun S, Zhao R, Xie Y, Liu Y: Photocatalytic degradation of aflatoxin B1 by activated carbon supported TiO2 catalyst. *Food Cont*, 100, 183-188, 2019. DOI: 10.1016/j.foodcont.2019.01.014
130. Xu C, Ye S, Cui X, Song X, Xie X: Modelling photocatalytic detoxification of aflatoxin B1 in peanut oil on TiO2 layer in a closed-loop reactor. *Biosys Eng*, 180, 87-95, 2019. DOI: 10.1016/j.biosystemseng.2019.01.018
131. Wu S, Wang F, Li Q, Zhou Y, He C, Duan N: Detoxification of DON by photocatalytic degradation and quality evaluation of wheat. *RSC Adv*, 9 (59): 34351-34358, 2019. DOI: 10.1039/c9ra04316k
132. Oms-Oliu G, Martín-Belloso O, Soliva-Fortuny R: Pulsed light treatments for food preservation. A review. *Food Bioprocess Technol*, 3 (1): 13-23, 2010.
133. Moreau M, Lescure G, Agoulon A, Svinareff P, Orange N, Feuilleley M: Application of the pulsed light technology to mycotoxin degradation and inactivation. *J Appl Toxicol*, 33 (5): 357-63, 2013. DOI: 10.1002/jat.1749
134. Soni A, Smith J, Thompson A, Brightwell G: Microwave-induced thermal sterilization-A review on history, technical progress, advantages and challenges as compared to the conventional methods. *Tr Food Sci Technol*, 97, 433-442, 2020. DOI: 10.1016/j.tifs.2020.01.030
135. Perez-Flores GC, Moreno-Martinez E, Mendez-Albores A: Effect of microwave heating during alkaline-cooking of aflatoxin contaminated maize. *J Food Sci*, 76 (2): T48-T52, 2011. DOI: 10.1111/j.1750-3841.2010.01980.x
136. Menon A, Stojceska V, Tassou SA: A systematic review on the recent advances of the energy efficiency improvements in non-conventional food drying technologies. *Tr Food Sci Technol*, 100, 67-76, 2020. DOI: 10.1016/j.tifs.2020.03.014
137. Kogelschatz U: Atmospheric-pressure plasma technology. *Plasma Physics and Controlled Fusion*, 46 (12B):B63, 2004. DOI: 10.1088/0741-3335/46/12B/006
138. Fridman A, Chirokov A, Gutsol A: Non-thermal atmospheric pressure discharges. *J Phys*, 38 (2):R1, 2005. DOI: 10.1088/0022-3727/38/2/R01
139. Misra NN, Yadav B, Roopesh MS, Jo C: Cold plasma for effective fungal and mycotoxin control in foods: Mechanisms, inactivation effects, and applications. *Compr Rev Food Sci Food Saf*, 18 (1): 106-120, 2019. DOI: 10.1111/1541-4337.12398
140. Siciliano I, Spadaro D, Prella A, Vallauri D, Cavallero MC, Garibaldi A, Gullino ML: Use of cold atmospheric plasma to detoxify hazelnuts from

aflatoxins. *Toxins (Basel)*, 8 (5):125, 2016. DOI: 10.3390/toxins8050125

141. Ouf SA, Mohamed AAH, El-Sayed WS: Fungal decontamination of fleshy fruit water washes by double atmospheric pressure cold plasma. *CLEAN-Soil Air Water*, 44 (2): 134-142, 2016. DOI: 10.1002/clen.201400575

142. Park BJ, Takatori K, Sugita-Konishi Y, Kim IH, Lee MH, Han DW, Chung KH, Hyun SO, Park JC: Degradation of mycotoxins using microwave-induced argon plasma at atmospheric pressure. *Surf Coat Technol*, 201 (9-11): 5733-5737, 2007. DOI: 10.1016/j.surfcoat.2006.07.092

143. Kriz P, Petr B, Zbynek H, Jaromir K, Pavel O, Petr S, Miroslav D: Influence of plasma treatment in open air on mycotoxin content and grain nutrients. *Plasma Med*, 5 (2-4): 145-148, 2015. DOI: 10.1615/PlasmaMed.2016015752

144. Iqdiham BM, Feizollahi E, Arif MF, Jeganathan B, Vasanthan T, Thilakarathna MS, Roopesh MS: Reduction of T-2 and HT-2 mycotoxins by atmospheric cold plasma and its impact on quality changes and germination of wheat grains. *J Food Sci*, 86 (4): 1354-1371, 2021. DOI: 10.1111/1750-3841.15658

145. Ten Bosch L, Pfohl K, Avramidis G, Wieneke S, Viol W, Karlovsky P: Plasma-based degradation of mycotoxins produced by *Fusarium*, *Aspergillus* and *Alternaria* species. *Toxins (Basel)*, 9 (3):97, 2017. DOI: 10.3390/toxins9030097

146. Adamović M, Stojanović M, Grubišić M, Ileš D, Milojković J: Importance of aluminosilicate minerals in safe food production. *Mac J Anim Sci*, 1, 175-180, 2011.

147. Magnoli AP, Texeira M, Rosa CA, Miazzo RD, Cavaglieri LR, Magnoli CE, Dalcero AM, Chiacchiera SM: Sodium bentonite and monensin under chronic aflatoxicosis in broiler chickens. *Poult Sci*, 90 (2): 352-357, 2011. DOI: 10.3382/ps.2010-00834

148. Chen Y, Kong Q, Chi C, Shan S, Guan B: Biotransformation of aflatoxin B1 and aflatoxin G1 in peanut meal by anaerobic solid fermentation of *Streptococcus thermophilus* and *Lactobacillus delbrueckii* subsp. *bulgaricus*. *Int J Food Microbiol*, 211: 1-5, 2015. DOI: 10.1016/j.ijfoodmicro.2015.06.021

149. Bhatti SA, Khan MZ, Saleemi MK, Saqib M, Khan A, Hassan Z: Protective role of bentonite against aflatoxin B1 and ochratoxin A-induced immunotoxicity in broilers. *J Immunotox*, 14 (1): 66-76, 2017. DOI: 10.1080/1547691X.2016.1264503

150. Sumantri I, Murti T, Van der Poel A, Boehm J, Agus A: Carry-over of aflatoxin B1-feed into aflatoxin M1-milk in dairy cows treated with natural sources of aflatoxin and bentonite. *J Indo Trop Anim Agric*, 37 (4): 271-277, 2012. DOI: 10.14710/jitaa.37.4.271-277

151. Gouda G, Khattab H, Abdel-Wahhab M, El-Nor SA, El-Sayed H, Kholif S: Clay minerals as sorbents for mycotoxins in lactating goat's diets: Intake, digestibility, blood chemistry, ruminal fermentation, milk yield and composition, and milk aflatoxin M1 content. *Small Rum Res*, 175, 15-22, 2019. DOI: 10.1016/j.smallrumres.2019.04.003

152. Tzou YM, Chan YT, Chen SE, Wang CC, Chiang PN, Teah HY, Hung JT, Wu JJ, Liu YT: Use 3-D tomography to reveal structural modification of bentonite-enriched clay by nonionic surfactants: Application of organo-clay composites to detoxify aflatoxin B1 in chickens. *J Hazard Mat*, 375, 312-319, 2019. DOI: 10.1016/j.jhazmat.2019.04.084

153. Kubena LF, Harvey RB, Huff WE, Elissalde MH, Yersin A G, Phillips TD, Rottinghaus GE: Efficacy of a hydrated sodium calcium aluminosilicate to reduce the toxicity of aflatoxin and diacetoxyscirpenol. *Poult Sci*, 72 (1): 51-59, 1993. DOI: 10.3382/ps.0720051

154. Mussaddeq Y, Begum I, Akhter S: Activity of aflatoxin adsorbents in poultry feed. *Pak J Biol Sci*, 10, 1697-1699, 2000.

155. Robinson A, Johnson NM, Strey A, Taylor JF, Marroquin-Cardona A, Mitchell NJ, Afriyie-Gyawu E, Ankrah NA, Williams JH, Wang JS, Jolly PE, Nachman RJ, Phillips TD: Calcium montmorillonite clay reduces urinary biomarkers of fumonisin B(1) exposure in rats and humans. *Food Addit Contam*, 29 (5): 809-818, 2012. DOI: 10.1080/19440049.2011.651628

156. Li Y, Tian G, Dong G, Bai S, Han X, Liang J, Meng J, Zhang H: Research progress on the raw and modified montmorillonites as adsorbents for mycotoxins: A review. *Appl Clay Sci*, 163, 299-311, 2018. DOI: 10.1016/j.clay.2018.07.032

157. Phillips TD, Wang M, Elmore SE, Hearon S, Wang JS: NovaSil clay for

the protection of humans and animals from aflatoxins and other contaminants. *Clays Clay Miner*, 67 (1): 99-110, 2019. DOI: 10.1007/s42860-019-0008-x

158. Masimango N, Remacle J, Ramaux J: The role of adsorption in the elimination of aflatoxin B1 from contaminated media. *Europ J Appl Micro Biotechnol*, 6, 101-105, 1978.

159. Decker WJ, Corby DG: Activated charcoal adsorbs aflatoxin B1. *Vet Hum Toxicol*, 22 (6): 388-389, 1980.

160. Hatch RC, Clark JD, Jain AV, Weiss R: Induced acute aflatoxicosis in goats: Treatment with activated charcoal or dual combinations of oxytetracycline, stanozolol, and activated charcoal. *Am J Vet Res*, 43 (4): 644-648, 1982. DOI: 10.2460/ajvr.1982.43.04.644

161. Ademoyero AA, Dalvi RR: Efficacy of activated charcoal and other agents in the reduction of hepatotoxic effects of a single dose of aflatoxin B1 in chickens. *Toxicol Lett*, 16 (1-2): 153-157, 1983. DOI: 10.1016/0378-4274(83)90024-3

162. Dalvi R, Ademoyero A: Toxic effects of aflatoxin B1 in chickens given feed contaminated with *Aspergillus flavus* and reduction of the toxicity by activated charcoal and some chemical agents. *Avian Dis*, 61-69, 1984. DOI: 10.2307/1590128

163. Davidson J, Babish J, Delaney K, Taylor D, Phillips T: Hydrated sodium calcium aluminosilicate decreases the bioavailability of aflatoxin in the chicken. *Poult Sci*, 6 (1): (Abstract) 1987.

164. Phillips TD, Kubena LF, Harvey RB, Taylor DR, Heidelbaugh ND: Hydrated sodium calcium aluminosilicate: A high affinity sorbent for aflatoxin. *Poult Sci*, 67 (2): 243-247, 1988. DOI: 10.3382/ps.0670243

165. Kubena L, Harvey R, Phillips T, Huff W: Modulation of aflatoxicosis in growing chickens by dietary addition of a hydrated sodium calcium aluminosilicate. *Poult Sci*, 67:106, 1988.

166. Doerr J: Effect of aluminosilicate on broiler chickens during aflatoxicosis. *Poult Sci*, 68 (1):45, 1989.

167. Harvey R, Kubena L, Phillips T, WEH, Corrier D: Prevention of clinical signs of aflatoxicosis with hydrated sodium calcium aluminosilicate added to diets. *Proc 20th Annu Meet Am Assoc Swine Pract*, 99-102, 1989.

168. Gelven RE: Approaches for alleviating toxic effects of aflatoxin in lactating dairy cows and weanling pigs. *MSc Thesis*, University of Missouri-Columbia, 2010.

169. Dvorak M: Ability of bentonite and natural zeolite to adsorb aflatoxin from liquid media. *Vet Med*, 34 (5): 307-316, 1989.

170. Lindemann M, Blodgett D, Schurig G, Kornegay E: Evaluation of potential ameliorators of aflatoxicosis in weanling/growing swine. *J Anim Sci*, 67:36, 1989.

171. Fukal L, Slamova A, Novak L, Sova Z: The effect of a high aflatoxin B1 concentration in feed on the weights of organs and strength of bones in grown-up chickens. *Biolog Chem Zivoc Vyroby-Veterinaria (Czechoslovakia)*. 26 (2), 1990.

172. Beaver RW, Wilson DM, James MA, Haydon KD, Colvin BM, Sangster LT, Pikul AH, Groopman JD: Distribution of aflatoxins in tissues of growing pigs fed an aflatoxin-contaminated diet amended with a high affinity aluminosilicate sorbent. *Vet Hum Toxicol*, 32 (1): 16-18, 1990.

173. Phillips TD, Clement BA, Kubena LF, Harvey RB: Detection and detoxification of aflatoxins: prevention of aflatoxicosis and aflatoxin residues with hydrated sodium calcium aluminosilicate. *Vet Hum Toxicol*, 32, 15-19, 1990.

174. Kubena LF, Harvey RB, Huff WE, Corrier DE, Phillips TD, Rottinghaus GE: Efficacy of a hydrated sodium calcium aluminosilicate to reduce the toxicity of aflatoxin and T-2 toxin. *Poult Sci*, 69 (7): 1078-1086, 1990. DOI: 10.3382/ps.0691078

175. Abdelhamid AM, el-Shawaf, el-Ayoty SA, Ali MM, Gamil T: Effect of low level of dietary aflatoxins on baladi rabbits. *Arch Tierernahr*, 40 (5-6): 517-537, 1990. DOI: 10.1080/17450399009421084

176. Sova Z, Pohunková H, Reisnerová H, Slámová A, Haisl K: Hematological and histological response to the diet containing aflatoxin B1 and zeolite in broilers of domestic fowl. *Acta Vet Brno*, 60 (1): 31-40, 1991.

177. Araba M, Wyatt R: Effects of sodium bentonite, hydrated sodium

calcium aluminosilicate NovaSil™, and ethacal on aflatoxicosis in broiler chickens. *Poult Sci*, 70 (6), 1991.

178. Kubena LE, Huff WE, Harvey RB, Yersin AG, Elissalde MH, Witzel DA, Giroir LE, Phillips TD, Petersen HD: Effects of a hydrated sodium calcium aluminosilicate on growing turkey poult during aflatoxicosis. *Poult Sci*, 70 (8): 1823-1830, 1991. DOI: 10.3382/ps.0701823

179. Bonna RJ, Aulerich RJ, Bursian SJ, Poppenga RH, Braselton WE, Watson GL: Efficacy of hydrated sodium calcium aluminosilicate and activated charcoal in reducing the toxicity of dietary aflatoxin to mink. *Arch Environ Contam Toxicol*, 20 (3): 441-447, 1991. DOI: 10.1007/BF01064418

180. Harvey RB, Kubena LE, Phillips TD, Corrier DE, Elissalde MH, Huff WE: Diminution of aflatoxin toxicity to growing lambs by dietary supplementation with hydrated sodium calcium aluminosilicate. *Am J Vet Res*, 52 (1): 152-156, 1991. DOI: 10.2460/ajvr.1991.52.01.152

181. Scheideler SE: Effects of various types of aluminosilicates and aflatoxin B1 on aflatoxin toxicity, chick performance, and mineral status. *Poult Sci*, 72 (2): 282-288, 1993. DOI: 10.3382/ps.0720282

182. Schell T, Lindemann M, Kornegay E, Blodgett D: Effects of feeding aflatoxin-contaminated diets with and without clay to weanling and growing pigs on performance, liver function, and mineral metabolism. *J Anim Sci*, 71 (5): 1209-1218, 1993. DOI: 10.2527/1993.7151209x

183. Harvey RB, Kubena LE, Elissalde MH, Phillips TD: Efficacy of zeolitic ore compounds on the toxicity of aflatoxin to growing broiler chickens. *Avian Dis*, 37 (1): 67-73, 1993. DOI: 10.2307/1591459

184. Lindemann MD, Blodgett DJ, Kornegay ET, Schurig GG: Potential ameliorators of aflatoxicosis in weanling/growing swine. *J Anim Sci*, 71 (1): 171-178, 1993. DOI: 10.2527/1993.711171x

185. Ramos AJ, Fink-Gremmels J, Hernandez E: Prevention of Toxic Effects of Mycotoxins by Means of Nonnutritive Adsorbent Compounds. *J Food Prot*, 59 (6): 631-641, 1996. DOI: 10.4315/0362-028X-59.6.631

186. Edrington TS, Sarr AB, Kubena LE, Harvey RB, Phillips TD: Hydrated sodium calcium aluminosilicate (HSCAS), acidic HSCAS, and activated charcoal reduce urinary excretion of aflatoxin M1 in turkey poults. Lack of effect by activated charcoal on aflatoxicosis. *Toxicol Lett*, 89 (2): 115-122, 1996. DOI: 10.1016/s0378-4274(96)03795-2

187. Edrington TS, Kubena LE, Harvey RB, Rottinghaus GE: Influence of a superactivated charcoal on the toxic effects of aflatoxin or T-2 toxin in growing broilers. *Poult Sci*, 76 (9): 1205-1211, 1997. DOI: 10.1093/ps/76.9.1205

188. Bailey R, Kubena L, Harvey R, Buckley S, Rottinghaus G: Efficacy of various inorganic sorbents to reduce the toxicity of aflatoxin and T-2 toxin in broiler chickens. *Poult Sci*, 77 (11): 1623-1630, 1998. DOI: 10.1093/ps/77.11.1623

189. Natour R, Yousef S: Adsorption efficiency of diatomaceous earth for mycotoxin. *Arab Gulf J Sci Res*, 16, 113-127, 1998.

190. Parlat SS, Yildiz AO, Oguz H: Effect of clinoptilolite on performance of Japanese quail (*Coturnix coturnix japonica*) during experimental aflatoxicosis. *Br Poult Sci*, 40 (4): 495-500, 1999. DOI: 10.1080/00071669987269

191. Flores CM, Dominguez JM, Diaz-De-Leon J: Modeling and experimental comparison of the differential adsorption of B1 and G1 aflatoxins on mineral aluminosilicate surfaces. *J Environ Pathol Toxicol Oncol*, 18 (3): 213-220, 1999.

192. Abdel-Wahhab MA, Nada SA, Amra HA: Effect of aluminosilicates and bentonite on aflatoxin-induced developmental toxicity in rat. *J Appl Toxicol*, 19 (3): 199-204, 1999. DOI: 10.1002/(sici)1099-1263(199905/06)19:3<199::aid-jat558>3.0.co;2-d

193. Ledoux DR, Rottinghaus GE, Bermudez AJ, Alonso-Debolt M: Efficacy of a hydrated sodium calcium aluminosilicate to ameliorate the toxic effects of aflatoxin in broiler chicks. *Poult Sci*, 78 (2): 204-210, 1999. DOI: 10.1093/ps/78.2.204

194. Miazza R, Rosa CA, De Queiroz Carvalho EC, Magnoli C, Chiacchiera SM, Palacio G, Saenz M, Kikot A, Basaldella E, Dalcero A: Efficacy of synthetic zeolite to reduce the toxicity of aflatoxin in broiler chicks. *Poult Sci*, 79 (1): 1-6, 2000. DOI: 10.1093/ps/79.1.1

195. Soufiani GN, Razmara M, Kermanshahi H, Velazquez AB, Daneshmand A: Assessment of aflatoxin B1 adsorption efficacy of natural and processed bentonites: *In vitro* and *in vivo* assays. *Appl Clay Sci*, 123: 129-133, 2016. DOI: 10.1016/j.clay.2016.01.019

196. Rosa CA, Miazza R, Magnoli C, Salvano M, Chiacchiera SM, Ferrero S, Saenz M, Carvalho EC, Dalcero A: Evaluation of the efficacy of bentonite from the south of Argentina to ameliorate the toxic effects of aflatoxin in broilers. *Poult Sci*, 80 (2): 139-44, 2001. DOI: 10.1093/ps/80.2.139

197. Aly SE, Abdel-Galil MM, Abdel-Wahhab MA: Application of adsorbent agents technology in the removal of aflatoxin B(1) and fumonisin B(1) from malt extract. *Food Chem Toxicol*, 42 (11): 1825-1831, 2004. DOI: 10.1016/j.fct.2004.06.014

198. Sumantri I, Herliani H, Yuliani M, Nuryono N: Effects of zeolite in aflatoxin B1 contaminated diet on aflatoxin residues and liver histopathology of laying duck. In, *IOP Conf Ser: Earth Environ Sci*, 2018

199. Rotter RG, Frohlich AA, Marquardt RR: Influence of dietary charcoal on ochratoxin A toxicity in Leghorn chicks. *Can J Vet Res*, 53 (4): 449-453, 1989

200. Huff WE, Kubena LE, Harvey RB, Phillips TD: Efficacy of hydrated sodium calcium aluminosilicate to reduce the individual and combined toxicity of aflatoxin and ochratoxin A. *Poult Sci*, 71 (1): 64-69, 1992. DOI: 10.3382/ps.0710064

201. Bauer J: Methods for detoxification of mycotoxins in feedstuffs. *Monatshefte fuer Veterinaermedizin (Germany)*, 49 (4): 175-181, 1994.

202. Galvano F, Pietri A, Bertuzzi T, Piva A, Chies L, Galvano M: Activated carbons: *In vitro* affinity for ochratoxin A and deoxynivalenol and relation of adsorption ability to physicochemical parameters. *J Food Prot*, 61 (4): 469-475, 1998. DOI: 10.4315/0362-028X-61.4.469

203. Khatoon A, Khan M Z, Abidin Z, Bhatti SA: Effects of feeding bentonite clay upon ochratoxin A-induced immunosuppression in broiler chicks. *Food Add Contam*, 35 (3): 538-545, 2018. DOI: 10.1080/19440049.2017.1411612

204. Galvano F, Pietri A, Bertuzzi T, Bognanno M, Chies L, Galvano M: Activated carbons: *In vitro* affinity for fumonisin B(1) and relation of adsorption ability to physicochemical parameters. *J Food Prot*, 60 (8): 985-991, 1997. DOI: 10.4315/0362-028X-60.8.985

205. Solfrizzo M, Carratu MR, Avantiaggiato G, Galvano F, Pietri A, Visconti A: Ineffectiveness of activated carbon in reducing the alteration of sphingolipid metabolism in rats exposed to fumonisin-contaminated diets. *Food Chem Toxicol*, 39 (5): 507-511, 2001. DOI: 10.1016/s0278-6915(00)00160-5

206. Vila-Donat P, Marín S, Sanchis V, Ramos AJ: Tri-octahedral bentonites as potential technological feed additive for Fusarium mycotoxin reduction. *Food Add Contam*, 37 (8): 1374-1387, 2020. DOI: 10.1080/19440049.2020.1766702

207. Smith TK: Dietary influences on excretory pathways and tissue residues of zearalenone and zearalenols in the rat. *Can J Physiol Pharmacol*, 60 (12): 1444-1449, 1982. DOI: 10.1139/y82-214

208. Bursian SJ, Aulerich RJ, Cameron JK, Ames NK, Steficek BA: Efficacy of hydrated sodium calcium aluminosilicate in reducing the toxicity of dietary zearalenone to mink. *J Appl Toxicol*, 12 (2): 85-90, 1992. DOI: 10.1002/jat.2550120204

209. Ramos A, Hernandez E: Resin colestiramina: Un adsorbente de zearalenona de alta afinidad. In, *Procc. XIV Congreso Nacional de Microbiología*. Zaragoza, Spain. 17-19 September, 1993.

210. Williams K, Blaney B, Peters R: Pigs fed Fusarium-infected maize containing zearalenone and nivalenol with sweeteners and bentonite. *Livest Prod Sci*, 39 (3): 275-281, 1994. DOI: 10.1016/0301-6226(94)90207-0

211. Chen Q, Lu Z, Hou W, Shi B, Shan A: Effects of modified maifanite on zearalenone toxicity in female weaner pigs. *It J Anim Sci*, 14 (2): 3597, 2015. DOI: 10.4081/ijas.2015.3597

212. Avantiaggiato G, Havenaar R, Visconti A: Assessing the zearalenone-binding activity of adsorbent materials during passage through a dynamic *in vitro* gastrointestinal model. *Food Chem Toxicol*, 41 (10): 1283-1290, 2003. DOI: 10.1016/S0278-6915(03)00113-3

213. Lemke SL, Grant PG, Phillips TD: Adsorption of zearalenone by organophilic montmorillonite clay. *J Agric Food Chem*, 46 (9): 3789-3796, 1998. DOI: 10.1021/jf9709461
214. Friend D, Trenholm H, Hartin K, Young J, Thompson B: Effect of adding potential vomitoxin (deoxynivalenol) detoxicants or aF. graminearum inoculated corn supplement to wheat diets fed to pigs. *Can J Anim Sci*, 64 (3): 733-741, 1984. DOI: 10.4141/cjas84-081
215. Avantiato G, Havenaar R, Visconti A: Evaluation of the intestinal absorption of deoxynivalenol and nivalenol by an *in vitro* gastrointestinal model, and the binding efficacy of activated carbon and other adsorbent materials. *Food Chem Toxicol*, 42 (5): 817-824, 2004. DOI: 10.1016/j.fct.2004.01.004
216. Young JC, Subryan LM, Potts D, McLaren ME, Gobran FH: Reduction in levels of deoxynivalenol in contaminated wheat by chemical and physical treatment. *J Agric Food Chem*, 34 (3): 461-465, 1986. DOI: 10.1021/jf00069a021
217. Kubena LF, Harvey RB, Bailey RH, Buckley SA, Rottinghaus GE: Effects of a hydrated sodium calcium aluminosilicate (T-Bind) on mycotoxicosis in young broiler chickens. *Poult Sci*, 77 (10): 1502-1509, 1998. DOI: 10.1093/ps/77.10.1502
218. Carson MS, Smith TK: Role of bentonite in prevention of T-2 toxicosis in rats. *J Anim Sci*, 57 (6): 1498-506, 1983. DOI: 10.2527/jas1983.5761498x
219. Buck W, Bratich P: Activated charcoal: Preventing unnecessary death by poisoning. *Vet Med*, 81, 73-77, 1986.
220. Galey FD, Lambert RJ, Busse M, Buck WB: Therapeutic efficacy of superactive charcoal in rats exposed to oral lethal doses of T-2 toxin. *Toxicol*, 25 (5): 493-499, 1987. DOI: 10.1016/0041-0101(87)90285-6
221. Poppenga RH, Lundeen GR, Beasley VR, Buck WB: Assessment of a general therapeutic protocol for the treatment of acute T-2 toxicosis in swine. *Vet Hum Toxicol*, 29 (3): 237-239, 1987.
222. Dwyer MR, Kubena LF, Harvey RB, Mayura K, Sarr AB, Buckley S, Bailey RH, Phillips TD: Effects of inorganic adsorbents and cyclopiazonic acid in broiler chickens. *Poult Sci*, 76 (8): 1141-1149, 1997. DOI: 10.1093/ps/76.8.1141
223. Huebner HJ, Lemke SL, Ottinger SE, Mayura K, Phillips TD: Molecular characterization of high affinity, high capacity clays for the equilibrium sorption of ergotamine. *Food Addit Contam*, 16 (4): 159-171, 1999. DOI: 10.1080/026520399284118
224. Sands DC, McIntyre JL, Walton GS: Use of activated charcoal for the removal of patulin from cider. *Appl Environ Microbiol*, 32 (3): 388-391, 1976. DOI: 10.1128/aem.32.3.388-391.1976
225. Dvorak Z: Mechanical engineering problems in preserving biological objects by temperature lowering. *Sb Ved Pr Lek Fak Karlovy Univ Hradci Kralove*, 33 (2): 115-125, 1990.
226. Jalili M, Jinap S, Son R: The effect of chemical treatment on reduction of aflatoxins and ochratoxin A in black and white pepper during washing. *Food Addit Contam*, 28 (4): 485-493, 2011. DOI: 10.1080/19440049.2010.551300
227. Javanmardi F, Khodaei D, Sheidaei Z, Bashiry M, Nayebedeh K, Vasseghian Y, Mousavi Khaneghah A: Decontamination of aflatoxins in edible oils: A comprehensive review. *Food Rev Int*, 38 (7): 1410-1426, 2022. DOI: 10.1080/87559129.2020.1812635
228. Park DL: Perspectives on mycotoxin decontamination procedures. *Food Addit Contam*, 10 (1): 49-60, 1993. DOI: 10.1080/02652039309374129
229. Natarajan KR: Chemical inactivation of aflatoxins in peanut protein ingredients. *J Environ Pathol Toxicol Oncol*, 11 (4): 217-227, 1992.
230. McKenzie KS, Sarr AB, Mayura K, Bailey RH, Miller DR, Rogers TD, Norred WP, Voss KA, Plattner RD, Kubena LF, Phillips TD: Oxidative degradation and detoxification of mycotoxins using a novel source of ozone. *Food Chem Toxicol*, 35 (8): 807-820, 1997. DOI: 10.1016/s0278-6915(97)00052-5
231. de Alencar ER, Faroni LRDA, Soares N FF, da Silva WA, da Silva Carvalho MC: Efficacy of ozone as a fungicidal and detoxifying agent of aflatoxins in peanuts. *J Sci Food Agric*, 92 (4): 899-905, 2012. DOI: 10.1002/jsfa.4668
232. Agriopoulou S, Koliadima A, Karaiskakis G, Kapelos J: Kinetic study of aflatoxins' degradation in the presence of ozone. *Food Cont*, 61, 221-226, 2016. DOI: 10.1016/j.foodcont.2015.09.013
233. Piemontese L, Messia MC, Marconi E, Falasca L, Zivoli R, Gambacorta L, Perrone G, Solfrizzo M: Effect of gaseous ozone treatments on DON, microbial contaminants and technological parameters of wheat and semolina. *Food Addit Contam*, 35 (4): 760-771, 2018. DOI: 10.1080/19440049.2017.1419285
234. Santos Alexandre AP, Vela-Paredes RS, Santos AS, Costa NS, Canniatti-Brazaca SG, Calori-Domingues MA, Augusto PED: Ozone treatment to reduce deoxynivalenol (DON) and zearalenone (ZEN) contamination in wheat bran and its impact on nutritional quality. *Food Addit Contam*, 35 (6): 1189-1199, 2018. DOI: 10.1080/19440049.2018.1432899
235. Jr AP, King J: Efficacy and safety evaluation of ozonation to degrade aflatoxin in corn. *J Food Sci*, 67 (8): 2866-2872, 2002. DOI: 10.1111/j.1365-2621.2002.tb08830.x
236. Trombete F, Porto Y, Freitas-Silva O, Pereira R, Direito G, Saldanha T, Fraga M: Efficacy of ozone treatment on mycotoxins and fungal reduction in artificially contaminated soft wheat grains. *J Food Process Preserv*, 41 (3): e12927, 2017. DOI: 10.1111/jfpp.12927
237. McKenzie K, Kubena L, Denvir A, Rogers T, Hitchens G, Bailey R, Harvey R, Buckley S, Phillips T: Aflatoxicosis in turkey poult is prevented by treatment of naturally contaminated corn with ozone generated by electrolysis. *Poult Sci*, 77 (8): 1094-1102, 1998. DOI: 10.1093/ps/77.8.1094
238. Li MM, Guan EQ, Bian K: Effect of ozone treatment on deoxynivalenol and quality evaluation of ozonized wheat. *Food Addit Contam*, 32 (4): 544-553, 2015. DOI: 10.1080/19440049.2014.976596
239. Sun C, Ji J, Wu S, Sun C, Pi F, Zhang Y, Tang L, Sun X: Saturated aqueous ozone degradation of deoxynivalenol and its application in contaminated grains. *Food Cont*, 69, 185-190, 2016. DOI: 10.1016/j.foodcont.2016.04.041
240. Wang L, Luo Y, Luo X, Wang R, Li Y, Li Y, Shao H, Chen Z: Effect of deoxynivalenol detoxification by ozone treatment in wheat grains. *Food Cont*, 66, 137-144, 2016. DOI: 10.1016/j.foodcont.2016.01.038
241. Qi L, Li Y, Luo X, Wang R, Zheng R, Wang L, Li Y, Yang D, Fang W, Chen Z: Detoxification of zearalenone and ochratoxin A by ozone and quality evaluation of ozonised corn. *Food Addit Contam*, 33 (11): 1700-1710, 2016. DOI: 10.1080/19440049.2016.1232863
242. Altug T, Yousef AE, Marth EH: Degradation of aflatoxin B1 in dried figs by sodium bisulfite with or without heat, ultraviolet energy or hydrogen peroxide. *J Food Prot*, 53 (7): 581-583, 1990. DOI: 10.4315/0362-028X-53.7.581
243. Abd Alla ES: Zearalenone: Incidence, toxigenic fungi and chemical decontamination in Egyptian cereals. *Nahrung*, 41 (6): 362-365, 1997. DOI: 10.1002/food.19970410610
244. Chlebicz A, Slizewska K: *In vitro* detoxification of aflatoxin B(1), deoxynivalenol, fumonisins, T-2 toxin and zearalenone by probiotic bacteria from genus *Lactobacillus* and *Saccharomyces cerevisiae* yeast. *Prob Antimicrob Proteins*, 12 (1): 289-301, 2020. DOI: 10.1007/s12602-018-9512-x
245. Bidura IGNG, Siti NW, Wibawa AAP, Puspani E, Candrawati DPMA: Improving the quality of tofu waste by mixing it with carrots and probiotics as a feed source of probiotics and β -carotene. *Int J Vet Sci*, 12, 407-413, 2023. DOI: 10.47278/journal.ijvs/2022.213
246. Akhtar T, Shahid S, Asghar A, Naeem MI, Aziz S, Ameer T: Utilisation of herbal bullets against Newcastle disease in poultry sector of Asia and Africa (2012-2022). *Int J Agri Biosci*, 12, 56-65, 2023. DOI: 10.47278/journal.ijab/2023.044
247. Coniglio MV, Luna MJ, Provencal P, Magnoli AP: Use of the probiotic *Saccharomyces cerevisiae* var. *boulardii* RC009 in the rearing stage of calves. *Int J Agri Biosci*, 12, 188-192, 2023. DOI: 10.47278/journal.ijab/2023.063
248. Kalita R, Pegu A, Baruah C: Prospects of probiotics and fish growth promoting bacteria in aquaculture: A review. *Int J Agri Biosci*, 12 (4): 234-244, 2023. DOI: 10.47278/journal.ijab/2023.070
249. Rashid S, Alsayeqh AF, Akhtar T, Abbas R Z, Ashraf R: Probiotics: alternative to antibiotics in poultry production. *Int J Vet Sci*, 12, 45-53, 2023. DOI: 10.47278/journal.ijvs/2022.175

250. Shah NP: Probiotic bacteria: Selective enumeration and survival in dairy foods. *J Dairy Sci.* 83 (4): 894-907, 2000. DOI: 10.3168/jds.S0022-0302(00)74953-8
251. Mehmood A, Nawaz M, Rabbani M, Mushtaq MH: Probiotic effect of *Limosilactobacillus fermentum* on growth performance and competitive exclusion of *Salmonella gallinarum* in poultry. *Pak Vet J*, 43 (4): 659-664, 2023. DOI: 10.29261/pakvetj/2023.103
252. Madrigal-Santillan E, Madrigal-Bujaidar E, Marquez-Marquez R, Reyes A: Antigenotoxic effect of *Saccharomyces cerevisiae* on the damage produced in mice fed with aflatoxin B(1) contaminated corn. *Food Chem Toxicol*, 44 (12): 2058-2063, 2006. DOI: 10.1016/j.fct.2006.07.006
253. Teniola OD, Addo PA, Brost IM, Farber P, Jany KD, Alberts JF, van Zyl WH, Steyn PS, Holzapfel WH: Degradation of aflatoxin B(1) by cell-free extracts of *Rhodococcus erythropolis* and *Mycobacterium fluoranthenorans* sp. nov. DSM44556(T). *Int J Food Microbiol*, 105 (2): 111-117, 2005. DOI: 10.1016/j.ijfoodmicro.2005.05.004
254. Gul ST, Alsayeqh AF: Probiotics improve physiological parameters and meat production in broiler chicks. *Int J Vet Sci*, 12, 182-191, 2023. DOI: 10.47278/journal.ijvs/2022.191
255. Raza A, Abbas RZ, Karadağoglu Ö, Raheem A, Khan AMA, Khalil MZ, Maheen N, Quddus A, Hussain A, Kanchev KP: Role of probiotics in increasing meat and egg production in poultry. *Kafkas Univ Vet Fak Derg*, 30, 753-760, 2024. DOI: 10.9775/kvfd.2024.32861
256. Dablood AS, Atwah B, Alghamdi S, Momenah MA, Saleh O, Alhazmi N, Mostafa YS, Alamri SA, Alyoubi WA, Alshammari NM: Could *Paenibacillus xylanexedens* MS58 be an ecofriendly antibiotic in poultry production? Impacts on performance, blood biochemistry, gut microbiota and meat quality. *Pak Vet J*, 44, 352-360, 2024. DOI: 10.29261/pakvetj/2024.180
257. Farzaneh M, Shi ZQ, Ghassempour A, Sedaghat N, Ahmadzadeh M, Mirabolfathy M, Javan-Nikkhah M: Aflatoxin B1 degradation by *Bacillus subtilis* UTBSP1 isolated from pistachio nuts of Iran. *Food Cont*, 23 (1): 100-106, 2012. DOI: 10.1016/j.foodcont.2011.06.018
258. Samuel MS, Sivaramakrishna A, Mehta A: Degradation and detoxification of aflatoxin B1 by *Pseudomonas putida*. *Int Biodeterior Biodegrad*, 86, 202-209, 2014. DOI: 10.1016/j.ibiod.2013.08.026
259. Rao KR, Vipin A, Hariprasad P, Appaiah KA, Venkateswaran G: Biological detoxification of Aflatoxin B1 by *Bacillus licheniformis* CFR1. *Food Cont*, 71, 234-241, 2017. DOI: 10.1016/j.foodcont.2016.06.040
260. Xu L, Eisa Ahmed MF, Sangare L, Zhao Y, Selvaraj JN, Xing F, Wang Y, Yang H, Liu Y: Novel aflatoxin-degrading enzyme from *Bacillus shackletonii* L7. *Toxins (Basel)*, 9 (1):36, 2017. DOI: 10.3390/toxins9010036
261. Shu X, Wang Y, Zhou Q, Li M, Hu H, Ma Y, Chen X, Ni J, Zhao W, Huang S, Wu L: Biological degradation of aflatoxin B(1) by cell-free extracts of *Bacillus velezensis* DY3108 with broad pH stability and excellent thermostability. *Toxins (Basel)*, 10 (8):330, 2018. DOI: 10.3390/toxins10080330
262. Wang L, Wu J, Liu Z, Shi Y, Liu J, Xu X, Hao S, Mu P, Deng F, Deng Y: Aflatoxin B(1) degradation and detoxification by *Escherichia coli* CG1061 isolated from chicken cecum. *Front Pharmacol*, 9:1548, 2018. DOI: 10.3389/fphar.2018.01548
263. Fang Q, Du M, Chen J, Liu T, Zheng Y, Liao Z, Zhong Q, Wang L, Fang X, Wang J: Degradation and detoxification of aflatoxin B1 by tea-derived *Aspergillus niger* RAF106. *Toxins (Basel)*, 12 (12):777, 2020. DOI: 10.3390/toxins12120777
264. Cai M, Qian Y, Chen N, Ling T, Wang J, Jiang H, Wang X, Qi K, Zhou Y: Detoxification of aflatoxin B1 by *Stenotrophomonas* sp. CW117 and characterization the thermophilic degradation process. *Environ Pollut*, 261:114178, 2020. DOI: 10.1016/j.envpol.2020.114178
265. Qiu T, Wang H, Yang Y, Yu J, Ji J, Sun J, Zhang S, Sun X: Exploration of biodegradation mechanism by AFB1-degrading strain *Aspergillus niger* FS10 and its metabolic feedback. *Food Cont*, 121:107609, 2021. DOI: 10.1016/j.foodcont.2020.107609
266. Fuchs E, Binder E M, Heidler D, Krska R: Structural characterization of metabolites after the microbial degradation of type A trichothecenes by the bacterial strain BBSH 797. *Food Addit Contam*, 19 (4): 379-386, 2002. DOI: 10.1080/02652030110091154
267. Young JC, Zhou T, Yu H, Zhu H, Gong J: Degradation of trichothecene mycotoxins by chicken intestinal microbes. *Food Chem Toxicol*, 45 (1): 136-143, 2007. DOI: 10.1016/j.fct.2006.07.028
268. He C, Fan Y, Liu G, Zhang H: Isolation and identification of a strain of *Aspergillus tubingensis* with deoxynivalenol biotransformation capability. *Int J Mol Sci*, 9 (12): 2366-2375, 2008. DOI: 10.3390/ijms9122366
269. Gao X, Mu P, Wen J, Sun Y, Chen Q, Deng Y: Detoxification of trichothecene mycotoxins by a novel bacterium, *Eggerthella* sp. DII-9. *Food Chem Toxicol*, 112, 310-319, 2018. DOI: 10.1016/j.fct.2017.12.066
270. Zhai Y, Zhong L, Gao H, Lu Z, Bie X, Zhao H, Zhang C, Lu F: Detoxification of deoxynivalenol by a mixed culture of soil bacteria with 3-epi-deoxynivalenol as the main intermediate. *Front Microbiol*, 10:2172, 2019. DOI: 10.3389/fmicb.2019.02172
271. Wang G, Wang Y, Ji F, Xu L, Yu M, Shi J, Xu J: Biodegradation of deoxynivalenol and its derivatives by *Devosia insulae* A16. *Food Chem*, 276, 436-442, 2019. DOI: 10.1016/j.foodchem.2018.10.011
272. Ju J, Tinyiro S E, Yao W, Yu H, Guo Y, Qian H, Xie Y: The ability of *Bacillus subtilis* and *Bacillus natto* to degrade zearalenone and its application in food. *J Food Process Preserv*, 43 (10):e14122, 2019. DOI: 10.1111/jfpp.14122
273. Wang Y, Wang G, Dai Y, Wang Y, Lee Y W, Shi J, Xu J: Biodegradation of deoxynivalenol by a novel microbial consortium. *Front Microbiol*, 10:2964, 2019. DOI: 10.3389/fmicb.2019.02964
274. Jia R, Cao L, Liu W, Shen Z: Detoxification of deoxynivalenol by *Bacillus subtilis* ASAG 216 and characterization the degradation process. *Europ Food Res Technol*, 247 (1): 67-76, 2021. DOI: 10.1007/s00217-020-03607-8
275. Xu J, Wang H, Zhu Z, Ji F, Yin X, Hong Q, Shi J: Isolation and characterization of *Bacillus amyloliquefaciens* ZDS-1: Exploring the degradation of zearalenone by *Bacillus* spp. *Food Cont*, 68, 244-250, 2016. DOI: 10.1016/j.foodcont.2016.03.030
276. Wang G, Yu M, Dong F, Shi J, Xu J: Esterase activity inspired selection and characterization of zearalenone degrading bacteria *Bacillus pumilus* ES-21. *Food Cont*, 77, 57-64, 2017. DOI: 10.1016/j.foodcont.2017.01.021
277. Štyriak I, Conková E, Kmec V, Böhm J, Razzazi E: The use of yeast for microbial degradation of some selected mycotoxins. *Mycotox Res*, 17 (Suppl 1): 24-27, 2001.
278. Benedetti R, Nazzi F, Locci R, Firrao G: Degradation of fumonisin B1 by a bacterial strain isolated from soil. *Biodegrad*, 17 (1): 31-38, 2006. DOI: 10.1007/s10532-005-2797-y
279. Lei Y, Zhao L, Ma Q, Zhang J, Zhou T, Gao C, Ji C: Degradation of zearalenone in swine feed and feed ingredients by *Bacillus subtilis* ANSB01G. *World Mycotox J*, 7 (2): 143-151, 2014. DOI: 10.3920/WMJ2013.1623
280. Zhao Z, Zhang Y, Gong A, Liu N, Chen S, Zhao X, Li X, Chen L, Zhou C, Wang J: Biodegradation of mycotoxin fumonisin B1 by a novel bacterial consortium SAAS79. *Appl Microbiol Biotechnol*, 103 (17): 7129-7140, 2019. DOI: 10.1007/s00253-019-09979-6
281. Stanley VG, Ojo R, Woldesenbet S, Hutchinson DH, Kubena LF: The use of *Saccharomyces cerevisiae* to suppress the effects of aflatoxicosis in broiler chicks. *Poult Sci*. 72 (10): 1867-1872, 1993. DOI: 10.3382/ps.0721867
282. Diaz DE, Hagler WM, Blackwelder JT, Eve JA, Hopkins BA, Anderson KL, Jones FT, Whitlow LW: Aflatoxin binders II: Reduction of aflatoxin M1 in milk by sequestering agents of cows consuming aflatoxin in feed. *Mycopathol*, 157 (2): 233-241, 2004. DOI: 10.1023/b:myco.0000020587.93872.59
283. Sampaio Baptista A, Horii J, Antonia Calori-Domingues M, Micotti da Glória E, Mastrodi Salgado J, Roberto Vizioli M: The capacity of manno-oligosaccharides, thermolysed yeast and active yeast to attenuate aflatoxicosis. *World J Microbiol Biotechnol*, 20 (5): 475-481, 2004. DOI: 10.1023/B:WIBI.0000040397.48873.3b
284. Tejada-Castaneda ZI, Avila-Gonzalez E, Casaubon-Huguenin MT, Cervantes-Olivares RA, Vasquez-Pelaez C, Hernandez-Baumgarten EM, Moreno-Martinez E: Biodegradation of aflatoxin-contaminated chick feed. *Poult Sci*, 87 (8): 1569-1576, 2008. DOI: 10.3382/ps.2007-00304

285. Kutz RE, Sampson JD, Pompeu LB, Ledoux DR, Spain JN, Vazquez-Anon M, Rottinghaus GE: Efficacy of Solis, NovasilPlus, and MTB-100 to reduce aflatoxin M1 levels in milk of early to mid lactation dairy cows fed aflatoxin B1. *J Dairy Sci*, 92 (8): 3959-3963, 2009. DOI: 10.3168/jds.2009-2031
286. Battacone G, Nudda A, Palomba M, Mazzette A, Pulina G: The transfer of aflatoxin M1 in milk of ewes fed diet naturally contaminated by aflatoxins and effect of inclusion of dried yeast culture in the diet. *J Dairy Sci*, 92 (10): 4997-5004, 2009. DOI: 10.3168/jds.2008-1684
287. Hernandez-Mendoza A, Guzman-De-Peña D, González-Córdova AF, Vallejo-Córdoba B, Garcia HS: *In vivo* assessment of the potential protective effect of *Lactobacillus casei* Shirota against aflatoxin B1. *Dairy Sci Technol*, 90 (6): 729-740, 2010. DOI: 10.1051/dst/2010030
288. Firmin S, Morgavi DP, Yiannikouris A, Boudra H: Effectiveness of modified yeast cell wall extracts to reduce aflatoxin B1 absorption in dairy ewes. *J Dairy Sci*, 94 (11): 5611-5619, 2011. DOI: 10.3168/jds.2011-4446
289. Abbes S, Salah-Abbes JB, Sharafi H, Jebali R, Noghabi KA, Oueslati R: Ability of *Lactobacillus rhamnosus* GAF01 to remove AFM1 *in vitro* and to counteract AFM1 immunotoxicity *in vivo*. *J Immunotoxicol*, 10 (3): 279-286, 2013. DOI: 10.3109/1547691X.2012.718810
290. Jebali R, Abbes S, Salah-Abbes JB, Younes RB, Haous Z, Oueslati R: Ability of *Lactobacillus plantarum* MON03 to mitigate aflatoxins (B1 and M1) immunotoxicities in mice. *J Immunotoxicol*, 12 (3): 290-299, 2015. DOI: 10.3109/1547691X.2014.973622
291. Liu N, Wang JQ, Jia SC, Chen YK, Wang JP: Effect of yeast cell wall on the growth performance and gut health of broilers challenged with aflatoxin B1 and necrotic enteritis. *Poult Sci*, 97 (2): 477-484, 2018. DOI: 10.3382/ps/pex342
292. Ali A, Khatoon A, Saleemi MK, Abbas RZ: Aflatoxins associated oxidative stress and immunological alterations are mitigated by dietary supplementation of *Pichia kudriavzevii* in broiler chicks. *Microb Pathog*, 161 (Pt A): 105279, 2021. DOI: 10.1016/j.micpath.2021.105279
293. Ali A, Khatoon A, Almohaimeed HM, Al-Sarraf F, Albiheyri R, Alotibi I, Abidin Z: Mitigative potential of novel *Lactobacillus plantarum* TISTR 2076 against the aflatoxins-associated oxidative stress and histopathological alterations in liver and kidney of broiler chicks during the entire growth period. *Toxins (Basel)*, 14 (10): 689, 2022. DOI: 10.3390/toxins14100689
294. Firmin S, Gandia P, Morgavi DP, Houin G, Jouany JP, Bertin G, Boudra H: Modification of aflatoxin B1 and ochratoxin A toxicokinetics in rats administered a yeast cell wall preparation. *Food Addit Contam*, 27 (8): 1153-1160, 2010. DOI: 10.1080/19440041003801174
295. El Barkouky E, Mohamed F, Atta A, Abu Taleb A, El Menawey M, Hatab M: Effect of *Saccharomyces cerevisiae* and vitamin C supplementation on performance of broilers subjected to ochratoxin A contamination. *Egyp Poult Sci*, 30 (1): 89-113, 2010.
296. Slizewska K, Nowak A, Smulikowska S: Probiotic preparation reduces faecal water genotoxicity and cytotoxicity in chickens fed ochratoxin A contaminated feed (*in vivo* study). *Acta Biochim Pol*, 63 (2): 281-286, 2016.
297. Mujahid H, Hashmi AS, Khan MZ, Tayyab M, Shezad W: Protective effect of yeast sludge and whey powder against ochratoxicosis in broiler chicks. *Pak Vet J*, 39, 588-592, 2019. DOI: 10.29261/pakvetj/2019.077
298. Hmood KA, Habeeb AH, Al-Mhanna KI: Antioxidant role of *Lactobacillus* sp. isolated from honey bee against histological effects of ochratoxin *in vivo*. *Al-Kufa Univ J Biol*, 11 (2): 67-80, 2019.
299. Dazuk V, Boiago MM, Rolim G, Paravisi A, Copetti PM, Bissacotti BF, Morsch VM, Vedovatto M, Gazoni FL, Matte F, Gloria EM, Da Silva AS: Laying hens fed mycotoxin-contaminated feed produced by *Fusarium* fungi (T-2 toxin and fumonisin B1) and *Saccharomyces cerevisiae* lysate: Impacts on poultry health, productive efficiency, and egg quality. *Microb Pathog*, 149: 104517, 2020. DOI: 10.1016/j.micpath.2020.104517
300. Alberts JF, Gelderblom WC, Botha A, van Zyl WH: Degradation of aflatoxin B(1) by fungal laccase enzymes. *Int J Food Microbiol*, 135 (1): 47-52, 2009. DOI: 10.1016/j.ijfoodmicro.2009.07.022
301. Taylor MC, Jackson CJ, Tattersall DB, French N, Peat TS, Newman J, Briggs LJ, Lapalnikar GV, Campbell PM, Scott C: Identification and characterization of two families of F420H2-dependent reductases from mycobacteria that catalyze aflatoxin degradation. *Mol Microbiol*, 78 (3): 561-575, 2010. DOI: 10.1111/j.1365-2958.2010.07356.x
302. Cao H, Liu D, Mo X, Xie C, Yao D: A fungal enzyme with the ability of aflatoxin B(1) conversion: Purification and ESI-MS/MS identification. *Microbiol Res*, 166 (6): 475-483, 2011. DOI: 10.1016/j.micres.2010.09.002
303. Zhao LH, Guan S, Gao X, Ma QG, Lei YP, Bai XM, Ji C: Preparation, purification and characteristics of an aflatoxin degradation enzyme from *Myxococcus fulvus* ANSM068. *J Appl Microbiol*, 110 (1): 147-155, 2011. DOI: 10.1111/j.1365-2672.2010.04867.x
304. Wang J, Ogata M, Hirai H, Kawagishi H: Detoxification of aflatoxin B1 by manganese peroxidase from the white-rot fungus *Phanerochaete sordida* YK-624. *FEMS Microbiol Lett*, 314 (2): 164-169, 2011. DOI: 10.1111/j.1574-6968.2010.02158.x
305. Yehia RS: Aflatoxin detoxification by manganese peroxidase purified from *Pleurotus ostreatus*. *Braz J Microbiol*, 45 (1): 127-133, 2014. DOI: 10.1590/S1517-83822014005000026
306. Ito M, Sato I, Ishizaka M, Yoshida S, Koitabashi M, Yoshida S, Tsushima S: Bacterial cytochrome P450 system catabolizing the *Fusarium* toxin deoxynivalenol. *Appl Environ Microbiol*, 79 (5): 1619-1628, 2013. DOI: 10.1128/AEM.03227-12
307. Feltrin ACP, Garcia SO, Caldas SS, Primel EG, Badiale-Furlong E, Garda-Bufferon J: Characterization and application of the enzyme peroxidase to the degradation of the mycotoxin DON. *J Environ Sci Health*, 52 (10): 777-783, 2017. DOI: 10.1080/03601234.2017.1356672
308. Carere J, Hassan YI, Lepp D, Zhou T: The enzymatic detoxification of the mycotoxin deoxynivalenol: Identification of DepA from the DON epimerization pathway. *Microb Biotechnol*, 11 (6): 1106-1111, 2018. DOI: 10.1111/1751-7915.12874
309. He WJ, Shi MM, Yang P, Huang T, Zhao Y, Wu AB, Dong WB, Li HP, Zhang JB, Liao YC: A quinone-dependent dehydrogenase and two NADPH-dependent aldo/keto reductases detoxify deoxynivalenol in wheat via epimerization in a *Devosia* strain. *Food Chem*, 321: 126703, 2020. DOI: 10.1016/j.foodchem.2020.126703
310. Tso KH, Lumsangkul C, Ju JC, Fan YK, Chiang HI: The potential of peroxidases extracted from the spent mushroom (*Flammulina velutipes*) substrate significantly degrade mycotoxin deoxynivalenol. *Toxins*, 13 (1): 72, 2021. DOI: 10.3390/toxins13010072
311. Shcherbakova L, Rozhkova A, Osipov D, Zorov I, Mikityuk O, Statsyuk N, Sinitsyna O, Dzhavakhiya V, Sinitsyn A: Effective zearalenone degradation in model solutions and infected wheat grain using a novel heterologous lactonohydrolase secreted by recombinant *Penicillium canescens*. *Toxins (Basel)*, 12 (8): 475, 2020. DOI: 10.3390/toxins12080475
312. Azam MS, Yu D, Liu N, Wu A: Degrading ochratoxin A and zearalenone mycotoxins using a multifunctional recombinant enzyme. *Toxins (Basel)*, 11 (5): 301, 2019. DOI: 10.3390/toxins11050301
313. Masching S, Naehrer K, Schwartz-Zimmermann HE, Sarandan M, Schaumberger S, Dohnal I, Nagl V, Schatzmayr D: Gastrointestinal degradation of fumonisin B(1) by carboxylesterase FumD prevents fumonisin induced alteration of sphingolipid metabolism in turkey and swine. *Toxins (Basel)*, 8 (3): 84, 2016. DOI: 10.3390/toxins8030084
314. Ahmad A, Humak F, Ahmad M, Altaf H, Qamar W, Hussain A, Ashraf U, Abbas RZ, Siddique A, Ashraf T: Phytochemicals as alternative anthelmintics against poultry parasites: A review. *Agrobiol Rec*, 12, 34-45, 2023. DOI: 10.47278/journal.abr/2023.015
315. Hegazy SA, Abd ES, Khorshed M, Salem F: Productive and immunological performance of small ruminants offered some medicinal plants as feed additives. *Int J Vet Sci*, 12, 120-125, 2023. DOI: 10.47278/journal.ijvs/2022.163
316. Krishnaveni P, Thangapandian M, Raja P, Rao G: Pathological and molecular studies on antitumor effect of curcumin and curcumin solid lipid nanoparticles. *Pak Vet J*, 43, 315-320, 2023. DOI: 10.29261/pakvetj/2023.022
317. Ratajac R, Pavličević A, Petrović J, Stojanov I, Orčić D, Štrbac F, Simin N: *In vitro* evaluation of acaricidal efficacy of selected essential oils against *Dermanyssus gallinae*. *Pak Vet J*, 44, 93-98, 2023. DOI: 10.29261/pakvetj/2023.123

318. Mohammad LM, Kamil AM, Tawfeeq RK, Jamal Ahmed S: Ameliorating effects of herbal mixture for dexamethasone induced histological changes in mice. *Int J Vet Sci*, 12, 126-131, 2023. DOI: 10.47278/journal.ijvs/2022.170
319. Rasheed M, Aljohani AS: Evaluation of anthelmintic effects of essential oil of Star Anise against *Ascaridia galli* of poultry. *Pak Vet J*, 44, 1223-1228, 2024. DOI: 10.29261/pakvetj/2024.294
320. Saeed Z, Abbas RZ, Khan MK, Saleemi MK: Anticoccidial activities of essential oil of *Amomum subulatum* in broiler chicks. *Pak J Agric Sci*, 60, 377-384, 2023.
321. Shi D, Zhou J, Zhao L, Rong X, Fan Y, Hamid H, Li W, Ji C, Ma Q: Alleviation of mycotoxin biodegradation agent on zearalenone and deoxynivalenol toxicosis in immature gilts. *J Anim Sci Biotechnol*, 9 (1):42, 2018. DOI: 10.1186/s40104-018-0255-z
322. Abbas R Z, Saeed Z, Bosco A, Qamar W, Subhani Z, Sorin CM, Kasli MAE, Munir F: Botanical control of coccidiosis in ruminants. *Pak J Agric Sci*, 60, 473-485, 2023.
323. Liu L, Xie M, Wei D: Biological detoxification of mycotoxins: Current status and future advances. *Int J Mol Sci*, 23 (3): 1064, 2022. DOI: 10.3390/ijms23031064
324. Ahmad S, Yousaf MS, Tahir SK, Rashid MA, Majeed KA, Naseem M, Raza M, Hayat Z, Khalid A, Zaneb H: Effects of co-supplementation of β -galacto-oligosaccharides and methionine on breast meat quality, meat oxidative stability and selected meat quality genes in broilers. *Pak Vet J*, 43, 428-434, 2023. DOI: 10.29261/pakvetj/2023.043
325. Zhao Y, Wang Q, Huang J, Chen Z, Liu S, Wang X, Wang F: Mycotoxin contamination and presence of mycobiota in rice sold for human consumption in China. *Food Cont*, 98, 19-23, 2019. DOI: 10.1016/j.foodcont.2018.11.014
326. Aboubakr M, Elmahdy AM, Taima S, Emam MA, Farag A, Alkafafy M, Said AM, Soliman A: Protective effects of N acetylcysteine and vitamin E against acrylamide-induced neurotoxicity in rats. *Pak Vet J*, 43, 262-268, 2023.
327. El-Sheikh ESA, Hamed IA, Alduwish MA, Momenah MA, Melebari SJ, Alsolmy SA, Alghamdi MS, Alharbi AA, Sherif RM, Shalaby AA: The ameliorative effect of vitamin C against sub-chronic thiamethoxam toxicity in male rats. *Pak Vet J*, 44, 803-811, 2024. DOI: 10.29261/pakvetj/2024.206
328. Gradelet S, Le Bon AM, Berges R, Suschetet M, Astorg P: Dietary carotenoids inhibit aflatoxin B1-induced liver preneoplastic foci and DNA damage in the rat: role of the modulation of aflatoxin B1 metabolism. *Carcinog*, 19 (3): 403-411, 1998. DOI: 10.1093/carcin/19.3.403
329. Klein PJ, Van Vleet TR, Hall JO, Coulombe RA, Jr: Dietary butylated hydroxytoluene protects against aflatoxicosis in Turkeys. *Toxicol Appl Pharmacol*, 182 (1): 11-19, 2002. DOI: 10.1006/taap.2002.9433
330. Sahoo PK, Mukherjee SC: Immunomodulation by dietary vitamin C in healthy and aflatoxin B1-induced immunocompromised rohu (*Labeo rohita*). *Comp Immunol Microbiol Infect Dis*, 26 (1): 65-76, 2003. DOI: 10.1016/s0147-9571(01)00038-8
331. Tedesco D, Steidler S, Galletti S, Tameni M, Sonzogni O, Ravarotto L: Efficacy of silymarin-phospholipid complex in reducing the toxicity of aflatoxin B1 in broiler chicks. *Poult Sci*, 83 (11): 1839-1843, 2004. DOI: 10.1093/ps/83.11.1839
332. Karakilcik AZ, Zerin M, Arslan O, Nazligul Y, Vural H: Effects of vitamin C and E on liver enzymes and biochemical parameters of rabbits exposed to aflatoxin B1. *Vet Hum Toxicol*, 46 (4): 190-192, 2004.
333. Solcan C, Gogu M, Floristean V, Oprisan B, Solcan G: The hepatoprotective effect of sea buckthorn (*Hippophae rhamnoides*) berries on induced aflatoxin B1 poisoning in chickens 1. *Poult Sci*, 92 (4): 966-974, 2013. DOI: 10.3382/ps.2012-02572
334. Li Y, Ma QG, Zhao LH, Guo YQ, Duan GX, Zhang JY, Ji C: Protective efficacy of alpha-lipoic acid against aflatoxin B1-induced oxidative damage in the liver. *Asian-Aust J Anim Sci*, 27 (6): 907-915, 2014. DOI: 10.5713/ajas.2013.13588
335. Sridhar M, Suganthi RU, Thammiah V: Effect of dietary resveratrol in ameliorating aflatoxin B1-induced changes in broiler birds. *J Anim Physiol Anim Nutr (Berl)*, 99 (6): 1094-1104, 2015. DOI: 10.1111/jpn.12260
336. Ghadiri S, Spalenza V, Dellafiora L, Badino P, Barbarossa A, Dall'Asta C, Nebbia C, Girolami F: Modulation of aflatoxin B1 cytotoxicity and aflatoxin M1 synthesis by natural antioxidants in a bovine mammary epithelial cell line. *Toxicol In Vitro*, 57, 174-183, 2019. DOI: 10.1016/j.tiv.2019.03.002
337. Cheng P, Ishfaq M, Yu H, Yang Y, Li S, Li X, Fazlani SA, Guo W, Zhang X: Curcumin ameliorates duodenal toxicity of AFB1 in chicken through inducing P-glycoprotein and downregulating cytochrome P450 enzymes. *Poult Sci*, 99 (12): 7035-7045, 2020. DOI: 10.1016/j.psj.2020.09.055
338. Atroschi F, Rizzo A, Biese I, Salonen M, Lindberg LA, Saloniemi H: Effects of feeding T-2 toxin and deoxynivalenol on DNA and GSH contents of brain and spleen of rats supplemented with vitamin E and C and selenium combination. *J Anim Physiol Anim Nutr*, 74 (1-5): 157-164, 1995. DOI: 10.1111/j.1439-0396.1995.tb00447.x
339. Wu L, Liao P, He L, Feng Z, Ren W, Yin J, Duan J, Li T, Yin Y: Dietary L-arginine supplementation protects weanling pigs from deoxynivalenol-induced toxicity. *Toxins (Basel)*, 7 (4): 1341-1354, 2015. DOI: 10.3390/toxins7041341
340. Lu Z: Dose-dependent fumonisin B (1) hepatotoxicity and hepatocarcinogenicity, detoxification of fumonisin B (1), and suppression by isoflavones of fumonisin B (1)-promoted hepatocarcinogenesis in rats. *Iowa State University*. 1997.
341. Gbore FA, Adu OA: Ameliorative potential of vitamin E on the impact of dietary fumonisin B1 on reproductive performance of female rabbits. *J Agric Rural Develop Trop Subtrop*, 118 (2): 161-169, 2017.
342. Ledur PC, Santurio JM: Cytoprotective effects of curcumin and silymarin on PK-15 cells exposed to ochratoxin A, fumonisin B(1) and deoxynivalenol. *Toxicon*, 185, 97-103, 2020. DOI: 10.1016/j.toxicon.2020.06.025
343. Bose S, Sinha SP: Modulation of ochratoxin-produced genotoxicity in mice by vitamin C. *Food Chem Toxicol*, 32 (6): 533-537, 1994. DOI: 10.1016/0278-6915(94)90110-4
344. Hoehler D, Marquardt RR: Influence of vitamins E and C on the toxic effects of ochratoxin A and T-2 toxin in chicks. *Poult Sci*, 75 (12): 1508-1515, 1996. DOI: 10.3382/ps.0751508
345. Grosse Y, Chekir-Ghedira I, Huc A, Obrecht-Pflumio S, Dirheimer G, Bacha H, Pfohl-Leszkowicz A: Retinol, ascorbic acid and alpha-tocopherol prevent DNA adduct formation in mice treated with the mycotoxins ochratoxin A and zearalenone. *Cancer Lett*, 114 (1-2): 225-229, 1997. DOI: 10.1016/s0304-3835(97)04669-7
346. Atroschi F, Biese I, Saloniemi H, Ali-Vehmas T, Saari S, Rizzo A, Veijalainen P: Significance of apoptosis and its relationship to antioxidants after ochratoxin A administration in mice. *J Pharm Pharm Sci*, 3 (3): 281-91, 2000.
347. Shalaby AM: The opposing effect of ascorbic acid (vitamin C) on ochratoxin toxicity in Nile tilapia (*Oreochromis niloticus*). 2004.
348. Zhai S, Ruan D, Zhu Y, Li M, Ye H, Wang W, Yang L: Protective effect of curcumin on ochratoxin A-induced liver oxidative injury in duck is mediated by modulating lipid metabolism and the intestinal microbiota. *Poult Sci*, 99 (2): 1124-1134, 2020. DOI: 10.1016/j.psj.2019.10.041
349. Leal M, Shimada A, Ruiz F, Gonzalez de Mejia E: Effect of lycopene on lipid peroxidation and glutathione-dependent enzymes induced by T-2 toxin *in vivo*. *Toxicol Lett*, 109 (1-2): 1-10, 1999. DOI: 10.1016/s0378-4274(99)00062-4
350. Ghedira-Chekir I, Maaroufi K, Zakhama A, Ellouz F, Dhouib S, Creppy EE, Bacha H: Induction of a SOS repair system in lysogenic bacteria by zearalenone and its prevention by vitamin E. *Chem Biol Interact*, 113 (1): 15-25, 1998. DOI: 10.1016/s0009-2797(98)00013-1
351. Shi B, Su Y, Chang S, Sun Y, Meng X, Shan A: Vitamin C protects piglet liver against zearalenone-induced oxidative stress by modulating expression of nuclear receptors PXR and CAR and their target genes. *Food Funct*, 8 (10): 3675-3687, 2017. DOI: 10.1039/C7FO01301A
352. Gao X, Xiao ZH, Liu M, Zhang NY, Khalil MM, Gu CQ, Qi DS, Sun LH: Dietary silymarin supplementation alleviates zearalenone-induced hepatotoxicity and reproductive toxicity in rats. *J Nutr*, 148 (8): 1209-1216, 2018. DOI: 10.1093/jn/nxy114
353. Su Y, Sun Y, Ju D, Chang S, Shi B, Shan A: The detoxification effect of vitamin C on zearalenone toxicity in piglets. *Ecotoxicol Environ Saf*, 158, 284-292, 2018. DOI: 10.1016/j.ecoenv.2018.04.046

RESEARCH ARTICLE

Hybrid Ensemble Model for Lactation Milk Yield Prediction of Holstein Cows

Derviş TOPUZ^{1(*)}  Selçuk TEKGÖZ² ¹ Niğde Ömer Halisdemir University, Niğde Zübeyde Hanım Vocational School of Health Services, Department of Health Services Science, TR-51240 Niğde-TÜRKİYE² Niğde Ömer Halisdemir University, Graduate School of Natural and Applied Sciences, Department of Interdisciplinary Disaster Management, TR-51240 Niğde-TÜRKİYE**(*) Corresponding author:**

Derviş Topuz

Phone: +90 388 221 2806

Cellular phone: +90 506 881 3838

E-mail: topuz@ohu.edu.tr

How to cite this article?

Topuz D, Tekgöz S: Hybrid ensemble model for lactation milk yield prediction of Holstein cows. *Kafkas Univ Vet Fak Derg*, 31 (5): 603-611, 2025.

DOI: 10.9775/kvfd.2025.34031

Article ID: KVFD-2025-34031

Received: 07.03.2025

Accepted: 13.08.2025

Published Online: 15.09.2025

Abstract

Machine learning (ML) algorithms are widely employed across various domains to identify patterns and relationships in large datasets, and to perform tasks such as prediction and classification. This study investigates the use of machine learning techniques to predict lactation milk yield in Holstein dairy cows within the field of veterinary sciences. The dataset comprises records from 128 cows, with lactation milk yield categorized into three classes low, medium, and high based on threshold values determined by expert opinion. The independent variables include Age (in days), Days in Milk (DIM), Service Period (in days), Calving Date, and Parity. To reduce the dimensionality of the dataset, Principal Component Analysis (PCA) and Linear Discriminant Analysis (LDA) were applied. The performance of nine classification algorithms was evaluated on both the original and reduced datasets using 10-fold cross-validation and bootstrap resampling methods. Due to class imbalance in the data, the weighted F1-score was used as the primary performance metric instead of accuracy. Among the original models, the highest weighted F1-scores were achieved by Decision Tree (DT), Gradient Boosting Machine (GBM), and Extreme Gradient Boosting (XGBoost), with scores of 0.47, 0.53, and 0.51, respectively. A hybrid ensemble model developed by combining these top-performing algorithms demonstrated superior performance, yielding a weighted F1-score of 1.00, an accuracy of 1.00, and an ROC-AUC of 1.00. These findings suggest that hybrid ensemble models can provide more effective and robust solutions in veterinary applications and similar research fields.

Keywords: Machine Learning, Decision tree, Gradient boosting machine, Xgboost, Milk yield, Holstein, F1-score, AUC, Hybrid model

INTRODUCTION

Livestock production is vital for global food security and demands ongoing research to boost productivity. Effective herd management enhances animal welfare, health, and profitability, which are key to sustainable milk production [1,2]. Machine learning (ML), a branch of artificial intelligence (AI), offers advanced tools to detect complex patterns, select relevant variables, and generate accurate predictions in this context [3]. ML and AI are widely used in fields such as veterinary science, enabling improved decision-making through big data and IoT technologies [4-6]. Recent advances have accelerated AI applications in livestock, including disease detection and biometric animal monitoring, enhancing real-time herd management [4,7-12].

Many studies apply ML to predict milk yield, but results often lack reliability under real farm conditions due to milk yield's multifactorial complexity [13,14]. Traditional accuracy metrics can mislead in imbalanced datasets; therefore, weighted F1-score and ROC-AUC are preferred for performance evaluation [15]. ML has shown promise in disease detection, reproductive performance prediction, and resource optimization in dairy farming [16-20].

This study evaluated nine ML algorithms to classify Holstein cows' lactation milk yield using a dataset of 128 records with five features. Dimensionality reduction via PCA and LDA was applied. Models were assessed using 10-fold cross-validation and 50 bootstrap samples, focusing on weighted F1-score and ROC-AUC due to class imbalance. A hybrid ensemble model combining top algorithms was developed to improve prediction accuracy



and robustness. The following sections detail the data, methods, results, and the enhanced performance of the hybrid model.

MATERIAL AND METHODS

Ethical Statement

This study does not require ethical permission.

Data and Preprocessing

The study dataset comprised 128 lactation records from Holstein cows, each with five features: age (days), days in milk (DIM), service period (days), calving date, and parity. The target variable, total lactation milk yield (kg), was classified into three categories (low, medium, high) based on expert thresholds, forming a multi-class classification task. Numerical features were normalized, categorical data numerically encoded, and outliers were removed using the Local Outlier Factor (LOF) method^[21] excluding nine samples. A robust scaler minimized the effect of extreme values. Descriptive statistics and correlation analysis were conducted to examine feature relationships and multicollinearity. Class imbalance was confirmed, necessitating weighted metrics for model evaluation.

Dimensionality reduction using Principal Component Analysis (PCA) and Linear Discriminant Analysis (LDA) was applied to reduce redundancy and noise: PCA reduced features from five to three components (97% variance retained), while LDA projected data onto two discriminant axes maximizing class separability. These reduced datasets were used to train classifiers, but as no significant performance gain was observed, hyperparameter tuning was conducted on models using the full feature set (128x5).

Machine Learning Algorithms

ML algorithms identify patterns in large datasets, enabling accurate predictions on unseen data^[22]. Successful ML application depends on choosing suitable algorithms and evaluation metrics^[23,24]. Fig.1 illustrates a typical ML approach.

Common ML tasks include classification and regression, which require different algorithms. In this study, nine supervised classifiers were implemented using Python 3.9.10 and Scikit-learn libraries.

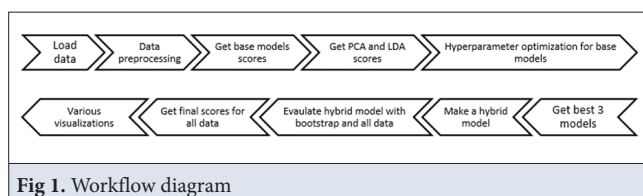


Fig 1. Workflow diagram

Decision Tree (DT): Tree-structured models split data by features and provide interpretable “if-then” rules. Pruning and tuning prevent overfitting^[25,26].

Gradient Boosting Machine (GBM): An ensemble method building trees sequentially to correct prior errors; sensitive to hyperparameters like learning rate and tree depth^[26].

Extreme Gradient Boosting (XGBoost): An optimized GBM variant with regularization and faster training, widely recognized for superior performance^[27], which has demonstrated strong performance in agricultural datasets^[28], also exhibits high tolerance to multicollinearity and missing data scenarios^[29].

Random Forest (RF): Ensemble of decision trees trained on bootstrap samples with random feature subsets, robust to overfitting and nonlinearities^[28-32].

K-Nearest Neighbors (KNN): Instance-based method classifying by majority vote of nearest neighbors using distance metrics; effective but computationally expensive in high dimensions^[33].

Hybrid Model: A voting ensemble combining DT, GBM, and XGBoost leveraged their complementary strengths to improve classification of milk yield (low, medium, high). Ensemble consensus reduces misclassification risk and enhances generalization.

Performance Evaluation Metrics and Validation

Due to class imbalance, traditional accuracy can be misleading^[11,34,35]. Thus, multiple metrics were used:

Accuracy: Ratio of correct predictions but less informative for imbalanced data (Eq. 1).

$$\text{Accuracy} = \frac{TP+TN}{FP+FN+TP+TN} \quad (1)$$

Here, *FP* denotes false positives and *FN* denotes false negatives.

Precision (P): Correct positive predictions among all positive predictions (Eq. 2).

$$\text{Precision (P)} = \frac{TP}{TP+FP} \quad (2)$$

Recall (R): Correct positive predictions among all actual positives (Eq. 3).

$$\text{Recall (R)} = \frac{TP}{TP+FN} \quad (3)$$

F1-score: Harmonic mean of precision and recall, balancing sensitivity and specificity, prioritized here with class-weighting to handle imbalance (Eq. 4)^[36,37].

$$F_1 = 2 \times \frac{P \times R}{P + R} \quad (4)$$

ROC-AUC: Threshold-independent measure of discrimination ability, calculated as weighted average over all class pairs (OvO approach)^[38].

Validation Techniques

10-Fold Cross-Validation: Dataset split into ten folds; each fold used once as test data to provide unbiased performance estimates (10% test, 90% train per fold) [39].

Bootstrap Sampling: To rigorously assess the statistical reliability, stability, and generalizability of model performance, a systematic bootstrap resampling strategy was employed in this study. This technique entails the generation of multiple resampled datasets by randomly drawing observations from the original dataset with replacement, thereby facilitating an evaluation of model behavior under varied sampling scenarios. Specifically, 50 independent bootstrap samples, each consisting of 10 randomly selected observations, were generated. These samples were subsequently used to investigate the variability in model predictions and to estimate performance stability and robustness [40]. Remarkably, the results demonstrated consistently perfect performance, with both accuracy and weighted F1-scores achieving 1.00 across all resampled datasets. These findings provide strong empirical evidence supporting the robustness, reliability, and invariance of the proposed models across varying data subsets. Furthermore, the bootstrap approach functioned as a powerful statistical tool for deriving more reliable estimates of model variance and predictive error, particularly in contexts characterized by limited data availability and potential shifts in data distribution. Overall, the methodology reinforces confidence in the models' generalization capability beyond the original training data, ensuring dependable performance in real-world applications.

Hyperparameter Tuning and Model Optimization

Hyperparameters external model settings were optimized via grid search combined with 10-fold CV to maximize

weighted F1-score. This ensured balanced performance across classes and avoided overfitting. Optimization was performed for DT, GBM, and XGBoost.

Hyperparameters were chosen considering model complexity, overfitting risk, and class differentiation. After tuning, each algorithm was retrained on the full dataset with optimal hyperparameters. This improved both individual model performance and the hybrid model's overall effectiveness. Results from the original and dimensionally reduced datasets are presented, comparing individual models and the hybrid ensemble. Evaluation focuses on metrics, especially the weighted F1-score, with comprehensive discussion of findings.

RESULTS

The creation of effective AI- and ML-based prediction systems requires a robust data pipeline, including: (1) data collection, (2) transformation into suitable formats, (3) secure storage, (4) analytical modeling and (5) presenting interpretable results. In this study, these steps were systematically applied to predict lactation milk yield. Nine classification algorithms were tested, and the effects of dimensionality reduction and model choice on performance were compared.

Step 1 - Data Collection: Relevant data were systematically gathered for analysis.

Step 2 - Data transformation: All features were standardized using the Robust Scaler (Eq. 5) and nine outliers were removed with the LOF algorithm [21].

$$\text{Robust Scaler } X_{\text{new}} = \frac{X - X_{\text{median}}}{\text{IQR}} \quad (5)$$

Step 3,4 - Data storage and data analysis: Basic statistics and correlations were examined to understand dataset

Table 1. Calculated Statistical Values for the Categories of the Dependent Variable (n=128)

Class	Number	Min.	Average	Median	Max.	Lower Bound	Upper Bound	Decision Boundaries
Low Milk Yield (0)	39	6208	7067.95	7203	7561	6926.22	7209.67	7561.2
Medium Milk Yield (1)	63	7563	8269.02	8296	8903	8168.42	8369.62	8915.6
High Milk Yield (2)	26	8924	9401.65	9409.5	9966	9289.31	9514	

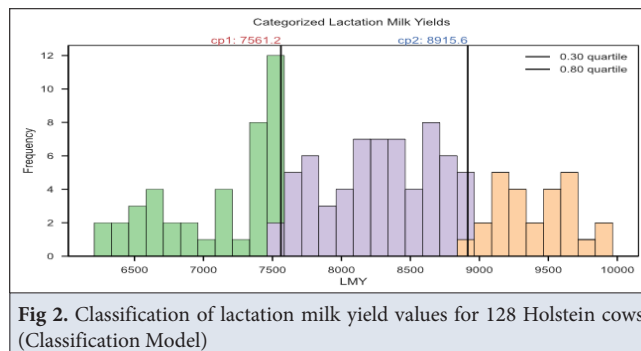


Fig 2. Classification of lactation milk yield values for 128 Holstein cows (Classification Model)

structure. A moderate negative correlation (-0.7) was found between the Milking Days Count (MDC) and Calving Date (CD), suggesting that cows with later calving dates tended to have fewer milking days. Based on expert opinion, the continuous dependent variable, lactation milk yield, was categorized into three classes (low, medium,

high) using the 30th and 80th percentiles (7.561,2 kg; 8.915,6 kg). Class imbalance was addressed by assigning higher weights to minority classes^[30]. Class distribution is shown in [Table 1](#), with a visual representation in [Fig. 2](#).

Class imbalance occurs when some classes have far more samples than others. To address this, class weights

Table 2. Performance results for all scenarios				
Algorithms		Performance Evaluation Criteria		
		Accuracy	F₁ Weighted	Roc-Auc Ovo Weighted
PCA	MLP	0.49	0.36	0.55
	LR	0.33	0.28	0.60
	KNN	0.45	0.42	0.53
	DT	0.45	0.44	0.56
	RF	0.48	0.44	0.60
	Adaboost	0.41	0.36	0.57
	GBM	0.45	0.43	0.56
	XGBoost	0.45	0.43	0.54
	LightGBM	0.41	0.40	0.57
LDA	MLP	0.52	0.41	0.58
	LR	0.34	0.27	0.61
	KNN	0.44	0.40	0.56
	DT	0.34	0.33	0.48
	RF	0.44	0.40	0.56
	Adaboost	0.47	0.40	0.58
	GBM	0.43	0.41	0.55
	XGBoost	0.41	0.40	0.53
	LightGBM	0.37	0.36	0.58
Before Hyperparameter Optimization	MLP	0.51	0.35	0.52
	LR	0.29	0.23	0.56
	KNN	0.45	0.41	0.54
	DT	0.30	0.29	0.46
	RF	0.45	0.42	0.56
	Adaboost	0.42	0.38	0.55
	GBM	0.46	0.45	0.56
	XGBoost	0.44	0.43	0.58
	LightGBM	0.38	0.37	0.57
After Hyperparameter Optimization	KNN	0.52	0.45	0.59
	DT	0.49	0.47	0.61
	RF	0.47	0.40	0.65
	Adaboost	0.46	0.44	0.58
	GBM	0.55	0.53	0.68
	XGBoost	0.47	0.51	0.62
	LightGBM	0.52	0.47	0.66
	Hybrid(DT+GBM+XGB)	1.00	1.00	1.00

were incorporated into the Decision Tree's Gini Index, emphasizing minority classes and improving model robustness ^[30]. Lactation milk yield was classified into low, medium, and high, with higher weights assigned to underrepresented groups.

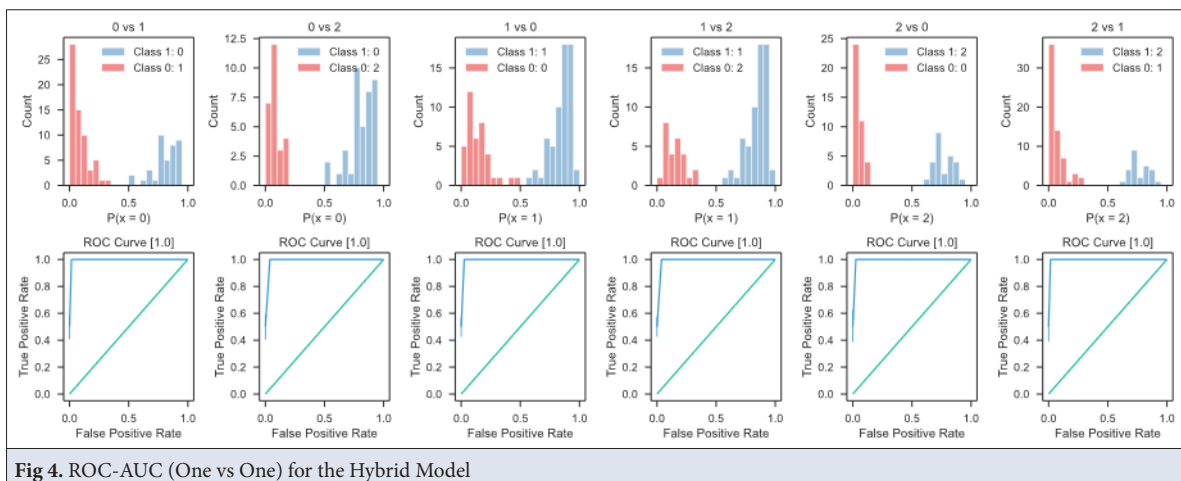
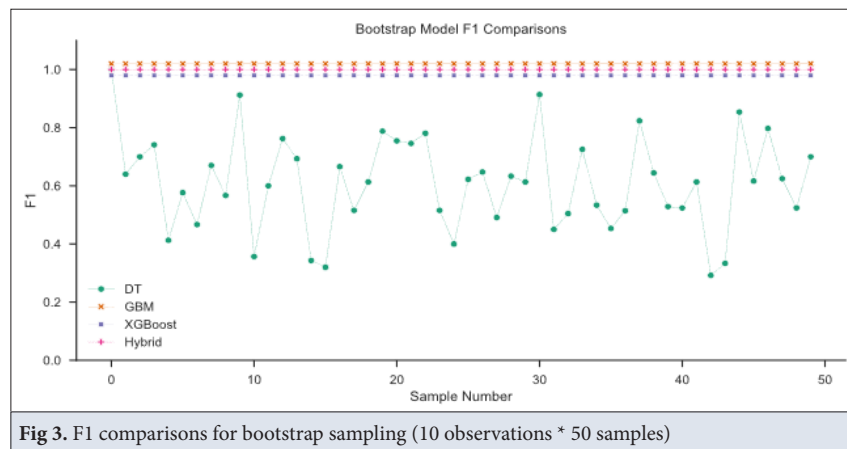
Following the training and hyperparameter tuning procedures described in previous sections, the models were evaluated on three different datasets: (a) the original feature set, (b) features reduced via Principal Component Analysis (PCA), and (c) features reduced via Linear Discriminant Analysis (LDA). Performance results for these scenarios, obtained via 10-fold cross-validation, are presented in *Table 2*.

The results obtained through PCA and LDA indicate that most models experienced either a slight decrease in performance or yielded comparable outcomes. This suggests that reducing the feature space to two components did not significantly enhance model learning. This finding is expected, as the original dataset contained only five features; thus, reducing it to two components may have resulted in some information loss. Nevertheless, the performance differences were generally minor for instance, the Random Forest (RF) model achieved a weighted F1 score of 0.42 on the original dataset and 0.40 with LDA.

These analyses provided valuable insights into the impact of dimensionality reduction on model performance. At this stage, the models achieving the highest F1 scores were GBM, XGBoost, and RF. The classification accuracies of the hybrid model developed using the bootstrap sampling method were compared with those of DT, GBM, and XGBoost. For this analysis, 50 bootstrap samples were generated, each containing 10 observations. Under these bootstrap sampling conditions, the accuracy scores of DT, GBM, XGBoost, and the hybrid model were evaluated. As a result, the average accuracy and weighted F1 score were obtained as 1.00.

Fig. 3 illustrates the distribution of weighted F1 scores for individual models across bootstrap samples. While the Decision Tree (DT) model shows considerable fluctuation, the other models and the hybrid model consistently achieved a perfect score, exhibiting the highest and most stable performance across all bootstrap subsets. The same experiment was repeated to verify accuracy, and identical results were obtained.

The proposed hybrid model's weighted ROC-AUC scores were evaluated across all possible pairwise class combinations using a One-vs-One (OvO) approach to provide a more detailed assessment of its performance.



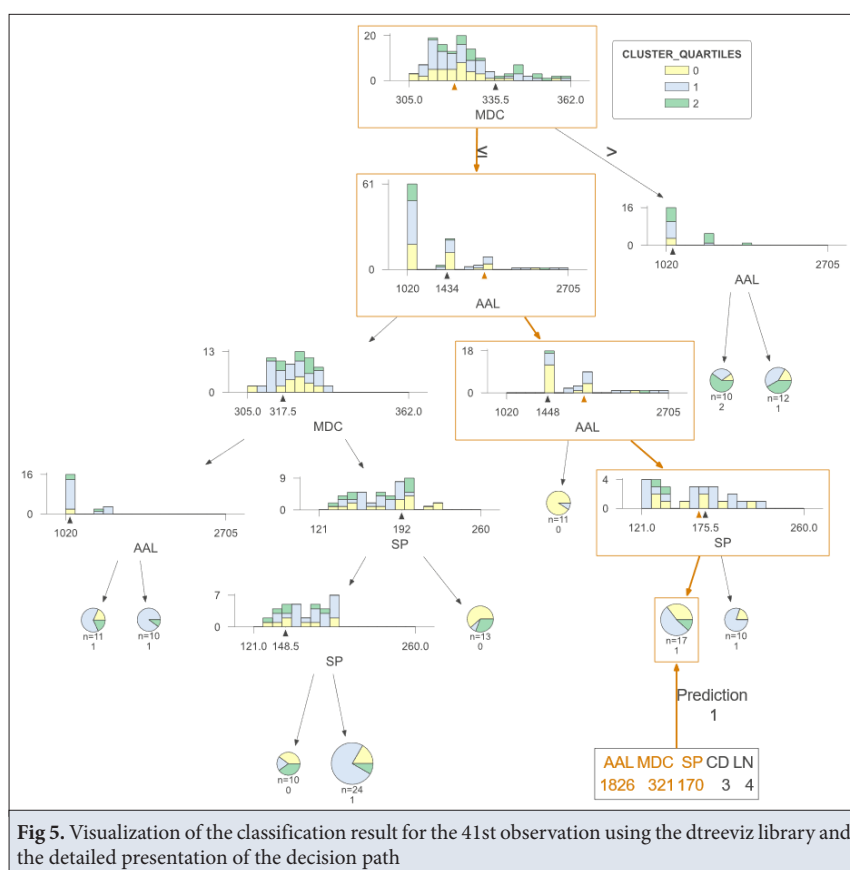


Fig 5. Visualization of the classification result for the 41st observation using the dtreeviz library and the detailed presentation of the decision path

These analyses offer a more comprehensive understanding of the model's ability to discriminate between classes, highlighting its effectiveness in multiclass classification scenarios. The AUC score for all possible pairs was 1.00. Visualizations of these findings are presented in Fig. 4.

Variable importance scores were calculated to identify the most influential variables in the decision-making process of the Decision Tree (DT), Gradient Boosting Machine (GBM), and XGBoost models, which yielded the best scores after hyperparameter optimization. Service Period (SP) was identified as the most important variable for the DT model, Animal's Age in Lactation (AAL) for the GBM model, and Milking Days Count (MDC) for the XGBoost model. These findings are intuitively significant, as longer milking durations and appropriate insemination intervals are generally associated with higher total milk production.

In addition, to analyze how the model makes individual predictions, a detailed examination of the decision path was conducted. In this context, the classification path followed by the Decision Tree model for cow number 41, which was selected to evaluate classification accuracy and overall model performance, is presented in Fig. 5. This approach serves as a crucial example for understanding the model's decision-making process more transparently. Such individual case studies reveal not only the statistical performance of the model but also its interpretability

for practical field applications [25].

The hybrid ensemble model, combining GBM, XGBoost, and DT via majority voting, outperformed all individual models, raising the best single-model F1-score (GBM: 0.53) to 1.00. This reflects the complementary strengths of tree-based and boosting methods, producing a robust classification framework. Cross-validation and bootstrap resampling helped mitigate overfitting, though the small, imbalanced dataset remains a limitation.

The study aimed to classify Holstein cows' milk yield (low, medium, high) using five features from 128 samples. Preprocessing included scaling, outlier removal, and correlation analysis. PCA and LDA were tested but discarded due to no performance gain. Nine algorithms were evaluated with weighted F1-score as the main metric. Boosting-based methods performed best after hyperparameter tuning, but the hybrid model achieved perfect separation, offering a reliable decision-support tool under similar constraints.

DISCUSSION

This study demonstrated that the lactation milk yield levels (low, medium, high) of Holstein cows can be classified with high accuracy using supervised machine learning algorithms. In particular, the hybrid model integrating the strengths of Decision Tree (DT), Gradient

Boosting Machine (GBM), and XGBoost achieved outstanding classification performance, with a weighted F1-score of 1.00. This result underscores the effectiveness of ensemble methods, even in the presence of challenges such as limited data and class imbalance. Previous studies have reported that boosting-based algorithms are capable of building robust and reliable models by reducing the risk of overfitting, especially in small and complex datasets [41-43]. In this study, the inclusion of biologically meaningful features such as age, number of lactations, insemination interval, and number of milking days played a crucial role in model performance. Proper integration of relevant biological and management-related factors directly enhanced classification accuracy. These findings emphasize that in cases of limited data, careful feature selection and preparation significantly improve model performance. Despite the pronounced class imbalance within the dataset, the model delivered high accuracy. In particular, the correct classification of low-yield cows was supported by highly sensitive performance metrics such as the weighted F1-score and ROC-AUC. The elimination of outliers, as well as preprocessing steps like data standardization and hyperparameter optimization, contributed significantly to reducing the negative impact of class imbalance. This finding confirms that appropriate data handling and modeling techniques can effectively address the challenges posed by imbalanced datasets [44-46].

This study makes a significant contribution to the development of decision support systems at the individual animal level. While previous research has primarily focused on farm-level management strategies using unsupervised learning techniques [13], the present study employs supervised algorithms to classify the lactation yield level of each cow individually. This enables the implementation of personalized, producer-specific management decisions. Furthermore, the use of a hybrid model that combines the complementary strengths of different algorithms has overcome the limitations of single-model approaches, resulting in more stable, reliable, and generalizable outcomes [47,48].

The study has several important limitations. First, the dataset used was exclusively composed of Holstein cattle from a single farm located in one geographic region. This restricts the generalizability of the model to other breeds (e.g., Jersey, Brown Swiss, Guernsey, Milking Shorthorn) or different environmental and management conditions. As highlighted in the literature, machine learning models often require retraining and validation to ensure their applicability across diverse environmental and operational contexts [49,50]. Secondly, the developed model was designed solely for classification purposes and does not provide quantitative predictions of milk yield. Employing regression-based models could offer more

functional insights for production planning by enabling direct estimation of milk output [51,52]. Lastly, the model focuses exclusively on milk yield and does not incorporate other key production parameters such as fertility, feed intake, and health status. Integrating these factors would enable the development of a more comprehensive and holistic decision support system [53,54].

The integration of data-driven decision support systems into animal production processes not only enhances production efficiency but also contributes to the development of sustainable management approaches that prioritize animal welfare [55,56]. Advanced studies in this direction will facilitate the real-time application of data-based models, enabling production processes to be managed in a more traceable, optimized, and ethically grounded manner. Consequently, this will lead to scientific and practical solutions aimed at improving both economic performance and ensuring animal health and welfare.

This study demonstrated that machine learning methods can effectively classify lactation milk yield levels in Holstein cows with high accuracy, even under limited and imbalanced data conditions. The superior performance of the hybrid model highlights the critical role of carefully selected biologically relevant variables and comprehensive data preprocessing strategies in model success. The findings support the development of individual animal-based, data-driven decision support systems and emphasize the potential of artificial intelligence applications to enhance both productivity and animal welfare in livestock farming. However, the model's reliance on data from a single breed and a geographically limited region presents a constraint regarding its generalizability. Future research should focus on validating the model across different breeds and environmental conditions, expanding it with regression-based approaches for quantitative yield prediction, and integrating additional key production parameters such as health, fertility, and feed intake.

Such advancements would facilitate the integration of data-driven AI applications into real-time, sustainable, and ethical livestock management systems ultimately contributing to improved economic performance and enhanced animal welfare.

DECLARATIONS

Availability of Data and Materials: Data and materials for this research are available upon request.

Acknowledgments: The corresponding author would like to express his heartfelt gratitude to his graduate student for the unwavering support during this research. The authors would also like to thank the reviewers for their careful, constructive, and insightful comments regarding this work.

Funding: This research did not receive any specific grant from funding.

Ethical Statement: This study does not require ethical permission.

Competing Interests: The authors declared that there is no conflict of interest.

Declaration of Generative Artificial Intelligence (AI): The authors declare that the article and/or tables and figures were not written/created by AI and AI-assisted technologies.

Author Contributions: DT and ST contributed to the design of this study. DT and ST participated in the sample collection, data analysis. DT and ST wrote the original draft. All authors contributed to data collection and discussion.

REFERENCES

1. Cozzi G, Brscic M, Gottardo F: Animal welfare as a pillar of a sustainable farm animal production. *Acta Agric Slov*, 2, 23-31, 2008. DOI: 10.14720/aas-s.2008.2.19200
2. Bell MJ, Wall E, Russell G, Roberts DJ, Simm G: Risk factors for culling in Holstein-Friesian dairy cows. *Vet Rec*, 167 (7): 238-240, 2010. DOI: 10.1136/vr.c4267
3. Bahoo S, Cucculelli M, Qamar D: Artificial intelligence and corporate innovation: A review and research agenda. *Technol Forecast Soc Change*, 188:122264, 2023. DOI: 10.1016/j.techfore.2022.122264
4. Rutten CJ, Velthuis AGJ, Steeneveld W, Hogeveen H: Invited review: Sensors to support health management on dairy farms. *J Dairy Sci*, 96 (4): 1928-1952, 2013. DOI: 10.3168/jds.2012-6107
5. Rorie RW, Bilby TR, Lester TD: Application of electronic estrus detection technologies to reproductive management of cattle. *Theriogenology*, 57 (1): 137-148, 2002. DOI: 10.1016/S0093-691X(01)00663-X
6. Firk R, Stamer E, Junge W, Krieter J: Automation of oestrus detection in dairy cows: A review. *Live Prod Sci*, 75 (3): 219-232, 2002. DOI: 10.1016/S0301-6226(01)00323-2
7. Fatima M, Pasha M: Survey of machine learning algorithms for disease diagnostic. *J Intell Learn Syst Appl*, 9 (1): 1-16, 2017. DOI: 10.4236/jilsa.2017.91001
8. Cihan P: Horse surgery and survival prediction with artificial intelligence models: Performance comparison of original, imputed, balanced, and feature-selected datasets. *Kafkas Univ Vet Fak Derg*, 30 (2): 233-241, 2024. DOI: 10.9775/kvfd.2023.30908
9. Koklu M, Ozkan IA: Multiclass classification of dry beans using computer vision and machine learning techniques. *Comput Electron Agric*, 174:105507, 2020. DOI: 10.1016/j.compag.2020.105507
10. Cihan P, Gökçe E, Kalıpsız O: A review of machine learning applications in veterinary field. *Kafkas Univ Vet Fak Derg*, 23 (4): 673-680, 2017. DOI: 10.9775/kvfd.2016.17281
11. Ozger ZB, Cihan P, Gokce E: A Systematic review of IoT technology and applications in animals. *Kafkas Univ Vet Fak Derg*, 30 (4): 411-431, 2024. DOI: 10.9775/kvfd.2024.31866
12. Cihan P, Saygılı A, Özmen NE, Akyüzlü M: Identification and recognition of animals from biometric markers using computer vision approaches: A review. *Kafkas Univ Vet Fak Derg*, 29 (6): 581-593, 2023. DOI: 10.9775/kvfd.2023.30265
13. Brotzman RL, Cook NB, Nordlund K, Bennett TB, Rivas AG, Döpfer D: Cluster analysis of dairy herd improvement data to discover trends in performance characteristics in large upper midwest dairy herds. *J Dairy Sci*, 98 (5): 3059-3070, 2015. DOI: 10.3168/jds.2014-8369
14. Van Klompenburg T, Kassahun A, Catal C: Crop yield prediction using machine learning: A systematic literature review. *Comput Electron Agric*, 177 (10):105709, 2020. DOI: 10.1016/j.compag.2020.105709
15. Liakos KG, Busato P, Moshou D, Pearson S, Bochtis D: Machine learning in agriculture: A review. *Sensors*, 18 (8):2674, 2018. DOI: 10.3390/s18082674
16. Topuz D: Lactation milk yield prediction with possibilistic logistic regression analysis. *Kafkas Univ Vet Fak Derg*, 27 (5): 547-557, 2021. DOI: 10.9775/kvfd.2020.25171
17. Curti PDF, Selli A, Pinto DL, Merlos-Ruiz A, Balieiro JCDC, Ventura RV: Applications of livestock monitoring devices and machine learning algorithms in animal production and reproduction: An overview. *Anim Reprod*, 20 (2):e20230077, 2023. DOI: 10.1590/1984-3143-AR2023-0077
18. Cihan P, Gökçe E, Atakişi O, Kırmızıgül AH, Erdoğan HM: Prediction of immunoglobulin G in lambs with artificial intelligence methods. *Kafkas Univ Vet Fak Derg*, 27 (1): 21-27, 2021. DOI: 10.9775/kvfd.. 2020.24642
19. Caraviello DZ, Weigel KA, Craven M, Gianola D, Cook NB, Nordlund KV, Fricke PM, Wiltbank MC: Analysis of reproductive performance of lactating cows on large dairy farms using machine learning algorithms. *J Dairy Sci*, 89 (12): 4703-4722, 2006. DOI: 10.3168/jds.S0022-0302(06)72521-8
20. Shine P, Murphy MD, Upton J, Scully T: Machine-learning algorithms for predicting on-farm direct water and electricity consumption on pasture based dairy farms. *Comput Electron Agric*, 150, 74-87, 2018. DOI: 10.1016/j.compag.2018.03.023
21. Breunig MM, Kriegel HP, Ng RT, Sander J: LOF: Identifying density-based local outliers. *In Proc Int Conf Manag Data*, 93-104, 2000. DOI: 10.1145/335191.335388
22. Nilsson NJ: Introduction to machine learning. An early draft of a proposed textbook, Robotic Library. Department of Computer Science, Stanford University, 1998.
23. Liu Y, Chen B, Qiao J: Development of a machine vision algorithm for recognition of peach fruit in natural scene. *Trans ASABE*, 54 (2): 695-702, 2011. DOI: 10.13031/2013.36472
24. Takma Ç, Atıl H, Aksakal V: Çoklu doğrusal regresyon ve yapay sinir ağı modellerinin laktasyon süt verimlerine uyum yeteneklerinin karşılaştırılması. *Kafkas Univ Vet Fak Derg*, 18 (6): 941-944, 2012. DOI: 10.9775/kvfd.2012.6764
25. Breiman L: Bagging predictors. *Mach Learn*, 24 (2): 123-140, 1996. DOI: 10.1007/BF00058655
26. Sarker IH: Machine learning: Algorithms, real-world applications and research directions. *SN Comput Sci*, 2 (3): 160, 2021. DOI: 10.1007/s42979-021-00592-x
27. Torlay L, Perrone-Bertolotti M, Thomas E, Baciú M: Machine learning XGBoost analysis of language networks to classify patients with epilepsy. *Brain Inform*, 4 (3): 159-169, 2017. DOI: 10.1007/s40708-017-0065-7
28. Şanlı T, Sıcaküz Ç, Yüregir OH: Comparison of the accuracy of classification algorithms on three data-sets in data mining: Example of 20 classes. *Int J Eng Sci Technol*, 12 (3): 81-89, 2020. DOI: 10.4314/ijest.v12i3.8
29. Hempstalk K, McParland S, Berry DP: Machine learning algorithms for the prediction of conception success to a given insemination in lactating dairy cows. *J Dairy Sci*, 98 (8): 5262-5273, 2015. DOI: 10.3168/jds.2014-8984
30. Gonzalez-Recio O, Weigel KA, Gianola D, Naya H, Rosa GJ: L2-boosting algorithm applied to high-dimensional problems in genomic selection. *Genet Res*, 92 (3): 227-237, 2010. DOI: 10.1017/S0016672310000261
31. Fawagreh K, Gaber MM, Elyan E: Random forests: from early developments to recent advancements. *Syst Sci Contr Eng*, 2 (1): 602-609, 2014. DOI: 10.1080/21642583.2014.956265
32. Zhu M, Xia J, Jin X, Yan M, Cai G, Yan J, Ning G: Class weights random forest algorithm for processing class imbalanced medical data. *IEEE Access*, 6, 4641-4652, 2018. DOI: 10.1109/ACCESS.2018.2789428
33. Jia BB, Zhang ML: Multi-dimensional classification via KNN feature augmentation: Pattern recognition. *Assoc Adv Artif Intell*, 106:107423, 2020. DOI: 10.1016/j.patcog.2020.107423
34. James G, Witten D, Hastie T, Tibshirani R: An introduction to statistical learning: 103 Springer Texts in Statistics New York: Springer, 2013. DOI: 10.1007/978-1-4614-7138-7
35. Sharma R, Kamble SS, Gunasekaran A, Kumar V, Kumar A: A systematic literature review on machine learning applications for sustainable agriculture supply chain performance. *Comput Oper Res*, 119:104926, 2020. DOI: 10.1016/j.cor.2020.104926
36. Lipton ZC, Elkan C, Narayanaswamy B: Optimal thresholding of classifiers to maximize F1 measure. *Mach Learn Knowl Discov Databases*,

8725, 225-239, 2014. DOI: 10.1007/978-3-662-44851-9_15

37. Shine P, Scully T, Upton J, Murphy MD: Multiple linear regression modelling of on-farm direct water and electricity consumption on pasture based dairy farms. *Comput Electron Agric*, 148, 337-346, 2018. DOI: 10.1016/j.compag.2018.02.020
38. Jaskowiak PA, Costa IG, Campello RJ: The area under the ROC curve as a measure of clustering quality. *Data Mining Knowl Discov*, 36 (3): 1219-1245, 2022. DOI: 10.1007/s10618-022-00829-0
39. Shine P, Scully T, Upton J, Shalloo L, Murphy MD: Electricity and direct water consumption on Irish pasture based dairy farms: A statistical analysis. *Appl Energy*, 210, 529-537, 2018. DOI: 10.1016/j.apenergy.2017.07.029
40. Sahinler S, Topuz D: Bootstrap and jackknife resampling algorithms for estimation of regression parameters. *JAQM*, 2 (2): 188-199, 2007.
41. Chen T, Guestrin C: Xgboost: A scalable tree boosting system. In: *Proceedings of the 22nd Acm Sigkdd International Conference on Knowledge Discovery and Data Mining*, San Francisco, 13-17 August, 785-794, 2016. DOI: 10.1145/2939672.2939785
42. Probst P, Wright MN, Boulesteix AL: Hyperparameters and tuning strategies for random forest. *WIREs Data Mining Knowl Discov*, 9 (3):e1301, 2019. DOI: 10.1002/widm.1301
43. Natekin A, Knoll A: Gradient boosting machines, a tutorial. *Front Neurobot*, 7 (21): 1-21, 2013. DOI: 10.3389/fnbot.2013.00021
44. Jafarigol E, Trafalis TA: A review of machine learning techniques in imbalanced data and future trends. *ArXiv Preprint*, 2023. DOI: 10.48550/arXiv.2310.07917
45. Haibo H, Garcia EA: Learning from imbalanced data. *IEEE Trans Knowl Data Eng*, 21 (9): 1263-1284, 2009. DOI: 10.1109/TKDE.2008.239
46. Buda M, Maki A, Mazurowski MA: A systematic study of the class imbalance problem in convolutional neural networks. *Neural Netw*, 106, 249-259, 2018. DOI: 10.1016/j.neunet.2018.07.011
47. Zhao ZQ, Zheng P, Xu ST, Wu X: Object detection with deep learning: A review. *IEEE Trans Neural Netw Learn Syst*, 30 (11): 3212-3232, 2019. DOI: 10.1109/TNNLS.2018.2876865
48. Dietterich TG: Ensemble methods in machine learning. In: *Multiple Classifier Systems, Lecture Notes in Computer Science*, 1857:1-15, Springer, Berlin, Heidelberg, 2000. DOI: 10.1007/3-540-45014-9-1
49. Parivendan SC, Sailunaz K, Neethirajan S: Socializing AI: Integrating social network analysis and deep learning for precision dairy cow monitoring. A critical review. *Animals*, 15 (13): 1835, 2025. DOI: 10.3390/ani15131835
50. Rios J: El acuerdo de paz entre el gobierno colombiano y las FARC: o cuando una paz imperfecta es mejor que una guerra perfecta. *Araucaria Rev Iberoam Filos Polit Humanid*, 19(38): 593-618, 2017. DOI: 10.12795/araucaria.2017.i38.28
51. Gonzalez-Recio O, Rosa GJ, Gianola D: Machine learning methods and predictive ability metrics for genome-wide prediction of complex traits. *Livest Sci*, 166, 217-231, 2014. DOI: 10.1016/j.livsci.2014.05.036
52. de Los Campos G, Hickey JM, Pong-Wong R, Daetwyler HD, Calus MP: Whole-genome regression and prediction methods applied to plant and animal breeding. *Genetics*, 193 (2): 327-345, 2013. DOI: 10.1534/genetics.112.143313
53. Pryce JE, Veerkamp RF: The incorporation of fertility indices in genetic improvement programs. *BSAS Occas Publ Fert*, 26 (1): 237-249, 2001. DOI: 10.1017/S0263967X00033711
54. Berry HL, Hogan A, Owen J, Rickwood D, Fragar L: Climate change and farmers mental health: Risks and responses. *Asia Pac J Public Health*, 23 (2): 119-132, 2011. DOI: 10.1177/1010539510392556
55. Wolfert S, Ge L, Verdouw C, Bogaardt MJ: Big data in smart farming - A review. *Agric Syst*, 153, 69-80, 2017. DOI: 10.1016/j.agry.2017.01.023
56. Eastwood C, Klerkx L, Ayre M, Dela Rue B: Managing socio-ethical challenges in the development of smart farming: From a fragmented to a comprehensive approach for responsible research and innovation. *J Agric Environ Ethics*, 32 (5): 741-768, 2019. DOI: 10.1007/s10806-017-9704-5

RESEARCH ARTICLE

Effects of Different Time Schedules for Regrouping on Socio-Positive Behaviors in Group-Housed Rabbit Does

Metin PETEK ^{1 (*)}  Sabine G. GEBHARDT-HENRICH ² 

¹ Bursa Uludag University, Faculty of Veterinary Medicine, Animal Science Department, TR-16059 Bursa - TÜRKİYE

² University of Bern, Vetsuisse Faculty, Veterinary Public Health Institute, Division of Animal Welfare, Center for Proper Housing: Poultry and Rabbits, Zollikofen, Bern, SWITZERLAND



(*) Corresponding author:

Metin Petek
Phone: +90 224 294 1352
Cellular phone: +90 554 959 5994
Fax: +90 224 294 1200
E-mail: petek@uludag.edu.tr

How to cite this article?

Petek M, Gebhardt-Henrich SG: Effects of different time schedules for regrouping on socio-positive behaviors in group-housed rabbit does. *Kafkas Univ Vet Fak Derg*, 31 (5): 613-618, 2025.
DOI: 10.9775/kvfd.2025.34134

Article ID: KVFD-2025-34134

Received: 26.03.2025

Accepted: 05.09.2025

Published Online: 15.09.2025

Abstract

Many studies have demonstrated that group housing of does often results in aggression and sometimes lesions due to biting. However, the positive interactions among reproducing does in group housing systems is less clear. The present descriptive study used video material of a part-time group housing system to examine socio-positive behaviour of does after postpartum separation of various lengths. The existing video records were collected from does which were kept in a part-time group housing system in a commercial farm. Each pen consisted of individual cages and two common areas. Three different time schedules/treatments for regrouping were applied in the study. Eight does were grouped on either day 12, 18 or 22 post-partum after insemination on day 8 post-partum. The does were individually marked using distinctive livestock spray markings. A previously developed ethogram of sociopositive behaviors and photos were used to identify the behavior. Individual behavior of does, its length and location were coded from 3.00 to 6.00 am and from 15.00 to 18.00 pm for every treatment. There were significant differences for the behaviour of locomotion, sharing the same feeder and lying in the common area among the groups ($P < 0.05$). There were no significant effects of daytime and treatment on the total number of behaviors and on the locations where any behaviour observed in the groups. As a conclusion; it was determined that the group housed rabbit does exhibit meaningful socio-positive behaviours. Lying in the common areas, running or walking were the most expressed positive behaviour by does in every treatment.

Keywords: Rabbit does, Part-time group housing, Positive behaviour

INTRODUCTION

In commercial rabbit production, the group housing system has been considered due to the public's concerns about rabbit welfare. In terms of the social nature of rabbits ^[1,2], a group housing system has the potential for socio-positive interactions between the does and potentially increase their welfare ^[3]. However, aggression and serious behavioural problems among rabbits sometimes might be common in group housing systems ^[4,5]. In addition, there might be a direct aggressive attack between kits and other does resulting injuries or death of kits. This is a crucial problem in terms of animal health and welfare in commercial production despite various efforts in practice to solve aggression among females.

Scientific research is looking for a balance between welfare and productivity through new housing designs, prioritizing the ethology of the species. Rabbit owners

should be encouraged to meet the need for rabbits to be housed with an appropriate conspecific in a suitably large, sheltered enclosure ^[6]. Effects of different types of flooring, cage sizes, densities, and group sizes are studied depending on the physiological and psychological needs of the productive stage of the animal ^[7]. In some studies ^[8-10], it has been stated that rabbits show lots of initiative to establish social contact, and this can help improving the wellbeing of the animals during their productive life and thus is an aspect of positive welfare.

Rabbit does are highly territorial, sensorial, and hierarchical animals and they rely on olfactory communication among each other ^[11]. A part-time group housing system allows the animals to express a wider spectrum of socio-positive behaviour and it provides an alternative for continuous group housing systems which have low production. Regrouping female rabbits in group-housing systems after the birth of their kits is common management practice



in rabbit production. But, the regrouping of female rabbits can lead to injuries and chronic stress ^[12], thereby compromising both animal welfare and production. Previous studies about group housing of female rabbits focused on agonistic behavior that may occur between the animals when hierarchy was established ^[13,14]. Rabbits in group housing can display a wider range of behavioural patterns, such as running, walking, and exploration ^[15]. Part-time group housing systems have proven to have potential but cannot yet be recommended in farms until major problems of increased aggression and injuries among does and kits are solved ^[16].

In recent years, there has been a new approach to exploring positive experiences for animals in their environment ^[17]. In contrast to previous studies focusing on the negative effects of re-grouping on rabbit welfare ^[18,19], very little attention has been given to the positive behavior of rabbit does. This study was conducted to determine the socio-positive behaviours of group housed rabbits after parturition, an area that has received insufficient exploration in the existing literature. Another aim of this study was to determine the location selected for behaviour and length of some positive indicators of rabbit does.

MATERIAL AND METHODS

Ethical Statement

Since the data were obtained from video recordings and no live animals were used in this study, ethical approval was not required.

Experimental Design

This study analyzed existing videos previously recorded on individual does for the study of agonistic behavior by Braconnier et al. ^[13] and Munari et al. ^[20]. The existing video records were collected from does which were kept in a part-time group housing system, including eight does per pen, on a commercial rabbit farm in Switzerland. They were reared according to a Swiss animal-friendly label programme, which requires group housing of females and a separated nest for each doe. In this part-time group housing system, the does were kept in groups with their kits during the lactation period.

Different postpartum (pp) regrouping schedules were used resulting in three different time schedules (treatments), which were applied in this study to evaluate their effects on socio-positive behaviors of does ^[13]: the first treatment group (T12) was group-housed at 12 days pp (day postpartum; dpp), the second one (T18) at 18 dpp and the third treatment group (T22) at 22 dpp after regrouping.

One day before parturition, the does were separated from each other. After artificial insemination applied 10 days after parturition (pp), the groups (T12, T18 and T22)

were re-grouped on day 12, on day 18 and on day 22 pp, respectively, by removing the separating grids of the separable areas and giving the does access to all areas of the pen.

Each treatment group consisted of 8 female animals. To facilitate individual monitoring, the does were individually differentiated using distinctive livestock spray markings and named according to the marks on their coats.

Housing Conditions and Feeding

Pen consisted of individual cages and two common areas. Common area one (Ca1) was situated on the ground level while common area two (Ca2), situated in front of the individual cages and food dispensers was located on the upper level. Common area one was covered with straw. The common area two consisted of two elevated platforms, one platform for each side, with a wooden floor where the (open) cages are situated. Each cage contained a nestbox with a feeder displayed outside on the common area and a nipple drinker. The boxes were open with free access to the common wooden platform during part of the breeding cycle. The does had ad libitum access to water, hay, and commercial rabbit pellets (UFA 925, UFA AG, Herzogenbuchsee, Switzerland).

Video Recording and Analysis

Video recording in the first treatment group was conducted between day 12 and 13 postpartum (T12), the second treatment group was filmed between day 18 and 19 (T18) and the last treatment group was filmed between day 22 and 23 (T22), shortly after regrouping. The socio positive and locomotory behaviors of animals were determined by watching the existing videos of selected hours in three groups. The positive behaviour was coded between 3.00-6.00 and between 15.00 to 18.00 for every treatment. In total, we analysed 18 h of continuous video of rabbit does ^[21]. An ethogram and photos made previously by Gebhard-Henrich et al. ^[21] and Niedermann ^[9] were used to code doe behaviors (*Table 1*). The ethogram was structured according to the behaviors displayed by does. All the activity that could be classified as positive behaviors were noted and coded according to the ethogram. All does were included in the analyses as focal animals. The behavior was registered in an excel table during the targeted time period. The activities that could be classified as positive behaviors (friendly interactions and non-aggressive locomotor exercise) were noted and coded as work-out, i.e. running or jumping (wo), sniffing (s), proximity (p), sharing the same box (sb), sharing the same feeder (fo) and lying in the common area (lca). The type of the behavior, location (in the lower, Ca1, or the upper level, Ca2, or both) and length of the state behavior were documented.

Table 1. Ethogram describing the positive behavior observed in does in the study

Behavior	Description
Proximity	Two does sharing common space in close proximity/within one animal length
Sharing the same box	At least two or more does share the same box with or without young ones
Sharing the same feeder	One does eats from another doe's feeder or two does feed at the same feeder with or without interactions
Sniffing	Two does with their noses sniffing each other without touching
Lying in common area	Does lie alone or together with others in any of common area
Locomotion/work-out	Work-out like walking, running or jumping

Statistical Analysis

The average percentage of the behaviour according to treatment, daytime and locations were calculated in the groups and presented with the graphs. Length of certain behaviour was expressed as mean \pm standard error for each treatment groups (T11, T18, T22) and time of day (am or pm). Two-way analysis of variance (ANOVA) was used to evaluate the effects of the treatment, time of day, and their interactions on the frequency of the behaviour after

normality of data distribution ^[23,24]. Statistical analyses were conducted using SPSS software, version 28 ^[25], with a significance level of $P < 0.05$ considered as statistically significant.

RESULTS

Frequency of total positive behaviors observed per hour between 03:00 and 06:00 am and pm are presented in *Fig. 1*. There were no significant effects of time of day ($P < 0.316$) and treatment ($P < 0.446$) on the total number of behaviors observed in the groups while time of day x treatment interaction for the total number of behaviour was found not to be significant ($P < 0.434$).

The total number of every positive behaviour as they occurred between am and pm period, including all treatments, are showed in *Fig. 2*. There were significant differences for the percentage of locomotion, sharing the same feeder and lying in the common area among the groups ($P < 0.05$).

The average length of some positive behaviours lasting longer than 50 sec. in all groups in selected time periods are presented in *Table 2*. There were no significant effects of day-time or treatment on the behaviour of sharing the same feeder and lying in the common area. No significant day time x treatment interactions was observed for sharing

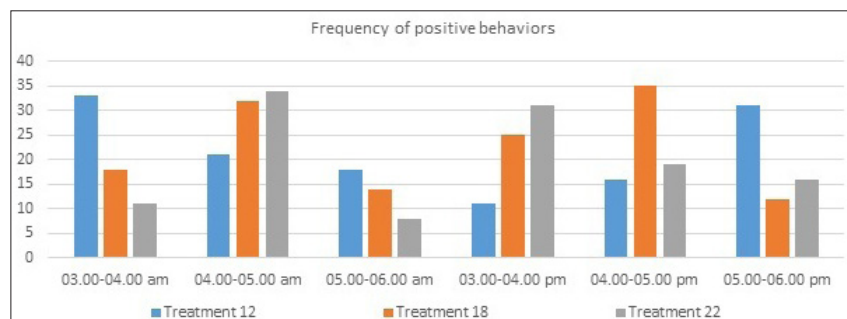


Fig 1. Frequency of total positive behaviors from 03:00 to 06:00 am and pm. The bars show the total number of positive behaviors, per hour. All the coded behaviors for each treatment (T12, T18, and T22) were summed together

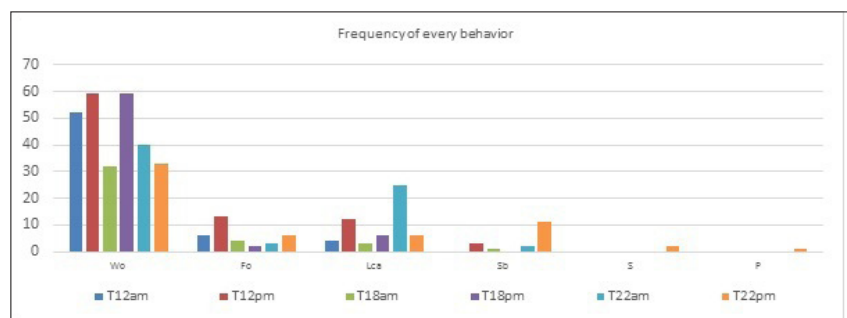
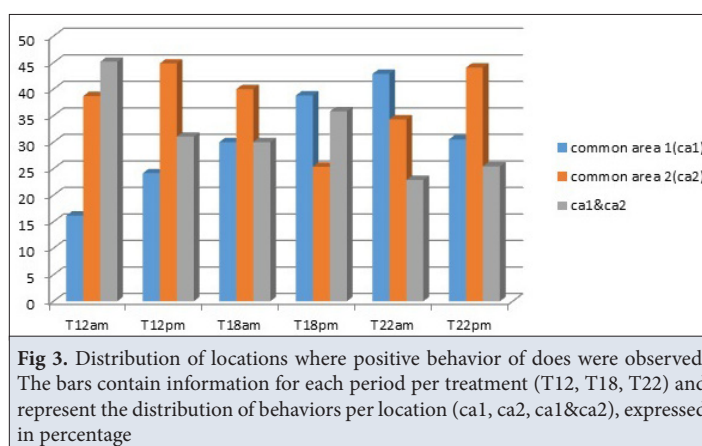


Fig 2. Distribution of every positive behavior per am or pm/per treatment (T12, T18, T22). The bars show the number of every positive behavior occurring between 03:00 to 06:00 am and 03:00 to 06:00 pm, per hour (Wo: Locomotion/work out, Fo: sharing the same feeder, Lca: lying in the common area, Sb: sharing the same box, S: sniffing, p: proximity)

Table 2. Average length of some behaviors observed in the groups (s)			
Treatment		Sharing the Same Feeder	Lying in Common Area
DayTime	am	214.72±42.31	316.85±59.30
	pm	114.63±42.12	347.58±50.25
Treatment	T12	181.87±36.16	324.13±64.87
	T18	120.00±63.46	275.25±79.44
	T22	192.17±51.81	397.27±55.44
DayTime x Treatment	amxT12	214.50±59.82	428.75±112.35
	amxT18	174.00±73.27	207.67±129.73
	amxT22	255.67±84.61	314.13±46.85
	pmxT12	149.23±40.65	219.50±64.87
	pmxT18	66.00±103.63	342.83±91.73
	pmxT22	128.67±59.82	480.40±100.49
ANOVA	DayTime	0.105	0.694
	Treatment	0.644	0.421
	DayTime x Treatment	0.877	0.080



the same feeder or lying in the common area behaviours of does.

Distribution of locations where positive behaviour was observed according to time of day is showed in Fig. 3. There were no significant effects of treatment ($P<0.250$) and daytime ($P<0.185$) on the locations where any behaviour observed. There were also no significant treatment x time of day interactions ($P<0.239$).

DISCUSSION

The welfare of rabbits is greatly influenced by the housing conditions in which they are kept. Group housing system allow breeding does to perform a wider behavioural freedom as running, jumping and social contact with other does [10]. In our study, a total of 385 activities described as positive behaviour was determined in group housed does. Of these positive behaviours, most of them occurred on day 12 and 18 of regrouping. Treatment 12 showed

most positive events (Fig. 1). In general, does were found to be least active between 05.00 to 06.00 am or pm. The lowest number of total behaviours was seen between from 05.00 to 06.00 am in T12 (11 activity in total) and T18 (8 activity) and from 04.00 to 05.00 pm in T18 (12 activity). Does in T12 were more active from 03.00 to 04.00 am and from 05.00 to 06.00 pm while does in T18 were showed more positive behaviour from 04.00 to 06.00 am and pm (56, in total) than at other times. Positive behaviours of does in T22 were the highest from 04.00 to 05.00 am (35 activity) and from 03.00 to 04.00 pm (31 activity). During the morning hours, the rabbits were less active, but during the afternoon they showed a tendency to interact with each other and move, except for treatment 22. In a study, Rooney et al. [26] reported that the mid-day period was the least active period for does.

As expected, workout (wo) like running and walking were the most expressed behaviours by does. It was found that

the frequency of locomotion in T12 pm and T18 pm was almost 58% of all total observed behaviours. Whereas, lying down was the most observed rabbit behaviour when housed in single cages ^[27]. Workout behaviour was followed by lying in the common area (lca), sharing the same feeder (Fo), and sharing the same box (Sb) behaviours for all groups. In general, feeding behaviour of rabbits varies along the day and approximately 60% of the solid ingestion takes places during the dark period ^[28]. Sniffing (s) and proximity (p) were only observed in T22. Di Vincenti and Rehling ^[29] reported that exploratory behaviour including sniffing, was found to be highest in group-housed rabbits in pens.

Behaviors of sharing the same feeder and lying in the common area lasted longer than 50 sec in every group. Although locomotion was the most common positive behaviour in the study we present the length of time for all these behavior. Because locomotion or work-out can be acceptable as event behaviors, because they lasted less than 1-4 s, sharing the same feeder and lying in the common area can be acceptable as state behaviors, because they lasted longer than 1-4 sec ^[30,31]. No significant differences for these behaviors between the groups were found in terms of daytime or treatment effects.

In general, the elevated common area (Ca2) was the most used location with 146 positive activities. The lowest ratio of positive behaviours in T12 was observed in ca1 (10 activities, in total) in both observation period. The amount of positive behaviours observed in all common areas was the highest in T12 during am and pm period (149 activities). The does in T22 preferred the ca1 during the morning period while they showed most positive behaviour in Ca2 during the afternoon. Ca1&Ca2 means that the does displayed the behaviour in both areas without interrupting. The most active does observed in both places at the same time was in T12 am.

In general, most results in our study were found to be consistent with the previous study of Niedermann ^[9]. This study is probably the first in terms of determining positive behaviour of group housed rabbit does but it has several limitations. Behavioural observations were only performed during the selected hours so some behaviours may have been missed ^[32]. The frequency of positive behaviour was found to be differed among individuals. It was much higher in two does and one of the other does did not display any of the positive behaviors during the observation period.

As conclusion, the group housed rabbit does exhibit meaningful socio-positive behaviours, suggesting that social interactions can play a beneficial role in their overall welfare. Lying in the common areas, running or walking were the most expressed positive behaviour by does in

every treatment. The data obtained from this study will contribute to understand assessment of common positive welfare and behavioural indicators of group housed rabbit does and select methods suitable for on-farm use. Furthermore, the findings will provide recommendations for the inclusion of aspects of positive welfare in farm animal welfare assessment schemes, esp. for group-housed does.

DECLARATIONS

Availability of Data and Materials: Datasets used in this experiment are available from the corresponding author on request.

Acknowledgements: A short report indicated the main findings of this paper as part of a Short-Term Scientific Mission (STSM) was published on the website of EU Cost Action project - CA21124-LIFT.

Funding Support: This research was partly supported by EU Cost Action project - CA21124 - LIFT: Lifting farm animal lives - laying the foundations for positive animal welfare (LIFT).

Competing Interest: The authors have no conflict of interest to declare in regard to this publication.

Declaration of Generative Artificial Intelligence (AI): The authors declare that the article, tables and figures were not written/created by AI and AI-assisted Technologies.

Author Contributions: Conceptualization: MP & SG, Data curation: MP & SG, Formal analysis: MP, Funding acquisition: MP & SG, Investigation: MP, Methodology: MP & SG, Project administration: MP & SG, Resources: SG, Software: SG, Supervision: SG, Validation: MP & SG, Visualization: MP & SG, Writing - original draft: MP, Writing-review and editing: MP & SG

REFERENCES

1. DiVincenti L Jr, Rehling AN: The social nature of european rabbits (*Oryctolagus cuniculus*). *J Am Assoc Lab Anim Sci*, 55 (6): 729-736, 2016.
2. Bill J, Rauterberg SL, Herbrandt S, Ligges U, Kemper N, Fels M: Agonistic behavior and social hierarchy in female domestic rabbits kept in semi-groups. *J Vet Behav*, 38, 21-31; 2020. DOI: 10.1016/j.jveb.2020.03.004
3. Cano, C, Carulla P, Villagrà A: Welfare, behavior, and housing of rabbits. In, Simões J, Monteiro JM (Eds): *Veterinary Care of Farm Rabbits*. Springer, Cham, 2024. DOI: 10.1007/978-3-031-44542-2_8
4. Szendro Z: Housing and welfare of growing rabbits. Part I: Groups size, space requirement and floor type. Lohman Information. <https://lohmman-breeders.com/files/downloads/PUBLICATIONS/LI/2024/LOHMANN-INFORMATION-housing-welfare-rabbits-EN.pdf> Accessed: October 08, 2024.
5. Kront O, Zita L, Kraus A, Moravcsíková Á, Frühauf Kolářová M, Bartoš L: Effects of genotype and housing system on rabbit does' aggressive behaviors and injuries in smallholding conditions. *Animals (Basel)*, 13 (8):1357, 2023. DOI: 10.3390/ani13081357
6. Burn C, Shields P: Do rabbits need each other? Effects of single versus paired housing on rabbit body temperature and behaviour in a UK shelter. *Anim Welfare*, 29 (2): 209-219, 2020. DOI: 10.7120/09627286.29.2.209
7. Garcia AV: Housing and rabbit welfare in breeding does. In, Argente MJ, Pardo MLGP, Dalton KP (Eds): *Lagomorpha Characteristics*. Open access peer-reviewed chapter. <https://www.intechopen.com/chapters/71955>, 2019. Accessed: January 20, 2025.
8. Dal Bosco A, Cartoni Mancinelli A, Hoy S, Martino M, Mattioli S, Cotozzolo E, Castellini C: Assessing the preference of rabbit does to social contact or seclusion: Results of different investigations. *Animals (Basel)*, 10

(2):286, 2020. DOI: 10.3390/ani10020286

9. **Niedermann H:** Sociopositive behavior in female breeding rabbits in part-time group housing. *Master's Thesis*, University of Zurich, 2022.

10. **Van Damme LGW, Ampe B, Delezie E, Rommers J, Tuytens FAM:** Social behaviour and personality profiles of breeding does housed part-time in group. *App Anim Behav Sci*, 267:106064, 2023. DOI: 10.1016/j.applanim.2023.106064

11. **Crowell-Davis S:** Rabbit behavior. *Vet Clin Exot Anim*, 24, 53-62, 2021. DOI: 10.1016/j.cvex.2020.09.002

12. **Hube D, Bill J, Knop ES, Herbrandt S, Kemper N, Fels M:** Physical injuries and hair corticosterone concentration in rabbit kits from single- and group-housed does kept on a commercial farm. *Animal*, 13 (2):196, 2023. DOI: 10.3390/ani13020196

13. **Braconnier M, Gomez Y, Gebhardt-Henrich SG:** Different regrouping schedules in semi group-housed rabbit does: Effects on agonistic behaviour, stress and lesions. *App Anim Behav Sci*, 228:105014, 2020. DOI: 10.1016/j.applanim.2020.105024

14. **Braconnier M, González-Mariscal G, Wauters J, Gebhardt-Henrich SG:** Levels of testosterone, progesterone and oestradiol in pregnant-lactating does in relation to aggression during group housing. *World Rabbit Sci*, 29, 247-261, 2021. DOI: 10.4995/wrs.2021.14897

15. **Ozella L, Sartore S, Macchi E, Manenti I, Mioletti S, Miniscalco B, Crosetto R, Ponzio P, Fiorilla E, Mugnai C:** Behaviour and welfare assessment of autochthonous slow-growing rabbits: The role of housing systems. *PLoS One*, 19 (7):e0307456, 2024. DOI: 10.1371/journal.pone.0307456

16. **Szendro Z, Trocino A, Hoy S, Xiccato G, Villagra A, Maertens L:** A review of recent research outcomes on the housing of farmed domestic rabbits: Reproducing does. *World Rabbit Sci*, 27 (1): 1-14, 2019. DOI: 10.4995/wrs.2019.10599

17. **EU CA 21124 Cost Action LIFT:** Lifting Farm Animal Lives - laying the foundations for positive animal welfare. <https://liftanimalwelfare.eu/>, 2022. Accessed: December 23, 2024.

18. **Da Silva KG, Borges TD, Costa LB, Dalmau A, Sotomaior CS:** Rabbit welfare protocols under Brazilian conditions: The applicability of welfare protocols in rabbit farms for different purposes - First results. *J Vet Behav*, 54:36-53, 2022. DOI: 10.1016/j.jveb.2022.06.002

19. **Coda KA, Fortman JD, García KD:** Behavioral effects of cage size and environmental enrichment in New Zealand white rabbits. *J Am Assoc Lab Anim Sci*, 59 (4): 356-364, 2020. DOI: 10.30802/AALAS-JAALAS-19-000136

20. **Munari C, Mugnai C, Braconnier M, Toscano MJ, Gebhardt-Henrich SG:** Effect of different management protocols for grouping does on

aggression and dominance hierarchies. *Appl Anim Behav Sci*, 227:104999, 2020. DOI: 10.1016/j.applanim.2020.104999

21. **Alfonso-Carrillo C, Martin E, De Blas C, Ibanez MA, Garcia-Ruiz AI, Garcia-Rebollar P:** Development of simplified sampling methods for behavioural data in rabbit does. *World Rabbit Sci*, 25, 87-94, 2017. DOI: 10.4995/wrs.2017.3627

22. **Gebhardt-Henrich GS, Braconnier M, Niedermann H:** Profitieren Zuchtkaninchen von der Gruppenhaltung? In, Düpjan S, Erhard M, Kemper N, Rauch E, Reiter K, Waiblinger S (Eds): Aktuelle Arbeiten zur artgemäßen Tierhaltung. 14-22, KTBL, Darmstadt, 2022.

23. **Snedecor GW, Cochran WG:** Statistical Methods. Eighth ed., Iowa State University Press, USA, 1989.

24. **Starbuck C:** Analysis of differences. In, The Fundamentals of People Analytics with applications in R. Springer, Cham. Springer, Switzerland, 2023.

25. **IBM Corp:** IBM SPSS Statistics for Windows, Version 28.0. Armonk, NY: IBM Corp, 2022.

26. **Rooney NJ, Baker PE, Blackwell EJ, Walker MG, Mullan S, Saunders RA, Suzanne DE:** Run access, hutch size and time-of-day affect welfare-relevant behaviour and faecal corticosterone in pair-housed pet rabbits. *App Anim Behav Sci*, 162:105919, 2024. DOI: 10.1016/j.applanim.2023.105919

27. **Huang Y, Breda J, Savietto D, Debrusse AM, Bonnemere JM, Gidenne T, Combes S, Fortun-Lamothe L:** Effect of housing enrichment and type of flooring on the performance and behaviour of female rabbits. *World Rabbit Sci*, 29, 275-285, 2021. DOI: 10.4995/wrs.2021.15848

28. **Gidenne T, García J, Lebas F, Licois D:** Nutrition and feeding strategy: Interactions with pathology. In, De Blas C, Wiseman J (Eds): Nutrition of the Rabbit. 179-199, Wallingford: CAB International, 2010.

29. **DiVincenti L Jr, Rehrig A:** Social behavior of adult male New Zealand white rabbits housed in groups or pairs in the laboratory. *J Appl Anim Welf Sci*, 20 (1): 86-94, 2017. DOI: 10.1080/10888705.2016.1247352







30. **Ferreira VHB, Simoni A, Germain K, Leterrier C, Lansade L, Collin A, Mignon-Grasteau S, Le Bihan-Duval E, Guettier E, Leruste H, Calandreau L, Guesdon V:** Working for food is related to range use in free-range broiler chickens. *Sci Rep*, 11:6253, 2021. DOI: 10.1038/s41598-021-85867-2

31. **Lehner PN:** Sampling methods in behavior research. *Poult Sci*, 71, 643-649, 1992. DOI: 10.3382/ps.0710643

32. **Mykytowycz R, Rowley I:** Continuous observations of the activity of the wild rabbit during 24 hour periods. *CSIRO Wildlife Res*, 3, 26 -31, 1958. DOI:10.1071/CWR9580026

RESEARCH ARTICLE

Evaluating the Multifunctional Therapeutic Potential of Phycocyanin: Antidiabetic, Antioxidant, Anticancer and Antimicrobial Effects on Metabolic, Oxidative, and Histopathological Parameters in Dithizone-Induced Diabetic Rats

Manal Abdullah ALDUWISH ¹  Nahed S. ALHARTHI ²  Asmaa Ali ALHARBI ³ 
Mody ALBALAWI ⁴  Amnah OBIDAN ⁴  Eman A. BEYARI ⁵  Hawazen K. AL-GHEFFARI ⁵ 
Amani Osman SHAKAK ^{6,7}  Aminah ALLOHIBI ⁷  Layla A. ALMUTAIRI ^{8 (*)} 
Suad Hamdan ALMASOUDI ⁹  Rabah N. ALSULAMI ¹⁰  Amin A. AL-DOAISS ¹¹ 
Abdelghafar Mohamed ABU-ELSAOUD ¹² 

¹ Department of Biology, College of Science and Humanities in Al-Kharj, Prince Sattam Bin Abdulaziz University, Alkarj 11942, SAUDI ARABIA

² Department of Medical Laboratory, College of Applied Medical Sciences in Al-Kharj, Prince Sattam Bin Abdulaziz University, Al-Kharj, 11942, SAUDI ARABIA

³ Department of Biochemistry, Faculty of Science, King Abdulaziz University, P.O. Box: 80200, Jeddah 21589, SAUDI ARABIA

⁴ Department of Biochemistry, Faculty of Science, University of Tabuk, Tabuk, 71491, SAUDI ARABIA

⁵ Department of Biological Sciences, Faculty of Science, King Abdulaziz University, Jeddah, SAUDI ARABIA

⁶ Biological Sciences Department, College of Science & Arts, King Abdulaziz University, Rabigh 21911, SAUDI ARABIA

⁷ Faculty of Medical Laboratory Sciences, University of Shendi, Shendi P.O. Box 142, SUDAN

⁸ Department of Biology, College of Science, Princess Nourah bint Abdulrahman University, P.O. Box 84428, Riyadh 11671, SAUDI ARABIA

⁹ Department of Biology, College of Sciences, Umm Al-Qura University, Makkah 21955, SAUDI ARABIA

¹⁰ Department of Biology, College of Applied Sciences, Umm Al-Qura University, SAUDI ARABIA

¹¹ Biology Department, College of Science, King Khalid University, P.O. Box 9004, Abha 61413, SAUDI ARABIA

¹² Department of Biology, College of Science, Imam Mohammad Ibn Saud Islamic University (IMSIU), Riyadh, 11623, SAUDI ARABIA

**(*) Corresponding author:**

Layla A. Almutairi

Phone: +966 50 021 2732

Fax: +966 50 021 2732

E-mail: laAlmutairi@pnu.edu.sa

How to cite this article?

Alduwish MA, Alharthi NS, Alharbi AA, Albalawi M, Obidan A, Beyari EA, Al-Gheffari HK, Shakak AO, Allohibi A, Almutairi LA, Almasoudi SH, Alsulami RN, Al-Doaiss AA, Abu-Elsaoud AM: Evaluating the multifunctional therapeutic potential of phycocyanin: Antidiabetic, antioxidant, anticancer and antimicrobial effects on metabolic, oxidative, and histopathological parameters in dithizone-induced diabetic rats. *Kafkas Univ Vet Fak Derg*, 31 (5): 619-634, 2025.

DOI: 10.9775/kvfd.2025.34347

Article ID: KVFD-2025-34347

Received: 03.05.2025

Accepted: 12.08.2025

Published Online: 20.08.2025

Abstract

Dithizone, a heavy metal chelator, induces diabetes in animals to model human diabetes. This study evaluates the effects of a phycocyanin extract (PE) from *Spirulina platensis* on growth, blood indices, oxidative status, gut microbiota, and tissue histology in dithizone-challenged rats, while also assessing its antidiabetic, antioxidant, anticancer, antimicrobial, and antiviral properties against HSV-1 and influenza A (H1N1) viruses. PE is rich in active compounds, notably C-Phycocyanin (1.2 mg/g). The extract demonstrated robust antioxidant activity by scavenging 92% of DPPH radicals, inhibited breast cancer cell line growth by 81%, and suppressed pathogenic microbes. It also reduced α -glucosidase and α -amylase activity by 75% and 80%. Antiviral assays indicated dose-dependent inhibition of HSV-1 (65% reduction in plaque formation, IC₅₀ = 42.5 μ g/mL) and H1N1 (58% viral load reduction, IC₅₀ = 50.3 μ g/mL), with suppression of viral entry, neuraminidase activity, and upregulation of antiviral genes (IFN- α and MX1). *In vivo*, 200 rats were divided into control, dithizone, PE-treated, and dithizone+PE groups for 30 days. PE treatment resulted in improved glucose control, lower HbA1c, enhanced insulin sensitivity, reduced malondialdehyde, increased glutathione, and favorable changes in gut bacteria. Gene expression of proinflammatory cytokines and precancerous markers (BCL-2, Nrf-2, OH, β -actin, IL-1 β , TNF- α , BAX, and Casp-3) was significantly reduced. Histological examination showed improved pancreatic and hepatic structure, and overall growth performance and blood profiles were enhanced. Collectively, PE mitigates metabolic disturbances from dithizone and shows promise as an antiviral agent, supporting its potential in functional foods and nutraceuticals.

Keywords: Phycocyanin, *Spirulina platensis*, Antidiabetic activity, Antioxidant activity, Anticancer, Antimicrobial, Antiviral, Dithizone-induced diabetic rats, Gut microbiota, Nutraceuticals



INTRODUCTION

With the global prevalence of chronic diseases like diabetes mellitus rising, there is increasing scientific emphasis on alternative and complementary therapies that offer beneficial effects across multiple pathological domains with minimal side effects. Diabetes mellitus, particularly, is a metabolic disorder marked by chronic hyperglycemia and is well known for its far-reaching consequences, triggering oxidative stress, tissue degeneration, dyslipidemia, chronic inflammation, heightened susceptibility to infections, and a higher incidence of certain cancers ^[1]. The dithizone-induced diabetic rat model has been widely utilized to simulate key aspects of human diabetes, including β -cell dysfunction, oxidative injury, and organ pathology, thereby providing a robust platform to evaluate interventions with both systemic and organ-specific effects ^[2].

Phycocyanin, a vibrant blue pigment-protein complex predominantly extracted from cyanobacteria such as *Spirulina platensis*, has emerged as a highly promising natural compound due to its diverse bioactive properties, notably its antidiabetic, antioxidant, anticancer, and antimicrobial activities ^[3,4]. Antidiabetic effects of phycocyanin have been demonstrated in several animal models, where phycocyanin supplementation results in significant reductions in fasting blood glucose and HbA1c levels, while also improving lipid profiles by lowering triglycerides, total cholesterol, and LDL cholesterol, and raising HDL cholesterol ^[5,6]. These metabolic improvements are often attributed to the restoration of pancreatic β -cell integrity, enhancement of endogenous insulin secretion, and activation of cellular signaling pathways such as AMPK and Akt, which collectively modulate gluconeogenesis, lipogenesis, and insulin responsiveness at a molecular level ^[7,8]. Phycocyanin not only plays a role in metabolism but is also a strong antioxidant. Its chemical structure allows it to neutralize harmful reactive oxygen species (ROS). By doing so, phycocyanin helps lower cell damage seen as reduced levels of malondialdehyde (MDA) and protein carbonylation. It also boosts the body's own antioxidants, such as superoxide dismutase (SOD), catalase, and glutathione peroxidase, making cells more resistant to oxidative stress ^[9,10]. Importantly, these protective mechanisms are mediated by upregulation of the Nrf2 pathway, conferring robust cellular defense against oxidative and inflammatory insults in tissues commonly affected by diabetes, such as the liver, kidney, and pancreas ^[10].

The anticancer potential of phycocyanin further distinguishes it from single-action natural compounds. Multiple studies have shown its ability to induce apoptosis, autophagy, and cell-cycle arrest in a range of tumor cell lines, while suppressing metastasis and angiogenesis by downregulating matrix metalloproteinases and vascular endothelial growth factors ^[11]. Notably, phycocyanin demonstrates selective cytotoxicity, effectively targeting

malignant cells with minimal toxicity toward normal tissues, and shows promise as an adjunct to conventional chemotherapeutics in preclinical models. In the context of diabetes, where the risk for carcinogenesis is elevated due to persistent inflammation and impaired immune surveillance, phycocyanin's anticancer effects are especially relevant, potentially addressing both primary and secondary disease mechanisms ^[12].

Another layer of phycocyanin's medicinal versatility is reflected in its broad-spectrum antimicrobial and immunomodulatory activities. The heightened infection risk observed in diabetic individuals is partly offset by phycocyanin's demonstrated ability to disrupt the membranes of pathogenic bacteria, inhibit biofilm formation, and modulate immune cell function, including the enhancement of lymphocyte proliferation, antibody production, and natural killer cell activity ^[13]. These actions contribute not only to the direct suppression of pathogen growth but also to faster recovery and reduced inflammatory complications in diabetic hosts. Animal studies, including those utilizing streptozin-induced diabetic rats have further validated phycocyanin's capacity to preserve histopathological integrity, protecting pancreatic islet architecture, reducing hepatic steatosis, and ameliorating renal and hepatic oxidative lesions ^[14].

The main gap lies in previous studies' reliance on broad or less specific disease models, fragmented evaluation of phycocyanin's therapeutic effects, and limited mechanistic clarity. The current study addresses these by utilizing the dithizone-induced diabetic rat, delivering comprehensive, mechanistic, and translational insights that advance phycocyanin research. Therefore, the objectives of this study are to comprehensively evaluate the medicinal potential of a phycocyanin extract derived from *Spirulina platensis* in mitigating dithizone-induced diabetes in rats. Specifically, the study aims to assess the impact of the extract on growth performance, metabolic and hematological parameters, oxidative stress markers, gut microbiota composition, and tissue histopathology. Furthermore, it investigates the extract's antidiabetic, antioxidant, anticancer, antimicrobial, and antiviral effects -particularly against HSV-1 and H1N1 viruses- alongside profiling its major phenolic compounds. Through these multifaceted approaches, the research seeks to elucidate the broad-spectrum health benefits and underlying mechanisms of phycocyanin extract in a relevant diabetes model.

MATERIALS AND METHODS

Ethical Approval

The animal study has been reviewed and approved by ZU-IACUC committee. was performed in accordance with the guidelines of the Egyptian Research Ethics Committee and the guidelines specified in the Guide for the Care and Use of Laboratory Animals (2024). Ethical code number

ZU-IACUC/2/F/497/2024. Written informed consent was obtained from the owners for the participation of their animals in this study.

***Spirulina platensis* Extract Preparation**

A pure culture of *Spirulina platensis* was recovered and grown using the Zarrouk medium created by Zarrouk in 1966. The composition of the Zarrouk medium included 1 g NaCl, 16.8 g NaHCO₃, 2.5 g NaNO₃, 0.5 g K₂HPO₄, 1 g K₂SO₄, 0.2 g MgSO₄·7H₂O, 0.04 g CaCl₂·2H₂O, 0.01 g FeSO₄·7H₂O, and 0.08 g EDTA per liter of water. Using a 1M KOH solution, the medium's pH was brought to 9.5. To initiate a fresh *Spirulina platensis* culture, 10 mL of a 5-day-old culture was added to a 250 mL amount of Zarrouk's media in 500 mL screw bottles. The bottles were placed in an environment with a constant temperature of 25± 2°C and exposed to continuous light from a 36W white fluorescent lamp with an intensity of 600-800 lux for ten days. The *Spirulina platensis* pure culture was successfully obtained through the effective streaking method on Zarrouk's media. Single culture from this strain was isolated using the streaking technique on Zarrouk's medium to produce a pure culture of *Spirulina platensis* [15]. The plates were carefully stored in an environment with a temperature of 25°C and a constant light exposure of 600 lux. Once the colonies were obtained, they were carefully collected and inspected under a microscope. Zarrouk's medium was then used to preserve the *Spirulina platensis* cells on slants.

Phycocyanin Extraction and Purification Process

To extract phycocyanin, wet biomass of *Spirulina platensis* was steeped in distilled water at a 1:25 (w/v) ratio for 24 h. Afterward, the mixture was centrifuged at 10,000 x g for 15 min at 4°C to remove cellular debris; the supernatant, containing the crude extract, was collected while the precipitate was discarded. The *Spirulina platensis* crude was adjusted to pH 7 using KOH solution (1N). The resulted crude extract was precipitated using various concentrations of ammonium sulphate (10, 15, and 40%). The efficiency of these saturation levels was then compared to the 25% ammonium sulfate method. The resulting solutions were left undisturbed for 2 h before undergoing centrifugation at 12,000 x g for 30 min. The blue precipitate obtained was subsequently dissolved in a 0.005 M Na-phosphate buffer (pH 7.0) to yield a clear solution, following the methodology described in Kamble et al. [16].

Chemical Composition of Phycocyanin Extract

The PE carbohydrate, protein, fat, moisture, fiber, and ash contents were examined using the methodology specified in AOAC [17]. Amino acid analysis is a technique that utilizes ion exchange liquid chromatography. It is widely

used in various domains to determine the qualitative and quantitative composition of substances accurately. Within biochrom systems, this fundamental concept has been enhanced to provide automated, rapid, and highly sensitive tests [18], known as classical amino acid analysis.

Phenolic Compounds Profile by LC-MS

Sample Preparation

Phenolic compounds were extracted from freeze-dried *phycocyanin* (100 mg) using 70% methanol (MeOH) in an ultrasonic bath (40 kHz, 30 min, 25°C). The extract was centrifuged (10,000 x g, 15 min, 4°C), filtered through a 0.22 µm PTFE syringe filter, and concentrated under a nitrogen stream at 40°C. The residue was reconstituted in 1 mL LC-MS grade methanol before analysis. To ensure accuracy, syringic acid-d₄ was used as an internal standard (IS), and recovery tests were performed by spiking samples with known phenolic standards. Solvent blanks were run between samples to prevent carryover contamination [19].

Chromatographic separation was performed on a C18 reversed-phase column (e.g., Zorbax Eclipse Plus, 2.1 x 100 mm, 1.8 µm) with a binary mobile phase consisting of (A) 0.1% formic acid in water and (B) 0.1% formic acid in acetonitrile. A gradient elution was applied as follows: 5% B (0-2 min), increased to 50% B (2-15 min), then to 95% B (15-20 min), held for 2 min (20-22 min), and finally re-equilibrated at 5% B (22-25 min). The flow rate was maintained at 0.3 mL/min, with a column temperature of 35°C and an injection volume of 5 µL.

Mass spectrometric detection was conducted using electrospray ionization (ESI) in negative mode with the following parameters and Full-scan data (m/z 50-1000) were acquired alongside targeted MS/MS for compound confirmation [20,21]. LC-MS data were processed using Agilent MassHunter, Thermo Xcalibur, or Skyline, with metabolite identification supported by METLIN, mzCloud, and GNPS databases.

Biological Activities of *Spirulina* Extract

Antidiabetic Activity

The α-glucosidase inhibitory activity of PE was calorimetrically assessed. Incubation of α-glucosidase with PE solutions (100, 150, 200, 250, and 300 µg/mL) was performed for 10 min at 37°C and pH 6.9. Subsequently, 50 µL of a 1 mM p-nitrophenyl-α-D-glucopyranoside solution (in phosphate buffer) was added. The reaction was terminated after a 10-min reaction period, and the optical density (OD) was measured at 405 nm. These values were then used in the equation [22].

$$\% \alpha - \text{glucosidase inhibition activity} = \frac{OD_{\text{control}} - OD_{\text{sample}}}{OD_{\text{control}}} \times 100 \quad (1)$$

Inhibitory activity against α-amylase was evaluated using

the methodology described by Nair et al.^[23] with minor adjustments. The process involved combining 50 µL of various PE concentrations with 1 mg/mL acarbose and 500 µL of α-amylase in a pH 6.8 phosphate buffer. This initial mixture was allowed to incubate for 10 min at room temperature. Subsequently, 500 µL of soluble starch was introduced, and the incubation continued under the same parameters. To terminate the reaction, 1 mL of 96 mM 3,5-dinitrosalicylic acid was added, followed by 5 min of steam heating and cooling to 25°C. The optical density was then determined at 540 nm, and these measurements were utilized in the relevant equation to ascertain the inhibitory activity.

$$\% \alpha - \text{amylase inhibition activity} = \frac{OD_{\text{control}} - OD_{\text{sample}}}{OD_{\text{control}}} \times 100 \quad (2)$$

Antioxidant Activity

The 2,2-diphenyl-1-picrylhydrazyl (DPPH) scavenging activity of PE was assessed as per Alsubhi et al.^[24]. A reaction between 0.5 mL of ethanolic DPPH and 1 mL of PE was incubated for 30 min in the dark, and the absorbance at 517 nm was measured spectrophotometrically. The IC₅₀ value reflects the minimum concentration required to scavenge 50% of the DPPH radical^[25]. The percentage of DPPH scavenging activity was calculated using the formula:

$$\% \text{ DPPH scavenging activity} = \frac{Abs_{\text{control}} - Abs_{\text{sample}}}{Abs_{\text{control}}} \times 100 \quad (3)$$

Antimicrobial Activity

The antibacterial properties of PE were tested against *Salmonella typhi*, *Bacillus cereus*, *Escherichia coli*, and *Staphylococcus aureus*. Microbial strains were preserved at 4°C by subculturing on nutrient agar slants. The antibacterial potential of the PE was evaluated using the agar well-disc diffusion method as per^[25]. After adding 50 mL of melted Muller-Hinton agar (MHA) to plates, a loopful of bacterial inoculum was evenly distributed across each plate's surface. Each plate was punctured with 8 mm wells, into which 6 mm discs soaked with 50 µL PE at levels of 100, 150, and 200 µg/mL were added. Negative control wells contained discs with water. MHA plates were then incubated for 24-48 h at 37°C. The diameters of inhibition zones (in mm) were measured to indicate antibacterial activity^[26].

The antifungal potential of PE concentrations (100, 150, 200, 250, and 300 µg/mL) was tested against pathogenic fungi: *Fusarium oxysporium*, *Fusarium oxysporium*, *Fusarium solai*, and *Aspergillus niger*. Antifungal activity of PE was quantified via a disc diffusion assay. Sabouraud dextrose agar plates were uniformly inoculated with fungal suspensions. Sterile paper discs, pre-loaded with varying concentrations of PE, were subsequently positioned on the inoculated media. Plates were incubated

at 28°C for a duration of seven days, after which the diameters of the observed inhibition zones were recorded in millimeters^[27].

Anticancer Activity

Cell Culture: MCF-7 breast carcinoma cells, acquired from Nawah Scientific Inc. (Mokatam, Cairo, Egypt), were cultured in DMEM media. This media was enriched with 100 mg/mL streptomycin, 100 units/mL penicillin, and 10% heat-inactivated fetal bovine serum. Cells were kept at 37°C in a humidified atmosphere with 5% (v/v) CO₂^[28].

Cytotoxicity Assay: The Sulforhodamine B (SRB) assay was used to determine cell viability. Briefly, 5x10³ cells/well were seeded in 96-well plates and incubated for 24 h. Cells were then treated with varying concentrations of drugs for 72 h. Following fixation with 10% trichloroacetic acid (TCA) and washing, cells were stained with 0.4% SRB for 10 min. After washing with 1% acetic acid and drying, protein-bound SRB was dissolved with 10 mM TRIS, and absorbance was measured at 540 nm using a microplate reader^[29].

$$\text{Cell survival rate (\%)} = \frac{OD_{\text{sample}} - OD_{\text{blank}}}{OD_{\text{control}} - OD_{\text{blank}}} \times 100 \quad (2)$$

Animal Behavior and Design Methodology

A total of 200 Sprague-Dawley white male albino rats from the Serum and Vaccine Center, Dokki, Giza, were used in the study, with an average weight of 150±10 g. Before the experiment, the rats were housed in cages that maintained a controlled temperature of 22-24°C and a 12-h light/12-h dark lighting schedule. This housing condition was maintained for at least 7 days. The rats were divided into five groups, each consisting of 40 (10 x 4). Subsequently, each group was assigned a distinct food item to consume for 28 days, according to the following distribution: Group I received a routine (basal) diet only. Group II received a diet and was injected intraperitoneally with 100 mg/kg b.w. dithizone (dissolved in olive oil) for 7 days. Group III received a routine (basal) diet supplemented with 100 mg/kg body weight of PE powder throughout the experimental period at the same time. Group IV received a routine (basal) diet mixed with 300 mg/kg body weight of PE powder. Group V received a mix of 300 mg/kg body weight of PE and 100 mg/kg of dithizone.

Biochemical Parameters

After the experiment, all rats were anesthetized using an R550 Multioutput Laboratory Small Animal Anesthesia Machine. This machine is designed for simultaneously anesthetizing 1-5 small animals, including rats, mice, cats, and rabbits. Each anesthesia channel can be controlled independently, and the gas flow to the induction box can be adjusted separately within a range of 0-2.0 L/min., and blood samples were obtained from the hepatic portal vein to assess the biochemical variables.

The blood samples were placed into heparin tubes to analyze the biochemical characteristics. The samples were thereafter centrifugated at 3,000 revolutions per minute for 15 min to isolate the serum. The levels of serum total cholesterol (TC), triglycerides (TG), and high-density lipoprotein cholesterol (HDL-c) were measured using enzymatic colorimetric techniques [30]. The VLDL-c concentration, measured in milligrams per deciliter, is calculated by dividing the triglyceride level by 5 [31]. The LDL-c was calculated using the following equation: The formula for calculating LDL cholesterol (LDL-c) in milligrams per deciliter (mg/dL) is as follows: $LDL-c = Total\ cholesterol\ (TC) - [HDL\ cholesterol\ (HDLc) + Very\ low-density\ lipoprotein\ cholesterol\ (VLDL-c)]$ [32]. The AST, ALT, AST/ALT ratio, and ALP were quantified using the methods outlined in reference [33]. The liver was extracted, and its tissues were washed in a chilled 0.9% saline solution (by weight or volume). The tissues were then quantified and stored at a temperature of -70°C. The levels of malondialdehyde (MDA) and the activities of superoxide dismutase (SOD), glutathione (GSH), and catalase (CAT) were estimated, following the steps described in reference [34]. Total antioxidant capacity (TAC) was also measured [35].

Liver Histopathology

The liver was preserved using 10% neutral buffered formalin immediately after removal from the animals. The fixed tissues were thereafter subjected to known histological tests [36].

Gene Expression

RNA extraction was performed using rat liver. The RNA globules were dissolved in diethylpyrocarbonate (DEPC)-treated water. The RNA concentration was measured using spectrophotometry at an optical density (OD) ratio of 260/280 [37]. The semiquantitative reverse transcription PCR used 3 µg of RNA. This process included subjecting the plate to denaturation in PCR thermocycler (Bio-Rad T100TM) at 70°C for 5 min.

Additionally, 0.5 nanograms of oligo (dT) primers were used. Two microliters of 10X RT buffer, two microliters of 10 mM dNTP, and one microliter of 100 M reverse transcriptase were mixed to make cDNA. The mixture was incubated at 42°C for 1 h and then heated at 70°C for 10 min to assure deactivation of the enzyme. To evaluate gene expression levels, densitometry was used to quantify mRNA expression, with β -actin mRNA serving as a reference standard (Table 1). The $2^{-\Delta\Delta CT}$ method was used to measure the expression levels of these genes using real-time PCR. The endogenous reference gene, actin, was used to standardize the analyzed genes. The CT values were used to examine the alterations in gene density and mRNA expression using a comparative approach.

Statistical Analysis

The data were analyzed using the SPSS program (Version 17.0). The data were reported as the mean \pm SE. Following a one-way ANOVA, Fisher's least significant difference (LSD) test was used to compare

Table 1. The primer sequence used for quantitative real-time PCR in liver rats with dithizone-induced toxicity

Gene	Entry Number	Product Size (bp)	Sequence
β -actin	NM_007393.4	140 bp	CCAGCCTTCCTTCTTGGGTA
			CAATGCCTGGGTACATGGTG
Bcl2	NM_009740	154 bp	AGCCTGAGAGCAACCCAAT
			AGCGACGAGAGAAGTCATCC
HO-1	NM_010442.1	125 bp	CGCCTCCAGAGTTTCCGCAT
			GACGCTCCATCACCGGACTG
Nrf2	NM_010902.3	139 bp	CGCCTGGGTTCACTGACTCG
			AGCACTGTGCCCTTGAGCTG
IL-1 β	NM_007393	304 bp	TAAGGCCAACCGTGAAAG
			GTACGACCAGAGGCATACAG
TNF- α	NM_000594.3	229 bp	AGGCAATAGGTTTGAGGGCCAT
			TCCTCCCTGCTCCGATTCCG
BAX	NM_001291428	108 bp	GGTTGTGCGCCCTTTCTA
			CGGAGGAAGTCCAATGTC
Casp-3	NM_004346.3	834 bp	GGAAGCGAATCAATGGACTCTGG
			GCATCGACATCTGTACCAGACC

the data. The statistical significance criterion was set at a P-value of ≤ 0.05 .

RESULTS

Chemical Composition of Phycocyanin Extract

The proximate composition analysis of the phycocyanin extract, conducted on a dry weight basis from three replicates, reveals its notable nutritional profile (Table 2). With a minimal moisture content of 3.0 g/100 g, the extract is primarily dry, contributing to its concentrated nature. It stands out as a significant protein source, comprising 65.0 g/100 g of crude protein, of which a remarkable 50.0 g/100 g is attributed specifically to phycocyanin. This high phycocyanin content underscores the efficacy of the extraction process. Additionally, the extract contains 20.0 g/100 g of total carbohydrates, with 8.5 g/100 g being dietary fiber, suggesting potential digestive benefits. Conversely, the lipid content is considerably low at 2.5 g/100 g, indicating a low-fat profile. The ash content, representing minerals, is 4.0 g/100 g. Overall, the phycocyanin extract provides a substantial energy content of 360 kcal, predominantly from its rich protein and carbohydrate composition, positioning it as a valuable ingredient for various applications requiring high protein and specific bioactive compounds.

Table 3 presents a detailed amino acid profile of PE, quantified in grams per 100 grams of protein. The analysis of the phycocyanin extract's amino acid profile, based on three replicates, indicates a high-quality protein source due to the presence of all essential amino acids. glutamic acid and aspartic acid are the most prevalent, at 112.4 mg/g protein and 98.2 mg/g protein respectively, playing crucial roles in protein structure and function. Notably, branched-chain amino acids (BCAAs) such as leucine (87.3 mg/g protein), valine (58.2 mg/g protein), and Isoleucine (39.6 mg/g protein) are well-represented, which is advantageous for muscle protein synthesis and recovery. Other essential amino acids like lysine (49.5 mg/g protein), threonine (42.1 mg/g protein), and phenylalanine (36.8 mg/g protein), along with sulfur-containing methionine (12.4 mg/g protein) and cysteine (8.3 mg/g protein), and the serotonin precursor tryptophan (14.2 mg/g protein), further contribute to the extract's comprehensive nutritional value. This complete and balanced amino acid composition suggests the phycocyanin extract's potential for use in nutritional supplements, functional foods, and other applications where a robust and readily available amino acid supply is desired.

Phenolic Compounds Profile of Phycocyanin Extract

Table 4 presents a comprehensive profile of phenolic compounds identified in *Spirulina* extract using LC-MS/MS in negative ionization mode. The LC-MS/MS analysis of

the phycocyanin extract, conducted in negative ionization mode, provides a detailed elucidation of its complex phytochemical composition, indicating a rich array of bioactive compounds. Expectedly, C-Phycocyanin subunit (1200.5 $\mu\text{g/g}$) and Allophycocyanin subunit (980.2 $\mu\text{g/g}$) are the most abundant constituents, consistent with the extract's primary nature. The fragmentation ions for C-Phycocyanin subunit are observed at m/z 1124, 843, 560, 397, while for Allophycocyanin subunit, they are 1320, 1056, 788, 512. A significant concentration of

Table 2. Proximate composition of phycocyanin extract (per 100 g dry weight \pm Standard Deviation)

Parameter	Content (g/100 g)
Moisture	3.0 \pm 0.5
Crude protein	65.0 \pm 5.0
Phycocyanin (of total protein)	50.0 \pm 4.0
Total carbohydrates	20.0 \pm 3.0
Dietary fiber	8.5 \pm 1.5
Total lipids	2.5 \pm 0.5
Ash	4.0 \pm 0.8
Energy Content	360 \pm 20 kcal

n = 3; data are presented as mean \pm SD. Different lowercase letters in the same column indicate significant variation at $P < 0.05$

Table 3. Amino Acid Profile of phycocyanin extract (g/100 g \pm Standard Deviation)

Amino Acid	Abbreviation	Content (mg/g protein)
Aspartic acid	Asp (D)	98.2 \pm 5.1
Glutamic acid	Glu (E)	112.4 \pm 6.3
Serine	Ser (S)	45.6 \pm 3.2
Glycine	Gly (G)	62.8 \pm 4.0
Histidine	His (H)	18.5 \pm 1.5
Arginine	Arg (R)	54.3 \pm 3.8
Threonine	Thr (T)	42.1 \pm 2.9
Alanine	Ala (A)	76.5 \pm 4.5
Proline	Pro (P)	33.7 \pm 2.1
Tyrosine	Tyr (Y)	28.9 \pm 8
Valine	Val (V)	58.2 \pm 3.6
Methionine	Met (M)	12.4 \pm 1.0
Cysteine	Cys (C)	8.3 \pm 0.7
Isoleucine	Ile (I)	39.6 \pm 2.4
Leucine	Leu (L)	87.3 \pm 5.2
Phenylalanine	Phe (F)	36.8 \pm 2.3
Lysine	Lys (K)	49.5 \pm 3.1
Tryptophan	Trp (W)	14.2 \pm 1.2

n = 3; data are presented as mean \pm SD. Different lowercase letters in the same column indicate significant variation at $P < 0.05$

Table 4. Phenolic compounds identified in phycocyanin extract by LC-MS/MS in negative ionization mode

Compound Name	Molecular Weight (g/mol)	Content (µg/g)	Fragmentation Ions (m/z)
C-Phycocyanin subunit	~28.000	1200.5	1124, 843, 560, 397
Allophycocyanin subunit	~30.500	980.2	1320, 1056, 788, 512
Phycocyanobilin	586.6	450.8	586, 299, 253, 165
Linolenic acid	278.4	320.3	277, 205, 149, 95
β-Carotene	536.9	210.7	536, 445, 321, 177
Pheophytin a	871.2	185.4	870, 592, 533, 461
Astaxanthin	596.8	150.9	595, 479, 401, 255
Zeaxanthin	568.9	132.6	567, 430, 375, 221
Chlorophyll a derivative	614.6	98.3	613, 555, 487, 329
Scytonemin	544.6	75.2	543, 468, 325, 211
Gallic acid	170.1	68.5	169, 125, 97, 79
Caffeic acid	180.2	55.7	179, 135, 107, 89
Ferulic acid	194.2	42.3	193, 149, 134, 117
Quercetin	302.2	38.9	301, 179, 151, 121
Kaempferol	286.2	29.6	285, 229, 185, 117
Apigenin	270.2	24.1	269, 225, 181, 117
Myricetin	318.2	18.7	317, 179, 137, 109
Indole-3-carboxylic acid	161.2	15.4	160, 116, 89, 71
p-Coumaric acid	164.2	12.8	163, 119, 93, 65
Sinapic acid	224.2	9.5	223, 178, 149, 121

Phycocyanobilin (450.8 µg/g) is also detected, presenting fragmentation ions at m/z 586, 299, 253, 165; this chromophore is crucial for the extract's antioxidant and anti-inflammatory properties. Beyond these core components, the extract contains an impressive profile of additional beneficial compounds. Notably, the essential fatty acid Linolenic acid (320.3 µg/g), with fragmentation ions at m/z 277, 205, 149, 95, is present. A strong suite of carotenoid antioxidants includes β-Carotene (210.7 µg/g) (fragmentation ions: m/z 536, 445, 321, 177), Astaxanthin (150.9 µg/g) (fragmentation ions: m/z 595, 479, 401, 255), and Zeaxanthin (132.6 µg/g) (fragmentation ions: m/z 567, 430, 375, 221), all recognized for their protective roles against oxidative stress and specific health benefits. Further enhancing the extract's complexity are chlorophyll derivatives like Pheophytin a (185.4 µg/g) and a Chlorophyll a derivative (98.3 µg/g), as well as the unique UV-absorbing compound Scytonemin (75.2 µg/g). A diverse group of phenolic acids, including Gallic acid (68.5 µg/g) with fragmentation ions at m/z 169, 125, 97, 79, Caffeic acid (55.7 µg/g), and Ferulic acid (42.3 µg/g), contribute significantly to the extract's antioxidant capacity. Prominent flavonoids such as Quercetin (38.9 µg/g) (fragmentation ions: m/z 301, 179, 151, 121), Kaempferol (29.6 µg/g), Apigenin (24.1 µg/g), and Myricetin (18.7

µg/g) further enrich the extract's biological activity, offering broad-spectrum antioxidant, anti-inflammatory, and potentially anti-carcinogenic effects.

Biological Activities of Phycocyanin Extract

Antioxidant Activity

Fig. 1 demonstrates the DPPH free radical scavenging activity of PE at concentrations ranging from 100 to 300 µg/mL, alongside that of the antioxidant

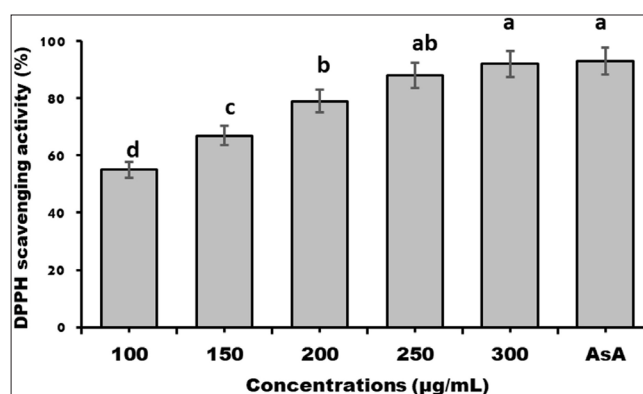


Fig 1. Antioxidant activity of phycocyanin extract against DPPH free radicals compared to ascorbic acid. Different lowercase letters above the columns indicate significant variation at $P < 0.05$

standard Ascorbic acid (AsA). *Fig. 1* illustrates a clear concentration-dependent relationship for *Spirulina* extract, with scavenging activity increasing from approximately 55% at 100 $\mu\text{g/mL}$ to around 67% at 150 $\mu\text{g/mL}$, further rising to about 80% at 200 $\mu\text{g/mL}$. The highest concentrations of PE, 250 $\mu\text{g/mL}$ and 300 $\mu\text{g/mL}$, exhibited potent scavenging activities of approximately 90-92%, statistically comparable to Ascorbic acid (93%). Statistical analysis revealed significant differences in scavenging activity between the lower concentrations of PE (100 and 150 $\mu\text{g/mL}$) and the higher concentrations (250 and 300 $\mu\text{g/mL}$) and Ascorbic acid. The IC_{50} value, representing the concentration required for 50% DPPH scavenging, can be inferred from the graph to be 120 $\mu\text{g/mL}$ for phycocyanin extract, highlighting its antioxidant potential. Ascorbic acid, with its high scavenging activity even at a concentration lower than the tested range, would have a considerably lower IC_{50} value, indicating its superior antioxidant potency compared to the tested concentrations of phycocyanin extract.

Anticancer Activity

The effect of PE on the viability of MCF-7 breast cancer cells was investigated through both microscopy and quantitative analysis (*Fig. 2*). The microscopic images illustrate the decreasing density and altered morphology of MCF-7 cells with increasing PE concentrations, with control cells appearing dense and healthy, while those treated with higher PE concentrations and doxorubicin show a sparse population with signs of cell damage (*Fig. 2-A,B,C,D*). The quantitative data, presented as a bar graph, reveals a clear dose-dependent inhibition of MCF-7 cell viability by PE. Starting with 62% viability at 100 $\mu\text{g/mL}$, the percentage of viable cells progressively decreased with increasing PE concentrations, reaching a low of 20% at 300 $\mu\text{g/mL}$ (*Fig. 2-E*). This significant reduction in viability at the highest PE concentration was comparable to the effect observed with the known chemotherapy drug doxorubicin. Statistical analysis confirmed the significant

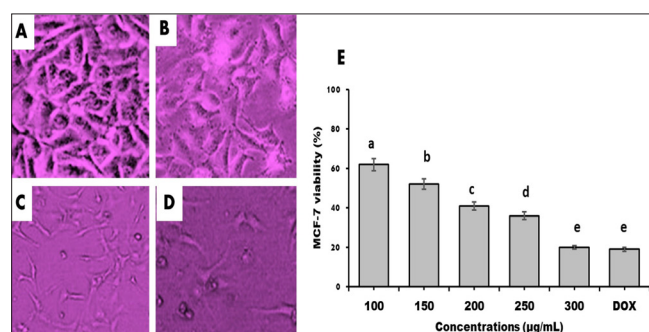


Fig 2. Microscopic images (A, B, C, D) of the effect of *phycocyanin* extract on the breast cancer cell lines compared to doxorubicin (DOX). (E) the effect of PE concentration on inhibition of the viability of MCF-7 cancer cells. Different lowercase letters above the columns indicate significant variation at $P < 0.05$

differences in cell viability across the increasing PE concentrations, highlighting the potent anti-proliferative activity of *Spirulina* extract against MCF-7 breast cancer cells in a dose-dependent manner, suggesting its potential as an anti-cancer agent.

Antidiabetic Activity

Fig. 3 illustrates the inhibitory effects PE at varying concentrations (100-300 $\mu\text{g/mL}$) on the activities of α -glucosidase (α -glu) and α -amylase (α -amyl), key

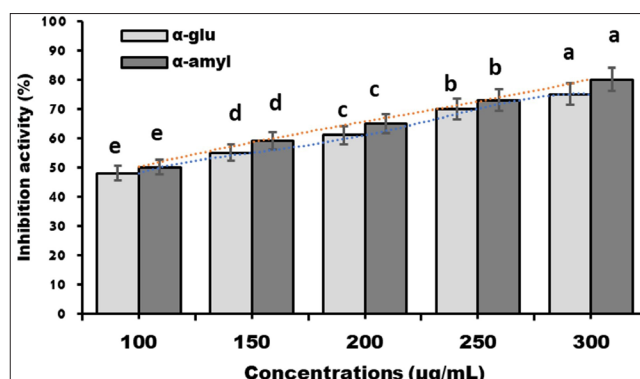


Fig 3. The inhibitory effect of PE concentrations on the activity of α -amylase and α -glucosidase. Different lowercase letters above the columns indicate significant variation at $P < 0.05$

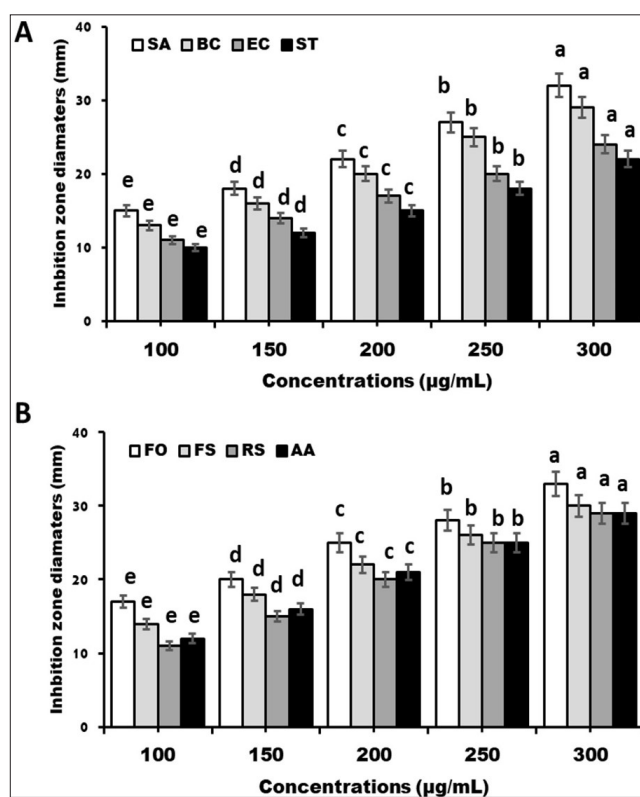


Fig 4. (A) Antibacterial activity of PE against pathogenic bacteria, *Staphylococcus aureus* (SA), *Bacillus cereus* (BC), *Escherichia coli* (EC), and *Salmonella typhi* (ST). (B) pathogenic fungi, *Fusarium oxysporium* (FO), *Fusarium solani* (FS), *Rhizoctonia solani* (RS), and *Alternaria alternata* (AA). Different lowercase letters on the columns indicate significant variation at $P < 0.05$

enzymes in carbohydrate metabolism relevant to diabetes management. For α -glucosidase, the inhibition activity increases from approximately 50% at 100 $\mu\text{g/mL}$ to around 75% at 300 $\mu\text{g/mL}$, representing a relative increase of 50% in inhibition over this concentration range. Similarly, α -amylase inhibition starts at roughly 52% at 100 $\mu\text{g/mL}$ and rises to about 80% at 300 $\mu\text{g/mL}$, showing a relative increase of approximately 54% in inhibition across the tested concentrations. Notably, the percentage of α -amylase inhibition is slightly higher at each concentration than that of α -glucosidase. Statistical analysis, denoted by the letters above the bars, confirms significant increases in inhibitory activities for both enzymes as the PE concentration rises. These findings suggest that *Spirulina* extract exhibits a dose-dependent ability to inhibit both α -glucosidase and α -amylase, with a slightly more pronounced inhibitory effect on α -amylase, indicating its potential as a natural agent for managing postprandial hyperglycemia in diabetes by hindering carbohydrate digestion and absorption.

Antimicrobial Activity

Fig. 4 presents the antimicrobial activity of PE at concentrations ranging from 100 to 300 $\mu\text{g/mL}$, measured by the diameter of the inhibition zone (mm) against several pathogenic microorganisms. Fig. 4-A illustrates the antibacterial activity of PE against four bacterial species: *S. aureus*, *B. cereus*, *E. coli*, and *S. typhi*. The results show a general trend of increasing inhibition zone diameters with increasing PE concentration for all tested bacteria. *S. aureus* consistently exhibited the largest inhibition zones across all concentrations, reaching approximately 32 mm at 300 $\mu\text{g/mL}$. *B. cereus* also showed significant inhibition, with the zone diameter increasing to 30 mm at the highest concentration. *E. coli* and *S. typhi* displayed moderate susceptibility to PE, with inhibition zones reaching approximately 24 mm and 22 mm, respectively, at 300 $\mu\text{g/mL}$. Statistical analysis, indicated by the letters above the bars, reveals significant differences in the inhibition zone diameters across the different PE concentrations for each bacterium, generally showing increased inhibition with higher concentrations.

Fig. 4-B demonstrates the antifungal activity of PE against four pathogenic fungal species: *Fusarium oxysporum*, *Fusarium solani*, *Rhizoctonia solani*, and *Alternaria alternata*. Similar to the antibacterial effects, the antifungal activity generally increased with higher PE concentrations. *F. oxysporum* showed the most sensitivity to PE, with the inhibition zone reaching approximately 30 mm at 300 $\mu\text{g/mL}$. *F. solani* also exhibited substantial inhibition, with the zone diameter increasing to around 29 mm at the highest concentration. *R. solani* and *A. alternata* displayed moderate sensitivity, with inhibition zones reaching approximately 25 mm and 28 mm, respectively, at 300

$\mu\text{g/mL}$. Statistical analysis again indicates significant differences in the inhibition zone diameters across the different PE concentrations for each fungus, with higher concentrations generally leading to larger inhibition zones.

Phycocyanin extract demonstrates both antibacterial and antifungal activities against the tested panel of pathogenic microorganisms in a concentration-dependent manner. The degree of susceptibility varied among the different species, with *S. aureus* and *F. oxysporum* showing the highest sensitivity to PE among the bacteria and fungi tested, respectively. These findings suggest the potential of PE as a natural source of antimicrobial and antifungal compounds.

Antiviral Activity

Fig. 5 clearly demonstrates the dose-dependent antiviral efficacy of the PE against both Herpes Simplex Virus type 1 (HSV-1) and Influenza A virus subtype H1N1. A consistent trend of increasing viral plaque reduction is observed for both viruses as the concentration of the substance rises from 50 $\mu\text{g/mL}$ to 300 $\mu\text{g/mL}$. Notably, the extract consistently exhibits greater effectiveness against HSV-1 across all concentrations, achieving a peak reduction approaching 90% at 300 $\mu\text{g/mL}$, compared to approximately 78-79% for H1N1 at the same concentration.

Fig. 6-A,B meticulously illustrate the phycocyanin extract's dose-dependent capacity to upregulate the relative expression of critical antiviral genes: Interferon-alpha (IFN- α) and Myxovirus resistance protein 1 (MX1). A clear and statistically significant increase in the fold change of both IFN- α and MX1 expression is observed as the extract's concentration rises from 50 $\mu\text{g/mL}$ to 300 $\mu\text{g/mL}$, unequivocally demonstrating its ability to stimulate these key components of the host's innate antiviral defense. The concomitant upregulation of IFN- α , a primary type I interferon, and MX1, a downstream interferon-stimulated

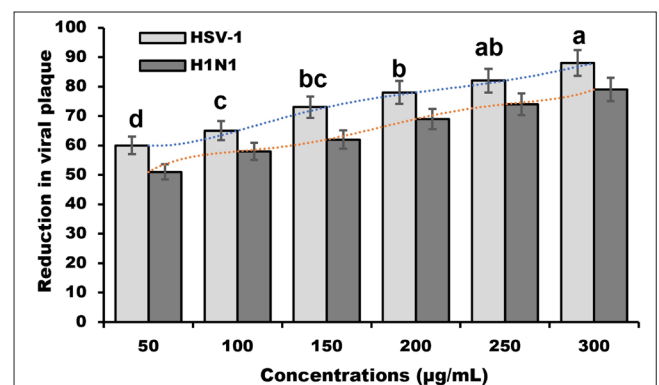
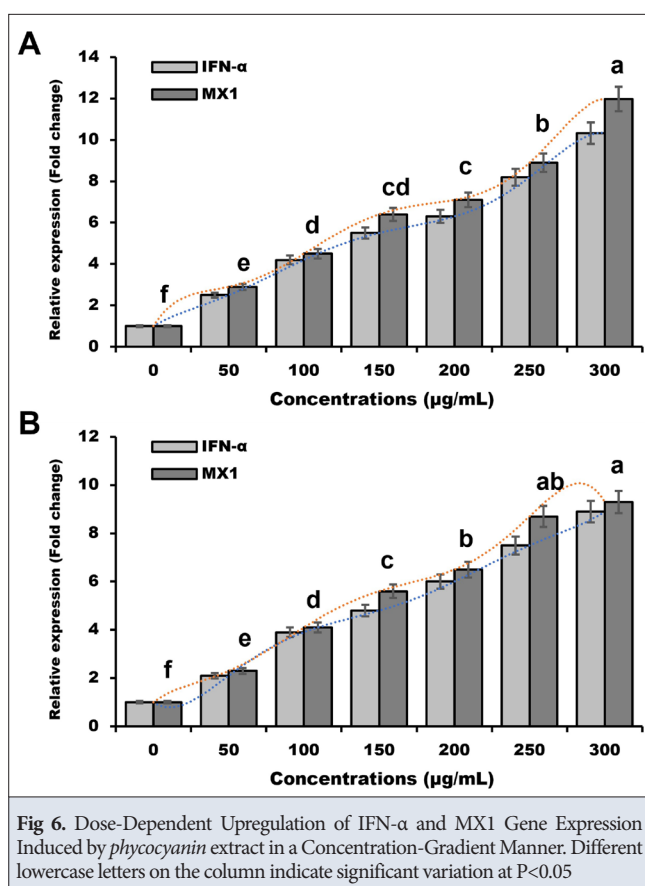


Fig 5. Dose-Dependent Antiviral Efficacy of *phycocyanin* extract Against HSV-1 and H1N1 Evaluated by Reduction in Viral Plaque Formation. Different lowercase letters on the column indicate significant variation at $P < 0.05$



gene, strongly suggests that the phycocyanin extract activates the interferon signaling pathway, leading to the production of essential antiviral effector molecules. While both panels show this robust induction, Panel A consistently exhibits a higher magnitude of gene expression, with IFN- α reaching approximately a 10-fold change and MX1 nearly a 12-fold change at 300 $\mu\text{g/mL}$, compared to approximately a 9-fold change for both in Panel B. These differences might stem from variations in experimental conditions or cell types, but the underlying immunostimulatory effect remains evident.

The findings showed the considerable antiviral activities of PE and that is clear in IC₅₀ where PE reduced 50% of viral plaque at 42.5 and 50 $\mu\text{g/mL}$ for HSV-1 and H1N1, respectively. Also, the CC₅₀ of PE was 110 and 142 $\mu\text{g/mL}$ for HSV-1 and H1N1, respectively.

Blood Biochemistry

Table 5 reveals a significant impact of dietary PE on various serum biochemical parameters in rats compared to the Positive Control (PC) group, which likely represents a state of induced dysfunction.

Regarding liver function, the PC group exhibited elevated liver enzymes. However, PE treatment at 100 mg/kg resulted in a 65.4% decrease in Aspartate transaminase

Table 5. The influence of dietary phycocyanin extract on the serum biochemical parameters of rats

Serum Biochemistry		Phycocyanin Extract Treatments (mg/kg)					P-value
		NC	PC	100	300	PC+PE	
Liver and kidney functions	AST (U/L)	105c	295a	102c	98d	112b	<0.0001
	ALT (U/L)	28b	58a	25c	22d	26c	<0.0001
	ALP (U/L)	115c	190a	105d	100d	125b	<0.0001
	AST/ALT ratio	3.75d	5.07a	4.01c	4.5b	4.3b	0.89
Lipid profile	Total cholesterol (mg/dL)	85d	288a	92c	81d	132b	<0.0001
	Triglycerides (mg/dL)	78d	195a	81c	76d	111b	<0.0001
	HDL (mg/dL)	56b	39c	66a	68a	54b	<0.0001
	LDL (mg/dL)	18d	35a	25c	22c	28b	<0.0001
	VLDL (mg/dL)	17c	38a	25b	21bc	25b	<0.0001
Oxidative stress	GSH (ng/mL)	2.1b	0.56d	2.9b	4.1a	1.8c	<0.0001
	SOD (U/mL)	42.3b	17.5d	48.3b	51.3a	36c	<0.0001
	CAT (ng/mL)	1.2b	0.41d	1.5ab	1.7a	0.87c	<0.0001
	MDA (nmol/mL)	3.5bc	18.5a	2.1c	1.5d	5.5b	<0.0001
	TAC (ng/mL)	1.45c	0.30e	1.8b	2.2a	1.22d	<0.0001
Diabetes markers	Glucose (mg/dL)	89bc	455a	91b	85c	97b	<0.0001
	HbA1c (%)	5.6c	14.3a	5.5c	5.2c	7.5b	<0.0001
	Insulin ($\mu\text{U/L}$)	16.6av	1.2c	17.5a	16.9ab	9.8b	<0.0001

$n = 3$; data are presented as mean \pm SD. Groups sharing the same lowercase letter within a row/column are not statistically different, while those with different letters show a statistically significant difference ($P < 0.05$); PE: Phycocyanin extract

Table 6. The influence of dietary phycocyanin extract on proinflammatory cytokines and cancerous genes (mean \pm SD)

Proinflammatory Cytokines/ Apoptosis Genes (Fold change)	Phycocyanin Extract Treatments (mg/kg)					P-value
	NC	PC	100	300	PC+PE	
BCL-2	1.0 \pm 0.0d	9.1 \pm 0.9a	1.2 \pm 0.5c	1.1 \pm 0.2cd	2.1 \pm 0.6b	<0.0001
Nrf-2	1.1 \pm 0.2d	7.5 \pm 0.5a	1.25 \pm 0.6c	1.15 \pm 1cd	1.5 \pm 0.5b	<0.0001
OH	1.2 \pm 0.6d	8.2 \pm 0.8a	1.3 \pm 0.2c	1.2 \pm 0.2cd	1.9 \pm 0.8b	<0.0001
B-actin	1.0 \pm 0.0d	10.5 \pm 0.3a	1.36 \pm 0.3c	1.18 \pm 0.3cd	2.5 \pm 6b	<0.0001
IL-1 β	1.00 \pm 0.09d	8.30 \pm 0.61a	1.20 \pm 0.11c	1.10 \pm 0.10cd	2.00 \pm 0.18b	<0.0001
TNF- α	1.05 \pm 0.07d	9.00 \pm 0.77a	1.24 \pm 0.13c	1.16 \pm 0.09cd	2.15 \pm 0.21b	<0.0001
BAX	1.00 \pm 0.08d	2.80 \pm 0.20a	1.30 \pm 0.10c	1.10 \pm 0.09cd	1.80 \pm 0.16b	<0.01
Casp-3	1.00 \pm 0.09d	3.10 \pm 0.23a	1.22 \pm 0.12c	1.13 \pm 0.10cd	1.95 \pm 0.17b	<0.01

n = 3; data are presented as mean \pm SD. Groups sharing the same lowercase letter within a row/column are not statistically different, while those with different letters show a statistically significant difference (*P*<0.05)

(AST), 300 mg/kg led to a 66.8% decrease, and the PC+PE group showed a 62.0% decrease in AST levels compared to the PC group. Similarly, Alanine Aminotransferase (ALT) levels decreased by 56.9%, 62.1%, and 55.2% in the 100 mg/kg, 300 mg/kg, and PC+PE groups. Alkaline Phosphatase (ALP) levels also saw substantial reductions of 47.4% in both the 100 mg/kg and 300 mg/kg PE groups, and 34.2% in the PC+PE group. The AST/ALT ratio showed a 19.5% increase in the 100 mg/kg group but decreased by 11.2% and 14.2% in the 300 mg/kg and PC+PE groups, respectively.

In terms of the lipid profile, the PC group displayed dyslipidemia. PE treatment at 100 mg/kg led to a 68.1% reduction in total cholesterol, while 300 mg/kg resulted in a 71.9% decrease, and PC+SPE showed a 54.2% decrease. Triglyceride levels decreased by 58.5%, 60.5%, and 43.1% in the respective SPE treatment groups. Notably, HDL increased by 69.2% with 100 mg/kg PE, 74.4% with 300 mg/kg PE, and 38.5% in the PC+PE group. The detrimental LDL cholesterol showed dramatic reductions of 87.8%, 89.3%, and 84.4%, while VLDL decreased by 55.3%, 44.7%, and 34.2% in the 100 mg/kg, 300 mg/kg, and PC+PE groups compared to the PC group (*Table 5*).

Regarding oxidative stress, the PC group showed signs of increased oxidative damage. PE treatment at 100 mg/kg led to a remarkable 417.9% increase in GSH levels, while 300 mg/kg resulted in a 632.1% increase, and PC+PE showed a 221.4% increase. Similarly, SOD activity increased by 176.0%, 193.1%, and 105.7%, and CAT activity increased by 317.1%, 361.0%, and 112.2% in the respective PE treatment groups. Conversely, MDA, a marker of lipid peroxidation, decreased significantly by 88.6%, 91.9%, and 70.3%. Total antioxidant capacity (TAC) also showed substantial increases of 500.0%, 633.3%, and 306.7% in the 100 mg/kg, 300 mg/kg, and PC+PE groups compared to the PC group.

Concerning diabetes markers, the PC group exhibited hyperglycemia and impaired glucose control. PE treatment at 100 mg/kg resulted in an 80.7% decrease in glucose levels, while 300 mg/kg led to an 81.3% decrease, and PC+PE showed a 78.7% decrease. HbA1c levels also decreased significantly by 61.5%, 63.6%, and 47.6% in the respective PE treatment groups. Notably, insulin levels showed dramatic increases of 1375.0% with 100 mg/kg PE, 1358.3% with 300 mg/kg PE, and 733.3% in the PC+PE group compared to the PC group (*Table 5*).

In summary, the PE-treated groups demonstrated substantial improvements across all measured parameters compared to the Positive Control group. The percentage changes highlight the considerable protective and healing potential of PE in mitigating liver dysfunction, dyslipidemia, oxidative stress, and hyperglycemia in this animal model. While the PE-only groups often showed more pronounced effects, the PC+PE group also exhibited significant improvements, suggesting that PE can offer benefits even in the presence of the inducing agent.

Proinflammatory Cytokines

The influence of dietary PE on pro-inflammatory cytokines revealed a consistent pattern of reduction across all measured markers compared to the Positive Control (PC) group (*Table 6*). Specifically, Bcl-2 levels decreased substantially by 86.8% and 87.9% in the 100 mg/kg (9.1 PC vs 1.2 at 100) and 300 mg/kg PE-treated groups (9.1 PC vs 1.1 at 300), respectively, with a notable 76.9% reduction in the PC+PE group (9.1 PC vs 2.1 at PC+PE). Similarly, Nrf-2 levels saw significant decreases of 83.3% (7.5 PC vs 1.25 at 100), 84.7% (7.5 PC vs 1.15 at 300), and 80.0% (7.5 PC vs 1.5 at PC+PE) in the corresponding treatment groups. The levels of OH also exhibited marked reductions of 84.1% (8.2 PC vs 1.3 at 100), 85.4% (8.2 PC vs 1.2 at 300), and 76.8% (8.2 PC vs 1.9 at PC+PE) in the 100 mg/kg, 300 mg/kg, and PC+PE

groups, respectively. The most pronounced decreases were observed in β -actin levels, with 87.0% (10.5 PC vs 1.36 at 100), 88.8% (10.5 PC vs 1.18 at 300), and 76.2% (10.5 PC vs 2.5 at PC+PE) reductions in the respective PE-treated groups. Moving to pro-inflammatory cytokines, IL-1 β levels significantly decreased by 85.5% (8.30 PC vs 1.20 at 100), 86.7% (8.30 PC vs 1.10 at 300), and 75.9% (8.30 PC vs 2.00 at PC+PE) in the 100 mg/kg, 300 mg/kg, and PC+PE groups, respectively. TNF- α levels also showed substantial reductions of 86.2% (9.00 PC vs 1.24 at 100), 87.1% (9.00 PC vs 1.16 at 300), and 76.1% (9.00 PC vs 2.15 at PC+PE) across these same groups. Furthermore, the extract demonstrated an influence on apoptosis-related genes. BAX levels decreased by 53.6% (2.80 PC vs 1.30 at 100), 60.7% (2.80 PC vs 1.10 at 300), and 35.7% (2.80 PC vs 1.80 at PC+PE) in the 100 mg/kg, 300 mg/kg, and PC+PE groups, respectively. Similarly, Casp-3 levels were reduced by 60.6% (3.10 PC vs 1.22 at 100), 63.5% (3.10 PC vs 1.13 at 300), and 37.1% (3.10 PC vs 1.95 at PC+PE) in the corresponding treatment groups. PE administration led to significant down-regulation of these pro-inflammatory markers and also mitigated the upregulation of BAX and Casp-3, suggesting a potent anti-inflammatory and potentially anti-apoptotic or protective effect in this experimental model. The consistent and substantial percentage decreases across all cytokines and treatment dosages underscore the potential of PE as an anti-inflammatory agent, even when administered in conjunction with the inducing agent in the PC+PE group. However, the PE-only groups generally exhibited slightly more pronounced effects. The p-values of <0.0001 or <0.01 for all parameters further confirm the high statistical significance of these observed effects.

Histology of Liver Tissue

Histological examination of rat liver tissue stained with Hematoxylin and Eosin (H&E) reveals distinct architectural features across the experimental groups. The control group (Fig. 7-A) exhibits a normal hepatic structure with well-organized hepatocyte cords radiating from central veins, clear sinusoids, and structurally sound portal triads. In contrast, the dithizone-challenged group (Fig. 7-B) displays significant liver damage, characterized by disorganization of hepatic cords, swollen hepatocytes potentially exhibiting vacuolation, and marked inflammation with an increased presence of inflammatory cells around structurally abnormal or congested portal triads. The phycocyanin-treated group (Fig. 7-C), receiving only phycocyanin, shows a liver morphology comparable to the control group, indicating no apparent adverse effects of phycocyanin alone on the liver tissue. Notably, the group treated with both dithizone and phycocyanin extract (Fig. 7-D) demonstrates a clear attenuation of the dithizone-induced liver damage.

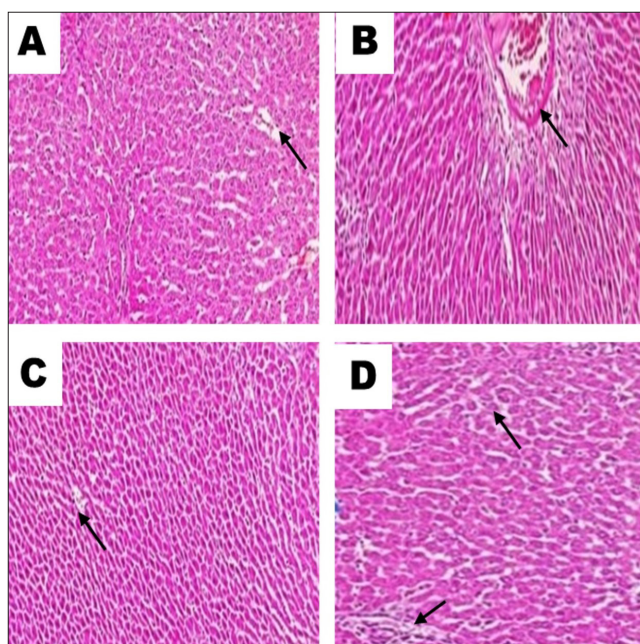


Fig 7. presents representative photomicrographs of rat liver tissue stained with Hematoxylin and Eosin (H&E) from different experimental groups. (A) Control Group, showcasing normal hepatic architecture with well-organized hepatocyte cords, clear sinusoids, and a structurally intact portal triad (black arrow), (B) Dithizone-Challenged Group, exhibiting significant liver damage characterized by disarrayed hepatic cords, cellular swelling (hepatocyte ballooning), inflammatory cell infiltration, and a congested or structurally altered portal triad (black arrow), (C) represents the *phycocyanin*-treated Group (PE alone), displaying liver tissue with a normal histological appearance, similar to the control group, with well-preserved hepatic architecture and a normal-looking portal triad (black arrow), indicating no adverse effects of *phycocyanin* extract alone, (D) Dithizone + *phycocyanin* extract (PE) Group, revealing a noticeable improvement in liver morphology compared to the dithizone-challenged group, with less cellular disorganization, reduced inflammation, and a relatively better-preserved portal triad (black arrows), suggesting the protective effect of *Phycocyanin* extract against dithizone-induced liver injury

While some signs of cellular disorganization and mild inflammation may still be present, the severity of the pathological changes is markedly reduced compared to the dithizone-challenged group, suggesting a protective effect of phycocyanin extract against chemical liver injury by preserving hepatic architecture and reducing cellular damage and inflammation.

DISCUSSION

Diabetes mellitus is a chronic metabolic disorder characterized by persistent hyperglycemia, with significant implications for oxidative stress, tissue damage, and elevated risks for secondary complications such as cancer, infections, and organ degeneration [38]. Dithizone-induced diabetes in animal models, especially rats, serves as a relevant and reproducible system to investigate drugs with multifaceted medicinal effects [39]. Among natural compounds, phycocyanin, a blue pigment-protein complex found in cyanobacteria such as *Spirulina*, has

drawn considerable attention due to its pronounced antioxidant, antidiabetic, anticancer, and antimicrobial activities ^[40].

Phycocyanin has demonstrated significant antidiabetic effects in various experimental models, including dithizone- and high-fat-diet-induced diabetic rodents. Its ability to lower fasting blood glucose (FBG) levels and improve glucose tolerance is attributed to several mechanisms. Recent *in vivo* studies show that administration of phycocyanin alleviates hyperglycemia, enhances glucose clearance during glucose tolerance tests, and improves pancreatic β -cell function as indicated by increased fasting insulin levels and improved HOMA- β indices in diabetic rodents ^[41,42]. These effects are mediated through the activation of AKT and AMPK signaling pathways in hepatic tissue, bolstering both insulin signaling and cellular glucose uptake ^[41]. Notably, the hypoglycemic action of phycocyanin, while progressive, is safe and maintains FBG within normal physiological ranges compared to control treatments with standard antidiabetic drugs such as metformin ^[41]. Diabetes is often accompanied by dyslipidemia and hepatic dysfunction, exacerbating the risk of cardiovascular complications. Phycocyanin treatment in diabetic rats leads to marked improvements in serum biochemical profiles, including reductions in triglycerides (TG), total cholesterol (TC), and liver transaminases (AST and ALT), while promoting healthy HDL cholesterol levels. Restoration of normal lipid metabolism is paralleled by suppressed hepatic steatosis and improved liver architecture, reflecting enhanced metabolic regulation. Collectively, these improvements not only mitigate diabetic complications but also reduce oxidative stress by limiting substrates for lipid peroxidation ^[43,44].

One of phycocyanin's most profound biological activities is its capacity to counteract oxidative stress, a major pathophysiological factor in diabetes and its complications. Dithizone-induced diabetic rats exhibit excessive formation of reactive oxygen species (ROS), leading to lipid peroxidation, protein glycation, and DNA damage. Supplementation with phycocyanin enhances endogenous antioxidant capacity, as evidenced by elevated superoxide dismutase (SOD) activity and reductions in malondialdehyde (MDA) levels-key biomarkers of oxidative injury. Furthermore, phycocyanin's chromophore, phycocyanobilin, acts as a potent free radical scavenger, directly neutralizing ROS and thus stabilizing cellular redox homeostasis ^[14,43,45].

Several intersecting pathways explain phycocyanin's antioxidant mechanisms, where phycocyanin upregulates nuclear factor erythroid 2-related factor 2 (Nrf2)-dependent transcription of antioxidant genes, as well as directly stimulating enzymatic antioxidants such as

catalase and glutathione peroxidase. This regulatory effect minimizes oxidative assaults on vital organs like the pancreas and liver, preserving their architecture and preventing necrosis or fibrosis ^[46,47].

Experimental and preclinical research has illuminated phycocyanin's anticancer properties. Mechanistically, phycocyanin arrests cancer cell proliferation through blockage of cell-cycle progression, triggers apoptosis and autophagy in neoplastic cells, and downregulates pro-angiogenic factors like VEGF ^[48]. In rodent models, phycocyanin administration not only reduces the incidence and volume of chemically-induced tumors (notably colon cancer in conjunction with diabetic models) but also suppresses metastasis by decreasing matrix metalloproteinases (MMPs) and hypoxia-inducible factor-1 α (HIF-1 α). Importantly, these anticancer activities are achieved with minimal toxicity to normal tissues, highlighting phycocyanin's selectivity for tumor cells.

Diabetes is a known risk factor for cancer, partly through persistent oxidative stress, chronic inflammation, and impaired immune surveillance. By ameliorating hyperglycemia, modulating immune response, and reducing oxidative damage, phycocyanin may decrease the promotional effect of diabetes on tumorigenesis ^[41,42].

Phycocyanin exhibits notable antimicrobial activity against various pathogenic bacteria, fungi, and viruses, which is particularly valuable given the elevated infection risk in diabetic individuals. Recent studies document its ability to disrupt bacterial cell membranes, inhibit biofilm formation, and neutralize bacterial toxins. These effects are effective against both Gram-positive and Gram-negative strains, making phycocyanin a potential candidate for managing diabetic infections, including those resistant to standard antibiotics ^[14].

Underlying the antimicrobial efficacy of phycocyanin is its broader immunomodulatory effect. Phycocyanin enhances lymphocyte proliferation, stimulates antibody production, and boosts natural killer cell activity. These responses are associated with quicker resolution of infections and reduced inflammation at infection sites, thereby improving recovery and preventing chronic complications in diabetic rats ^[49].

Dithizone-induced diabetes primarily damages pancreatic β -cells, resulting in islet cell degeneration, necrosis, and inflammatory infiltration. Histological investigations reveal that phycocyanin administration preserves islet architecture, limits infiltration by inflammatory cells, and facilitates regeneration of β -cells. This protective effect coincides with the improvement in insulin secretion and normalization of glucose homeostasis ^[39]. Diabetes induces hepatic steatosis and renal tubular

degeneration. Phycocyanin reconstructs normal liver and kidney morphology in diabetic rats, preventing fatty infiltration, sinusoidal dilatation, and fibrotic changes. Its antioxidant action underlies the reduction of hepatic lipid peroxidation, while improved serum markers (reduced ALT, AST, and creatinine) corroborate these findings at the functional level [14,45,49].

Microscopic observation of treated diabetic rats shows attenuation of oxidative lesions, restoration of normal cellular ultrastructure, and reduction of apoptotic cell death in multiple organs. These changes indicate that phycocyanin not only prevents but may also reverse diabetes-related tissue injury. By improving insulin sensitivity and lipid profiles, phycocyanin reorients whole-organism metabolism toward a healthier state, countering hyperphagia, polydipsia, weight loss, and fatigue commonly observed in diabetic rats. Its comprehensive effect on both glucose and lipid metabolism distinguishes it from single-action antidiabetic agents [41,42].

Oxidative stress serves as a nexus linking metabolic dysregulation, tissue injury, infection susceptibility, and carcinogenesis in diabetic models. Phycocyanin's multifactorial properties create a positive feedback loop amelioration of oxidative stress reduces secondary tissue damage and cancer risk, which further supports metabolic control and immune competence. Although most recent studies have utilized high-fat-diet and streptozotocin-induced models, available data strongly suggest these effects extend to dithizone-induced diabetes due to the similarity in pathological mechanisms: loss of insulin-producing β -cells, heightened oxidative stress, and secondary organ involvement [42,49]. Phycocyanin's robust antioxidant, antihyperglycemic, and tissue-protective qualities make it a promising agent for experimental validation in dithizone-induced diabetic rats.

Phycocyanin possesses an array of therapeutic effects antidiabetic, antioxidant, anticancer, and antimicrobial that operate synergistically to alleviate the metabolic, oxidative, and histopathological complications of diabetes. Its mechanisms include improving glycemic control, restoring lipid metabolism, enhancing endogenous antioxidant responses, inducing apoptosis in cancer cells, protecting tissues against oxidative and inflammatory damage, and reducing infection risks through direct antimicrobial actions and immune modulation. Future research should focus on translating these capabilities into clinical settings, precisely mapping its molecular targets in various diabetic and cancer models, and optimizing its delivery for maximal efficacy. Nevertheless, phycocyanin stands as a powerful phytochemical, with promising multifunctional therapeutic potential in the management of diabetes and associated complications

DECLARATIONS

Availability of Data and Materials: The datasets used and/or analyzed during the current study are available from the corresponding author (L. A. Almutairi) on reasonable request.

Competing Interests: The authors declared that there is no conflict of interest.

Acknowledgment: The authors gratefully acknowledge Princess Nourah bint Abdulrahman University Researchers Supporting Project number (PNURSP2025R457), Princess Nourah bint Abdulrahman University, Riyadh, Saudi Arabia. The authors extend their appreciation to the Deanship of Research and Graduate Studies at King Khalid University for funding this work through Large Research Project under grant number RGP2/178/46.

Funding: Princess Nourah bint Abdulrahman University Researchers Supporting Project number (PNURSP2025R457), Princess Nourah bint Abdulrahman University, Riyadh, Saudi Arabia. Deanship of Research and Graduate Studies at King Khalid University for funding this work through Large Research Project under grant number RGP2/178/46.

Declaration of Generative Artificial Intelligence (AI): The author declare that the article tables and figures were not written or created by AI and AI-assisted technologies.

Author Contributions: Conceptualization, MAA, NSA, AMA, AAA, MA, AO, EAB, HKAG, AOS, LAA, SHA, and RNA, formal analysis, HKAG, AOS, LAA, SHA, AAA, and RNA, investigation, MAA, NSA, AAA, MA, AO, and EAB, data curation, HKAG, AOS, LAA, SHA, and RNA, writing original draft preparation, MAA, NSA, AAA, MA, AAA, AO, and EAB, writing final manuscript and editing, HKAG, AOS, LAA, SHA, and RNA, visualization and methodology, MAA, NSA, AAA, MA, AO, EAB, HKAG, AAA, AOS, LAA, SHA, and RNA. All authors have read and agreed to the published version of the manuscript.

REFERENCES

1. Morya S, Kumar Chattu V, Khalid W, Zubair Khalid M, Siddeeg A: Potential protein phycocyanin: An overview on its properties, extraction, and utilization. *Int J Food Prop*, 26, 3160-3176, 2023. DOI: 10.1080/10942912.2023.2271686
2. García-Gómez C, Aguirre-Cavazos DE, Chávez-Montes A, Ballesteros-Torres JM, Orozco-Flores AA, Reyna-Martínez R, Torres-Hernández ÁD, González-Meza GM, Castillo-Hernández SL, Gloria-Garza MA, Kačániová M, Ireneusz-Kluz M, Elizondo-Luevano JH: Phycobilins versatile pigments with wide-ranging applications: Exploring their uses, biological activities, extraction methods and future perspectives. *Mar Drugs*, 23 (5):201, 2025. DOI: 10.3390/md23050201
3. Chavda V, Patel S: Hyperglycaemic metabolic complications of ischemic brain: Current therapeutics, anti-diabetics and stem cell therapy. *CNS Neurol Disord Drug Targets*, 22, 832-856, 2023. DOI: 10.2174/1871527321666220609200852
4. Qamar F, Sultana S, Sharma M: Animal models for induction of diabetes and its complications. *J Diabetes Metab Disord*, 22, 1021-1028, 2023. DOI: 10.1007/s40200-023-01277-3
5. Ou Y, Lin L, Yang X, Pan Q, Cheng X: Antidiabetic potential of phycocyanin: Effects on KKAY mice. *Pharm Biol*, 51, 539-544, 2013. DOI: 10.3109/13880209.2012.747545
6. Prabakaran G, Sampathkumar P, Kavisri M, Moovendhan M: Extraction and characterization of phycocyanin from *Spirulina platensis* and evaluation of its anticancer, antidiabetic and antiinflammatory effect. *Int J Biol Macromol*, 153, 256-263, 2020. DOI: 10.1016/j.ijbiomac.2020.03.009
7. Munawaroh HSH, Gumilar GG, Nurjanah F, Yuliani G, Aisyah S,

- Kurnia D, Wulandari AP, Kurniawan I, Ningrum A, Koyande AK, Show PL: *In-vitro* molecular docking analysis of microalgae extracted phycocyanin as an anti-diabetic candidate. *Biochem Eng J*, 161:107666, 2020. DOI: 10.1016/j.bej.2020.107666
8. Ziyaei K, Abdi F, Mokhtari M, Daneshmehr MA, Ataie Z: Phycocyanin as a nature-inspired antidiabetic agent: A systematic review. *Phytomedicine*, 119:154964, 2023. DOI: 10.1016/j.phymed.2023.154964
9. Gabr GA, El-Sayed SM, Hikmal MS: Antioxidant activities of phycocyanin: A bioactive compound from *Spirulina platensis*. *J Pharm Res Int*, 32, 73-85, 2020. DOI: 10.9734/jpri/2020/v32i230407
10. Liu R, Qin S, Li W: Phycocyanin: Anti-inflammatory effect and mechanism. *Biomed Pharmacother*, 153:113362, 2022. DOI: 10.1016/j.biopha.2022.113362
11. Braune S, Krüger-Genge A, Kammerer S, Jung F, Küpper JH: Phycocyanin from *Arthrospira platensis* as potential anti-cancer drug: Review of *in vitro* and *in vivo* studies. *Life*, 11 (2):91, 2021. DOI: 10.3390/life11020091
12. Ravi M, Tentu S, Baskar G, Rohan Prasad S, Raghavan S, Jayaprakash P, Jeyakanthan J, Rayala SK, Venkatraman G: Molecular mechanism of anti-cancer activity of phycocyanin in triple-negative breast cancer cells. *BMC Cancer*, 15:768, 2015. DOI: 10.1186/s12885-015-1784-x
13. Bougateg H, Hadrich F, Gazbar M, Sila A, Chamkha M, Bougateg A: Development of a novel method for the extraction of phycocyanin pigment from *Spirulina platensis* and assessment of its antioxidant, antimicrobial, and anticancer activities. *Biomass Convers Biorefin*, 15, 8001-8013, 2025. DOI: 10.1007/s13399-024-05540-2
14. Husain A, Khanam A, Alouffi S, Shahab U, Alharazi T, Maarfi F, Khan S, Hasan Z, Akasha R, Farooqui A, Ahmad S: C-phycocyanin from cyanobacteria: A therapeutic journey from antioxidant defence to diabetes management and beyond. *Phytochem Rev*, 2024:1-19, 2024. DOI: 10.1007/s11101-024-10045-x
15. Jiang L, Yu S, Chen H, Pei H: Enhanced phycocyanin production from *Spirulina subsalsa* via freshwater and marine cultivation with optimized light source and temperature. *Bioresour. Technol*, 378:129009, 2023. DOI: 10.1016/j.biortech.2023.129009
16. Kamble SP, Gaikar RB, Padalia RB, Shinde KD: Extraction and purification of C-phycocyanin from dry *Spirulina* powder and evaluating its antioxidant, anticoagulation and prevention of DNA damage activity. *J Appl Pharm Sci*, 3, 149-153, 2013.
17. AOAC: Official Methods of Analysis. 18th ed., Association of Official Analytical Chemists, Arlington, VA., USA, 2012.
18. Pearson D: The Chemical Analysis of Food. 6th ed., 504-530, Church Hill, Livingstone, Edinburgh, 1981.
19. Hajiyevea S, Cankilic MY, Kilic V, Gorgulu S, Patrignani F, Lanciotti R: An insight into the potential antioxidant, anticancer and antimicrobial activities of *Geitlerinema* sp. C-phycocyanin extracts. *Algal Res*, 85:103836, 2025. DOI: 10.1016/j.algal.2024.103836
20. Shrivastava A, Gupta VB: Methods for the determination of limit of detection and limit of quantitation of the analytical methods. *Chron Young Sci*, 2 (1): 21-25, 2011. DOI: 10.4103/2229-5186.79345
21. Alkhudaydi HMS, Muriuki EN, Spencer JP: Determination of the polyphenol composition of raspberry leaf using LC-MS/MS. *Molecules*, 30 (4):970, 2025. DOI: 10.3390/molecules30040970
22. Carneiro AdA, Sinoti SBP, de Freitas MM, Simeoni LA, Fagg CW, Magalhães PdO, Silveira D, Fonseca-Bazzo YM: Hydroethanolic extract of *Morus nigra* L. leaves: A dual PPAR- α/γ agonist with anti-inflammatory properties in lipopolysaccharide-stimulated RAW 264.7. *Plants*, 11 (22):3147, 2022. DOI: 10.3390/plants11223147
23. Nair SS, Kavrekar V, Mishra A: *In vitro* studies on alpha amylase and alpha glucosidase inhibitory activities of selected plant extracts. *Eur J Exp Biol*, 3, 128-132, 2013.
24. Alsubhi NH, Al-Quwaie DA, Alrefaei GI, Alharbi M, Binothman N, Aljadani M, Saad A: Pomegranate pomace extract with antioxidant, anticancer, antimicrobial, and antiviral activity enhances the quality of strawberry-yogurt smoothie. *Bioengineering*, 9 (12):735, 2022. DOI: 10.3390/bioengineering9120735
25. Alowaiesh BF, Alhaithloul HAS, Saad AM, Hassanin AA: Green biogenic of silver nanoparticles using polyphenolic extract of olive leaf wastes with focus on their anticancer and antimicrobial activities. *Plants*, 12 (6):1410, 2023. DOI: 10.3390/plants12061410
26. Sayed-Ahmed ETA, Salah KBH, El-Mekawy RM, Rabie NA, Ashkan ME, Alamoudi SA, Alruhaili MH, Al Jaouni SK, Almuhayawi MS, Selim S, Saad AM, Namir M: The preservative action of protein hydrolysates from legume seed waste on fresh meat steak at 4°C: Limiting unwanted microbial and chemical fluctuations. *Polymers*, 14 (15):3188, 2022. DOI: 10.3390/polym14153188
27. El-Saadony MT, Saad AM, Najjar AA, Alzahrani SO, Alkhatib FM, Shafi ME, Selem E, Desoky EM, Fouda SEE, El-Tahan AM, Hassan MAA: The use of biological selenium nanoparticles to suppress *Triticum aestivum* L. crown and root rot diseases induced by *Fusarium* species and improve yield under drought and heat stress. *Saudi J Biol Sci*, 28, 4461-4471, 2021. DOI: 10.1016/j.sjbs.2021.04.043
28. Rubinstein LV, Shoemaker RH, Paull KD, Simon RM, Tosini S, Skehan P, Scudiero DA, Monks A, Boyd MR: Comparison of *in vitro* anticancer-drug-screening data generated with a tetrazolium assay versus a protein assay against a diverse panel of human tumor cell lines. *J Natl Cancer Inst*, 82, 1113-1117, 1990. DOI: 10.1093/jnci/82.13.1113
29. Allam RM, Al-Abd AM, Khedr A, Sharaf OA, Nofal SM, Khalifa AE, Mosli HA, Abdel-Naim AB: Fingolimod interrupts the cross talk between estrogen metabolism and sphingolipid metabolism within prostate cancer cells. *Toxicol Lett*, 291, 77-85, 2018. DOI: 10.1016/j.toxlet.2018.04.008
30. Chu SY, Jung JH, Park MJ, Kim SH: Risk assessment of metabolic syndrome in adolescents using the triglyceride/high-density lipoprotein cholesterol ratio and the total cholesterol/high-density lipoprotein cholesterol ratio. *Ann Pediatr Endocrinol Metab*, 24, 41-48, 2019. DOI: 10.6065/apem.2019.24.1.41
31. Bijland S, Pieterman EJ, Maas AC, van der Hoorn JW, van Erk MJ, van Klinken JB, Havekes LM, van Dijk KW, Princen HM, Rensen PC: Fenofibrate increases very low density lipoprotein triglyceride production despite reducing plasma triglyceride levels in APOE* 3-Leiden. CETP mice. *J Biol Chem*, 285, 25168-25175, 2010. DOI: 10.1074/jbc.M110.123992
32. Sampson M, Ling C, Sun Q, Harb R, Ashmaig M, Warnick R, Sethi A, Fleming JK, Otvos JD, Meeusen JW, Delaney SR, Jaffe AS, Shamburek R, Amar M, Remaley AT: A new equation for calculation of low-density lipoprotein cholesterol in patients with normolipidemia and/or hypertriglyceridemia. *JAMA Cardiol*, 5, 540-548, 2020. DOI: 10.1001/jamacardio.2020.0013
33. Cheng CH, Chu CY, Chen HL, Lin IT, Wu CH, Lee YK, Hu PJ, Bair MJ: Subgroup analysis of the predictive ability of aspartate aminotransferase to platelet ratio index (APRI) and fibrosis-4 (FIB-4) for assessing hepatic fibrosis among patients with chronic hepatitis C. *J Microbiol Immunol Infect*, 53, 542-549, 2020. DOI: 10.1016/j.jmii.2019.09.002
34. Alatawi FS, Faridi UA, Alatawi MS: Effect of treatment with vitamin D plus calcium on oxidative stress in streptozotocin-induced diabetic rats. *Saudi Pharm J*, 26, 1208-1213, 2018. DOI: 10.1016/j.sjps.2018.07.012
35. Pappas A, Tsiokanos A, Fatouros IG, Poullos A, Kouretas D, Goutzourelas N, Giakas G, Jamurtas AZ: The effects of *Spirulina* supplementation on redox status and performance following a muscle damaging protocol. *Int J Mol Sci*, 22:3559, 2021. DOI: 10.3390/ijms22073559
36. Chen JC, Fang C, Zheng RH, Chen ML, Kim DH, Lee YH, Bailey C, Wang KJ, Lee JS, Bo J: Environmentally relevant concentrations of microplastics modulated the immune response and swimming activity, and impaired the development of marine medaka *Oryzias latipes* larvae. *Ecotoxicol Environ Saf*, 241:113843, 2022. DOI: 10.1016/j.ecoenv.2022.113843
37. Saif GB, Khan IA: Association of genetic variants of the vitamin D receptor gene with vitiligo in a tertiary care center in a Saudi population: A case-control study. *Ann Saudi Med*, 42, 96-106, 2022. DOI: 10.5144/0256-4947.2022.96
38. González P, Lozano P, Ros G, Solano F: Hyperglycemia and oxidative stress: an integral, updated and critical overview of their metabolic interconnections. *Int J Mol Sci*, 24:9352, 2023. DOI: 10.3390/ijms24119352
39. Algul S, Ozcelik O: Comprehensive review of animal models in diabetes research using chemical agents. *Lab Anim*, 59, 356-363, 2025. DOI:

10.1177/00236772241296199

40. Papadaki S, Tricha N, Panagiotopoulou M, Krokida M: Innovative bioactive products with medicinal value from microalgae and their overall process optimization through the implementation of life cycle analysis - An overview. *Mar Drugs*, 22:152, 2024. DOI: 10.3390/md22040152

41. Hao S, Li F, Li Q, Yang Q, Zhang W: Phycocyanin protects against high glucose high fat diet induced diabetes in mice and participates in AKT and AMPK signaling. *Foods*, 11 (20):3183, 2022. DOI: 10.3390/foods11203183

42. Husain A, Alouffi S, Khanam A, Akasha R, Farooqui A, Ahmad S: Therapeutic efficacy of natural product 'C-phycocyanin' in alleviating streptozotocin-induced diabetes via the inhibition of glycation reaction in rats. *Int J Mol Sci*, 23:14235, 2022. DOI: 10.3390/ijms232214235

43. Bahrini I, Alamoudi M, Alazami M, Alrashdi J, Alouche N: Protective effects of C-Phycocyanin from *Spirulina platensis* against pancreatic inflammation, lymphocyte infiltration, impaired carbohydrate digestion, and glucose metabolism dysregulation in diabetic rats. *J Agric Food Res*, 2025:101951, 2025. DOI: 10.1016/j.jafr.2025.101951

44. Biryulina N, Sidorova YS, Zorin S, Petrov N, Guseva G, Mazo V, Kochetkova A: Evaluation of the combined effect of *Arthrospira platensis* biomass phycocyanin concentrate and soy protein on male Wistar rats fed a high-fat diet with added cholesterol. *Vopr Pitan*, 94 (2): 73-84, 2025. DOI: 10.33029/0042-8833-2025-94-2-73-84

45. Zheng J, Inoguchi T, Sasaki S, Maeda Y, McCarty MF, Fujii M, Ikeda N, Kobayashi K, Sonoda N, Takayanagi R: Phycocyanin and phycocyanobilin from *Spirulina platensis* protect against diabetic nephropathy by inhibiting oxidative stress. *Am J Physiol Regul Integr Comp Physiol*, 304 (2): 110-120, 2013. DOI: 10.1152/ajpregu.00648.2011

46. Xu F, Yang F, Qiu Y, Wang C, Zou Q, Wang L, Li X, Jin M, Liu K, Zhang S, Zhang Y, Li B: The alleviative effect of C-phycocyanin peptides against TNBS-induced inflammatory bowel disease in zebrafish via the MAPK/Nrf2 signaling pathways. *Fish Shellfish Immunol*, 145:109351, 2024. DOI: 10.1016/j.fsi.2023.109351

47. Puengpan S, Phetrungnapha A, Sattayakawee S, Tunsophon S: Phycocyanin attenuates skeletal muscle damage and fatigue via modulation of Nrf2 and IRS-1/AKT/mTOR pathway in exercise-induced oxidative stress in rats. *PLoS One*, 19:e0310138, 2024. DOI: 10.1371/journal.pone.0310138

48. Jayanti DAPIS, Abimanyu IGAM, Azzamudin H: *Spirulina platensis*'s phycocyanobilin as an antiangiogenesis by inhibiting VEGFR2-VEGFA pathway in breast cancer: *In silico* study. *J Smart Bioprospe Technol*, 2 (3): 87-91, 2021. DOI: 10.21776/ub.jsmartech.2021.002.03.87

49. Hoseini F, Hoseini S, Fazilati M, Ebrahimie E, Hoseini F, Choopani A: Evaluation of C-phycocyanin effects with drug purity on the immune system through its effect on interferon-gamma (INF- γ). *Int J Med Rev*, 8, 188-193, 2021. DOI: 10.30491/ijmr.2021.270381.1181

RESEARCH ARTICLE

Assessment of Testicular Artery Blood Flow Using Doppler Ultrasonography and Its Correlation with Spermatological Parameters in Kangal Shepherd Dogs

Burcu ESİN ¹ (*)  Cumali KAYA ¹  Çağatay ESİN ² ¹ Department of Animal Reproduction and Artificial Insemination, Faculty of Veterinary Medicine, University of Ondokuz Mayıs, TR-55200 Samsun - TÜRKİYE² Department of Internal Medicine, Faculty of Veterinary Medicine, University of Ondokuz Mayıs, TR-55200 Samsun - TÜRKİYE

(*) Corresponding author:

Burcu ESİN

Phone: +90 362 312 1919

E-mail: burcuyalcin@omu.edu.tr

How to cite this article?

Esin B, Kaya C, Esin Ç: Assessment of testicular artery blood flow using doppler ultrasonography and its correlation with spermatological parameters in Kangal Shepherd dogs. *Kafkas Univ Vet Fak Derg*, 31 (5): 635-643, 2025.

DOI: 10.9775/kvfd.2025.34432

Article ID: KVFD-2025-34432

Received: 14.05.2025

Accepted: 11.08.2025

Published Online: 19.08.2025

Abstract

This study investigated the relationship between testicular artery hemodynamics and spermatological parameters in Kangal Shepherd dogs of different age groups using Doppler ultrasonography and computer-assisted sperm analysis. Fourteen clinically healthy, sexually mature Kangal Shepherd dogs were categorized into adult (3-5 years, n=7) and senior (7-9 years, n=7) groups. Each dog underwent three evaluations at two-week intervals, including a Doppler ultrasonographic assessment of suprastesticular, intratesticular, and marginal arteries and comprehensive spermatological analysis. Testicular arterial blood flow was assessed by measuring peak systolic velocity, end-diastolic velocity, pulsatility index (PI), and resistive index (RI). Spermatological assessments included total motility, progressive motility, sperm concentration, and morphological analysis. The results revealed significant age-related alterations in testicular blood flow parameters, with senior dogs exhibiting increased PI and RI values. Moreover, strong negative correlations were identified between Doppler indices and spermatological parameters. Conversely, positive correlations were found between vascular resistance parameters and morphological sperm defects, particularly in the head, tail, and midpiece regions. The strongest correlations were observed in the left intratesticular artery, with RI showing a very strong negative correlation with motility ($r=-0.91$) and a very strong positive correlation with total morphological defects ($r=0.92$). In conclusion, this study shows that testicular blood flow, assessed via Doppler ultrasonography, is closely linked to sperm parameters in Kangal Shepherd dogs, underscoring its value in clinical reproductive functions, especially for age-related changes.

Keywords: Doppler velocimetry, Kangal Shepherd dogs, Spermatological parameters, Testicular artery, Ultrasonography

INTRODUCTION

Fertility in male dogs is influenced by various intrinsic and extrinsic factors, including age, hormonal balance, testicular vascularization, and environmental conditions ^[1]. Among these, testicular blood flow (TBF) has gained particular attention in recent years, as Doppler ultrasonography (DU) parameters such as the pulsatility index (PI) and resistive index (RI)-have been proposed as potential indicators of sperm quality in dogs ^[2]. In clinical practice, DU is a valuable, non-invasive tool used to evaluate the hemodynamic characteristics of blood flow in various arteries and veins. It is widely employed for vascular assessment in multiple organs, including

the liver, mammary glands, kidneys, placenta, and fetal structures. In recent years, research has increasingly focused on the Doppler parameters of the testicular artery (TA) in different animal species ^[3-6]. This focus is of critical importance, as impaired blood supply in the TA is considered a significant contributor to male infertility ^[7].

The testicular artery, which arises from the abdominal aorta, supplies blood to the testes. After passing through the inguinal ring to reach the spermatic cord, it travels along the posterior surface of the testis, emerging near the proximal pole. The artery then penetrates the tunica albuginea and follows a relatively straight course typically without branching-through the tunica vasculosa, a



vascular layer beneath the capsule that extends along the epididymal margin of the testis.

In human medicine; Color Doppler (CD), Pulsed Wave Doppler (PW) and Power Doppler (PD) are routinely performed to evaluate the andrological status of the testes [8] as these modalities offer a simple yet accurate method of measuring blood flow by integrating anatomical and hemodynamic information [9]. In veterinary medicine, several studies have investigated the application of DU in dogs for evaluating TBF under both physiological and pathological conditions [10,11]. Although still considered a relatively novel technique in veterinary practice, testicular DU holds great potential for future development and clinical utility.

The testicular parenchyma is a high-metabolism tissue; any disruption in the transport of nutrients and oxygen via the blood can have adverse effects on the morphology and function of the testis [12]. Studies in dogs have shown a relationship between hemodynamic parameters of testicular artery blood flow and semen-related parameters [13,14]. Venianaki et al. [15] studied hemodynamic parameters of testicular artery blood flow in Beagles during prepubertal, pubertal and postpubertal ages. They obtained significant correlations between the hemodynamic parameters they obtained and semen evaluation parameters [15]. Souza et al. [16] reported possible changes in hemodynamic parameters of testicular artery blood flow during the peri-pubertal period; in general, these parameters can be used as indicators of future semen quality [17-19]. However, since the animals evaluated in the study were of different breeds, this did not support standardization of the results.

The testicular artery originates from the abdominal aorta and supplies blood to the testes via several branches. It first gives rise to the suprastesticular artery, located along the spermatic cord, then enters the testis and continues as the marginal artery along the epididymal border, and finally branches into the intratesticular artery that penetrates the testicular parenchyma [13]. The intratesticular artery runs through the mediastinum testis and provides direct perfusion to the seminiferous tubules. Among these, the intratesticular artery is particularly important because it supplies the active spermatogenic tissue. Alterations in blood flow parameters (e.g., RI, PI) within this artery are closely linked to sperm motility, morphology, and concentration. Therefore, detailed Doppler assessment of these arteries can provide critical insights into testicular function and male dog fertility [15,16].

In addition to evaluating testicular artery blood flow, the objective and quantitative assessment of spermatological parameters is essential for determining male reproductive performance. A complete andrological examination

-including physical evaluation of the testes and semen analysis- is fundamental for assessing testicular function. Computer-assisted sperm analysis (CASA) systems offer objective and reproducible measurements of sperm motility by tracking and analyzing the movement characteristics of individual sperm cells. Beyond motility, a comprehensive semen evaluation also includes sperm concentration and morphological assessment, both of which are critical for understanding the functional competence of spermatozoa [19].

Despite the clinical value of integrating vascular and spermatological data, there remains a need for more studies investigating the relationship between testicular hemodynamics and detailed semen quality parameters in dogs [2]. In particular, studies are needed on local or regional breeds such as the Kangal Shepherd dog, which may exhibit different reproductive physiology influenced by genetic background and environmental conditions [20].

This study investigated age-related changes in testicular artery hemodynamics and their potential association with semen quality in Kangal Shepherd dogs. Adult (3-5 years) and senior (7-9 years) dogs were compared regarding Doppler ultrasonographic parameters and spermatological findings. In addition to examining the effects of aging on testicular blood flow, the study also sought to determine whether alterations in vascular dynamics are correlated with differences in semen quality between the two age groups.

MATERIAL AND METHODS

Ethical Statement

This study was conducted at the Animal Hospital of the Faculty of Veterinary Medicine, Ondokuz Mayıs University, and was approved by the Animal Ethics Committee of Ondokuz Mayıs University (Approval No: 2024/41).

Experimental Design

A total of 14 healthy, sexually mature male Kangal Shepherd dogs were enrolled in the study. The dogs were categorized into two age groups: adult (n=7; 3.5±1.5 years; 48.98±1.02 kg) and senior (n=7; 7±1.5 years; 50±6.94 kg). All animals were presented to the university hospital for routine procedures such as vaccination or artificial insemination. Before participation, informed consent was obtained from all dog owners.

Each animal underwent a complete physical examination and a detailed reproductive tract evaluation. Only clinically healthy dogs without any observable physical or reproductive disorders, and with no known history of reproductive diseases, were included in the study. Testicular Doppler ultrasonography and spermatological

evaluations were performed three times on each dog, at two-week intervals.

All dogs were maintained on a standardized diet throughout the study to minimize variability and ensure uniform metabolic conditions. Dogs diagnosed with orchitis, testicular morphological abnormalities, systemic illness, or those that failed to provide semen samples were excluded from the study.

Testicular Doppler Ultrasonography

Testicular blood flow was assessed in all dogs before semen collection. All ultrasonographic examinations were conducted by the same experienced ultrasonographer involved in the study. The dogs were positioned supine without sedation to minimize potential interference from anesthetic agents on TBF measurements. Vetus 9 (Mindray®) equipment equipped with a microconvex probe operating at 6.5-7.5 MHz was used for the ultrasound. A thin layer of ultrasound gel was applied to the skin, and the transducer was placed on the testes of the animals, which were positioned in dorsal recumbency [21].

Color Doppler ultrasonography was used to assess the testicular artery (TA) and visualize blood flow in both the right and left testes. TBF was evaluated in the suprastesticular, intratesticular, and marginal testicular arteries (*Fig. 1*). During each measurement, at least three consecutive Doppler waveforms were recorded and averaged to enhance measurement accuracy (*Fig. 2*). For each region

of both testicles, Hemodynamic PSV, EDV, PI and RI measurements were repeated three times and averaged. Doppler parameters were automatically calculated and recorded by the ultrasound system.

Collection of Semen Samples and Spermatological Analysis

Semen was collected from each dog three times, at two-week intervals using digital stimulation, to ensure that the animals met the minimum reproductive requirements [22]. During each collection, the ejaculate was divided into three distinct fractions: pre-sperm, sperm-rich, and post-sperm fractions. For spermatological assessments, only the sperm-rich fraction was used, as it contains the highest concentration of spermatozoa and provides the most reliable parameters for assessing semen quality. Parameters assessed included total motility (%), progressive motility (%), sperm concentration (mL), and sperm morphology (%). During evaluation, semen was maintained at a constant temperature of 37°C.

To ensure homogeneity, the fresh spermatozoa were diluted with a tris-based extender to achieve a final concentration of $50\text{-}100 \times 10^6$ spermatozoa/mL [23]. Prior to computer-assisted analysis, semen samples were subjected to macroscopic evaluation, including assessment of ejaculate volume, color, and consistency. Subsequently, a CASA system (Sperm Class Analyser, Version 6.5.0.91, Microptic, Barcelona, Spain) was utilized to assess sperm concentration, motility (%), progressive motility (%), and morphology.

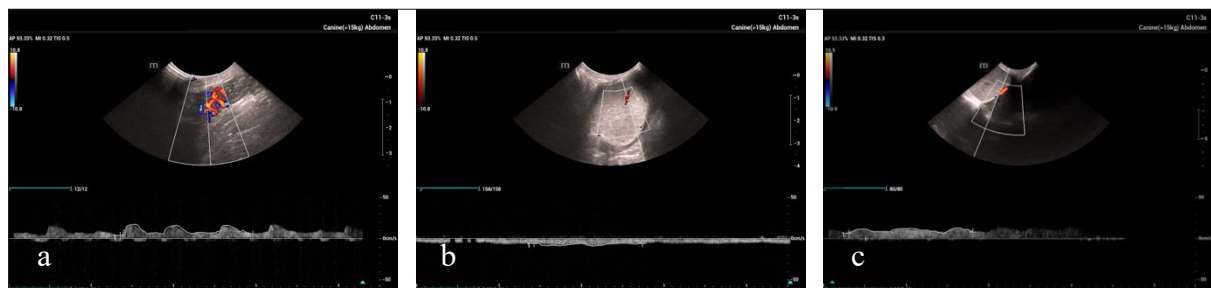


Fig 1. Doppler waveform of the testicular artery in dogs: suprastesticular (a), intratesticular (b), and marginal (c)

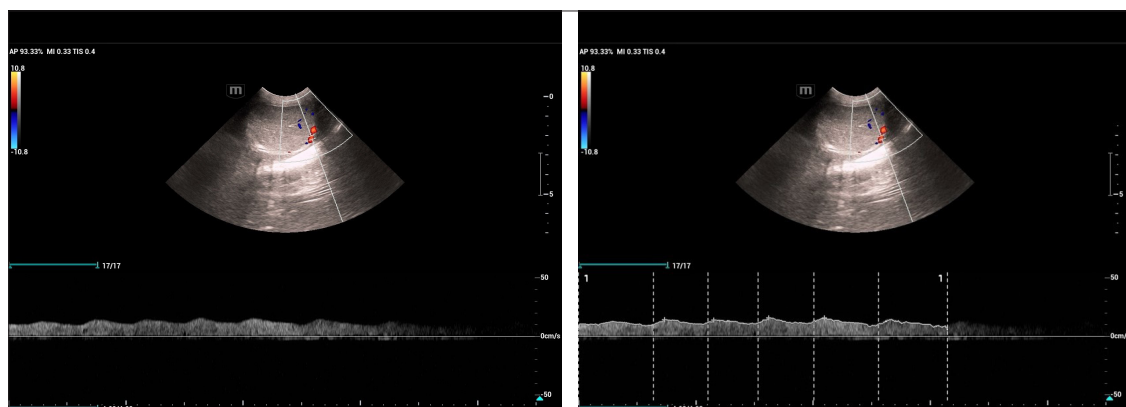


Fig 2. Spectral Doppler measurement of the testicular marginal artery

Sperm morphology was evaluated using the "Sperm Blue" kit" (Microptic"), and the results were also analyzed via the CASA system [24]. The Sperm Blue kit stains various parts of the sperm (head, midpiece, and tail) in different shades of azure, allowing for detailed morphological assessment. Sperm smears were prepared for each dog, allowed to air dry at room temperature, and stained following the manufacturer's instructions. At least 200 spermatozoa were assessed per animal, and the percentage of abnormal spermatozoa was determined.

Dogs were randomly selected for inclusion in the study, regardless of their initial sperm parameters as assessed by the CASA system, as the objective was to evaluate the natural variability of testicular hemodynamics and its association with spermatological parameters across different age groups.

Statistical Analysis

IBM SPSS Statistics for Windows, Version 21.0 (IBM Corp., NY, USA), was used for all statistical analyses. For each dog, repeated measurements taken at two-week intervals were averaged, and these mean values were used for statistical analysis to avoid pseudo-replication. Before hypothesis testing, the normality of the data distribution was assessed using the Shapiro-Wilk test, complemented by visual inspection of histograms and Q-Q plots. Additionally, skewness and kurtosis values were examined to further confirm the distribution characteristics of the variables. For normally distributed data, differences between the adult and senior groups were evaluated using the Independent Samples t-test. Homogeneity of variances was assessed with Levene's test, and the appropriate t-test results (assuming equal or unequal variances) were reported accordingly.

Doppler ultrasonographic measurements, including PSV, EDV, PI, and RI of the suprastesticular, marginal, and intratesticular arteries in both the right and left testes, were normally distributed and thus analyzed using parametric tests (Independent Samples t-test). In contrast, spermatological parameters such as motility, progressive motility, sperm concentration, and morphological defects (head, midpiece, tail, and total morphological defects) did not follow a normal distribution. Although these variables exhibited homogeneity of variances, they were analyzed using the non-parametric Mann-Whitney U test due to their deviation from normality.

Spearman's rank correlation coefficient (ρ) was used to assess the relationships between Doppler parameters and spermatological variables. The strength of correlations was interpreted based on the absolute value of ρ . A P-value of less than 0.05 was considered statistically significant for all tests.

RESULTS

Doppler ultrasonographic evaluation revealed significant age-related alterations in testicular arterial blood flow (*Table 1*). In the right testis, the suprastesticular artery exhibited significantly higher PSV values in the senior group compared to the adult group ($P<0.01$). In contrast, EDV and RI were significantly lower in adults ($P<0.01$). Intratesticular arterial flow in the right testis also demonstrated significantly elevated PSV and PI values in the adult group ($P<0.01$), whereas RI was lower ($P<0.05$). No significant differences were observed in EDV values between the groups. In contrast, marginal artery measurements in the right testis revealed no significant differences in PSV, EDV, or RI values ($P>0.05$), although PI was significantly higher in adult dogs ($P<0.05$).

Similar trends were observed in the left testis. In the suprastesticular artery, senior group exhibited significantly higher PSV and PI values ($P<0.05$ and $P<0.01$, respectively) and lower EDV and RI values compared to adult group ($P<0.05$ and $P<0.01$, respectively). The intratesticular artery on the left side also significantly reduced RI and PI values in the adult group ($P<0.01$ and $P<0.05$, respectively). However, the marginal artery showed no significant differences between groups in most parameters ($P>0.05$). These findings suggest that testicular arterial hemodynamics, particularly within the suprastesticular and intratesticular arteries, are significantly influenced by age in large-breed dogs.

Significant differences between the adult and senior groups were observed in all spermatological parameters (*Table 2*). Total motility and progressive motility were significantly higher in adult dogs ($P<0.01$ and $P<0.001$, respectively), while senior dogs exhibited markedly reduced motility levels. Similarly, sperm concentration was significantly higher in the adult group compared to the senior group ($P<0.01$). In contrast, morphological abnormalities were significantly more prevalent in the senior group. The mean percentages of head, midpiece, and tail defects were significantly higher in older dogs ($P<0.01$ or $P<0.001$), resulting in a significantly increased total defect percentage in the senior group ($P<0.001$). These findings suggest a clear age-related decline in semen quality, characterized by reduced motility and increased morphological abnormalities in senior dogs.

Significant correlations between Doppler ultrasonographic vascular hemodynamics and spermatological parameters in the study dogs are presented in *Fig. 3*.

The correlation analysis between Doppler ultrasonographic indices and spermatological parameters is detailed in *Table 3*. A strong negative correlation was observed between right suprastesticular PSV and total motility ($r=-$

Table 1. Comparison of doppler ultrasonographic parameters of the testicular arteries between adult and senior dogs

Doppler Ultrasonography			Groups of Animals (Mean±SD)		P
			Adult Group	Senior Group	
Right Testis Doppler Parameters	Supratesticular artery	PSV (cm/s)	18.15±0.93	22.14±2.11	<0.01**
		EDV (cm/s)	5.73±1.45	3.67±0.33	<0.01**
		RI	0.67±0.08	0.83±0.14	<0.01**
		PI	1.27±0.28	1.93±0.05	<0.01**
	Intratesticular artery	PSV (cm/s)	4.44±0.5	6.15±1.49	<0.01**
		EDV (cm/s)	3.21±0.47	3.48±0.47	>0.05
		RI	0.27±0.04	0.41±0.10	<0.05*
		PI	0.36±0.05	0.57±0.14	<0.01**
	Marginal artery	PSV (cm/s)	13.71±2.04	14.42±2.05	>0.05
		EDV (cm/s)	6.97±1.57	6.23±0.49	>0.05
		RI	0.48±0.11	0.55±0.05	>0.05
		PI	0.77±0.18	1.07±0.08	<0.05*
Left Testis Doppler Parameters	Supratesticular artery	PSV (cm/s)	18.15±1.47	20.74±1.68	<0.05*
		EDV (cm/s)	5.73±1.45	3.84±0.34	<0.05*
		RI	0.68±0.1	0.81±0.1	<0.01**
		PI	1.76±1.08	1.93±0.3	<0.01**
	Intratesticular artery	PSV (cm/s)	9.72±1.42	5.73±1.27	>0.05
		EDV (cm/s)	3.85±0.61	3.87±0.61	>0.05
		RI	0.29±0.01	0.52±0.1	<0.01**
		PI	0.43±0.03	0.54±0.08	<0.05*
	Marginal artery	PSV (cm/s)	14.20±1.96	14.69±1.38	>0.05
		EDV (cm/s)	6.81±1.83	6.32±0.63	>0.05
		RI	0.48±0.06	0.53±0.04	>0.05
		PI	0.65±0.1	0.72±0.17	>0.05

*P<0.05, **P<0.01, SD: standard deviation

0.81, P<0.01), progressive motility (r=-0.84, P<0.01), and sperm concentration (r=-0.87, P<0.01). Conversely, right supratesticular PSV showed strong positive correlations with head defects (r=0.85), tail defects (r=0.77), and total morphological defects (r=0.76).

Similarly, the right supratesticular RI was negatively correlated with motility (r=-0.82), progressive motility (r=-0.84), and concentration (r=-0.71) while exhibiting positive associations with head (r=0.75), tail (r=0.73), and total defects (r=0.75). The PI in the same artery

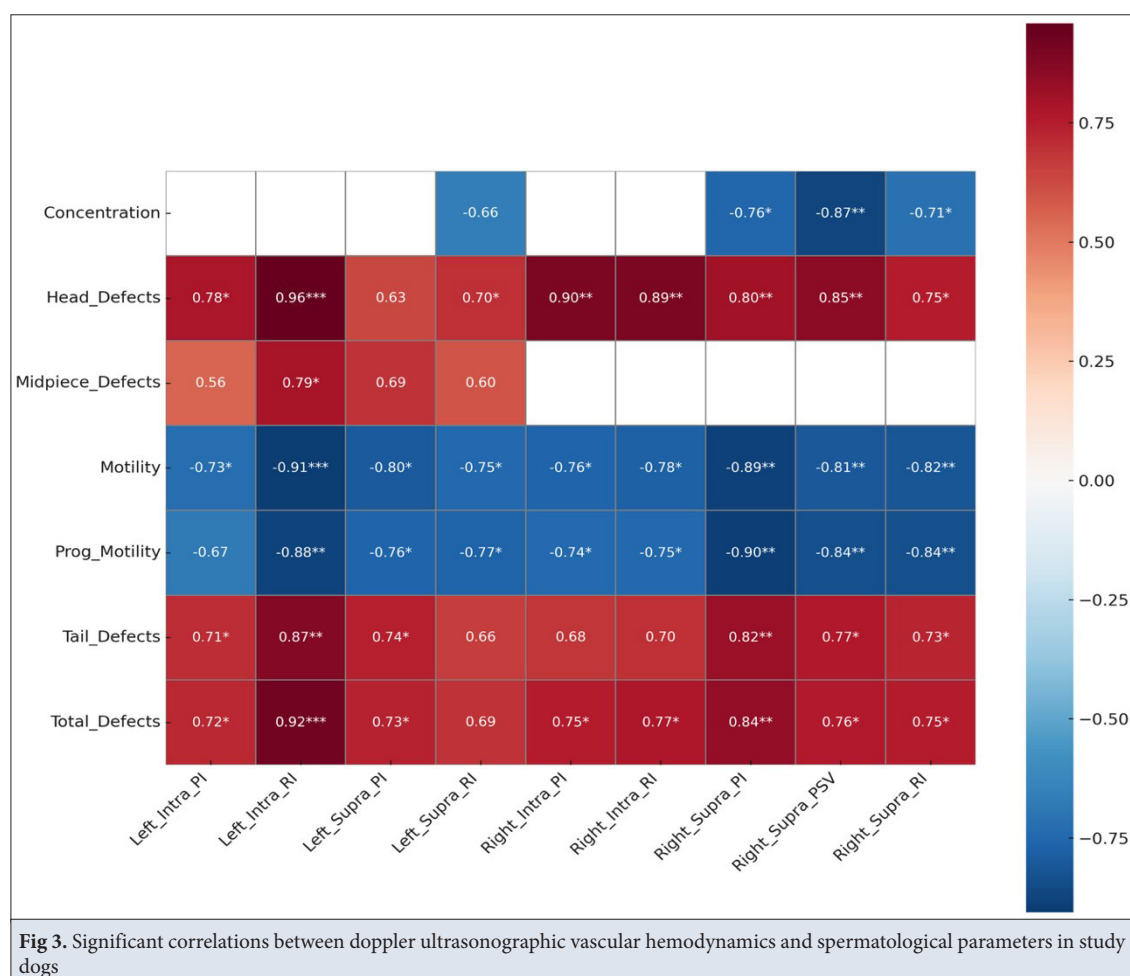
also demonstrated strong negative correlations with motility (r=-0.88), progressive motility (r=-0.90), and concentration (r=-0.76), alongside strong positive correlations with head (r=0.81), tail (r=0.82), and total defects (r=0.84).

In the right intratesticular artery, RI showed strong negative correlations with motility (r=-0.78) and progressive motility (r=-0.75) and strong positive correlations with head (r=0.89), tail (r=0.70), and total morphological defects (r=0.77). PI values followed a

Table 2. Comparison of spermatological parameters between adult and senior groups

Spermatological Parameters	Adult group			Senior group			P
	Mean±SD	Median	Interquartile Range	Mean±SD	Median	Interquartile Range	
Motility	78.71±6.08	80.13	8.38	33.71±6.27	31.23	8.38	<0.01**
Progressive Motility	68.95±5.38	72.23	10.98	13.62±4.29	13.34	6.94	<0.001***
Concentration	368.19±33.19	380	41.98	184.27±37.85	178.67	74.84	<0.01**
Head Defects	1.42±0.78	1	1	6.14±1.57	6	2	<0.001***
Midpiece Defects	4.42±0.53	4	1	9±2.08	9	4	<0.01**
Tail Defects	4±0.81	4	2	12.42±1.61	12	3	<0.001***
Total Defects	9.85±0.89	10	3	27.57	3.64	8	<0.001***

*P<0.05, **P<0.01, ***P<0.001, SD: standard deviation

**Fig 3.** Significant correlations between doppler ultrasonographic vascular hemodynamics and spermatological parameters in study dogs

similar trend, being negatively correlated with motility ($r=-0.76$) and progressive motility ($r=-0.74$) and positively correlated with head ($r=0.90$), tail ($r=0.68$), and total defects ($r=0.74$).

For the left testis, left suprastesticular RI showed strong negative correlations with motility ($r=-0.75$) and

progressive motility ($r=-0.77$) and a moderate negative correlation with sperm concentration ($r=-0.66$). Positive correlations were observed with head ($r=0.70$), midpiece ($r=0.60$), tail ($r=0.66$), and total defects ($r=0.69$). Left suprastesticular PI was also negatively associated with motility ($r=-0.80$) and progressive motility ($r=-0.76$)

and positively associated with head ($r=0.63$), midpiece ($r=0.69$), tail ($r=0.74$), and total defects ($r=0.73$).

The strongest associations were found in the left intratesticular artery. RI exhibited very strong negative correlations with motility ($r=-0.91$) and progressive motility ($r=-0.88$) and very strong positive correlations with head ($r=0.96$), midpiece ($r=0.79$), tail ($r=0.87$), and total morphological defects ($r=0.92$). Lastly, left intratesticular PI showed a strong negative correlation with motility ($r=-0.72$), a moderate negative correlation with progressive motility ($r=-0.67$), and positive associations with head ($r=0.78$), midpiece ($r=0.56$), tail ($r=0.71$), and total defects ($r=0.72$).

DISCUSSION

This study evaluated the relationship between testicular artery hemodynamics and spermatological parameters in Kangal Shepherd dogs across different age groups. The hemodynamic data revealed that PSV, PI, and RI values measured in the supratesticular and intratesticular arteries were significantly elevated in senior dogs, whereas end-diastolic velocity (EDV) values were significantly lower. No significant differences were observed between the left and right testicles in any hemodynamic parameters, and the measurements remained consistent across different examination days.

Regarding the spermatological findings, adult dogs exhibited significantly higher total motility, progressive motility, and sperm concentration than their senior group. Conversely, the incidence of morphological defects -specifically in the head, midpiece, and tail regions- was significantly higher in the senior group. Correlation analysis demonstrated a strong negative association between increased arterial resistance and pulsatility and sperm motility and concentration. In contrast, a positive correlation was identified with morphological abnormalities.

Age-related changes in testicular blood flow have been extensively documented in human medicine. Doppler ultrasonography studies have consistently shown that advancing age is associated with increased PSV, decreased EDV and elevated PI and, RI values in the testicular arteries [25]. These hemodynamic alterations reflect diminished vascular elasticity and impaired microcirculation within aging testicular tissue. The consequent reduction in testicular perfusion contributes to the decline in spermatogenic function commonly observed in older men. Clinically, such age-related Doppler changes are increasingly utilized as non-invasive indicators of subclinical testicular dysfunction and as part of the broader assessment of male reproductive health. Accordingly, testicular Doppler ultrasonography

has become an important diagnostic modality in the evaluation of age-associated testicular decline and male infertility [26].

In veterinary medicine, assessing testicular blood flow using Doppler ultrasonography has proven to be a valuable diagnostic tool [27,28]. Numerous studies have demonstrated a positive relationship between testicular arterial blood flow and spermatological parameters, including overall sperm quality [13,17,22]. In Doppler evaluations conducted across various animal species -including dogs [17], rams [6] and stallions [5]- hemodynamic parameters such as PI and RI have been extensively studied. These indices, in particular, have been widely accepted as reliable indicators of testicular perfusion status and potential markers of sperm quality [15].

Considering the relevant literature, Souza et al. [22] reported the PI index values in the range of 0.7-1.15 and the RI index values in the range of 0.4-0.7 in the study conducted to examine the Doppler velocimetry parameters of the testicular artery in dogs. In 2015, conducted another study including the measurement and evaluation of the velocimetry parameters of the marginal testicular artery. In this study, the PI index results ranged from 0.4 to 0.7 and the RI index results ranged from 0.3 to 0.6. In addition, PSV and EDV values were obtained significantly lower in infertile dogs. RI and PI values did not differ between fertile and infertile dogs [29]. Venianaki et al. [15] studied the doppler examination of the testicular artery in dogs from birth to adolescence and reported the PI index values in the range of 0.1-0.5 and the RI index values in the range of 0.1-0.4. Based on these results, it can be said that the doppler velocymetric values of the testicular artery measured by us are consistent with other studies.

In the context of infertility and aging, increases in PI and RI observed in testicular arteries are thought to be associated with impaired testicular microcirculation and reduced parenchymal perfusion. Elevated PI and RI values reflect increased resistance to arterial blood flow and diminished diastolic velocity, which in turn hampers the delivery of oxygen and nutrients essential for spermatogenesis [30]. In vascular pathologies such as varicocele, increased RI and PI values have been reported, indicating compromised testicular microvascular function [31]. Moreover, aging-related changes including the disruption of elastin-collagen balance, the development of endothelial dysfunction, and structural thickening of arterial walls contribute to diminished vascular compliance and heightened arterial resistance. This leads to a more pulsatile pattern of blood flow to the testes, resulting in elevated PI and RI parameters, which may ultimately contribute to germinal epithelial damage and a decline in spermatogenic activity.

Several studies have attempted to establish reference values

for testicular blood flow in dogs and to elucidate their association with spermatological parameters [14,16,32,33]. In a study conducted by de Souza et al.^[29] to define regional differences in testicular arterial blood flow in clinically post-pubertal and pre-pubertal dogs, they found that PSV, EDV, RI and PI values were significantly lower in pre-pubertal dogs compared to post-pubertal dogs in testicular hemodynamic values. Zelli et al.^[33] reported a negative correlation between PI and RI with total progressive motility, while PSV was also negatively associated with the live of sperm. This result is inconsistent with that obtained by England et al.^[32] who could not prove a relationship between RI and PI with total sperm output or percentage of live of sperm. Trautwein et al.^[19] investigated the effect of testicular arterial blood flow on sperm motility and spermatozoa morphology in dogs and reported a correlation between Doppler velocimetry parameters and motility.

In the present study, PI and RI values, which have been previously proposed as potential indicators of sperm quality in dogs [33], were consistent with those reported in earlier studies. A strong negative correlation was identified between testicular arterial RI and PI values and key spermatological parameters such as sperm motility and concentration, which tended to decline with age. Conversely, RI and PI values were positively correlated with the incidence of morphological abnormalities, which increased with age. These findings suggest that age-related impairment in testicular blood flow, as reflected by elevated vascular resistance parameters, may negatively influence spermatogenesis. Consequently, the increase in vascular resistance with age may play a critical role in the deterioration of male fertility.

Trautwein et al.^[19] investigated the effect of testicular artery blood flow on epididymal sperm motility and spermatozoa morphology in dogs and reported a positive correlation between Doppler velocimetry parameters PSV, PI and RI and motility parameters. In 2020, Lemos et al.^[14] reported a positive correlation between sperm concentration and PSV and EDV in their study comparing normozoospermic and non-normozoospermic groups. In our study, a negative correlation was obtained between sperm concentration and PSV.

In our study, PSV values were higher in senior dogs than in the adult group; however, a significant decrease in sperm concentration was observed. This apparent paradox may indicate a compensatory vascular response to age-related microcirculatory impairment. Elevated PSV in the presence of increased PI and RI suggests that while systolic pressure rises to maintain perfusion, overall flow efficiency declines due to elevated resistance. This high-resistance, low-efficiency state hampers effective oxygen and nutrient delivery to the testicular tissue,

thereby compromising spermatogenesis [33,34].

Additionally, a study examining the Doppler examination of testicles in dogs of different sizes reported that the velocitometric index values varied depending on the size and weight of the dog [16]. Larger and heavier dog breeds show different velocitometric parameter values compared to smaller dog breeds. In our study, correlations between velocitometric values and spermatological parameters were applied to Kangal Shepherd dogs. The differences in our findings with the study conducted by Lemos et al.^[14]. In the study, evaluations were made using more than one breed. Therefore, this difference may have been observed.

In conclusion, Doppler velocimetric evaluation plays an important role in the evaluation of reproduction in male dogs. This study shows that spermatological parameters can be associated with testicular arterial blood flow in male Kangal Shepherd dogs of different age groups. It also forms the basis for establishing basic reference values that can be used for clinical diagnosis. Due to the differences in these parameters depending on the location of measurement, season, age, breed, laterality and operator, further research is needed to determine reference physiological parameters according to species and breed and to establish reference values for species of certain sizes.

DECLARATIONS

Availability of Data and Materials: The datasets and analysed during the current study available from the corresponding author (BE) on reasonable request.

Ethical Statement: This study was conducted at the Animal Hospital of the Faculty of Veterinary Medicine, Ondokuz Mayıs University, and was approved by the Animal Ethics Committee of Ondokuz Mayıs University (Approval No: 2024/41).

Funding Support: There is no funding source.

Conflict of Interest: The authors declare that they have no conflicts of interest.

Declaration of Generative Artificial Intelligence (AI): The authors declare that the article, tables and figures were not written/created by AI and AI-assisted Technologies.

Author Contributions: BE: Writing—original draft, Project administration, Methodology, Data curation, Conceptualization. BE, CK and ÇE: Methodology, Conceptualization, Writing – review & editing.


REFERENCES

1. Arlt SP, Reichler IM, Herbel J, Schäfer-Somi S, Riege L, Leber J, Frehner B: Diagnostic tests in canine andrology - What do they really tell us about fertility? *Theriogenology*, 196, 150-156, 2023. DOI: 10.1016/j.theriogenology.2022.11.008
2. Stefanizzi E, Valenčáková A, Schmiesterová K, Figurová M, Horňáková I: The use of Doppler ultrasonography in the examination of testicles in dogs. *Acta Vet Brno*, 72 (4): 453-467, 2022. DOI: 10.2478/acve-2022-0037
3. Bigliardi E, Denti L, De Cesaris V, Bertocchi M, Di Ianni F, Parmigiani E, Bresciani C, Cantoni AM: Colour Doppler ultrasound imaging of blood

- flows variations in neoplastic and non-neoplastic testicular lesions in dogs. *Reprod Domest Anim*, 54 (1): 63-71, 2019. DOI: 10.1111/rda.13310
4. Trautwein LGC, Souza AK, Martins MIM: Can testicular artery Doppler velocimetry values change according to the measured region in dogs? *Reprod Domest Anim*, 54 (4): 687-695, 2019. DOI: 10.1111/rda.13410
5. Ortiz-Rodriguez JM, Anel-Lopez L, Martín-Muñoz P, Álvarez M, Gaitskell-Phillips G, Anel L, Rodríguez-Medina P, Peña FJ, Ortega Ferrusola C: Pulse Doppler ultrasound as a tool for the diagnosis of chronic testicular dysfunction in stallions. *PLoS One*, 12 (5): e0175878, 2017. DOI: 10.1371/journal.pone.0175878
6. Batissaco L, Celeghini ECC, Pinaffi FLV, de Oliveira BMM, de Andrade AFC, Recalde ECS, Fernandes CB: Correlations between testicular hemodynamic and sperm characteristics in rams. *Braz J Vet Res Anim Sci*, 50 (5): 384-395, 2013. DOI: 10.11606/issn.2318-3659.v50i5p384-395
7. Konovalenko S, Kritsak M, Stechyshyn I, Pavliuk B: Male infertility as a consequence of endogenous and exogenous factors. *Pharmacologyonline*, 3, 265-274, 2021.
8. Dubinsky TJ, Chen P, Maklad N: Color-flow and power Doppler imaging of the testes. *World J Urol*, 16, 35-40, 1998. DOI: 10.1007/s003450050023
9. Atilla MK, Sargin H, Yilmaz Y, Odabas O, Keskin A, Aydin S: Undescended testes in adults: clinical significance of resistive index values of the testicular artery measured by Doppler ultrasound as a predictor of testicular histology. *J Urol*, 158 (3): 841-843, 1997. DOI: 10.1016/S0022-5347(01)64332-5
10. Samir H, Radwan F, Watanabe G: Advances in applications of color Doppler ultrasonography in the andrological assessment of domestic animals: A review. *Theriogenology*, 161, 252-261, 2021. DOI: 10.1016/j.theriogenology.2020.12.002
11. Bracco C, Gloria A, Contri A: Ultrasound-based technologies for the evaluation of testicles in the dog: Keystones and breakthroughs. *Vet Sci*, 10 (12):683, 2023. DOI: 10.3390/vetsci10120683
12. Colli LG, Belardin LB, Echem C, Akamine EH, Antoniassi MP, Andretta RR, Mathias LS, Rodrigues SF de P, Bertolla RP, de Carvalho MHC: Systemic arterial hypertension leads to decreased semen quality and alterations in the testicular microcirculation in rats. *Sci Rep*, 9 (1):11047, 2019. DOI: 10.1038/s41598-019-47157-w
13. Moxon R, Bright L, Pritchard B, Bowen IM, de Souza MB, da Silva LDM, England GCW: Digital image analysis of testicular and prostatic ultrasonographic echogenicity and heterogeneity in dogs and the relation to semen quality. *Anim Reprod Sci*, 160, 112-119, 2015. DOI: 10.1016/j.anireprosci.2015.07.012
14. Lemos H, Dorado J, Hidalgo M, Gaivão I, Martins-Bessa A: Assessment of dog testis perfusion by colour and pulsed-doppler ultrasonography and correlation with sperm oxidative DNA damage. *Top Companion Anim Med*, 41:100452, 2020. DOI: 10.1016/j.tcam.2020.100452
15. Venianaki AP, Barbagianni MS, Fthenakis GC, Galatos AD, Gouletsou PG: Doppler examination of the testicular artery of Beagle-breed dogs from birth to puberty. *Tomography*, 9 (4): 1408-1422, 2023. DOI: 10.3390/tomography9040112
16. de Souza MB, Barbosa CC, England GCW, Mota Filho AC, Sousa CV, de Carvalho GG, Silva HV, Pinto JN, Linhares JCS, Silva LDM: Regional differences of testicular artery blood flow in post pubertal and pre-pubertal dogs. *BMC Vet Res*, 11 (47): 1-6, 2015. DOI: 10.1186/s12917-015-0363-3
17. Zelli R, Troisi A, Ngonput AE, Cardinali L, Polisca A: Evaluation of testicular artery blood flow by Doppler ultrasonography as a predictor of spermatogenesis in the dog. *Res Vet Sci*, 95 (2): 632-637, 2013. DOI: 10.1016/j.rvsc.2013.04.023
18. Carrillo JD, Soler M, Lucas X, Agut A: Colour and pulsed Doppler ultrasonographic study of the canine testis. *Reprod Domest Anim*, 47 (4): 655-659, 2012. DOI: 10.1111/j.1439-0531.2011.01937.x
19. Trautwein LGC, Souza AK, Cardoso GS, da Costa Flaiban KKM, de Oliveira Dearo AC, Martins MIM: Correlation of testicular artery Doppler velocimetry with kinetics and morphologic characteristics of epididymal sperm in dogs. *Reprod Domest Anim*, 55 (6): 720-725, 2020. DOI: 10.1111/rda.13672
20. Akyazi I, Ograk YZ, Eraslan E, Arslan M, Matur E: Livestock guarding behaviour of Kangal dogs in their native habitat. *Appl Anim Behav Sci*, 201, 61-66, 2018. DOI: 10.1016/j.applanim.2017.12.013
21. Yayla S, Ozturk S, Aksoy O, Kilic E, Yildiz S: Normal ultrasonographic anatomy of the prostate in Kars Shepherd dogs. *Kafkas Univ Vet Fak Derg*, 18 (1): 27-30, 2012. DOI: 10.9775/kvfd.2011.4528
22. de Souza MB, da Cunha Barbosa C, Pereira BS, Monteiro CLB, Pinto JN, Linhares JCS, da Silva LDM: Doppler velocimetric parameters of the testicular artery in healthy dogs. *Res Vet Sci*, 96 (3): 533-536, 2014. DOI: 10.1016/j.rvsc.2014.03.008
23. Nazeri E, Niasari-Naslaji A, Ghasemzadeh-Nava H, Panahi F: The effect of varying concentrations of chicken plasma egg yolk and glycerol on the viability of canine sperm following short and long-term preservation. *Iran J Vet Res*, 24 (1): 6-13, 2023. DOI: 10.22099/IJVR.2022.43403.6339
24. Tekin K, Kurtde E, Salmanoglu B, Uysal O, Stelletta C: Osteopontin concentration in prostates fractions: A novel marker of sperm quality in dogs. *Vet Sci*, 10 (11):646, 2023. DOI: 10.3390/vetsci10110646
25. Yang H, Chryssikos T, Houseni M, Alzeair S, Sansovini M, Iruvuri S, Torigian DA, Zhuang H, Dadparvar S, Basu S: The effects of aging on testicular volume and glucose metabolism: An investigation with ultrasonography and FDG-PET. *Mol Imaging Biol*, 13, 391-398, 2011. DOI: 10.1007/s11307-010-0341-x
26. Wang JJ, Wang SX, Tehmina, Feng Y, Zhang RF, Li XY, Sun Q, Ding J: Age-related decline of male fertility: mitochondrial dysfunction and the antioxidant interventions. *Pharmaceuticals*, 15 (5): 519, 2022. DOI: 10.3390/ph15050519
27. Semiz I, Tokgöz Ö, Tokgoz H, Voyvoda N, Serifoglu I, Erdem Z: The investigation of correlation between semen analysis parameters and intraparenchymal testicular spectral Doppler indices in patients with clinical varicocele. *Ultrasound Q*, 30 (1): 33-40, 2014. DOI: 10.1097/RUQ.0000000000000055
28. Esin C: Effect of systemic hypertension on prostatic arterial hemodynamics in dogs with benign prostate hyperplasia. *Kafkas Univ Vet Fak Derg*, 18 (1): 27-32, 2025. DOI: 10.9775/kvfd.2024.32734
29. de Souza MB, England GCW, Mota Filho AC, Ackermann CL, Sousa CVS, de Carvalho GG, Silva HVR, Pinto JN, Linhares JCS, Oba E: Semen quality, testicular B-mode and Doppler ultrasound, and serum testosterone concentrations in dogs with established infertility. *Theriogenology*, 84 (5): 805-810, 2015. DOI: 10.1016/j.theriogenology.2015.05.015
30. Ok F, Durmus E, Ayaz M: The role of the resistive index in predicting testicular atrophy after orchiopexy in unilateral undescended testis. *Pediatr Surg Int*, 39 (1): 38, 2022. DOI: 10.1007/s00383-022-05336-3
31. Dalili AR, Madani AH, Joni SS: The comparison of resistance Index of testicular artery using color Doppler ultrasound in infertile men undergoing varicocele. *J Reprod Infertil*, 22 (2): 110, 2021. DOI: 10.18502/jri.v22i2.5796
32. England GCW, Bright L, Pritchard B, Bowen IM, de Souza MB, Silva LDM, Moxon R: Canine reproductive ultrasound examination for predicting future sperm quality. *Reprod Domest Anim*, 52 (52): 202-207, 2017. DOI: 10.1111/rda.12825
33. Zelli R, Orlandi R, Troisi A, Cardinali L, Polisca A: Power and pulsed doppler evaluation of prostatic artery blood flow in normal and benign prostatic hyperplasia-affected dogs. *Reprod Domest Anim*, 48 (5): 768-773, 2013. DOI: 10.1111/rda.12159
34. Claus LAM, Barca Junior FA, Junior CK, Pereira GR, Fávoro PDC, Ferreira FP, Galdioli VH, Seneda MM, Ribeiro ELA: Testicular shape, scrotal skin thickness and testicular artery blood flow changes in bulls of different ages. *Reprod Domest Anim*, 56 (7): 1034-1039, 2021. DOI: 10.1111/rda.13947

RESEARCH ARTICLE

How Light and Stocking Density Affect the Morphometric and Mechanical Traits of Quail Tibiotarsus?

İ. Gökçe YILDIRIM ¹  Figen SEVİL KİLİMCİ ¹ (*)  Komal KHAN ²  Firuze TÜRKER YAVAŞ ¹ 
Ece KOÇ YILDIRIM ³  Sanan RAZA ⁴ 

¹ Aydın Adnan Menderes University, Faculty of Veterinary Medicine, Department of Veterinary Anatomy, TR-09016 Aydın - TÜRKİYE

² University of Veterinary & Animal Sciences, Anatomy Section, Department of Basic Sciences, 35200, Jhang Campus, PAKISTAN

³ Aydın Adnan Menderes University, Faculty of Veterinary Medicine, Department of Veterinary Physiology, TR-09016 Aydın - TÜRKİYE

⁴ University of Veterinary & Animal Sciences, Department of Clinical Sciences, Theriogenology Section, 35200 Jhang Campus, PAKISTAN



(*) Corresponding author:

Figen Sevil Kilimci

Phone: +90 256 220 6000/6094

Cellular phone: +90 535 361 3488

E-mail: fsevil@adu.edu.tr

How to cite this article?

Yıldırım İG, Sevil Kilimci F, Khan K, Türker Yavaş F, Koç Yıldırım E, Raza S: How Light and Stocking Density Affect the Morphometric and Mechanical Traits of Quail Tibiotarsus? *Kafkas Univ Vet Fak Derg*, 31 (5): 645-652, 2025.
DOI: 10.9775/kvfd.2025.34495

Article ID: KVFD-2025-34495

Received: 20.05.2025

Accepted: 13.09.2025

Published Online: 19.09.2025

Abstract

Quails (*Coturnix coturnix japonica*) are a significant migratory bird species, widely recognised for their rapid growth and efficient production of meat and eggs, making them an important component of the poultry industry. Despite their economic importance, the impact of environmental factors, particularly light and stocking density, on their skeletal health remains an area requiring further investigation. This study addresses this gap by examining how these factors influence the morphometric and mechanical properties of quail long bones. This study aimed to investigate the effects of different light colors and stocking densities on the morphometric and mechanical properties of long bones in Japanese quails. The experiment utilised three different light colors (white, blue, and green) and two different stocking densities (100 cm²/animal and 200 cm²/animal). A total of 120 Japanese quails (72 male, 48 female) were used to evaluate morphometric (length, diameter) and mechanical (bending strength, stiffness) properties. It was determined that light color significantly affected bone stiffness but had no marked effect on bone strength and elastic modulus. Furthermore, it was observed that the morphometric and mechanical properties of female quail bones were higher than those of males. These findings highlight the impact of light on quail bone health and open new avenues for future research. Stocking density was found to have no significant effect on bone properties.

Keywords: Biomechanics, Bone, Light-emitting diodes, Quail, Tibiotarsus

INTRODUCTION

The quail (*Coturnix coturnix*) is a migratory avian species with a wide distribution across Eurasia and Africa. It is also known for its unique taste characteristics in meat and eggs, rapid reproductive activity, and short-term capital recovery.

Despite a wide market for quail meat and eggs, quail management, including lighting requirements, housing density, and other welfare variables, is still not well-developed at extensive or intensive production levels ^[1].

Some researchers indicated that lighting is one of the most important environmental factors affecting poultry performance and physical activity ^[2]. Light plays a

significant role in growth, skeletal development, welfare, and reproductive performance. Rozenboim et al. ^[3] suggested that green light increases body weight, but blue and green light-emitting diodes (LEDs) combination was found much more effective than green. Studies have shown a positive correlation between specific light intensities and broiler activity, increasing pressure and load on bones, and supporting bone development ^[4,5]. Light can also cause changes in some skeletal-related metabolic pathways, such as calcium and phosphorus metabolism ^[6]. Appropriate photoperiods have increased body weight, cortical bone formation, and bone mineralisation ^[7]. The tibiotarsus length and weight of broiler chickens were positively affected by intermittent lighting ^[8].



Cage characteristics and conditions are also important environmental factors affecting animal production traits. High housing density has been shown to worsen skeletal problems and progressively reduce walking ability [9,10].

Bone exhibits viscoelastic properties, meaning that its mechanical characteristics are directly influenced by its density, porosity, and micro-architecture [11]. In mechanical testing, the slope of the elastic region on the force-displacement curve represents the extrinsic stiffness or rigidity of the bone structure, while the elastic modulus quantifies the intrinsic stiffness of the bone material itself. The maximum stress the bone can withstand before failure is termed its ultimate strength, a parameter independent of its size and shape. However, the force required to break the bone-referred to as the breaking load or fracture force-does vary with bone size, distinguishing it from intrinsic strength [12]. Light can also cause changes in some skeletal-repeated metabolic pathways such as calcium and phosphorus metabolism [6].

Since light affects the metabolic structure of bone tissue, studies in this field evaluate both intrinsic and morphometric properties of bone tissue. In light of all this information, the study aimed to investigate the morphometric and mechanical effects of three different light colours on quail long bones in two animal groups with different housing densities.

MATERIALS AND METHODS

Ethical Statement

This study was approved by the Animal Experiments Local Ethics Committee of Aydın Adnan Menderes University, under the number 64583101/2023/29.

Animals and Experimental Design

The bones used in the study were obtained from a completed study at the Poultry Research Unit of the Veterinary Faculty of Aydın Adnan Menderes University.

In the study, the right tibiotarsus bones of a total of 120 quails (*Coturnix coturnix japonica*), aged 42 days, with an

average weight of 226 ± 30.19 g female and 228 ± 28.84 g male (mean \pm SD), including eight females and 12 males in each group, were used (Table 1).

The quails used in the research were raised at the Poultry Research Unit of the Veterinary Faculty of Aydın Adnan Menderes University for 42 days. The chicks were randomly selected on the first day of hatching and divided into groups. From the first day, they were separated into rooms with three different lighting applications, where light colour, temperature, and humidity values were controlled. The quails were fed *ad libitum* with feed containing 2910 kcal/kg ME and 24% CP during the growing period of 0-14 days, and 2900 kcal/kg ME and 22% CP during the development period of 15-42 days (NRC, 1994). Fresh water was provided daily *ad libitum* through a nipple drinker system. The quails were housed in four-tier brooding cages, each tier measuring 25x45x90 cm and equipped with heaters, feeders, and drinkers that remained constant in location and number throughout the trial. A continuous lighting program of 24 h of light - 0 h of darkness was applied to all groups throughout the study. The feeders and drinkers in the compartments were checked twice daily during the research period. Lighting was provided with LED bulbs emitting white, green, and blue light. Adjustable thermostatic automatic heaters were used in each compartment of the cages to maintain the desired ambient temperature. Humidity levels were also maintained at $60 \pm 5\%$ throughout the trial.

Different 9 W LED bulbs (CT-4277 CATA, Türkiye) emitting blue (480 nm), green (560 nm), and white light (400-770 nm) at an intensity of 20 lx were positioned above the cages. Throughout the experiment, the photoperiod was set at 24 h of light and 0 hours of darkness (24L:0D).

The housing density of the quails was arranged in two separate groups. A floor area of 200 cm²/animal was provided in the normal-density housing groups. In the high-density housing groups, a floor area of 100 cm²/animal was provided. In the normal housing groups, each cage compartment contained 20 quails, while in the high-density groups, each compartment contained 40 quails.

Table 1. The experimental groups for research study

Test Groups	Color	Density of Placement	Number of Males	Number of Females	Number of Animals
Group I	White Light	100 cm ² /animal	12	8	20
Group II	Blue Light	100 cm ² /animal	12	8	20
Group III	Green Light	100 cm ² /animal	12	8	20
Group IV	White Light	200 cm ² /animal	12	8	20
Group V	Blue Light	200 cm ² /animal	12	8	20
Group VI	Green Light	200 cm ² /animal	12	8	20
Total			72	48	120

Prior to the study, 20 animals were randomly selected from this group.

On the 42nd day of the study, decapitation was performed. Subsequently, the right and left legs of each quail were collected and stored in zipped plastic bags at +4°C to prevent tissue damage (for 24 h). The dissection of the legs was performed 24 h later to extract the tibiotarsus bones. The same person carefully performed the cleaning process of the bones without damaging the periosteum and bone tissue. To preserve their properties until the measurements and mechanical test stage, the bones were wrapped in gauze moistened with physiological saline and stored in Ziplock bags at -25°C [13].

Preparation of Samples for Biomechanical Test

Before the mechanical test, the bones were slowly thawed firstly at +4°C and then soaked in sterile physiological saline at +20°C. Subsequently, the lengths of the bones

were measured with a calliper, and their midpoint was marked to determine the loading points. The bones' mediolateral and craniocaudal periosteal diameters (outer diameters) were measured at the pre-determined loading point.

Mechanical Test: Three-Point Bending Test

The Zwick/Roell Z0.5 mechanical testing machine located at Aydın Adnan Menderes University, TARBIYOMER, was used for the mechanical test (Fig. 1). The distance between the support points for the three-point bending test was determined based on the length and diameter values of the obtained bones. Since the length values between the groups are very close, the support points were selected as fixed. The midpoints of the bone lengths were designated as the loading points. Two support points were selected so that the loading point was precisely in the middle, and the support distance was selected as 20 mm. During the test,

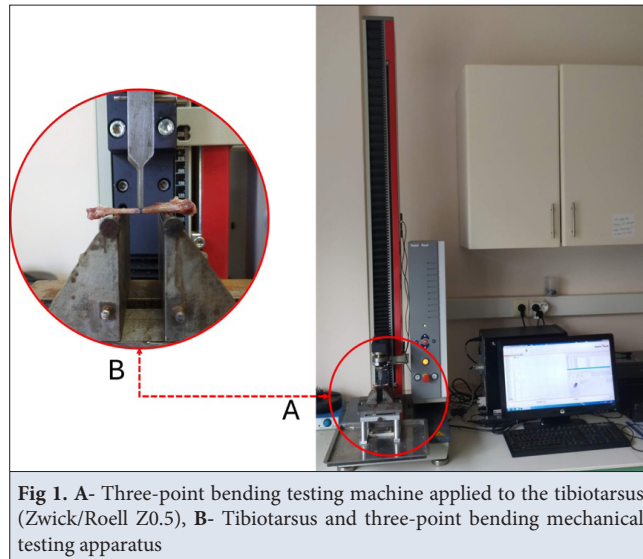


Fig 1. A- Three-point bending testing machine applied to the tibiotarsus (Zwick/Roell Z0.5), **B-** Tibiotarsus and three-point bending mechanical testing apparatus

Table 2. Effect of Gender, colored light, stocking density of bone morphometric measurements in the Quails^{1,2}

Parameters		N	L (mm)	DExt _{ML} (mm)	DInt _{ML} (mm)	DExt _{CrCd} (mm)	DInt _{CrCd} (mm)
Gender	Male	72	52.088±0.209	3.013±0.032	1.778±0.025	2.724±0.019	1.451±0.026
	Female	48	53.613±0.256	3.221±0.040	1.774±0.031	2.839±0.023	1.463±0.032
Colored light	White	40	52.666±0.286	3.042±0.44	1.721±0.034	2.783±0.026	1.433±0.036
	Blue	40	52.512±0.286	3.120±0.44	1.759±0.034	2.750±0.026	1.468±0.036
	Green	40	53.373±0.286	3.188±0.44	1.802±0.034	2.812±0.026	1.470±0.036
Stocking density	100 cm ² /Quails	60	52.848±0.234	3.128±0.036	1.741±0.28	2.799±0.021	1.474±0.029
	200 cm ² /Quails	60	52.853±0.234	3.105±0.036	1.781±0.028	2.764±0.021	1.439±0.029
P	Gender		0.000	0.000	0.388	0.000	0.784
	Colored light		0.081	0.072	0.248	0.281	0.704
	Stocking density		0.988	0.679	0.318	0.294	0.395

¹ Data presented as Mean ± SD

² The interaction between groups was not significant for investigated traits (P>0.05)

Table 3. Effect of Gender, colored light, stocking density of bone biomechanical properties in the Quails^{1,2}

Parameters		N	Moment of Inertia (mm ⁴)	Force (N)	Deformation (mm)	Stiffness (N/mm)	Strength (MPa)	Elastic Modulus (MPa)
Gender	Male	72	2.743±0.937	45.910±0.923	0.727±0.021	83.276±1.738	119.137±3.058	5317.593±145.076
	Female	48	3.387±1.147	55.452±1.130	0.710±0.026	95.092±2.129	121.56±3.745	4921.957±177.681
Colored light	White	40	2.992±1.282	49.699±1.264	0.717±0.029	87.954±2.380	121.245±4.187	5165.824±198.653
	Blue	40	2.947±1.282	50.425±1.264	0.733±0.029	85.716±2.380	122.613±4.187	5143.890±198.653
	Green	40	3.256±1.282	51.918±1.264	0.705±0.029	93.883±2.380	117.186±4.187	5049.610±198.653
Stocking density	100cm ² /Quails	60	3.155±1.047	50.716±1.032	0.732±0.024	89.009±1.943	118.666±3.418	5022.712±162.200
	200cm ² /Quails	60	2.975±1.047	50.646±1.032	0.705±0.024	89.359±1.943	122.030±3.418	5216.838±162.200
P	Gender		0.000	0.000	0.337	0.000	0.617	0.087
	Stocking density		0.188	0.425	0.535	0.047	0.636	0.908
	Colored light		0.227	0.900	0.343	0.899	0.488	0.399

¹ Data presented as Mean ± SD² The interaction between groups was not significant for investigated traits (P>0.05)

a preload of 1N was applied, and the bones were loaded at a rate of 10mm/min until they fractured [14,15]. After the test, a Force (N) - Deformation (mm) graph was obtained for each bone. The fractured bones' mediolateral and craniocaudal endosteal diameters (inner diameters) were also measured at the loading point, for later calculations.

From the graphs obtained after the three-point bending test, the stiffness value of each bone was calculated, and the inner and outer diameter values of the bones were used to calculate the moment of inertia (inertia moments) and cortical indexes of the bones. Using this calculated moment of inertia and stiffness values, each bone's ultimate strength and elastic modulus were determined [14,15].

Statistical Analysis

Statistical data was evaluated using the SPSS statistical package program (version 22.0, SPSS Inc., Chicago, IL, US) and R Studio software (version 4.4.2, Inc, Boston, MA, USA). Normal distribution of the data was checked by Shapiro-willk test. DExt_{ML}, I, F values that did not show normal distribution were logarithmically and DExt_{CrCd}, deformation values were reverse transformed. Levene's homogeneity test was used to check whether the values were homogeneous. General linear model (Univariate-GLM) method was used for comparison between groups. Bonferroni test was used to check the significance of differences between groups. The significance of differences between groups was set at P≤0.05, shown using asterisk. All results were reported as means ± SD.

RESULTS

In this study, the morphometric measurements (L, DExt)

and mechanical properties (moment of inertia, bone breaking force, and stiffness values) of quail bones, along with their variations according to gender, light color, and stocking density, are detailed in [Table 2](#) and [Table 3](#).

According to the [Table 2](#) and [Table 3](#), the morphometric (L, DExt) and mechanical properties of quail bones (moment of inertia, bone breaking force and stiffness values) differed between genders (P<0.000). In addition, although there was a significant difference in stiffness of bones among the light groups (P=0.047), but the used post hoc test could not measure the differences among the groups. No significant difference was seen in the results of all the parameters among differently stocked groups. In addition, the statistical analysis also showed that there were no interactions between the two provided stocking density rates on biomechanical parameters of quail bones.

Correlation analyses were performed separately for sex, stocking density, and light colour groups ([Fig. 2](#), [Fig. 4](#))

The correlation matrices revealed distinct gender-specific patterns in the relationships between structural and mechanical properties. In males, external measurements demonstrated robust correlations with mechanical properties, particularly the DExt_{ML} showing strong negative correlations with Elastic Modulus (r ≈ -0.8) and Strength (r ≈ -0.6). Similarly, in males, DExt_{CrCd} exhibited substantial negative correlations with Elastic Modulus (r ≈ -0.7) and Strength (r ≈ -0.5). Conversely, females displayed generally weaker correlations, with DExt_{ML} showing moderate negative correlations with Elastic Modulus (r ≈ -0.6) and Strength (r ≈ -0.4). The Imm⁴ parameter demonstrated notable positive correlations with mechanical properties in both genders, though the relationship was more pronounced in males (r ≈ 0.7 with

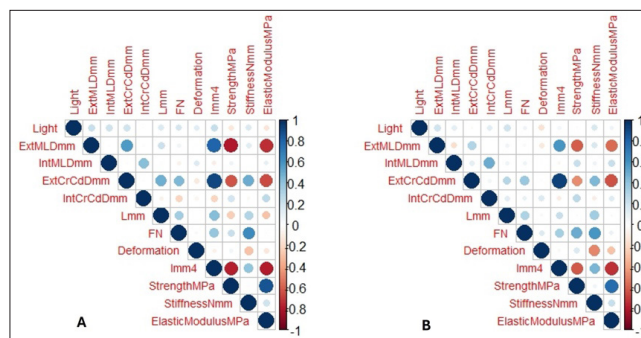


Fig 2. A comparative analysis of correlation patterns the male groups (A), female groups (B) under stocking density conditions. Red colours: negative correlation, Blue Colours: positive correlation

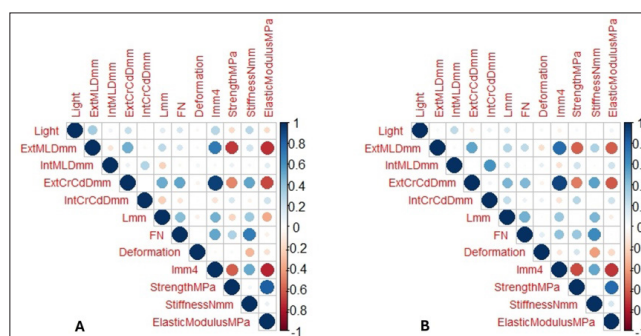


Fig 3. A comparative analysis of correlation patterns the normal-density groups (A), the high-density groups (B), under stocking density conditions. Red colours: negative correlation, Blue colours: positive correlation

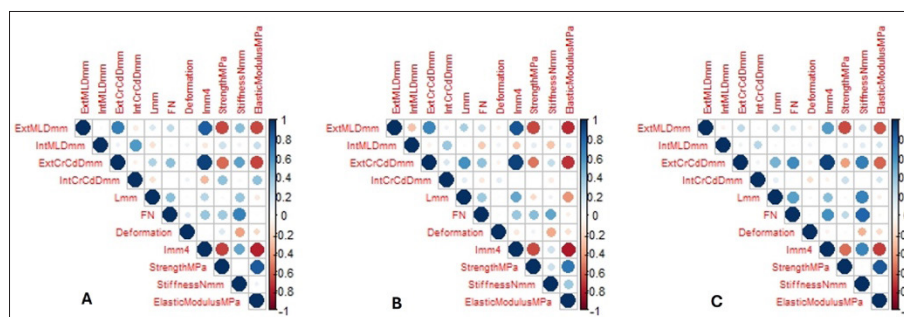


Fig 4. A comparative analysis of correlation patterns under white (A), blue (B), and green (C) light condition. Red colours: negative correlation, Blue colours: positive correlation

Strength) compared to females ($r \approx 0.6$ with Strength). Internal measurements (DInt_{ML} and DInt_{CrCd}) exhibited weaker correlations compared to external measurements across both genders (Fig. 2).

Correlation analysis revealed distinct patterns between normal-density (A) and high-density (B) bone specimens. In normal-density specimens, external measurements (DExt_{ML}) showed strong negative correlations with mechanical properties, particularly with Modulus of Elasticity ($r \approx -0.8$) and Strength ($r \approx -0.6$). The DExt_{CrCd} parameter also showed significant correlations with mechanical properties (with Modulus of Elasticity $r \approx -0.7$). Similarly, high-density specimens showed generally

weaker correlations between external measurements and mechanical properties; DExt_{ML} showed moderate correlations with Modulus of Elasticity ($r \approx -0.6$) and Strength ($r \approx -0.4$). Interestingly, the Imm⁴ parameter showed strong positive correlations with mechanical properties in both density groups. However, it was slightly more pronounced in normal density specimens (with $r \approx 0.7$ Strength) than in high density specimens ($r \approx 0.6$). Internal measurements (DInt_{ML} and DInt_{CrCd}) showed relatively weak correlations in both density groups, suggesting that external dimensions may be more reliable predictors of mechanical properties, especially in normal density bone specimens (Fig. 3).

Correlation matrices provide insights into the structural-mechanical relationships of bone samples by revealing distinct patterns across the three lighting conditions. Under all lighting conditions (A), external measurements showed the strongest correlations with mechanical properties. Specifically, DExt_{ML} showed robust negative correlations with Elastic Modulus and Strength, while DExt_{CrCd} showed similarly strong correlations with mechanical parameters. Similarly, under blue light conditions (B), correlations between external measurements and mechanical properties weakened moderately. The DExt_{ML} parameter maintained negative correlations with Elastic Modulus and Strength, albeit with reduced strength. Green light conditions (C) revealed a pattern in which correlation strengths generally remained weaker than those observed under white and blue light. The relationship between external measurements and mechanical properties remained negative. Internal measurements (DInt_{ML} and DInt_{CrCd}) showed relatively consistent, but weak correlations across all three lighting conditions, while the Imm⁴ parameter consistently showed strong negative correlations with mechanical properties across all lighting conditions, with slightly varying magnitudes (Fig. 4).

DISCUSSION

The findings of this study shed light on the intricate relationship between light exposure and bone health in Japanese quails. They reveal that the colour of LED light can significantly impact bone stiffness, albeit without marked effects on bone strength and elastic modulus. These results align with the hypothesis that environmental factors, such as light wavelength, play a critical role in avian development and welfare.

The gender effect on bones revealed that the moment of inertia was significantly higher in females than in male quail bones. This result was supported by the previous observation that the diaphysis cross-sectional area of bone was greater in females than in male quails [16]. Our study was also consistent with research findings on broiler males and females, which showed higher densitometric and geometric parameters in females compared to male broilers [17,18]. There was the possibility of female quail adaptation to bear a heavy weight by bone geometrical changes, which resulted in increased diameters. Although strength and stiffness were found to be significantly ($P < 0.000$) higher in female quails than in male quails, bone strength was not affected by gender. In a previous study by Rath et al. [19], bone strength in broilers was not affected by gender. Our study was also consistent with the findings of studies conducted on female and male chickens, which showed higher densitometric and geometric parameters in female chickens compared to male chickens [17], and that bones are more sensitive to physical loads during growth;

therefore, the results are generally characterized by an increase in bone mass through periosteum and endosteal apposition, with or without changes in mineral density [20].

It has been reported that bone density increases with age in females compared to males [17] and that the effects of the egg-laying mechanism and hormones increase bone density [21]. There were findings that the effects on sex-related bone traits became more pronounced in the later stages of the birds' lives [22], which may be an important factor affecting the bone strength of these quails. The different LED lights increased bone stiffness in the quails exposed to "Green" light, which is particularly intriguing. Specifically, the linear model analysis reveals a statistically significantly higher stiffness in the green group, suggesting that the wavelength or intensity of green light may promote bone quality aspects that are not immediately apparent through gross morphological measurements. The reason could be the fact that birds possess high peak sensitivity between wavelengths of 545 to 575 nm (green light). This result was in accordance with the previous findings of Rozenboim et al. [3], who found that green light was associated with increased growth of broiler birds. This finding was also in line with prior research focused primarily on blue and green wavelengths [23,24], which suggested that a broader spectrum of light colours, including those closer to the yellow wavelength, may influence avian bone physiology. That's why, in this study, green light also influenced the biomechanical properties of the bones to some extent.

However, the influence of light colour on the birds was seen as trivial, suggesting insignificant improvement in strength and elastic modulus of the quail bones [25]. Multiple variables, including dimensions, strength, and elastic modulus of quail bones, among the different light-exposed groups (White, Blue, Green), did not reveal statistically significant differences. These findings show that while lighting conditions may influence growth and behaviour in poultry, their direct impact on the quail's bone physical and biomechanical properties may require a more nuanced understanding of a larger study group [2,26].

Our results add to the growing body of evidence that light colour has a physiological impact on bone development. This agrees with studies in broiler chickens, where light intensity and color significantly influence skeletal health [4,5]. Previous studies highlighted the role of light in modulating skeletal muscle development and possibly bone quality through mechanisms such as enhanced activity levels or altered metabolic pathways affecting bone density and strength [2,24].

Housing birds at higher densities has been found associated with leg weakness and poor walking ability [27]. However, this study did not follow the previous findings.

Further research is needed on how environmental factors synergize to affect bone health and integrity in poultry, potentially focusing on biochemical or morphological differences [28,29].

The correlation analysis of morphological and biomechanical data revealed complex relationships between bone architecture and mechanical properties. The analysis demonstrated that external dimensions serve as reliable predictors of mechanical properties in bone architecture, with higher bone stiffness specifically related to increased moment of inertia and periosteal mediolateral diameter. This finding aligns with previous research in which wider tibial bones of Lohmann Dual exhibited greater rigidity than the narrow tibia of Ross 308 chicken [30]. However, the bone strength and elastic modulus showed negative correlations with diameter and moment of inertia, which could be attributed to the dependence of strength not only on bone geometry but also on cortical thickness, porosity, and trabecular framework [14].

These structural-mechanical relationships demonstrated distinct patterns influenced by multiple factors, including gender and density variations. Gender-specific differences indicated sexual dimorphism's role, with males exhibiting stronger correlations between dimensional and mechanical parameters compared to females, suggesting the necessity of gender-specific approaches in structural measurements. Additionally, density-dependent variations showed that normal-density samples maintained stronger correlations between dimensional and mechanical parameters compared to high-density samples.

In addition, the observed relationships between structural and mechanical properties in bone analysis revealed relatively similar correlation patterns with the choice of lighting conditions, but with minor differences. This similarity in correlation patterns under different lighting conditions suggested that lighting protocols could be evaluated similarly in bone morphometry and mechanical property assessments. The illumination conditions significantly impacted these structural-mechanical relationships, with white light providing the most pronounced correlations and potentially offering optimal conditions for structural-mechanical assessments. In contrast, blue and green light conditions demonstrated moderate correlation strengths, which might be more suitable for specific analytical purposes. This variation across different lighting conditions emphasizes the critical importance of implementing standardized illumination protocols in bone morphometry and mechanical property assessments in veterinary research settings.

However, this study had several limitations that should be considered when interpreting the results. First of all, the tibiotarsus bone, which is frequently preferred in

poultry studies, was used and its effects on other bones were not investigated. Additionally, while three different LED light colors were tested, the study did not investigate the effects of different light intensities or photoperiods that could affect bone development. Finally, the study did not include biochemical markers of bone metabolism or histological analysis, which could provide deeper insights into the mechanisms underlying the observed effects of light exposure on bone properties.

In conclusion, the impact of sex on bone properties was clear, with female quail bones showing significantly higher values for moment of inertia, fracture strength, and hardness compared to male quail bones. This finding aligns with the adaptation of female quails to support heavier body weights, indicating sex-specific mechanisms in bone development. However, stocking density did not significantly affect bone parameters, which contradicts previous research and warrants further investigation. Overall, this study highlights the intricate nature of bone development and the impact of environmental factors. While lighting conditions do not appear to affect bone morphology, the differences in hardness significantly suggest that optimal light exposure is essential. This opens up avenues for future research into these interactions.

DECLARATIONS

Availability of Data and Materials: Data this used available on request from the corresponding authors (F. Sevil Kilimci).

Acknowledgments: We would like to thank Assistant Professor Dr. Solmaz KARAARSLAN for her support during the statistics phase and Associate Professor Dr. Mehmet KAYA for her support in providing materials.

Financial Support: This research did not receive any specific grant from funding agencies in the public, commercial, or not-for-profit sectors.

Conflict of Interest: We certify that there is no conflict of interest with any financial organization regarding the material discussed in the manuscript.

Declaration of Generative Artificial Intelligence (AI): The authors used AI technologies only to improve readability and language.

Author Contributions: IGY, FSK, and FTY: Conceptualization, Data curation, Formal analysis. IGY, EKY, KK, and SR: Investigation, Methodology, Project administration. FSK and FTY: Software, Resources. FSK, and IGY: Supervision, Validation, Visualization: FSK, IGY, KK, and SR: Writing - original draft, Writing - review & editing.

REFERENCES

1. El Sabry MI, Hassan SSA, Zaki MM, Stino FKR: Stocking density: A clue for improving social behavior, welfare, health indices along with productivity performances of quail (*Coturnix coturnix*) - A review. *Trop Anim Health Prod*, 54:83, 2022. DOI: 10.1007/s11250-022-03083-0
2. Zhao RX, Cai CH, Wang P, Zheng L, Wang JS, Li KX, Liu W, Guo XY, Zhan XA, Wang KY: Effect of night light regimen on growth performance, antioxidant status and health of broiler chickens from 1 to 21 days of age.

Asian-Australas J Anim Sci, 32 (6): 904-911, 2019. DOI: 10.5713/ajas.18.0525

3. Rozenboim I, Biran I, Chaiseha Y, Yahav S, Rosenstrauch A, Sklan D, Halevy O: The effect of a green and blue monochromatic light combination on broiler growth and development. *Poult Sci*, 83 (5): 842-845, 2004. DOI: 10.1093/ps/83.5.842

4. Mohammed HM, Ibrahim M, Saleem AS: Effect of different light intensities on performance, welfare and behavior of turkey poult. *J Adv Vet Anim Res*, 3 (1):18, 2016. DOI: 10.5455/javar.2016.c126

5. Skrbic Z, Lukic M, Petricevic V, Bogosavljevic-Boskovic S, Rakonjac S, Doskovic V, Tolimir N: Effects of light intensity in different stocking densities on tibial measurements and incidence of lesions in broilers. *Biotechnol Anim Husb*, 35 (3): 243-252, 2019. DOI: 10.2298/bah1903243s

6. Abu Tabeeh MAS, Abbas RJ: The effect of color light and stocking density on tibial measurements and levels of calcium and phosphorus in bone and serum of broilers and layers chickens. *Int J Sci Technol*, 11 (2): 36-42, 2016. DOI: 10.12816/0033530

7. Cui YM, Wang J, Zhang HJ, Feng J, Wu SG, Qi GH: Effect of photoperiod on growth performance and quality characteristics of tibia and femur in layer ducks during the pullet phase. *Poult Sci*, 98 (3): 1190-1201, 2019. DOI: 10.3382/ps/pey496

8. Yildiz H, Petek M, Sonmez G, Arican I, Yilmaz B: Effects of lighting schedule and ascorbic acid on performance and tibiotarsus bone characteristics in broilers. *Turk J Vet Anim Sci*, 33 (6): 469-476, 2009. DOI: 10.3906/vet-0802-1

9. Shynkaruk T, Long K, LeBlanc C, Schwean-Lardner K: Impact of stocking density on the welfare and productivity of broiler chickens reared to 34 d of age. *J Appl Poult Res*, 32:100344, 2023. DOI: 10.1016/j.japr.2023.100344

10. Buijs S, Van Poucke E, Van Dongen S, Lens L, Baert J, Tuytens FAM: The influence of stocking density on broiler chicken bone quality and fluctuating asymmetry. *Poult Sci*, 91 (8): 1759-1767, 2012. DOI: 10.3382/ps.2011-01859

11. Turner CH: Biomechanics of bone: determinants of skeletal fragility and bone quality. *Osteoporos Int*, 13 (2): 97-104, 2002. DOI: 10.1007/s001980200000

12. Turner CH, Burr DB: Basic biomechanical measurements of bone: A tutorial. *Bone*, 14 (4): 595-608, 1993. DOI: 10.1016/8756-3282(93)90081-K

13. Süzer B: Biomechanical comparison of the effects of the storage temperature on tibiotarsus in Japanese quail. *J Res Vet Med*, 40 (2): 131-135, 2021. DOI: 10.30782/jrvrm.1027065

14. Khan K, Kilimci FS, Kara ME: Biomechanical tests: Applications and their reliability for the prediction of bone strength in broiler chicken. *MAE Vet Fak Derg*, 6 (2): 85-92, 2021. DOI: 10.24880/maeuvfd.936262

15. Standarts A. Shear and three-point bending test of animal bone. ANSI/ASAE S459 DEC01, USA. 2003.

16. Tomaszewska E, Knaga S, Dobrowolski P, Lamorski K, Jabłoński M, Tomczyk-Warunek A, Jarda K, Hudaib M, Hudaib-Stasiak M, Borsuk G, Muszyński S: The effect of bee pollen on bone biomechanical strength and trabecular bone histomorphometry in tibia of young Japanese quail (*Coturnix japonica*). *PloS One*, 15 (3):e0230240, 2020. DOI: 10.1371/journal.pone.0230240

17. Charuta A, Dzierżeczka M, Komosa Ł, Kalinowski M, Pierzchała M:

Age- and sex-related differences of morphometric, densitometric and geometric parameters of tibiotarsal bone in Ross broiler chickens. *Folia Biol (Krakow)*, 61 (3-4): 211-220, 2013. DOI: 10.3409/fb61_3-4.211

18. Charuta A, Dzierżeczka M, Komosa M, Biesiada-Drzazga B, Działa-Szczepańczyk E, Cooper RG: Age- and sex-related changes in mineral density and mineral content of the tibiotarsal bone in quails during post-hatching development. *Kafkas Univ Vet Fak Derg*, 19 (1): 31-36, 2013. DOI: 10.9775/kvfd.2012.7055

19. Rath NC, Balog JM, Huff WE, Huff GR, Kulkarni GB, Tierce JF: Comparative differences in the composition and biomechanical properties of tibiae of seven- and seventy-two-week-old male and female broiler breeder chickens. *Poult Sci*, 78 (8): 1232-1239, 1999. DOI: 10.1093/ps/78.8.1232

20. Regmi P, Smith N, Nelson N, Haut RC, Orth MW, Karcher DM: Housing conditions alter properties of the tibia and humerus during the laying phase in Lohmann white Leghorn hens. *Poult Sci*, 95, 198-206, 2016. DOI: 10.3382/ps/pev209

21. Dacke CG, Sugiyama T, Gay CV: The role of hormones in the regulation of bone turnover and eggshell calcification. In: Scanes CG (Ed): *Sturkie's Avian Physiology*. 6th ed., 549-575, Academic Press, 2015.

22. Yalçın S, Özkan S, Coşkun E, Bilgen G, Delen Y, Kurtulmuş Y, Tanyalçın T: Effects of strain, maternal age and sex on morphological characteristics and composition of tibial bone in broilers. *Br Poult Sci*, 42 (2): 184-190, 2001. DOI: 10.1080/00071660120048429

23. Cao J, Liu W, Wang Z, Xie D, Jia L, Chen Y: Green and blue monochromatic lights promote growth and development of broilers via stimulating testosterone secretion and myofiber growth. *J Appl Poult Res*, 17, 211-218, 2008. DOI: 10.3382/japr.2007-00043

24. Cao J, Wang Z, Dong Y, Zhang X, Li J, Chen Y: Effect of combinations of monochromatic lights on growth and productive performance of broilers. *Poult Sci*, 91 (12): 3013-3018, 2012. DOI: 10.3382/ps.2012-02413

25. Remonato Franco B, Shynkaruk T, Crowe T, Fancher B, French N, Gillingham S, Schwean-Lardner K: Light color and the commercial broiler: Effect on behavior, fear, and stress. *Poult Sci*, 101 (11):102052, 2022. DOI: 10.1016/j.psj.2022.102052

26. Lewis PD: A review of lighting for broiler breeders. *Br Poult Sci*, 47 (4): 393-404, 2006. DOI: 10.1080/00071660600829092

27. Abudabos AM, Samara EM, Hussein EOS, Al-Ghadi MQ, Al-Atiyat RM: Impacts of stocking density on the performance and welfare of broiler chickens. *Ital J Anim Sci*, 12 (1):e11, 2013. DOI: 10.4081/ijas.2013.e11

28. James CG, Stanton LA, Agoston H, Ulici V, Underhill TM, Beier F: Genome-wide analyses of gene expression during mouse endochondral ossification. *PLoS One*, 5 (1):e8693, 2010. DOI: 10.1371/journal.pone.0008693

29. Zhang H, Zeng Q, Bai S, Wang J, Ding X, Xuan Y, Su Z, Zhang K: Effect of graded calcium supplementation in low-nutrient density feed on tibia composition and bone turnover in meat ducks. *Br J Nutr*, 120 (11): 1217-1229, 2018. DOI: 10.1017/S0007114518002556

30. Harash G, Richardson KC, Alshamy Z, Hünigen H, Hafez HM, Plendl J, Al Masri S: Basic morphometry, microcomputed tomography and mechanical evaluation of the tibiotarsal bone of a dual-purpose and a broiler chicken line. *PLoS One*, 15 (3):e0230070, 2020. DOI: 10.1371/journal.pone.0230070

RESEARCH ARTICLE

Comparative Performance of Convolutional Neural Network Models in Wing Morphometric Classification of Honey Bee Populations Across Europe

Berkant İsmail YILDIZ ¹ (*) ¹ Akdeniz University, Faculty of Agriculture, Department of Agricultural Biotechnology, TR-07058 Antalya - TÜRKİYE

(*) Corresponding author:

Berkant İsmail Yıldız

Cellular phone: +90 542 516 29 85

E-mail: berkantyildiz@gmail.com

How to cite this article?

Yıldız Bİ: Comparative performance of convolutional neural network models in wing morphometric classification of honey bee populations across Europe. *Kafkas Univ Vet Fak Derg*, 31 (5): 653-659, 2025.
DOI: 10.9775/kvfd.2025.34544

Article ID: KVFD-2025-34544

Received: 25.05.2025

Accepted: 06.10.2025

Published Online: 06.10.2025

Abstract

Accurate identification of *Apis mellifera* populations is essential for conserving biodiversity, optimizing breeding programs, and understanding environmental adaptation processes. Traditional morphometric approaches, while informative, face significant limitations due to their labor-intensive nature and inefficiency when applied to large-scale datasets. To address these challenges, this study applies a comparative evaluation of Convolutional Neural Network (CNN) models for country-level classification of honey bee populations using forewing images. A total of 2,500 high-resolution forewing images-500 from each of Croatia, Poland, Romania, Spain, and Greece-were selected to represent diverse geographical regions. Following biologically appropriate preprocessing and data augmentation, the images were analyzed through a comparative evaluation of three pre-trained CNN models - VGG16, InceptionV3, and ResNet50. All models were fine-tuned through transfer learning, and classification performance was systematically assessed using accuracy, precision, recall, and F1-score metrics. Among the evaluated models, VGG16 achieved the highest classification accuracy at 95%, outperforming InceptionV3 and ResNet50. These results highlight not only the high predictive power of CNN models in morphologically distinguishing honey bee populations, but also demonstrate the relative strengths of different CNN models. Furthermore, the study underscores the advantages of automated CNN-based workflows over manual morphometric methods in terms of speed, objectivity, and scalability. By integrating CNN models into morphometric analysis, this research provides robust and reproducible tools for apicultural studies, population-level biodiversity monitoring, and applied breeding strategies.

Keywords: Automated population classification, Convolutional Neural Networks (CNNs), Deep learning in biodiversity, Honey bee, Wing morphometrics

INTRODUCTION

The western honey bee (*Apis mellifera*) plays a central role in sustaining pollination networks that underpin the functioning of natural ecosystems, while also serving as an indispensable component of global agricultural production systems. Pollination services directly influence approximately 75% of flowering plant species and contribute to around 35% of global food production, thereby supporting both biodiversity and food security worldwide ^[1]. However, in recent decades, various stressors-including climate change, pesticide use in agriculture, and habitat fragmentation-have led to significant declines in local honey bee populations. These threats pose serious risks not only at ecological but also economic and genetic levels, challenging the long-term sustainability of apiculture and pollination services ^[2,3].

In this context, accurate identification and monitoring of local genetic lineages are crucial for understanding intra-species adaptation dynamics and for developing strategic conservation efforts to safeguard native populations. Traditional morphometric analyses have long been employed as the primary approach for identifying subspecies and geographic variants of honey bees. Among these, forewing venation patterns have historically served as key morphological indicators for differentiating populations ^[4]. Nevertheless, this method is increasingly inadequate for modern biometric applications due to its dependency on expert interpretation, labor-intensive and time-consuming processes, and limited scalability for large datasets. Furthermore, the reliance on visual assessments introduces subjectivity, which in turn compromises the reproducibility and standardization of results ^[5].

In recent years, rapid advancements in artificial intelligence



and computer vision have enabled the fast, objective, and high-throughput analysis of morphological data. These developments form the foundation for automated systems that increasingly complement human expertise in image-based classification tasks. Convolutional Neural Networks (CNNs) have emerged as powerful and flexible models that overcome the limitations of traditional morphometric approaches, owing to their data-driven learning strategies and multi-layered architectures [6]. CNNs are implemented through diverse architectures that emphasize different strategies for feature extraction and network depth. Prominent examples used in transfer learning include VGG16, which emphasizes a simple yet deep layer organization; ResNet50, which introduced residual connections to allow the training of very deep networks without degradation problems; and InceptionV3, which incorporates multi-scale convolutional filters for efficient feature extraction [7]. A key strength of CNNs lies in their ability to autonomously learn both local and global patterns embedded in image data, eliminating the need for manual feature engineering. Particularly in symmetrical structures such as wing morphology, CNNs effectively capture subtle variations—even those imperceptible to the human eye—that carry taxonomic significance, thus demonstrating high discriminative power in complex morphological pattern recognition tasks [8-10]. These capabilities not only enhance classification performance but also meet core requirements of modern biometric analysis, such as reproducibility, scalability, and adaptability. Consequently, CNN-based systems signify a paradigm shift in morphometric evaluation, paving the way for more comprehensive and objective strategies with the potential to progressively replace traditional methods [11].

Various CNN-based approaches have been proposed in the literature for the classification of honey bee subspecies. For example, De Nart et al. [12] compared different CNN models using 9,887 wing images from seven subspecies and reported that ResNet50 achieved an accuracy above 94%. Similarly, the DeepWings© system developed by Rodrigues et al. [13] employed a hybrid CNN-SVM framework on images from 26 subspecies and achieved an average accuracy of 86.6%. Oleksa et al. [14] on the other hand, made a significant contribution to addressing the issue of data sharing in this field by providing a large-scale open-access dataset comprising 26,481 honey bee wing images collected from different regions across Europe. However, this open-access dataset has so far been utilized mainly for classical morphometric or statistical analyses, and applications of multi-class CNN-based classification remain absent. More broadly, most existing studies have concentrated on subspecies-level identification, leaving the automated classification of geographic population variation largely underexplored.

In this study, a total of 2,500 forewing images of honey bees

from Croatia, Poland, Romania, Spain, and Greece were used to achieve automated morphological classification of populations at the country level. To this end, three different CNN architectures-VGG16, InceptionV3, and ResNet50-were implemented through transfer learning, and the classification performance of each model was evaluated based on metrics such as accuracy, precision, recall, and F1-score. The study aims to fill a critical gap in the literature by focusing on geographic population-level classification, which has received limited attention, and by providing a comparative performance analysis of CNN-based models. This approach offers the potential to overcome the limitations of traditional morphometric methods by enabling faster, more objective, and scalable classification processes.

MATERIAL AND METHODS

Ethical Statement

This study did not involve any procedures requiring ethical approval.

Material

In this study, a total of 2,500 forewing images of worker honey bees (*Apis mellifera*) from various regions of Europe were used. The images were obtained from a public domain dataset published by Oleksa et al. and hosted on the Zenodo platform [14]. The original dataset contains 26,481 forewing images collected from 13 European countries; however, for the purposes of this study, only the data from five countries-Croatia, Poland, Romania, Spain, and Greece-with sufficient sample sizes were included in the analysis (Fig. 1).

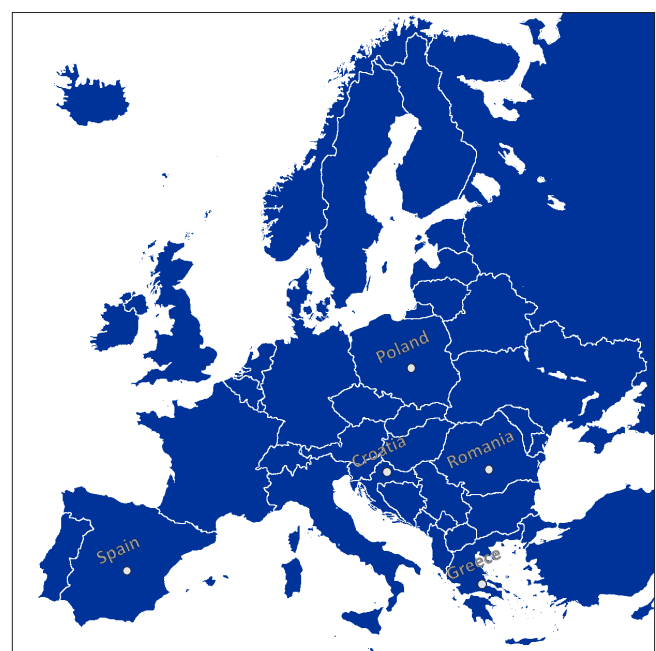


Fig 1. Locations from which honey bee samples were collected

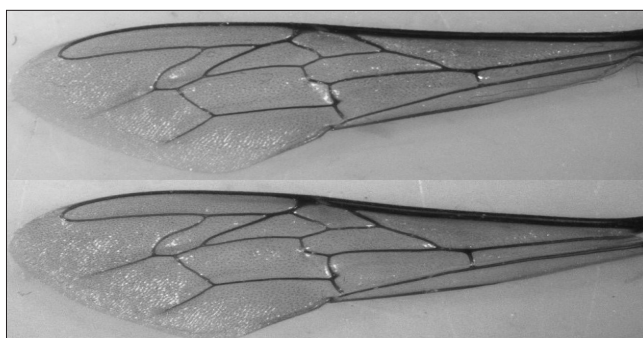


Fig 2. Example of a honey bee forewing with the image quality used in the analyses

For each country, a balanced subset consisting of 500 wing images was created by applying a stratified random sampling procedure across multiple geographic locations included in the dataset. This approach ensured that each country class was equally represented while partially reflecting its internal geographic variation. The images were obtained by mounting the wings of worker bees between microscopic slides and capturing them digitally under controlled optical conditions. All images were in high-resolution, PNG format and were used directly for analysis without any manual annotation or segmentation procedures (Fig. 2). The image files followed a naming convention beginning with ISO 3166-1 alpha-2 country codes (e.g., GR-0001-wing01.png) and were organized into separate, ZIP archives for each country.

Preprocessing

A total of 2,500 wing images in .PNG format were subjected to preprocessing to standardize their dimensions prior to analysis. All images were resized to an input resolution of 224×224 pixels and converted into three-channel tensors in RGB format. Pixel values were normalized from the original 0-255 range to a 0-1 scale. No manual segmentation, background removal, or landmark annotation was applied; the images were analyzed in their raw form.

Data Augmentation

To address the limited number of samples in the dataset and to better capture intra-country morphological variation, data augmentation techniques were applied. This process aimed to reduce the risk of overfitting during model training and to enhance the model's ability to recognize generalizable morphological patterns.

From each original wing image, synthetic variations were generated using the following transformations:

- Random horizontal flipping
- Random rotation up to $\pm 15^\circ$
- Random width and height shifts of up to $\pm 10\%$

- Random zooming within a $\pm 10\%$ range

- Minor pixel brightness variations (brightness range: 0.8-1.2)

These transformations were implemented in real time (on-the-fly) on the training data using the ImageDataGenerator class from the Keras library. Data augmentation was applied only to the training set; the validation and test sets were evaluated in their raw, unaltered forms.

CNN Architectures

In this study, three widely used Convolutional Neural Network (CNN) architectures were evaluated for the classification of honey bee wing images: VGG16, ResNet50, and InceptionV3. These models represent different design principles: VGG16 with its simple but deep layer organization is a common reference in transfer learning; ResNet50 introduces residual connections that allow the training of very deep networks without degradation problems; and InceptionV3 employs multi-scale convolutional filters within its modules, enabling efficient extraction of diverse features from complex images [7]. All architectures were implemented through transfer learning using pre-trained ImageNet weights. During training, the initial layers were frozen and only the final layers were fine-tuned for task-specific adaptation.

The input dimensions were standardized to $224 \times 224 \times 3$ across all models. The original classification layers were replaced with a fully connected dense layer of five neurons, each representing one country class, with softmax activation applied to generate probabilities for class membership.

For training, the Adam optimization algorithm was employed with a learning rate of 0.0001. Each architecture was trained independently, and classification performance was evaluated separately to ensure fair comparison.

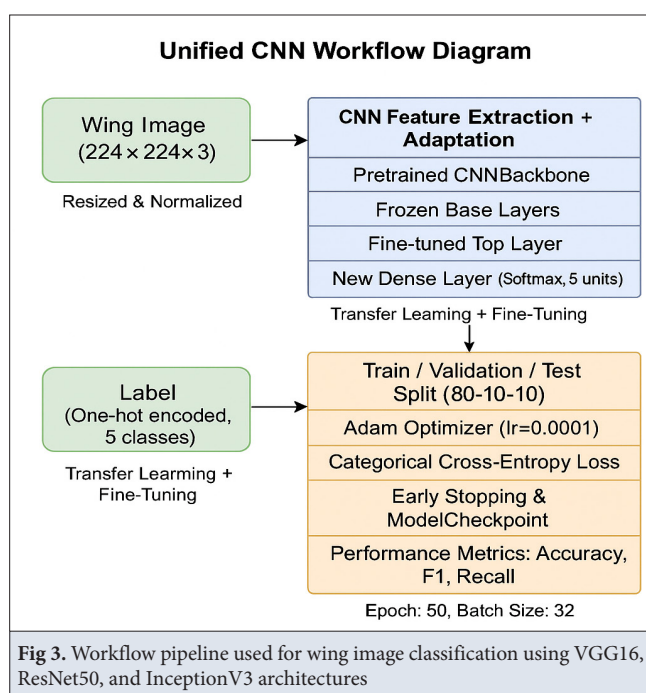
Model Training

The dataset was divided into 80% training and 20% test sets, with 10% of the training data reserved for validation. Stratified sampling was applied to preserve class distribution across subsets. All CNN models were trained independently for a maximum of 50 epochs with a batch size of 32. To prevent overfitting, early stopping was applied, terminating training if validation loss (val_loss) did not improve for five consecutive epochs. The Adam optimizer was used with a learning rate of 0.0001, and categorical cross-entropy was selected as the loss function due to the multi-class classification task and its compatibility with the softmax activation function. The ModelCheckpoint callback was employed to save the weights corresponding to the epoch with the best validation performance.

All analyses were conducted in Python on the Google Colab platform. Models were implemented with TensorFlow 2.11 and Keras, supported by NumPy, Scikit-learn, Matplotlib, and Seaborn libraries, and training was performed on an NVIDIA Tesla T4 GPU-enabled system.

Evaluation Metrics

To evaluate the classification performance of the models, several metrics were computed on the test dataset. These included accuracy, precision, recall, and F1-score. To provide a comprehensive assessment of each model's ability to correctly identify all classes, these metrics were reported both per class and as macro-averaged scores (Fig. 3).



In addition, confusion matrices and Receiver Operating Characteristic (ROC) curves were visualized for each model. Class-wise recall and specificity levels were analyzed in detail. The confusion matrices were used to identify which classes were most frequently misclassified with one another, while the ROC curves and the corresponding Area Under the Curve (AUC) values reflected the overall discriminative power of the models.

PCA-Based Morphological Distribution Analysis

In addition to the classification performance achieved by the deep learning models, Principal Component Analysis (PCA) was performed to further explore inter-individual morphological patterns. For this analysis, shape features derived from each wing image were computed using Hu moments. Hu moments consist of seven statistical values that are invariant to geometric transformations such as

rotation, scaling, and translation, and are commonly used to describe object shapes in a stable manner. Each individual was represented as a seven-dimensional feature vector based on the computed Hu moments, and these vectors were subsequently reduced to two dimensions using the PCA algorithm. The resulting PCA plots visually illustrated morphometric similarities and differences among individuals and allowed for the analysis of class-level overlaps.

RESULTS

The classification performance of the three Convolutional Neural Network (CNN) architectures is summarized in Table 1. Among them, VGG16 achieved the highest accuracy at 95%, with precision, recall, and F1-score values of 0.95, reflecting balanced and consistent recognition across all classes. InceptionV3 followed with 93% accuracy and comparable precision-recall metrics (≈ 0.93). ResNet50 showed the lowest overall accuracy (90%) but maintained a relatively high precision (0.93), suggesting a more conservative classification approach that may have reduced false positives.

As shown in Fig. 4-A,B,C, the confusion matrices provide a comparative overview of class-wise discrimination. VGG16 reached 100% accuracy for Spain (ES) and Greece (GR), with precision and recall values of 1.00, likely due to distinctive morphological traits in these populations. In contrast, classification errors occurred in Croatia (HR), where 14 samples were misclassified as Poland (PL) (recall = 0.86), and in PL, where four samples were assigned to HR (recall = 0.96). Romania (RO) showed moderate confusion with seven misclassifications into HR and PL. For ResNet50 (Fig. 4-B), ES, GR, and RO were perfectly classified, but minor errors occurred in HR (recall = 0.97). The greatest difficulty was observed in PL: only 55 of 100 samples were correctly identified, with 45 misclassified as HR, leading to sharp declines in both precision and recall. The InceptionV3 model (Fig. 4-C) also achieved 100% accuracy for ES and GR. However, HR showed weaker performance, with 23 samples classified as PL and one as RO (recall = 0.76). Precision in PL was reduced by nine misclassifications from HR, while recall remained relatively high (91/100 correctly classified). For RO, only two misclassifications into HR were observed, and the overall recognition was strong.

Table 1. Average classification performance metrics by model

Model	Accuracy	Precision	Recall	F1-Score	Support
VGG16	0.95	0.95	0.95	0.95	500
ResNet50	0.90	0.93	0.90	0.90	500
InceptionV3	0.93	0.93	0.93	0.93	500

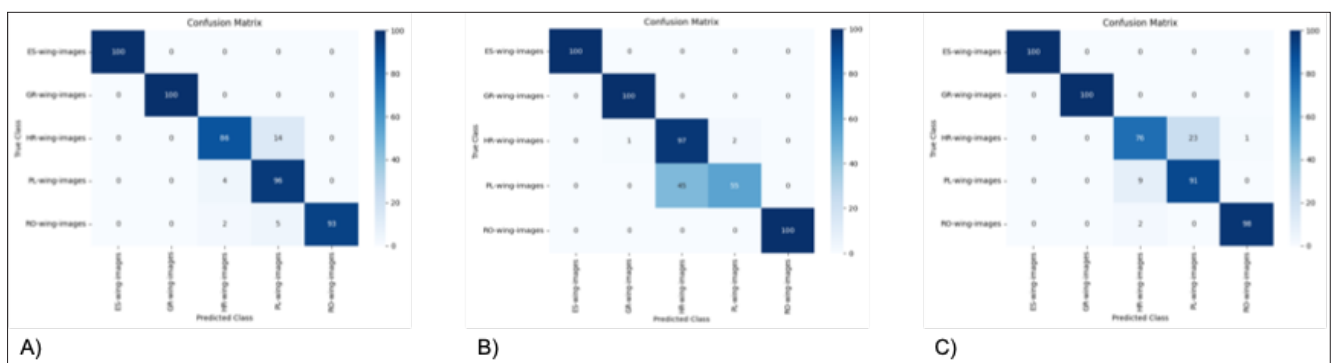


Fig 4. Confusion matrices illustrating the classification performance of different CNN models. (A) VGG16, (B) ResNet50, and (C) InceptionV3. Each matrix displays the actual versus predicted class distributions, highlighting the ability of each model to distinguish among honey bee wing images from different populations

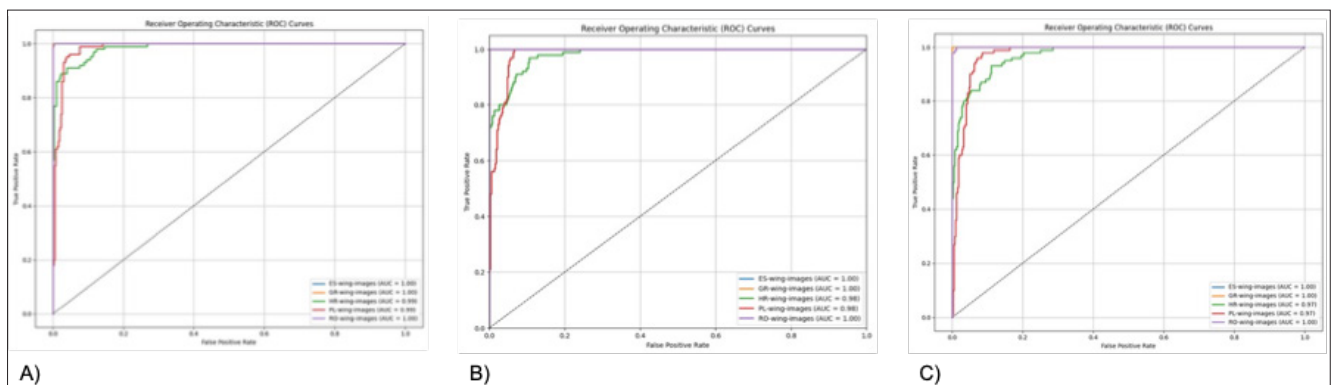


Fig 5. ROC curves demonstrating the classification performance of the CNN models. (A) VGG16, (B) ResNet50, and (C) InceptionV3. The curves illustrate the trade-off between true positive and false positive rates across different classification thresholds. AUC values are reported to quantify the overall discriminative ability of each model

Receiver Operating Characteristic (ROC) curves for the three CNN architectures (Fig. 5-A,B,C) demonstrated consistently high inter-class discriminative performance. For Spain (ES), Greece (GR), and Romania (RO), all models achieved an Area Under the Curve (AUC) value of 1.00, confirming perfect separation without classification errors. This finding highlights the distinctiveness of the wing patterns in these populations and the strong ability of CNNs to capture such features. By contrast, slight reductions in AUC values were observed for Croatia (HR) and Poland (PL), with VGG16 achieving the highest scores (0.99), followed by ResNet50 (0.98) and InceptionV3 (0.97). These differences indicate that morphological similarities between HR and PL created a greater challenge for accurate separation. The ROC curve slopes further suggest that InceptionV3 performed comparatively weaker for these classes. Overall, ROC analysis confirmed VGG16 as the most consistent model, ResNet50 as balanced, and InceptionV3 as relatively limited in discriminative ability for certain populations.

In addition to the classification analyses, a Principal Component Analysis (PCA) was performed using shape features derived from Hu moments to further explore

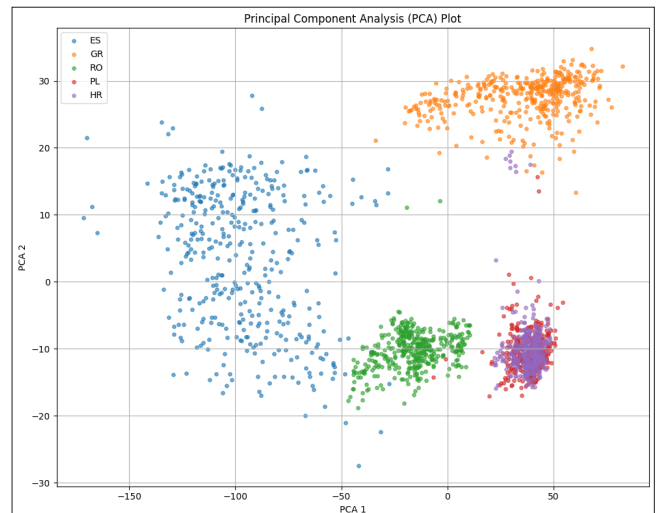


Fig 6. Two-dimensional PCA plot illustrating the morphological variation of honey bee wing images from five different populations. Each point represents a single individual, and colors indicate country-specific groupings (ES, GR, RO, PL, HR). The first two principal components collectively explain 80.09% of the total variance

morphological similarities and differences among the samples. The first two principal components together explained 80.09% of the total variance, indicating that most of the morphological variation was effectively captured.

As shown in *Fig. 6*, the five country groups generally formed distinct clusters; however, a marked overlap was observed between Croatia (HR) and Poland (PL). This overlap was also reflected in the CNN misclassification patterns, where up to 45% of PL samples were assigned to HR by ResNet50.

DISCUSSION

The findings of this study demonstrated that CNN-based models can classify honey bee populations with high overall accuracy, particularly when using wing image data. Among the evaluated architectures, VGG16 consistently outperformed ResNet50 and InceptionV3 across accuracy, precision, recall, and F1-score metrics, indicating its robustness and balance in handling class distinctions. These results align with previous studies, such as De Nart et al.^[12], which demonstrated the applicability of CNN-based classification to honey bee wing images, supporting the notion that such models offer higher-resolution discrimination than traditional morphometric approaches. Taken together, these findings indicate that while all models produced highly accurate results for certain classes, classification performance declined notably due to recurring misclassifications between the HR and PL classes. The consistent confusion between Croatia (HR) and Poland (PL) may be rooted not only in algorithmic limitations but also in biological similarity. According to Mahalanobis distance values reported by Oleksa et al.^[14], the distance between the HR and PL populations was calculated as 3.91—the smallest among the five countries analyzed in this study. Thus, it can be inferred that these classification errors reflect not only model-specific weaknesses but also genuine morphometric proximity, which naturally influences the learning process of the models.

Previous studies have employed a variety of CNN architectures for classifying bee wing images, thereby providing useful comparative benchmarks. De Nart et al.^[12] evaluated ResNet50, MobileNetV2, InceptionV3, and Inception-ResNetV2 architectures on approximately 9,887 honey bee wing images and reported accuracies exceeding 92%, with Inception-based models achieving the strongest performance in many classes. Similarly, Spiesman et al.^[15] demonstrated that convolutional neural networks, specifically EfficientNetV2L, can achieve high accuracy (up to 98.1%) when classifying challenging bee taxa using forewing images, reinforcing the value of morphological image-based approaches for species-level identification. In a broader insect context, Sauer et al.^[16] developed a CNN for distinguishing mosquito species based solely on wing images and achieved a macro-F1 score of about 0.90 using RGB images, demonstrating that even highly similar wing venation patterns can be

reliably differentiated with well-trained architectures. In the present study, VGG16 delivered the best performance. This outcome may be attributed to the model's balance between complexity and regularization, which allowed it to generalize effectively on a limited dataset without overfitting. ResNet50, while robust for deep feature learning due to its residual connections, tended to perform more conservatively in morphologically similar classes, leading to reduced recall. InceptionV3, although designed to capture multi-scale features, was less effective than VGG16 in separating the HR-PL populations. Collectively, these findings suggest that in contexts where repetitive and fine-scale morphological traits dominate—such as forewing venation—simpler architectures may offer an optimal trade-off between capacity and generalization. The observed performance differences support the view that architecture choice should be carefully aligned with the morphological complexity of the problem under investigation.

Beyond the performance comparisons, another important distinction is methodological. Unlike landmark-based approaches such as DeepWings® software developed by Rodrigues et al.^[13] and Garcia et al.^[17] or similar systems that rely on predefined vein coordinates, our method did not require any manual extraction of morphometric landmarks. Instead, the CNN models directly processed raw wing images, learning discriminative features in a data-driven manner. This represents a methodological shift in wing morphometrics, as it removes observer-dependent steps and allows the models to capture subtle and potentially more informative morphological patterns that may be overlooked in landmark-based analyses. Such an approach enhances objectivity, reduces preprocessing effort, and expands the scalability of morphometric studies to large datasets.

The applications of artificial intelligence in apiculture extend far beyond classification. For example, DeepBee® achieved over 98% accuracy in detecting eggs, larvae, and honey, outperforming traditional observation^[18]. Other approaches, such as those of Voudiotis et al.^[19], integrated cameras with deep learning to identify Varroa-infested bees with 86% accuracy. Deep learning has also been applied to more complex biological features: Lösel et al.^[20] distinguished brain structures of bees and wasps using micro-CT and CNNs. In addition, Kongsilp et al.^[21] combined Mask R-CNN with Kalman filtering to track waggle dances within hives. Collectively, these studies highlight the versatility of deep learning in tackling diverse apicultural challenges, ranging from colony health monitoring to behavioral analysis.

This study demonstrated that CNN-based models can classify honey bee populations with high accuracy based on wing morphology, with the VGG16 architecture

exhibiting particularly balanced and reliable performance. The recurrent overlaps observed between morphologically similar populations, such as HR and PL, reflect not only model-related challenges but also genuine biological proximities. Beyond these results, the present work introduces a distinctive contribution by demonstrating that accurate classification can be achieved without manual landmark extraction, relying instead on fully automated, data-driven feature learning from raw wing images. This methodological simplification enhances objectivity and scalability, making the approach more suitable for large-scale morphometric applications. Future research may further improve class-level discrimination and generalization capacity by incorporating more diverse datasets and advanced modeling strategies, but the present findings already establish CNN-based workflows as a robust and innovative framework for population-level analyses in apicultural research.

DECLARATION

Availability of Data and Materials: The dataset used in this study is publicly available on Zenodo at <https://zenodo.org/records/7244070>.

Acknowledgements: The author declares no acknowledgements.

Funding Support: The author received no funding for this study.

Competing Interest: The author declares that there are no competing interest.

Declaration of Generative Artificial Intelligence (AI): The author declare that the article, tables and figures were not written/created by AI and AI-assisted Technologies.

REFERENCES

- Klein AM, Vaissière BE, Cane JH, Steffan-Dewenter I, Cunningham SA, Kremen C, Tscharntke T: Importance of pollinators in changing landscapes for world crops. *Proc Biol Sci*, 274 (1608): 303-313, 2007. DOI: 10.1098/rspb.2006.3721
- Potts SG, Imperatriz-Fonseca V, Ngo HT, Aizen MA, Biesmeijer JC, Breeze TD, Dicks LV, Garibaldi LA, Hill R, Settele J, Vanbergen AJ: Safeguarding pollinators and their values to human well-being. *Nature*, 540 (7632): 220-229, 2016. DOI: 10.1038/nature20588
- Vercelli M, Novelli S, Ferrazzi P, Lentini G, Ferracini C: A qualitative analysis of beekeepers' perceptions and farm management adaptations to the impact of climate change on honey bees. *Insects*, 12 (3):228, 2021. DOI: 10.3390/insects12030228
- Ruttner F: Biogeography and Taxonomy of Honeybees. Springer Berlin, Heidelberg, 1988.
- Tofilski A: Using geometric morphometrics and standard morphometry to discriminate three honeybee subspecies. *Apidologie*, 39 (5): 558-563, 2008. DOI: 10.1051/apido:2008037
- Alzubaidi L, Zhang J, Humaidi AJ, Al-Dujaili A, Duan Y, Al-Shamma O, Farhan L: Review of deep learning: Concepts, CNN architectures, challenges, applications, future directions. *J Big Data*, 8:53, 2021. DOI: 10.1186/s40537-021-00444-8
- Zhao X, Wang L, Zhang Y, Han X, Deveci M, Parmar M: A review of convolutional neural networks in computer vision. *Artif Intell Rev*, 57 (4):99, 2024. DOI: 10.1007/s10462-024-10721-6
- Buschbacher K, Ahrens D, Espeland M, Steinhage V: Image-based species identification of wild bees using convolutional neural networks. *Ecol Inform*, 55:101017, 2020. DOI: 10.1016/j.ecoinf.2019.101017
- Geldenhuys DS, Josias S, Brink W, Makhubele M, Hui C, Landi P, Bingham J, Hargrove J, Hazelbag MC: Deep learning approaches to landmark detection in tsetse wing images. *PLoS Comput Biol*, 19 (6):e1011194, 2023. DOI: 10.1371/journal.pcbi.1011194
- Ansari MA, Crampton A, Garrard R, Cai B, Attallah M: A Convolutional Neural Network (CNN) classification to identify the presence of pores in powder bed fusion images. *Int J Adv Manuf Technol*, 120 (7): 5133-5150, 2022. DOI: 10.1007/s00170-022-08995-7
- LeCun Y, Bengio Y, Hinton G: Deep learning. *Nature*, 521 (7553): 436-444, 2015. DOI: 10.1038/nature14539
- De Nart D, Costa C, Di Prisco G, Carpana E: Image recognition using convolutional neural networks for classification of honey bee subspecies. *Apidologie*, 53 (1):5, 2022. DOI: 10.1007/s13592-022-00918-5
- Rodrigues PJ, Gomes W, Pinto MA: DeepWings©: Automatic wing geometric morphometrics classification of honey bee (*Apis mellifera*) subspecies using deep learning for detecting landmarks. *Big Data Cogn Comput*, 6 (3):70, 2022. DOI: 10.3390/bdcc6030070
- Oleksa A, Căuia E, Siceanu A, Puškadija Z, Kovačić M, Pinto MA, Rodrigues PJ, Hatjina F, Charistos L, Bouga M, Prešern J, Kandemir İ, Rašić S, Kusza S, Tofilski A: Honey bee (*Apis mellifera*) wing images: A tool for identification and conservation. *GigaScience*, 12:giad019, 2023. DOI: 10.1093/gigascience/giad019
- Spiesman BJ, Gratton C, Gratton E, Hines H: Deep learning for identifying bee species from images of wings and pinned specimens. *PloS one*, 19 (5):e0303383, 2024. DOI: 10.1371/journal.pone.0303383
- Sauer FG, Werny M, Nolte K, Villacañas de Castro C, Becker N, Kiel E, Lühken R: A convolutional neural network to identify mosquito species (Diptera: Culicidae) of the genus *Aedes* by wing images. *Sci Rep*, 14 (1):3094, 2024. DOI: 10.1038/s41598-024-53631-x
- García CAY, Rodrigues PJ, Tofilski A, Elen D, McCormak GP, Oleksa A, Henriques D, Ilyasov R, Kartashev A, Bargain C, Fried B, Pinto MA: Using the software DeepWings© to classify honey bees across Europe through wing geometric morphometrics. *Insects*, 13 (12): 1132, 2022. DOI: 10.3390/insects13121132
- Alves TS, Pinto MA, Ventura P, Neves CJ, Biron DG, Junior AC, De Paula Filho DL, Rodrigues PJ: Automatic detection and classification of honey bee comb cells using deep learning. *Comput Electron Agric*, 170:105244, 2020. DOI: 10.1016/j.compag.2020.105244
- Voudiotis G, Moraiti A, Kontogiannis S: Deep learning beehive monitoring system for early detection of the Varroa mite. *Signals*, 3 (3): 506-523, 2022. DOI: 10.3390/signals3030030
- Lösel PD, Monchanin C, Lebrun R, Jayme A, Relle JJ, Devaud JM, Heuveline V, Lihoreau M: Natural variability in bee brain size and symmetry revealed by micro-CT imaging and deep learning. *PLoS Comput Biol*, 19 (10):e1011529, 2023. DOI: 10.1371/journal.pcbi.1011529
- Kongsilp P, Taetragool U, Duangphakdee O: Individual honey bee tracking in a beehive environment using deep learning and Kalman filter. *Sci Rep*, 14 (1):1061, 2024. DOI: 10.1038/s41598-023-44718-y

RESEARCH ARTICLE

Component Identification of Buyang Huanwu Decoction and the Effect of Main Components on Preventing Muscle Atrophy

Lan ZHOU¹  Shu LUO¹  Linglian MENG¹  Guangyao WANG¹  Lijing ZHANG¹  Haoxin WU¹ (*) 

¹ College of Traditional Chinese Medicine, Nanjing University of Chinese Medicine, 210023 Nanjing, CHINA



(*) **Corresponding author:** Haoxin WU
Phone: +86-25-85389102
E-mail: 290366@njucm.edu.cn

How to cite this article?

Zhou L, Luo S, Meng L, Wang G, Zhang L, Wu H: Component identification of BYHWD and the effect of main components on preventing muscle atrophy. *Kafkas Univ Vet Fak Derg*, 31 (5): 661-667, 2025.
DOI: 10.9775/kvfd.2025.34593

Article ID: KVFD-2025-34593

Received: 04.06.2025

Accepted: 22.08.2025

Published Online: 15.09.2025

Abstract

Buyang Huanwu Dcoction (BYHWD) is a traditional Chinese medicine that has been widely used for the clinical treatment of skeletal muscle atrophy which is a common complication after motor neuron injury and seriously affects the recovery of skeletal muscle function. This study aimed to explore the main components of Buyang Huanwu decoction and its possible mechanism for treating skeletal muscle and nerve atrophy in mice. Total fibular nerve injury model was established by using total fibular nerve clamp surgery. Main component of decoction was detected by HPLC and LC-MS, the morphology of skeletal muscle samples was observed using hematoxylin-eosin staining (H&E) and laser lens, and the expressions of muscular atrophy related proteins were detected by Western blot. Astragaloside is the main components of BYHWD, it promotes the recovery of injured neuroskeletal muscle and significantly inhibits the atrophy of related muscle tissue ($P < 0.05$). Denervation of skeletal muscle is closely related to autophagy, and Astragaloside can effectively inhibit autophagy after skeletal muscle injury. Astragaloside, the main component of BYHWD, promotes the recovery of skeletal muscle denervation by inhibiting autophagy.

Keywords: Astragaloside, Autophagy, Buyang Huanwu Decoction, Motor neuron injury, Neurogenic atrophy

INTRODUCTION

Muscle is a plastic tissue that continuously adjusts its shape, size, and function according to internal and external stimuli ^[1]. Local muscle atrophy is divided into disuse atrophy and denervation atrophy. Disuse atrophy often occurs in patients who are bedridden for a long time, or in patients with joint breaking for a long time, while denervation atrophy is mainly caused by neurological diseases or traumatic violence that damages skeletal muscle nerves ^[2]. Trauma or inflammation makes the nerves at the injury site undernourished, and the related skeletal muscles receive nerve impulses restricted, which in turn causes related muscle atrophy ^[3]. Compared with disuse atrophy, skeletal muscle denervation atrophy is more serious, and its treatment has always been the main focus of relevant clinical workers ^[4]. At present, the treatment of muscle atrophy is mostly limited to physical rehabilitation training and the treatment of a small number of hormone drugs. Therefore, an in-depth exploration of the pathogenic mechanism of muscle atrophy is crucial for taking targeted interventions, paying off muscle function, and improving the quality of the patient's life ^[5].

BYHW Decoction is a traditional prescription of traditional Chinese medicine. BYHWD is often used to treat the sequelae of cerebrovascular accidents (such as stroke), including facial paralysis, aphasia, hemiplegia, paraplegia and other diseases of Qi deficiency and blood stasis ^[6]. Nowadays, it is mostly used to treat neurological injury-related diseases such as cerebrovascular disease, facial nerve palsy, polio sequelae, sciatica, concussion sequelae, etc., and has achieved remarkable clinical effects ^[7].

In this study, we mainly analyzed the main pharmacological components of BYHWD, and studied the inhibitory effect of its main components on denervation of tibial anterior muscle in mice with peroneal nerve injury through animal experiments.

MATERIAL AND METHODS

Ethical Approval

All procedures performed involving animals were in accordance with the ethical standards of the Institutional Animal Care and Use Committee (IACUC) of Nanjing University of Chinese Medicine (No. 202203A041).



Animals

SPF grade, male, 6 weeks old, body weight 200 ± 10 g, 42 SD rats, purchased from Changzhou Cavens Laboratory Animal Co., Ltd. Laboratory animal license number: SCXK (Su) 2016-0010. All experimental animals began formal experiments after one week of adaptive feeding.

Animal Model

Rats were weighed, 10% chloral hydrate (300 g/mL) was injected intraperitoneally for anesthesia, and the surgical area of the left femur was routinely prepared and disinfected. Take a 1.5 cm incision in the middle of the left posterior femur, cut the skin and fascia in turn, free and fully expose the femur of the sciatic nerve, and perform the common peroneal nerve clamp down. With 14 cm hemostatic forceps, the upper total teeth clamp the common peroneal nerve 3 times, 10 seconds/time, 10 sec apart each time; the width of the crush injury is 5 mm. The distal end of the injury was marked with 9-0 non-invasive sutures, and the surgical incision was sutured layer by layer. After the rats woke up, they were put back into the cage for normal feeding. All animals were injected with the corresponding drug intraperitoneally on the 2nd day after modeling, and the normal group and the model group were injected with the same amount of normal saline for 7 days. After 18 days of surgical modeling, all rats were euthanized, and the tibial anterior muscle tissues on the left and right sides of the rats were taken respectively. The tibial anterior muscle tissue was divided into three parts for storage: 2.5% glutaraldehyde solution was fixed at 4°C; -80°C was stored at low temperature; 4% paraformaldehyde solution was fixed at room temperature for subsequent detection.

Experimental Grouping

The first part of the experiment: Normal group (replaced by the right healthy side of the model group); (2) Model group; (3) Astragaloside group (20 mg/kg); (4) Capillary isoflavone group (20 mg/kg); (5) Ferulic acid group (100 mg/kg); (6) Paeoniflorin group (20 mg/kg); (7) Ligustrazine group (100 mg/kg); (8) Mecobalamine positive control group (600 µg/kg), 6 in each group. Intraperitoneal injection was started two days after modeling and lasted for a total of 7 days.

The second part of the experiment: Base on the first experiment, the main active ingredient group + FOXO agonist was added, and 40 mg/kg of FOXO agonist was injected intraperitoneally every day for 7 consecutive days. Intraperitoneal injection was started two days after modeling, which lasted for a total of 7 days. The normal group and the model group were injected with the same amount of normal saline.

HPLC and LC-MS Experiments

HPLC: Precisely weigh 0.55 mg of pilus isoflavones, ferulic acid, paeoniflorin, and ligustrazine samples, place them in 10 mL brown volumetric flasks, add 70% methanol solution to dissolve and dilute to scale, and make a sample containing 0.055 mg per mL. Reference solution. Precisely weigh Buyang Huanwu Decoction and add methanol to dissolve, centrifuge the supernatant, and put the bandwidth evaluation in a 5 mL volumetric flask, shake well, and get it. Detection conditions: mobile phase: A 0.05% H_3PO_4 aqueous solution; B 0.1% methanol; chromatographic column: Symmetry C18, 4.6 x 250 mm; flow rate: 0.6 mL/min; column temperature: 30°C; injection volume: 5 µL; DAD detector Detection wavelength: 320 nm.

LC-MS: Take 0.0050 g of Astragaloside reference substance, weigh it precisely, place it in a 10 mL volumetric flask, add an appropriate amount of methanol to dissolve and dilute to scale, and make a solution containing 0.5 mg per 1 mL. Precisely weigh BYHW Decoction and add methanol to dissolve, centrifuge the supernatant, and put the bandwidth evaluation in a 5 mL volumetric flask, shake well. Detection conditions: Column: ACQUITY UPLCTMBEH C18 (1.7 µm, 50 mm * 2.1 mm); Column temperature: 35°C; Mobile phase: A 0.1% formic acid water (positive ion mode)/water, B acetonitrile; Flow rate: 0.2 Lmin; Injection volume: 5 µL; Autosampler temperature/TEM: 15°C.

Western Blot

Samples were cracked in RIPA lysis buffer plus PMSF in low temperature, and BCA assay kit (Santa Cruz, California, USA) detected total protein concentration. Prepared protein samples were separated in SDS-PAGE and transferred into 0.22 µm PVDF membranes and incubated with prepared antibodies. Finally, enhanced chemiluminescence (ECL, ThermoFisher, MA, USA) visualized this membrane. Antibodies against FOXO/p-FOXO and GAPDH were purchased from Abcam (Cambridge, MA, USA). Antibodies against MuRF-1, Atg5, Beclin-1, LC3I and LC3II were purchased from Proteintech Group (Proteintech Group, Wuhan, China).

H&E Staining

Pretibial muscle tissue was dissected from each group. The prepared muscle tissue slices were dewaxed and hydrated. After washed by water, synovial tissue slices were staining in hematoxylin solution for 5 min. Next, differentiated by 1% hydrochloric alcohol for 15s, the slices were washed with water. And then synovial tissue slices were stained by eosin solution for 1 min. Finally, muscle tissue slices were dehydrated, transparentized and sealed by neutral gum, observed under an optical microscope (Olympus, Tokyo, Japan).

Immunohistochemistry Staining

Pretibial muscle tissues were dissected from each group. First, Pretibial muscle tissue was fixed in 4% formaldehyde, embedded in paraffin. Each paraffin block was cut into 5 mm sections with a cryostat. The prepared Pretibial muscle tissue slices were dewaxed and hydrated followed washed by water. Secondly, Pretibial muscle tissue slices were sealed in 5 % normal goat serum for 30 min at room temperature. And then the slices were incubated with primary (p-FOXO 1:60, FOXO 1:300, LC3 1:300, Atg5 1:150, Beclin-1 1:100) antibody overnight at 4°C. After washing with PBS, the slices were incubated with biotinylated goat anti-rabbit IgG for 1 h. Finally, the slices were stained by DAB until a color change, and was observed under microscope (Olympus, Tokyo, Japan).

Masson Staining

Collect the tibial anterior muscle tissue, take out all the tissues, and dehydrate them sequentially through a layer of ethanol in a dehydrator. Put the melted paraffin into the embedding frame, place it on a -20°C freezer to cool, take it out of the embedding frame after the wax block solidifies and trim it, and place the embedded paraffin block in a 4°C refrigerator for setting. Slice after setting for 10 h. Briefly, Masson staining was performed on a 10 µm cryosection of muscle fixed with 95% alcohol for 20 min. Sections then were incubated with different solutions supplemented in Masson's Trichrome Stain Kit. At the end, the section was dehydrated with 95% alcohol for 10 sec, two rinses in anhydrous alcohol for 10 sec, and two rinses in xylene for 1 min each. The sections were mounted with Neutral balsam for imaging and fibrosis quantification. Muscle fibrosis quantification was performed by using Image J.

Transmissive Electron Microscope

Take rat tibial anterior muscle tissue, wash it with

normal saline, immediately put it in a pre-chilled 2.5% glutaraldehyde solution, and fix it overnight at 4°C. After all tissues were fixed, the rat tibial anterior muscle tissue was cut into tissue blocks of 1 mm³ size. Replace the 1% osmium acid solution, let it stand at 4°C for 2 h, and wash 3 times again with 1 x PBS. The tissue samples to be inspected were subjected to 50% (15 min), 70% (15 min), 80% (15 min), 90% (15 min), 95% (15 min), 100% (20 min), 100% (20 min) ethanol layer dehydration. After the transition of propylene oxide permeation, the samples were embedded with resin, and ultra-thin sections (thickness 70-90 nm) of lead citrate solution and 50% ethanol saturated solution of dioxy uranium acetate were stained for 15 min respectively. Under transmission electron microscope, images were collected to observe the ultrastructure of tissue samples.

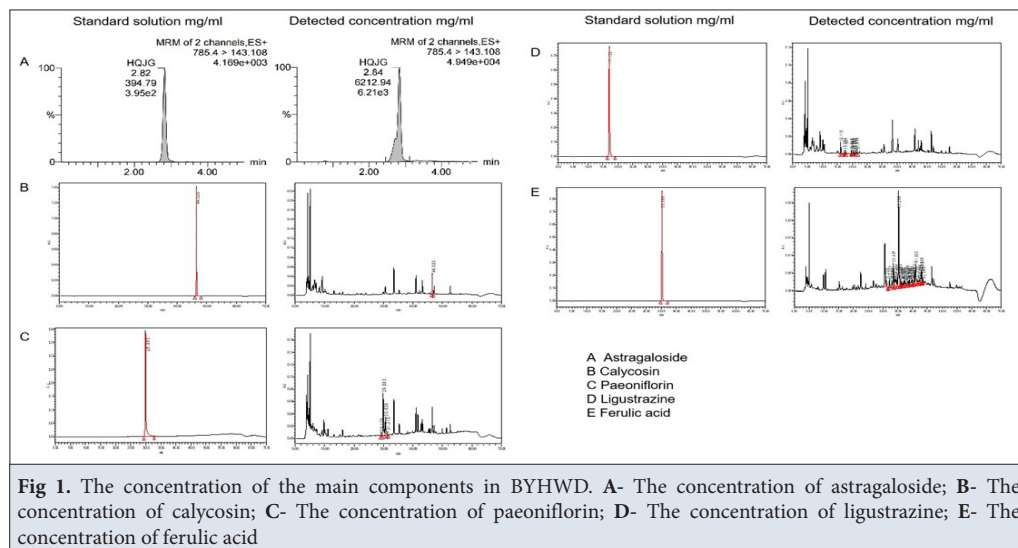
Data Processing and Statistical Methods

The data obtained from the experiment were expressed by mean ± standard error (Mean ± SEM), and all data were processed and statistically analyzed using GraphPad Prism 6. The t-test was used for the comparison between the mean values of the two groups of samples, and the ANOVA test was used for the comparison between the mean values of multiple groups of samples. P<0.05 indicates that the difference is statistically significant.

RESULTS

The Ingredients Contained in BYHWD

In order to study the main components of BYHW Decoction, HPLC and LC-MS were used to detect the contents of Isoflavones, Ferulic Acid, Paeoniflorin, Ligustrazine and Astragaloside in the medicinal solution, respectively. The analysis results showed that, the content of Astragaloside in the decoction (3.78 mg/mL) (*Fig. 1-A*) is much larger than that of other components,



Isoflavone (0.11 mg/mL) (Fig. 1-B), Ferulic Acid (0.14 mg/mL) (Fig. 1-C), Paeoniflorin (1.48 mg/mL) (Fig. 1-D), Ligustrazine (0.0063 mg/mL) (Fig. 1-E). The experimental results clearly indicate that astragaloside is the dominant chemical substance that dissolves after the BYHW decoction is boiled, suggesting that it may be one of the key substances underlying the efficacy of this compound formula. This also reflects the significant role of astragalus as the principal herb in the formula.

Astragaloside Inhibits the Atrophy Level of Skeletal Muscle After Nerve Injury

After determining the concentration of each component, we tested the therapeutic effect of each component on de-neuromuscular atrophy using mecobalamine tablets as positive control in animal models. HE staining results showed that compared with control group, muscle tissue of each treatment group was damaged to varying degrees. On the other hand, the degree of muscle tissue loss was significantly reduced in the treatment group compared with the blank model group (Fig. 2-A). Except for the positive control of mecobalamine, Astragaloside group was the closest to normal tissues in terms of tissue morphology. The electron microscopy results of muscle tissue were similar to those of HE (Fig. 2-B), which indicates that Astragaloside may be the main pharmacodynamic component.

Autophagy Plays an Important Role in Skeletal Muscle Denervation Atrophy

Based on previous studies on skeletal muscle, the ubiquitin-proteasome pathway or the autophagic lysosome pathway is the most likely deep cause of skeletal muscle denervation

on atrophy. To this end, we examined and compared the expression levels of key proteins of these two signaling pathways in normal tissues and model tissues (Fig. 2-C). As shown in Fig. 2-C, the expression level of LC3II/I and the ratio of LC3II/I in the model group were both increased, indicating the improved autophagy level of muscle cells. During autophagy formation, cytoplasmic type LC3 (LC3-I) will enzymolysis a small section of polypeptide and transform into membrane type (LC3-II). The increase of LC3-II represents the initiation of autophagy, and the LC3-II/I ratio can also estimate the level of autophagy. These results suggests that autophagy is the underlying cause of denervation atrophy in skeletal muscle.

Astragaloside Fights Skeletal Muscle Denervation by Inhibiting Muscle Autophagy

To verify this hypothesis, we treated animal model with Astragaloside alone, with autophagy labeled protein FOXO agonist as a control. The experimental results showed that the muscle dry-wet ratio in the model group was significantly improved after receiving Astragaloside treatment, but the data of group E was significantly decreased after the using of FOXO agonist (Fig. 3-A,B,C), suggesting that the using of autophagy agonist could inhibit the therapeutic effect of Astragaloside on skeletal muscle denervation. Masson staining showed that the blue collagen fiber tissue of Astragaloside group was significantly less than that of model group, and the blue area of FOXO agonist group showed obvious expansion (Fig. 3-D). Under electron microscope (Fig. 3-E), the number of scattered autophagosomes in Astragaloside group was significantly reduced, but the number of autophagosomes was significantly increased after the use of FOXO agonist.

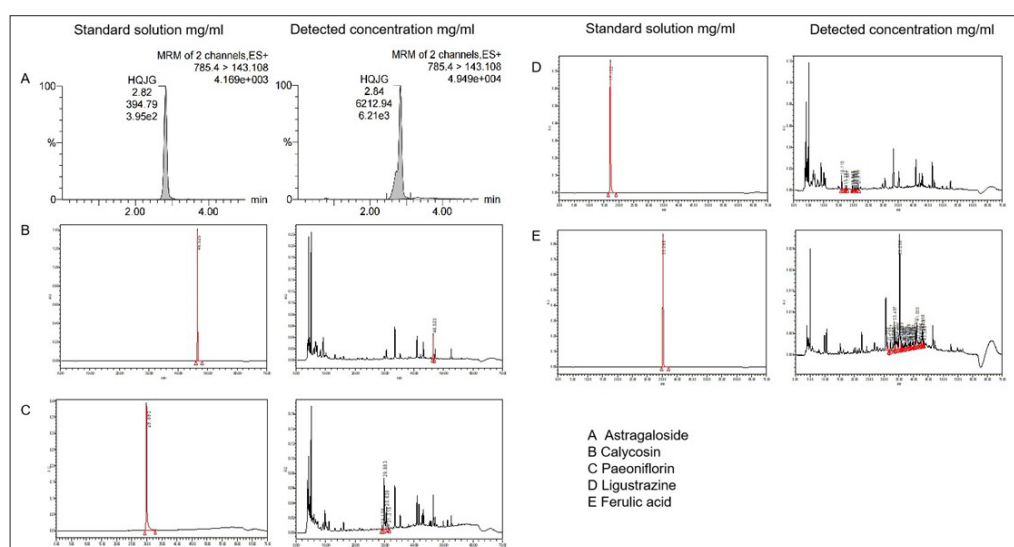
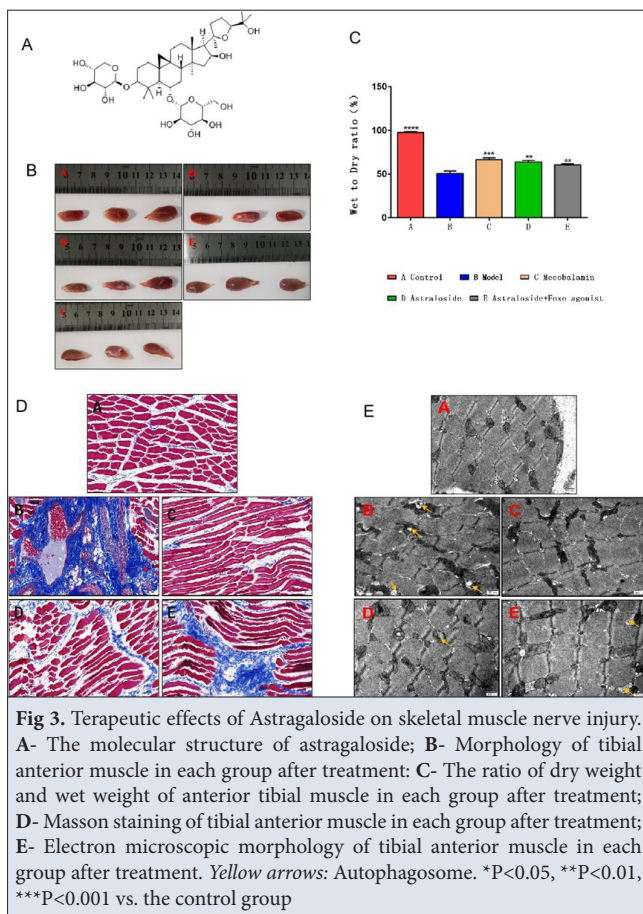


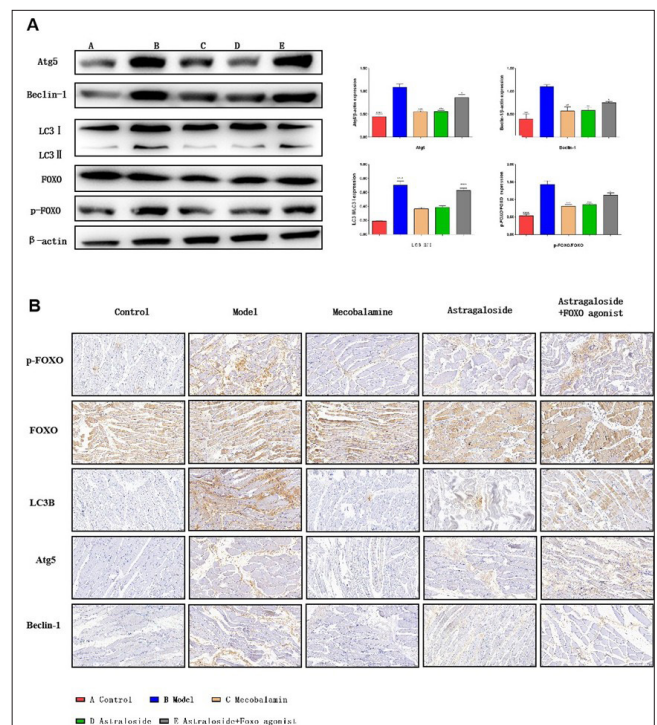
Fig 2. Therapeutic effects of each monomeric component on skeletal muscle atrophy. A-H&E staining results of muscle tissues after treatment in each group; B- Electron microscopic images of muscle tissue in each group after treatment; C- Expression levels of key proteins in muscular atrophy related signaling pathways (M: Model) (**P<0.01, ***P<0.001 vs. the control group)



These results suggest that Astragaloside inhibits skeletal muscle denervation via lysosomal autophagy.

Astragaloside Inhibits Skeletal Muscle Denervation Autophagy Through FOXO Related Pathway

Autophagy is a highly conserved and multi-step metabolic process that maintains homeostasis of the intracellular environment by degrading damaged proteins, cellular metabolites and diseased organelles. The occurrence and development of many diseases are associated with changes in autophagy activity, and the autophagy related gene microtubule-associated protein 1 light chain 3, LC3 and autophagy related gene-5 (ATG5) are both important genes involved in the regulation of autophagy activity. In our results, the expression level of LC3 and Atg5 protein were significantly upregulated after animal model was established and down-regulated after treatment which indicates us the important role of autophagy in skeletal muscle denervation atrophy (Fig. 4-A,B). Besides, studies have shown that FOXO can activate the autophagy mechanism of different cell types by affecting the expression of autophagy genes which including ATG5. Therefore, we used FOXO agonists as a distraction to determine whether autophagy in muscle tissue after motor nerve injury is mediated by changes in the FOXO pathway. As predicted, the addition of FOXO agonists reversed the



efficacy of the treatment in both the mecobalamin and astragaloside groups.

DISCUSSION

In this study, starting from the basic composition of traditional Chinese medicine, the contents of the five most important components in the BYHWD, Isoflavones, Ferulic acid, Paeoniflorin, Ligustrazine and Astragaloside, were detected by HPLC and LC-MS methods [8]. All monomers have a certain inhibitory effect on skeletal muscle atrophy caused by nerve injury in vivo. Among them, Astragaloside has the highest concentration in decoction, and its monomer has the most obvious inhibitory effect on muscle atrophy [9]. Pharmacologically speaking, Astragaloside has many pharmacological activities, it can effectively activate mononuclear macrophage system, stimulate macrophage and T cell function to play an antiviral effect; Astragaloside can prevent adrenal hyperplasia and thymus atrophy in the alert phase of stress response, and prevent abnormal changes in the resistance phase and exhaustion phase of stress response so as to play an anti-stress role [10]. In addition, Astragaloside can also enhance cell metabolism, promote blood circulation, and improve cardiopulmonary function in some cases [11].

In terms of clinical research, Astragaloside has a good

curative effect in the treatment of the body after nerve injury. Qi et al.^[12] used BYHWD to feed rats after spinal cord injury. The experimental results show that the decoction can inhibit PAF. The application of BYHW significantly improved the motor function of rats; the research results of Zhao et al.^[13] team on the gerbil model of ischemia-reperfusion injury showed that BYHWD could protect the nerve function of gerbils after reperfusion injury by improving brain microcirculation. A study indicated that BYHWD can inhibit the apoptosis of nerve cells caused by hypoxia by eliminating reactive oxygen species and NO^[14]. Our results show that the inhibitory effect of BYHWD on skeletal muscle denervation may be produced by inhibiting skeletal muscle cell autophagy.

Whether it is the expression of autophagy-related proteins after monomer treatment, or the immunohistochemical results of autophagy-related proteins in tissues, and the number of autophagy corpuscles in tissues under electron microscopy, the results of autophagy-related detection showed significant changes among the groups^[15]. This also directly affects the wet-to-weight ratio and cross-sectional area of skeletal muscle after treatment. Autophagy is a dynamic process through which cytoplasmic components can be decomposed into basal components and then re-entered into the cytoplasm for reuse^[16]. Autophagy is also a major protective mechanism that allows cells to survive a variety of stress conditions, such as nutrient or growth factor deprivation, hypoxia, reactive oxygen species (ROS), DNA damage, and more^[17]. MuRF-1 encodes E3s ubiquitin ligase, which is essential for protein ubiquitination degradation and determines the degradation rate of this pathway^[18]. However, from the detection results of samples, there was no significant difference in the expression of MuRF-1 in normal tissue and model group, but there was significant difference in the expression of LC3, the signature protein of the autophagic lysosome pathway^[17]. Under basic conditions, low levels of autophagy exist in all types of cells, but stimuli such as nutritional deficiencies or hypoxia may lead to up-regulation of autophagy levels^[19].

After the injury of the common peroneal nerve, the conduction of nerve impulses is hindered, resulting in the disuse of some muscle fibers controlled downstream, resulting in disuse muscular atrophy^[20]. At the same time, the release of acetylcholine from the peripheral parts of the damaged nerve fibers decreases, and sympathetic nerve nutrition weakens, resulting in muscle atrophy^[21]. Our findings reveal a possible mechanism of muscle disuse atrophy, that is, after motor nerve injury, downstream skeletal muscle due to lack of nutritional factors in order to maintain mixing, the level of autophagy in skeletal muscle cells increases, and the number of muscle fibers decreases, resulting in muscle atrophy. Combined with the research

results of Cheng et al.^[22], on the one hand, BYHWD strengthened the microcirculation downstream of injury and alleviated the lack of nutritional factors caused by nerve injury, on the other hand, its main component, Astragaloside, can effectively reduce the expression of autophagy related proteins in skeletal muscle, thereby inhibiting skeletal muscle atrophy.

Motor nerve injury induces muscle atrophy via autophagy activation and nutrient deficiency. BYHWD alleviates atrophy by improving microcirculation and its component Astragaloside suppresses autophagy, offering a therapeutic strategy for nerve injury-related muscle wasting.

DECLARATIONS

Data Availability Statement: All processed data and models used during the study are available from the corresponding author (HW) by request.

Acknowledgments: We would like to thank all the researchers and study participants for their contributions.

Funding Support: This study was supported by The General project of Natural Science Foundation of Jiangsu Province (Grant No. BK20201399).

Ethical Approval

All procedures performed in the studies involving animals were in accordance with the ethical standards of the Institutional Animal Care and Use Committee (IACUC) of Nanjing University of Chinese Medicine (No. 202203A041).

Declaration of Conflicting Interests: The author(s) declared no potential conflicts of interest.

Declaration of Generative Artificial Intelligence: We declare that the article and tables/figures are not written by AI.

Authors' Contribution: L.Z. and HW: fully responsible for the study designing, Research fields, Drafting, Finalizing the paper; S.L., L.M., and G.W.: Wrote the manuscript and drew the pictures, Collected and organize literature; H.W. and L.Z.: Proofread the manuscript. All authors have reviewed and agreed to the published version of the manuscript.

REFERENCE

1. Cohen S, Nathan JA, Goldberg AL: Muscle wasting in disease: Molecular mechanisms and promising therapies. *Nat Rev Drug Discov*, 14 (1): 58-74, 2015. DOI: 10.1038/nrd4467
2. Baehr LM, Hughes DC, Waddell DS, Bodine SC: SnapShot: Skeletal muscle atrophy. *Cell*, 185 (9):1618-1618.e1, 2022. DOI: 10.1016/j.cell.2022.03.028
3. Braun TP, Zhu X, Szumowski M, Scott GD, Grossberg AJ, Levasseur PR, Graham K, Khan S, Damaraju S, Colmers WF, Baracos VE, Marks DL: Central nervous system inflammation induces muscle atrophy via activation of the hypothalamic-pituitary-adrenal axis. *J Exp Med*, 208 (12): 2449-2463, 2011. DOI: 10.1084/jem.20111020
4. Derde S, Hermans G, Derese I, Güiza F, Hedström Y, Wouters PJ, Bruyninckx F, D'Hoore A, Larsson L, Van den Berghe G, Vanhorebeek I: Muscle atrophy and preferential loss of myosin in prolonged critically ill patients. *Crit Care Med*, 40 (1): 79-89, 2012. DOI: 10.1097/CCM.0b013e31822d7c18
5. Faruk MO, Ichimura Y, Komatsu M: Selective autophagy. *Cancer Sci*, 112

(10): 3972-3978, 2021. DOI: 10.1111/cas.15112

6. Fu Y, Cai J, Xi M, He Y, Zhao Y, Zheng Y, Zhang Y, Xi J, He Y: Neuroprotection effect of astragaloside IV from 2-DG-induced endoplasmic reticulum stress. *Oxid Med Cell Longev*, 2020:9782062, 2020. DOI: 10.1155/2020/9782062

7. Wang H, He Y, Wan L, Li C, Li Z, Li Z, Xu H, Tu C: Deep learning models in classifying primary bone tumors and bone infections based on radiographs. *npj Precis Onc*, 9:72, 2025. DOI: 10.1038/s41698-025-00855-3

8. Peng J, Ge C, Shang K, Liu S, Jiang Y: Comprehensive profiling of the chemical constituents in Dayuanyin decoction using UPLC-QTOF-MS combined with molecular networking. *Pharm Biol*, 62 (1): 480-498, 2024. DOI:10.1080/13880209.2024.2354341

9. Glick D, Barth S, Macleod KF: Autophagy: cellular and molecular mechanisms. *J Pathol*, 221 (1): 3-12, 2010. DOI: 10.1002/path.2697

10. Lattouf NA, Tomb R, Assi A, Maynard L, Mesure S: Eccentric training effects for patients with post-stroke hemiparesis on strength and speed gait: A randomized controlled trial. *NeuroRehabilitation*, 48 (4): 513-522, 2021. DOI:10.3233/NRE-201601

11. Li C, Zhang Y, Liu J, Kang R, Klionsky DJ, Tang D: Mitochondrial DNA stress triggers autophagy-dependent ferroptotic death. *Autophagy*, 17 (4): 948-960, 2021. DOI: 10.1080/15548627.2020.1739447

12. Qi YN, Tan MS, Wang YL, Wang W, Wu XJ, Hao QY, Yi P, Yang F, Tang XS: Effect of Buyanghuanwu decoction on the expression of platelet activating factor after acute spinal cord injury in rats. *Zhongguo Gu Shang*, 31 (2): 170-174, 2018. DOI: 10.3969/j.issn.1003-0034.2018.02.015

13. Zhao YN, Wu XG, Li JM, Chen CX, Rao YZ, Li SX: Effect of BuYangHuanWu recipe on cerebral microcirculation in gerbils with ischemia-reperfusion. *Sichuan Da Xue Xue Bao Yi Xue Ban*, 41 (1): 53-56, 2010.

14. Rodriguez-Aller M, Gurny R, Veuthey JL, Guillaume D: Coupling ultra high-pressure liquid chromatography with mass spectrometry:

Constraints and possible applications. *J Chromatogr A*, 1292, 2-18, 2013. DOI: 10.1016/j.chroma.2012.09.061

15. Shi H, Zhou P, Gao G, Liu PP, Wang SS, Song R, Zou YY, Yin G, Wang L: Astragaloside IV prevents acute myocardial infarction by inhibiting the TLR4/MyD88/NF- κ B signaling pathway. *J Food Biochem*, 45 (7):e13757, 2021. DOI: 10.1111/jfbc.13757

16. Urbńska K, Orzechowski A: The secrets of alternative autophagy. *Cells*, 10 (11):3241, 2021. DOI: 10.3390/cells10113241

17. Wang C, Haas M, Yeo SK, Sebt S, Fernández ÁE, Zou Z, Levine B, Guan JL: Enhanced autophagy in Becn1F121A/F121A knockin mice counteracts aging-related neural stem cell exhaustion and dysfunction. *Autophagy*, 18 (2): 409-422, 2022. DOI: 10.1080/15548627.2021.1936358

18. Wang F, Zhao Y, Chen S, Chen L, Sun L, Cao M, Li C, Zhou X: Astragaloside IV alleviates ammonia-induced apoptosis and oxidative stress in bovine mammary epithelial cells. *Int J Mol Sci*, 20 (3):600, 2019. DOI: 10.3390/ijms20030600

19. Yang Z, Lin P, Chen B, Zhang X, Xiao W, Wu S, Huang C, Feng D, Zhang W, Zhang J: Autophagy alleviates hypoxia-induced blood-brain barrier injury via regulation of CLDN5 (claudin 5). *Autophagy*, 17 (10): 3048-3067, 2021. DOI: 10.1080/15548627.2020.1851897

20. Zhang M, Yi Y, Gao BH, Su HF, Bao YO, Shi XM, Wang HD, Li FD, Ye M, Qiao X: Functional characterization and protein engineering of a triterpene 3-/6-/2'-O-glycosyltransferase reveal a conserved residue critical for the regiospecificity. *Angew Chem Int Ed Engl*, 61:e202113587, 2022. DOI: 10.1002/anie.202113587

21. Zhang ZQ, Song JY, Jia YQ, Zhang YK: Buyanghuanwu decoction promotes angiogenesis after cerebral ischemia/reperfusion injury: Mechanisms of brain tissue repair. *Neural Regen Res*, 11 (3): 435-440, 2016. DOI: 10.4103/1673-5374.179055

22. Cheng M, Li T, Hu E, Yan Q, Li H, Wang Y, Luo J, Tang T: A novel strategy of integrating network pharmacology and transcriptome reveals

antiapoptotic mechanisms of Buyang Huanwu Decoction in treating

intracerebral hemorrhage. *J Ethnopharmacol*, 319 (Pt 1):117123, 2024. DOI:

10.1016/j.jep.2023.117123

RESEARCH ARTICLE

First Report of Gastroenteritis Caused by *Citrobacter braakii* in a Yellow-margined Box Turtle (*Cuora flavomarginata*)

Min CHEN ¹  Yifan SONG ¹  Chongfeng LIU ¹  Ningning CHEN ¹  Junzeng XUE ^{1, (*)} 

¹ College of Oceanography and Ecological Science, Shanghai Ocean University, Shanghai, 201306, CHINA



(*) Corresponding author:

Junzeng Xue
Phone: +86 021 61900428
E-mail: jzxue@shou.edu.cn

How to cite this article?

Chen M, Song Y, Liu C, Chen N, Xue J:
First report of gastroenteritis caused by
Citrobacter braakii in a yellow-margined
box turtle (*Cuora flavomarginata*). *Kafkas
Univ Vet Fak Derg*, 31 (5): 669-677, 2025.
DOI: 10.9775/kvfd.2025.34626

Article ID: KVFD-2025-34626

Received: 14.06.2025

Accepted: 27.09.2025

Published Online: 06.10.2025

Abstract

To determine the pathogen responsible for gastroenteritis mortality in a yellow-margined box turtle (*Cuora flavomarginata*). A dominant single colony, A1, was isolated from the liver lesions of the diseased *C. flavomarginata* on the farm. Based on 16S rDNA sequencing and comparative analysis in NCBI, the isolate showed 99.58% similarity to *Citrobacter braakii*. Antimicrobial susceptibility testing revealed that strain A1 was resistant to multiple antibiotics. The pathogenicity of the strain was confirmed through experimental infection in red-eared sliders (*Trachemys scripta elegans*), which resulted in clinical signs consistent with gastroenteritis. Histopathological examination of infected tissues revealed inflammatory cell infiltration in the gastric submucosa and lamina propria, as well as degenerative changes in hepatocytes, including cytoplasmic loosening, mild edema, and cholestasis. Additionally, structural alterations were observed in the intestinal mucosa, accompanied by inflammatory infiltration. Our study demonstrates that *C. braakii* is one of the pathogenic agents responsible for gastroenteritis in turtles. Preliminary discussions were conducted from the perspectives of pathogenicity, antimicrobial susceptibility, and histopathology, thereby providing a theoretical foundation for the prevention of turtle diseases caused by this microorganism.

Keywords: Antimicrobial resistance, *Citrobacter braakii*, *Cuora flavomarginata*, Experimental infection, Histopathology, Turtle

INTRODUCTION

The yellow-margined box turtle (*C. flavomarginata*) belongs to the family Emydidae and the genus *Cuora* ^[1-3]. It is highly valued for its edible, medicinal, and ornamental qualities, and is easily domesticated. These attributes have driven intensive wild harvesting, resulting in severe declines in population. Consequently, it is now afforded legal protection at both national and international levels ^[4]. Intensive artificial breeding has been developed to meet market demand. However, high-density farming practices often lead to frequent disease outbreaks, including pneumonia, shell rot, peptic ulcer, and cystic disease. In 2021, Du et al. ^[5] reported fatal duodenal perforation in a juvenile yellow-margined box turtle caused by *Chelonobacter oris*, and in 2016, *Aeromonas hydrophila* was documented to cause keratitis in this species ^[6]. Among these various diseases, bacterial gastroenteritis is a common and clinically significant problem in *C. flavomarginata*. To date, gastrointestinal diseases related to turtles have been described in Chinese grass turtles (*Mauremys reevesii*) ^[7], yellow pond turtles (*Mauremys mutica*) ^[8], leatherback

turtle (*Dermochelys coriacea*) ^[9], and red-footed turtles (*Chelonoidis carbonarius*) ^[10], which are caused by *Escherichia coli*, *Salmonella* spp., *Aeromonas punctata*, *Aeromonas sobria*, *Vibrio metschnikovii*, *Photobacterium damsela* subsp. *piscicida*, and *Clostridium perfringens*. However, scarce information is available on *C. braakii* as a bacterial pathogen in turtles.

C. braakii is considered to be an important human and aquaculture pathogen. It has been documented to cause disease in a wide range of aquatic species, including the red claw crayfish (*Cherax quadricarinatus*) ^[11], black carp (*Mylopharyngodon piceus*) ^[12], spiny frog (*Quasipaa spinosa*) ^[13], rainbow trout (*Oncorhynchus mykiss*) ^[14], catfish (*Silurus asotus*) ^[15], *Melanotaenia praecox* ^[16], and other aquatic animals. As a typical opportunistic pathogen, it can also cause inflammation and bacteremia in human tissue ^[17,18]. Infections with *C. braakii* are frequently characterized by necrotizing inflammation and immunosuppression in host species, especially poikilothermic aquatic ones ^[19]. The bacterium demonstrates considerable tissue invasiveness and environmental adaptability in such hosts ^[20]. Given that



C. flavomarginata is a poikilothermic aquatic reptile whose immune function is highly susceptible to environmental stress, its immune responses may share similarities with those reported in fish and amphibians. We therefore hypothesized that *C. braakii* poses a comparable pathogenic threat to this turtle species.

This study demonstrates the association of *C. braakii* with severe gastroenteritis in *C. flavomarginata*. We systematically characterized its phenotypic and biochemical characteristics, pathogenicity, antibiotic resistance profile, and histopathological changes induced by infection. These findings offer a scientific basis for the clinical diagnosis and control of bacterial gastroenteritis in this species. They also hold practical significance for protecting the health of captive populations of this endangered turtle.

MATERIAL AND METHODS

Ethical Statement

All animal experimental procedures in this study strictly adhered to international ethical guidelines for animal experimentation and relevant Chinese regulations. The experimental protocol was reviewed and approved by the Academic Committee of the College of Oceanography and Ecological Science at Shanghai Ocean University and received formal approval from the Shanghai Ocean University Animal Ethics Committee (Approval No. SHOU-DW-2024-300).

Isolation and Identification of the Pathogen

On November 25, 2024, we obtained a diseased *C. flavomarginata* (230 g in weight) from a commercial farm in Shanghai, exhibiting multiple clinical signs. The individual initially presented with lethargy, significantly reduced food intake, and diminished activity. These symptoms were subsequently accompanied by the excretion of green feces. The abnormal manifestations persisted for more than 48 h and showed no improvement following initial routine surface disinfection and isolation. The condition progressed to include complete anorexia, redness and swelling around the anus, dark brown fecal excretion, limb edema, and sunken orbits. The turtle eventually became severely debilitated and succumbed to the illness. The moribund turtles were immediately transported to the laboratory on ice packs for immediate microbiological analysis. The body surface of dead turtles was disinfected with 75% ethanol (Huankai Microbiology Science and Technology Co., Ltd., China), and necropsy was performed under aseptic conditions. Liver lesions were aseptically streaked with a sterilized loop onto LB agar (Huankai Microbiology Science and Technology Co., Ltd., China) and violet red bile glucose agar (VRBGA) plates (Hangzhou Microbiology Reagent Co., Ltd., China). The inoculated plates were

incubated aerobically at 37°C for 24 h. A predominant bacterial colony was repeatedly subcultured on fresh LB agar to obtain a pure isolate, designated strain A1. For phenotypic characterization, strain A1 was cultured on LB agar at 37°C for 24 h, and colony morphology was recorded. Based on relevant literature and the characteristics of *enterobacteria*, Biochemical profiling was performed using Bacterial Biochemical Identification kit (Hangzhou Microbial Reagent Co., China), including tests for glucose fermentation, lysine decarboxylase, ornithine decarboxylase, H₂S production, peptone water, lactose fermentation, dulcitol fermentation, phenylalanine deaminase, urea, citrate, sucrose fermentation ^[21]. Results were interpreted according to *Bergey's Manual of Systematic Bacteriology*.

The genomic DNA of the pathogenic isolate was extracted using a bacterial DNA kit (Personal Biotechnology Co., Ltd., China), and the 16S rDNA gene region was amplified by PCR using the universal primers 27F (5-AGAGTTTGATCCTGGCTCAG-3) and 1492R (5-GGT TACCTTGTTACGACTT-3). The PCR amplification reaction mixture (50 µL) consisted of: 1 µL genomic DNA (20 ng/µL), 5 µL 10xBuffer (containing 2.5 mM Mg²⁺), 1 µL Taq polymerase (5 U/µL), 1 µL dNTP mix (10 mM), 1.5 µL of each primer (10 µM), and 39.0 µL ddH₂O. The mixture was gently flicked to combine the components, and droplets on the tube wall were collected by brief centrifugation. Amplification was carried out in a thermal cycler under the following conditions: initial denaturation at 95°C for 5 min; 35 cycles of denaturation at 95°C for 30 s, annealing at 58°C for 30 s, and extension at 72°C for 90 s; and a final extension at 72°C for 7 min. After amplification, 3 µL of the PCR product was analyzed by 1% agarose gel electrophoresis to confirm the presence of the target amplicon. The PCR products were purified and sequenced by Shenzhen MicroUnion Technology Group Co., Ltd. (China), and the sequencing was performed on an ABI3730-XL genetic analyzer. The obtained sequence was analyzed using the BLAST algorithm on the NCBI website (<https://www.ncbi.nlm.nih.gov>, accessed on December 7, 2024) to identify the species with the greatest sequence similarity to our isolate. Sequences with high similarity scores and from related aquaculture pathogens were selected for further analysis. A phylogenetic tree was constructed using the neighbor-joining method ^[22] in MEGA5.1 software (<http://www.megasoftware.net/>, accessed on December 7, 2024). The tree was subjected to a confidence test with 1000 bootstrap replications.

Experimental Infection

Trachemys scripta elegans and *C. flavomarginata* both belong to the class *Reptilia*, order *Testudines*, and suborder *Cryptodira* ^[23,24]. They share numerous ecological and biological traits, including a freshwater habitat, an

omnivorous diet, and similarities in the anatomical structure of the digestive system, physiological functions, and basic immune responses [25-27]. Disease reports also indicate that these species are susceptible to common health issues, such as pneumonia [28] and ophthalmitis [29], which present with similar clinical manifestations upon pathogenic bacterial infection [30]. Furthermore, in adherence to the “3R Principles” (Replacement, Reduction, and Refinement) and due to ethical as well as institutional regulatory constraints -specifically, the lack of approved animal ethics protocol for experimental work involving *C. flavomarginata* at our institution- the present study selected *Trachemys scripta elegans* as the infection model to investigate gastroenteritis caused by *C. braakii*.

After strain A1 was cultured at a constant temperature for 24 h, the bacterial lawn was harvested with 0.85% sterilized saline. The bacterial suspension was adjusted to a concentration of 3×10^8 CFU/mL. Twenty healthy *Trachemys scripta elegans* (carapace length: 9.0 ± 2.0 cm; body weight: 110 ± 20 g) were purchased from a farm in Jinhua, Zhejiang Province. The turtles were fed ad libitum twice daily for 14 days in an aerated tap water environment maintained at 28°C according to established husbandry protocols. No signs of disease or abnormalities were observed during this period. The turtles were then equally divided into two groups: a control group and an experimental group, with 10 individuals in each group. The experimental group received an intraperitoneal injection of 0.2 mL of the bacterial suspension, whereas the control group received an equal volume of sterile saline. The injected turtles were housed in individual tanks (80 x 47 x 28 cm) and fed normally throughout the experimental period. Survival rates and clinical signs were monitored and recorded daily for 45 days. Mortality of the *Trachemys scripta elegans* was monitored and recorded daily following the initiation of the infection experiment. For the purpose of survival analysis, a death was coded as “1”. Censored data -defined as individuals that either survived until the end of the study period or died from causes unrelated to the experimental infection- were coded as “0”. All data were compiled and subjected to statistical analysis using GraphPad Prism software (version 10.1.2). Survival rates across groups were compared using the Log-rank (Mantel-Cox) test. A two-tailed *P* value of less than 0.05 was considered statistically significant.

Histopathology

The main organs of the digestive system (liver, intestine, and stomach) were collected from deceased *Trachemys scripta elegans* and fixed in 4% paraformaldehyde solution for histopathological analysis. Following fixation, the tissues were dehydrated through a graded ethanol series, cleared in xylene, embedded in paraffin, sectioned, and stained with hematoxylin and eosin (H&E). The prepared

sections were then examined under a light microscope for observation, photography, and assessment of pathological changes.

Antimicrobial Susceptibility Assay

The Kirby-Bauer (K-B) disk diffusion method was employed. Four antibiotic disks were placed on each agar plate. The plates were then incubated at 28°C for 18 to 24 h. Following incubation, the diameters of the zones of inhibition were measured using manual calipers. Each experiment was performed in triplicate, and the average diameter was calculated for analysis. The antimicrobial susceptibility results were interpreted according to the standards provided by the Clinical and Laboratory Standards Institute (CLSI) [31].

RESULTS

Autopsy of the diseased *Trachemys scripta elegans* revealed several pathological changes. These included an enlarged liver and gallbladder with necrotic and congested tissues, a stomach with blood on its outer wall, and intestines that were inflated with blood, had inelastic walls, and showed erosion of the hind-gut (Fig. 1). In the experimental infection, individuals in the experimental group exhibited progressive mortality, culminating in 100% cumulative mortality by day 45. The initial mortality occurred on day 4, with a peak mortality period observed between days 15 and 30. The final death was recorded on day 45. In contrast, all turtles in the control group remained healthy throughout the experimental period, with no mortality observed (Fig. 2). The survival analysis revealed a statistically significant difference between the two groups (Log-rank test, $\chi^2 = 4.907$, *df* = 1, $*p = 0.0267$). Consistent with the survival curve, the infected group exhibited a significantly lower survival rate compared to the control group, demonstrating that the experimental bacterial infection significantly reduced the survival of *Trachemys scripta elegans*.

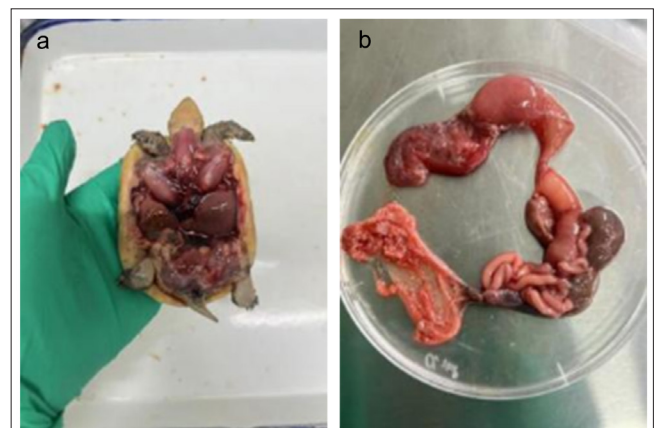


Fig 1. Anatomical diagram of a diseased turtle

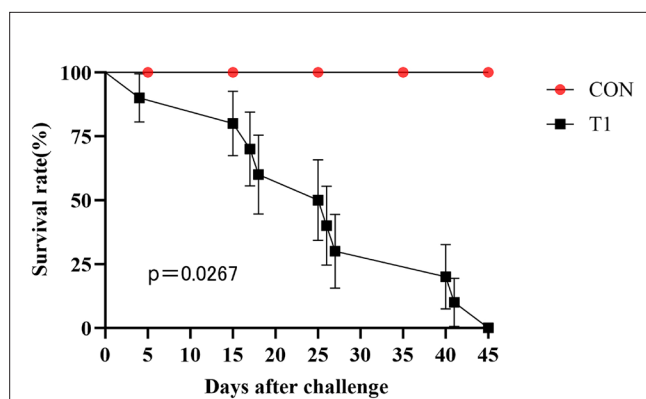


Fig 2. Survivals of experimental *Trachemys scripta elegans* infected intraperitoneally with strain A1 for Forty Five days (CON, 0 CFU/mL; T1, 3×10^6 CFU/mL)

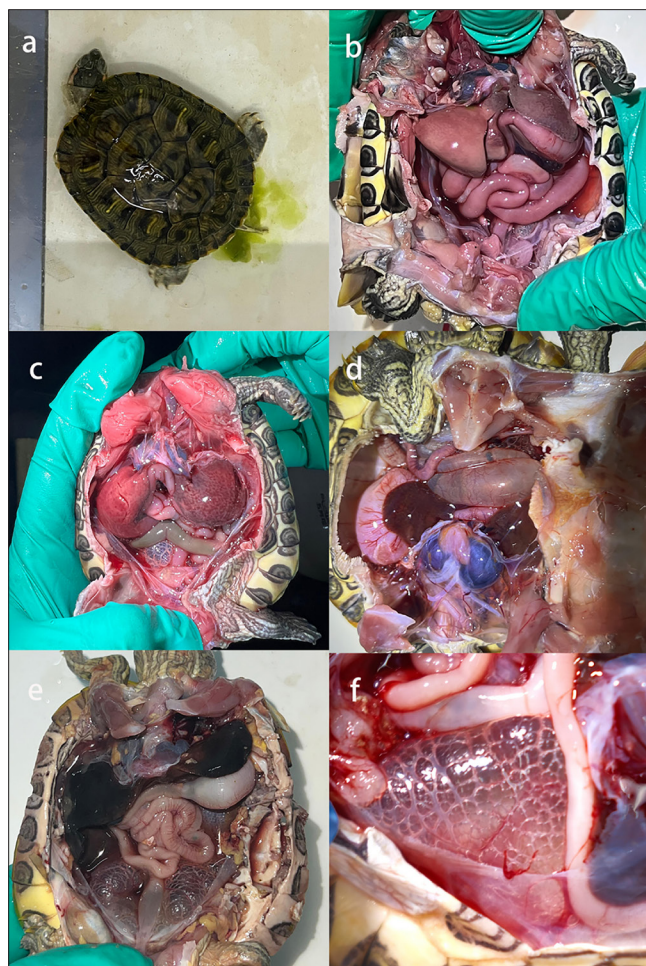


Fig 3. Symptoms and anatomical diagram of the onset of *Trachemys scripta elegans*. a- Typical gastroenteritis symptoms of dead turtles, b, c, d- dissection of the turtle infected with *C. braakii*, e, f- pneumonia symptoms

In the experimental group, infected turtles exhibited a range of clinical signs, including tail floating, anal mucus discharge, diarrhea with greenish stools (Fig. 3-a), and a progressive reduction in food intake leading to complete anorexia. Occasional open-mouth breathing, limb edema

and weakness were also observed. Upon dissection, pathological findings included hemorrhagic streaks on the outer stomach wall, intestinal distension with serosal hemorrhage, and swollen and partially eroded livers (Fig. 3-b,c,d). Some affected individuals also showed severe pulmonary emphysema (Fig. 3-e,f). The clinical manifestations and postmortem lesions observed in *Trachemys scripta elegans* were consistent with those previously described in *C. flavomarginata*. The original challenge strain, A1, was successfully reisolated from the infected *Trachemys scripta elegans* and confirmed through molecular and phenotypic analyses. Accordingly, Koch's postulates were fulfilled, confirming the pathogenic potential of *C. braakii* strain A1 in this host species.

Observation and Identification of Strain A1

After 24 h of incubation, strain A1 formed circular, convex, smooth, moist colonies with entire margins, measuring approximately 1-2 mm in diameter. The colonies exhibited a milky white and translucent appearance (Fig. 4-a).

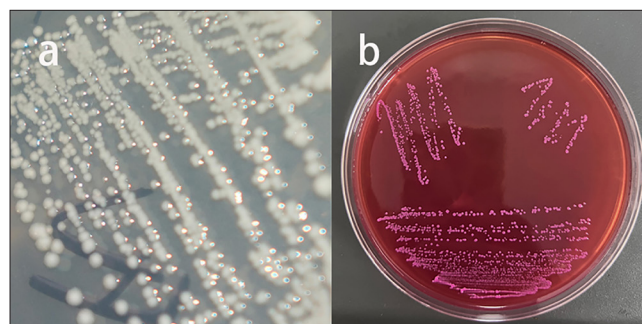


Fig 4. Morphological observation of strain A1

Table 1. Physiological and biochemical characteristics of strain A1 and the reference strain *C. braakii* CICC 21598

Test Item	Strain A1	<i>C. braakii</i> CICC 21598
Glucose fermentation	+	+
Lysine decarboxylase	+	+
Ornithine decarboxylase	+	+
H ₂ S production	+	+
Peptone water	+	+
Lactose fermentation	+	+
Dulcitol fermentation	+	+
Phenylalanine deaminase	-	-
Urea	-	-
Citrate	+	+
Sucrose fermentation	-	-

+ positive; - negative. The reference strain CICC 21598 was obtained from the China Center of Industrial Culture Collection (CICC)

On violet red bile dextrose agar (VRBGA), the colonies developed a distinct pink coloration (Fig. 4-b). According to the results of the biochemical identification test of strain A1, glucose, lysine, ornithine, H₂S production, peptone water, lactose, dulcitol, and citrate were positive, and phenylalanine, urea, and Sucrose were negative (Table 1). These biochemical characteristics are consistent with those of *C. braakii*, supporting the preliminary identification of strain A1 as *C. braakii*. Genomic DNA was extracted from strain A1 using a commercial kit and served as the template for PCR amplification. Amplified products were separated by 1% agarose gel electrophoresis, which yielded a target band of approximately 1,500 bp (Fig. 5). The 16S rDNA sequence of strain A1 was deposited in GenBank under accession number PX129799.1. BLAST analysis revealed 99.58% similarity with *C. braakii* (accession no.

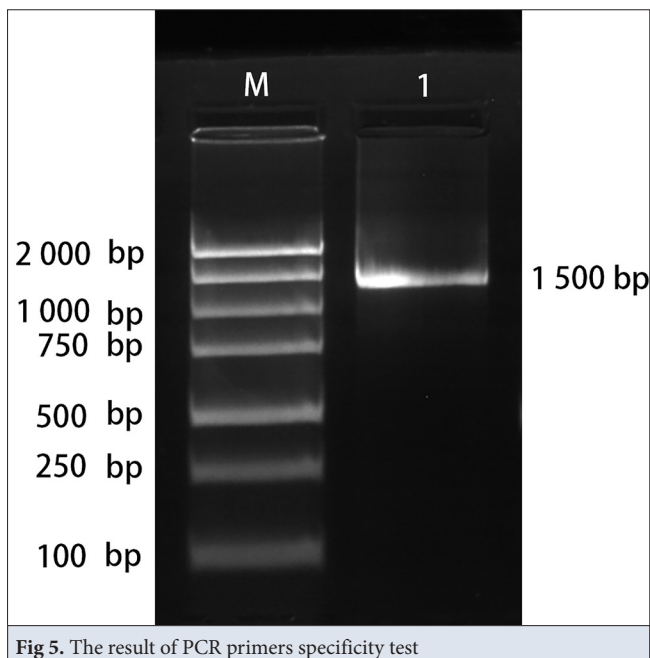


Fig 5. The result of PCR primers specificity test

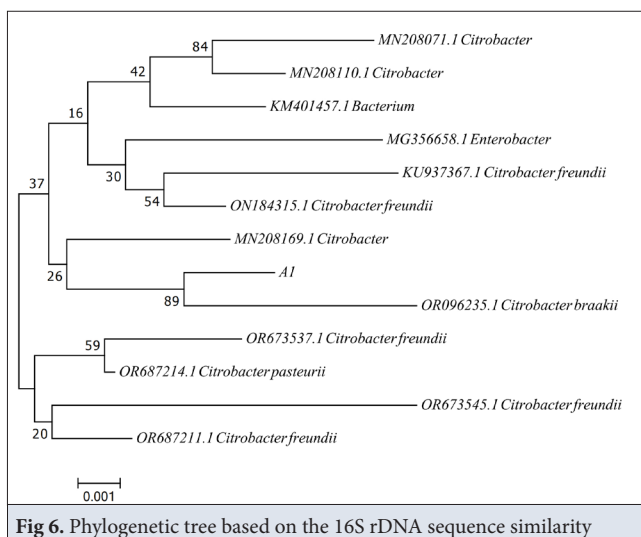


Fig 6. Phylogenetic tree based on the 16S rDNA sequence similarity

CP113163.1). Phylogenetic analysis further confirmed that strain A1 clusters within the same clade as *C. braakii* reference strains (Fig. 6).

Histopathological Analysis

Histopathological examination of the deceased turtles revealed that the hepatocytes were polygonal in shape, with scant eosinophilic cytoplasm and mild hydropic degeneration. Scattered inflammatory cell infiltration and cholestasis were observed within the hepatic parenchyma (Fig. 7-a, arrow 2). Increased brown pigment deposits were noted in focal areas (Fig. 7-a, arrow 1). Marked fibrous tissue proliferation was evident in the portal areas, accompanied by disorganization of the hepatic plate architecture. Hepatic sinusoids were distinct and contained numerous nucleated erythrocytes (Fig. 7-a, arrow 3). In the intestinal tissue, villi were seen projecting into the lumen. The mucosal lamina propria exhibited a significant reduction in glandular structures, with some glands displaying slight architectural irregularity. Prominent fibrous tissue proliferation and extensive inflammatory cell infiltration were observed in the lamina propria (Fig. 7-c, arrow 2). The muscularis mucosae was mildly thickened, and scattered inflammatory cells were present in both the submucosa and the lamina propria (Fig. 7-c, arrow 1). In the stomach, certain glandular structures appeared irregular, with a noticeable decrease in gland number and increased inflammatory cell infiltration (Fig. 7-e, arrow 2). The lamina propria showed substantial fibrous hyperplasia and abundant inflammatory cell infiltration (Fig. 7-e, arrow 1). The

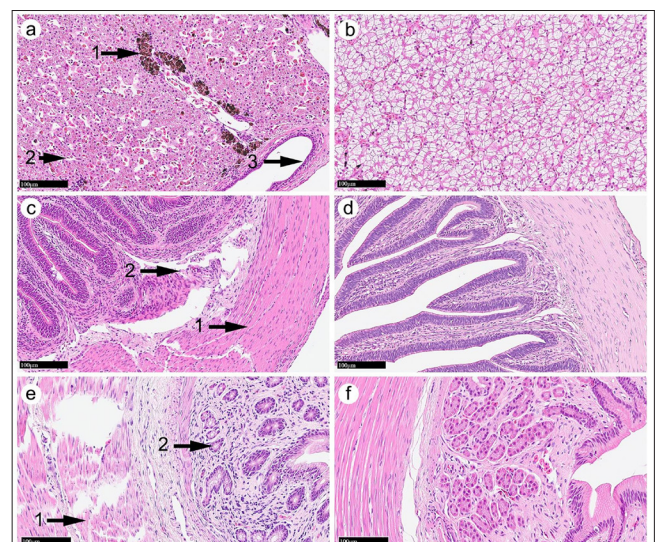


Fig 7. H&E staining of diseased and normal experimental turtles. a- Liver of diseased *Trachemys scripta elegans* (20×, H&E), b- Liver of healthy *Trachemys scripta elegans* (20×, H&E), c- Intestinal tract of diseased *Trachemys scripta elegans* (20×, H&E), d- Intestinal tract of healthy *Trachemys scripta elegans* (20×, H&E), e- Stomach of diseased *Trachemys scripta elegans* (20×, H&E), f- Stomach of healthy *Trachemys scripta elegans* (20×, H&E)

Table 2. Susceptibility of strain A1 to antimicrobials

Antimicrobials	Content (µg/disk)	Zone Diameter Breakpoints (mm)			Inhibition Zone Diameter (mm)	Susceptibility
		S	I	R		
Ampicillin (AMP)	10	≥17	14~16	≤13	11	R
Amikacin (AMK)	30	≥17	15~16	≤14	18	S
Piperacillin (PIP)	100	≥21	18~20	≤17	28	S
Cephalexin (CN)	30	≥18	15~17	≤14	11	R
Cefazolin (CZ)	30	≥18	15~17	≤14	6	R
Cefuroxime (CXM)	30	≥18	15~17	≤14	23	S
Cefoperazone (CPZ)	75	≥21	16~20	≤15	30	S
Ceftriaxone (CTR)	30	≥27	25~26	≤25	30	S
Ceftazidime (CAZ)	30	≥18	15~17	≤14	28	S
PenicillinG (PEN)	1	≥21	18~20	≤17	6	R
Gentamicin (GEN)	10	≥15	13~14	≤12	22	S
Kanamycin (KAN)	30	≥18	14~17	≤13	9	R
Streptomycin(S)	10	≥15	12~14	≤11	11	R
Tetracycline (TET)	30	≥19	15~18	≤14	15	I
Minocycline (MI)	30	≥19	15~18	≤14	18	I
Doxycycline (DO)	30	≥16	13~15	≤12	12	R
Polymyxin B (PB)	300	≥12	8~11	≤7	11	I
Vancomycin (VAN)	30	≥13	9~12	≤8	6	R
Lincosamide (LCM)	2	≥31	24~30	≤23	6	R
Erythromycin (E)	15	≥23	14~22	≤13	6	R

S: susceptible; I: intermediately susceptible; R: resistant

muscularis mucosae was slightly thickened, and scattered inflammatory cells were identified within the submucosa and lamina propria.

Antimicrobial Susceptibility of Pathogenic Strain

The antimicrobial susceptibility profile of strain A1 is summarized in Table 2. The strain was susceptible to amikacin, gentamicin, piperacillin, cefuroxime, cefuroxime, cefoperazone, ceftazidime, and ceftriaxone. Conversely, it was resistant to ampicillin, cephalixin, cefazolin, penicillin G, kanamycin, streptomycin, doxycycline, vancomycin, lincosamide, and erythromycin. Intermediate susceptibility was observed for tetracycline, minocycline, and polymyxin B. These results indicate that strain A1 exhibits a multidrug-resistant phenotype, with resistance observed to narrow-spectrum beta-lactams (penicillin G and first-generation cephalosporins) and specific aminoglycosides (kanamycin and streptomycin).

DISCUSSION

This study is the first to identify and confirm *C. braakii* as an emerging pathogen associated with lethal gastroenteritis in *C. flavomarginata*. Notably, we observed and documented several previously unreported clinical signs

-including limb edema, respiratory distress- which provide critical insights into its unique pathogenic presentation in turtles. The findings reveal specific gross lesions, antimicrobial resistance patterns, and characteristic histopathological changes induced by this bacterium. Together with physiological, biochemical, and pathogenicity analyses, this research not only expands the known spectrum of reptilian bacterial pathogens but also establishes a crucial reference for understanding the pathogenic mechanisms of *C. braakii* in *chelonians*. These results offer valuable theoretical and practical guidance for developing targeted disease control strategies for this species.

Our findings indicate that *C. braakii* is a primary causative agent of severe gastroenteritis in turtles. Turtle gastroenteritis, a common reptilian disease, is characterized by well-documented clinical signs and pathological features. In the initial stages, infected turtles typically exhibit lethargy, reduced mobility, and anorexia. Their feces are soft and poorly formed, ranging in color from green to yellow-brown or dark brown. In severe cases, watery diarrhea with a foul odor is observed. Advanced disease is marked by sunken eyes

and abnormal feces, which may be egg-white-like, black, or liver-colored. Terminal stages often involve complete anorexia, leading to death from progressive debilitation. Gross pathological examination revealed a pronounced inflammatory response in the digestive tract. The gastrointestinal mucosa exhibits erosions and ulcerations, often accompanied by excessive mucus production, severe hemorrhage, or petechiae. The lumen may contain a white, clear, or milky gelatinous exudate. The liver frequently exhibits pale yellow lesions, consistent with secondary hepatic involvement^[32-34]. However, limb edema and severe pulmonary emphysema appear to be a novel feature of *C. braakii* infection, distinguishing it from infections caused by common pathogens such as *Salmonella* spp., *Escherichia coli*, or *Aeromonas hydrophila*^[35]. These findings are consistent with a study in night herons (*Nycticorax nycticorax*)^[36], which reported that *C. braakii* infection can cause depression, anorexia, dyskinesia, and diarrhea. Furthermore, this pathogen has been isolated from the liver and intestine of diseased *Procambarus clarkii* and *Andrias davidianus* exhibiting diarrhea and dehydration^[37,38]. The high virulence of *C. braakii* strains from rhesus monkeys (*Macaca mulatta*) was demonstrated in animal models. Collectively, these reports from diverse species corroborate our findings and underscore the significant pathogenic capacity of *C. braakii*. This cross-species pathogenicity underscores its role as an emerging multi-host opportunistic pathogen. The mechanism underlying its gastroenteric effects likely involves the induction of significant inflammation and damage to the gastrointestinal mucosa^[39,40].

Antimicrobial susceptibility testing revealed that *C. braakii* exhibited high resistance to lincosamide and macrolide antibiotics, consistent with findings in red crayfish^[41]. In contrast, its susceptibility to β -lactams, tetracyclines, and aminoglycosides differed from profiles reported elsewhere. Notably, predominant resistance was observed against narrow-spectrum β -lactams, a finding corroborated by Li et al.^[37]. These variations in antimicrobial susceptibility may be attributed to differences in host species, environmental conditions, and selective pressures from the unregulated or excessive use of broad-spectrum antibiotics. Such practices promote the emergence and dissemination of resistant strains. For example, the multidrug resistance gene *cfr* was detected in *C. braakii* isolates from chicken farm environments in Jiangxi, China^[42]. Additionally, the carbapenemase gene *blaKPC-2* and the plasmid-mediated colistin resistance gene *mcr-1* have been identified in this species^[43,44]. The presence of these resistance genes poses serious challenges for clinical management and complicates the control of *C. braakii* infections. Furthermore, *C. braakii* infection often triggers a multi-tissue inflammatory response, leading to clinical

manifestations including anorexia, digestive dysfunction, and diarrhea. In severe cases, the infection can be fatal^[45]. Characteristic histopathological features include gastric mucosal erosion or ulceration, submucosal hemorrhage with inflammatory cell infiltration, and mild to moderate glandular hyperplasia with structural disorganization, congestion, edema, and inflammation. Additional features involve swelling of the intestinal epithelial mucosa with extensive submucosal inflammatory cell infiltration, as well as hepatic erythrocyte accumulation and pigment deposition^[46]. The pathological observations in this study were consistent with these previously described changes. However, we identified additional specific alterations, including polygonal hepatocytes with cytoplasmic vacuolization and cholestasis, fibrotic tissue proliferation in portal areas, disorganized hepatic cord structures, abnormal protrusion of intestinal villi into the lumen, and fibrosis in the gastric lamina propria. These discrepancies may arise from variations in host immune status, bacterial virulence, environmental stressors, and genetic background^[47]. The stomach, intestine, and liver were identified as the primary organs affected by *C. braakii*. This targeting of vital digestive organs likely explains the high mortality rates associated with clinical symptoms such as anorexia and diarrhea^[48].

These findings have direct clinical and managerial implications for aquaculture. In cases where farmed turtles exhibit symptoms including anorexia, lethargy, and digestive disturbances, infection with *C. braakii* should be included as a differential diagnosis. This suspicion is reinforced by necropsy findings such as dull yellow hepatic lesions with white flocculent material, gastrointestinal hemorrhage, necrosis, and the presence of gelatinous exudate. Confirmatory diagnosis should rely on bacteriological isolation followed by 16S rDNA sequencing. Given that the isolated strain exhibited multi-drug resistance to commonly used β -lactams (e.g., ampicillin, penicillin G), aminoglycosides (e.g., kanamycin), and macrolides (e.g., erythromycin), empirical use of these antibiotics should be avoided to prevent treatment failure and the spread of resistance. Instead, alternative strategies such as phage therapy (e.g., phage vB-CbrM-HP1, which has proven effective in reducing *C. braakii* load in fish^[49]) could be considered due to its high specificity and favorable safety profile^[50]. From a management perspective, stringent biosecurity measures are essential. These include optimizing water quality, ensuring feed hygiene, maintaining controlled stocking densities, and implementing regular disinfection of ponds and equipment. Furthermore, quarantine protocols for newly introduced animals are critical to prevent pathogen introduction. Finally, as *C. braakii* is a zoonotic pathogen capable of infecting humans, these

measures are also vital for protecting occupational health and preventing cross-contamination.

However, this study has several limitations. Firstly, the bacterial isolate was derived from a single dominant strain (A1) obtained from a limited sample size (n=1) at one farm, which may not represent the full genetic diversity of *C. braakii* pathogens. Secondly, although justified by ethical considerations and the physiological similarities of the digestive system, the use of a surrogate model (*Trachemys scripta elegans*) for the challenge experiment may not perfectly recapitulate the natural infection process in the primary host, *C. flavomarginata*. Finally, while our work focused on pathogen identification, pathological characterization, and antimicrobial susceptibility testing, the underlying molecular mechanisms -including key virulence factors (e.g., adhesins, toxins) and resistance genes (e.g., AmpC β -lactamases, aminoglycoside-modifying enzymes)- remain uncharacterized. Future studies should expand the sample size to include geographically diverse strains, prioritize challenge experiments in the original host species where feasible, and employ genomic and molecular techniques to comprehensively elucidate the pathogenic and resistant mechanisms of *C. braakii*.

DECLARATIONS

Availability of Data and Materials: The data given in this study may be obtained from the corresponding author (Junzeng XUE) on reasonable request.

Acknowledgements: We sincerely thank all those who contributed to this research and the manuscript submission process. We are also grateful to the reviewers for their valuable comments, which significantly improved the quality of this paper.

Funding Support: This research did not receive any specific grant from funding agencies in the public, commercial, or not-for-profit sectors.

Ethical Approval: All animal experimental procedures in this study strictly adhered to international ethical guidelines for animal experimentation and relevant Chinese regulations. The experimental protocol was reviewed and approved by the Academic Committee of the College of Oceanography and Ecological Science at Shanghai Ocean University and received formal approval from the Shanghai Ocean University Animal Ethics Committee (Approval No. SHOU-DW-2024-300).

Competing Interests: The authors declare that there is no conflict of interest.

Declaration of Generative Artificial Intelligence (AI): The authors declare that the article, tables and figures were not written/created by AI and AI-assisted Technologies.

Author Contributions: MC: Conceptualization, Study Design, Data Curation, Methodology, Formal Analysis, Investigation, Writing - Original Draft. YS: Supervision, Writing - Review and Editing. CL: Supervision, Visualization. NC: Investigation, Supervision. JX: Project Administration, Funding Acquisition, Final Approval.

REFERENCES

- Liao PF, Li L, Liu CT, Ding YJ, Huang QY, Hu YW, Ge CT, Xu JH, Zhang XD: Isolation, identification, biological characteristics, and genomic study of a *Providencia rettgeri* strain. *Acta Hydrobiol Sin*, 48 (12): 2109-2121, 2024. DOI: 10.7541/2024.2024.0085
- Wang H, Duan GQ, Hua XH, Hu YT, Liu AM: Development and characterization of 40 SNP markers of endangered species *Cuora flavomarginata* by whole-genome resequencing. *Conserv Genet Resour*, 16 (4): 273-277, 2024. DOI: 10.1007/s12686-024-01366-2
- Cheng AP, Huang CC, Tsai CF, Chan FC, Zheng YT, Wang CC, Chen HC, Hung KH: Optimization and application of a forensic microsatellite panel for two endangered freshwater turtle species (*Cuora flavomarginata* and *Mauremys mutica*) in Taiwan. *Glob Ecol Conserv*, 58:e03502, 2025. DOI: 10.1016/j.gecco.2025.e03502
- Lin YF, Wu SH, Lin TE, Mao JJ, Chen TH: Population status and distribution of the Endangered yellow-margined box turtle (*Cuora flavomarginata*) in Taiwan. *Oryz*, 44 (4): 581-587, 2010. DOI: 10.1017/S0030605310000797
- Du MZ, Zhao Y, Jia YG: Exploration of the pathogen of infection in the death case of the yellow-margined box turtle. *Chinese J Anim Sci*, 57 (7): 88-91, 2021.
- Musgrave KE, Diehl K, Mans C: *Aeromonas Hydrophila* keratitis in freshwater turtles. *J Exot Pet Med*, 25 (1): 26-29, 2016. DOI: 10.1053/j.jepm.2015.12.003
- Zhao CG, Zhao NX: Occurrence and prevention of gastrointestinal diseases in *Mauremys reevesii*. *Sci Fish Farm*, 1, 65-66, 2018.
- He CW, Song XQ, Tang HY: Isolation and identification of pathogens associated with diarrhea in *Mauremys mutica*. *Chinese Vet Sci*, 8, 56-57, 2003. DOI: 10.16656/j.issn.1673-4696.2003.08.017
- Poppi L, Zaccaroni A, Pasotto D, Dotto G, Marcer F, Scaravelli D, Mazzariol S: Post-mortem investigations on a leatherback turtle *Dermochelys coriacea* stranded along the Northern Adriatic coastline. *Dis Aquat Organ*, 100 (1): 71-76, 2012. DOI: 10.3354/dao02479
- Weese JS, Staempfli HR: Diarrhea associated with enterotoxigenic *Clostridium perfringens* in a red-footed turtle (*Geochelone carbonaria*). *J Zoo Wildl Med*, 31 (2): 265-266, 2000. DOI: 10.1638/1042-7260(2000)031[0265:DAWECP]2.0.CO;2
- Zhang SY, Zheng RZ, Ai TS, Yu YZ, Zhang LQ, Zhou WD, Deng P, Ding GZ: Isolation, identification and antimicrobial susceptibility test of *C. braakii* from *Procambarus clarkii*. *Jiangsu Agric Sci*, 46 (12): 129-131, 2018.
- Wang JZ, Geng XY, Zhu SX, Dong WL, Jia XY, Shan XF, Gao YF: Isolation, identification and drug susceptibility test of *C. braakii* from *Mylopharyngodon piceus*. *Chinese Vet Sci*, 46 (5): 602-606, 2016.
- Chen XY, Zheng QZ, Song TT, Zheng SJ, Zheng RQ: Pathogen identification and antimicrobial susceptibility testing of cataracts in spiny frogs (*Quasipaa spinosa*). *J Zhejiang Agric Sci*, 57 (7): 1141-1143+1151, 2016.
- Altun S, Duman M, Buyukekiz AG, Ozyigit MO, Karatas S, Turgay E: Isolation of *C. braakii* from rainbow trout (*Oncorhynchus mykiss*). *Isr J Aquac Bamiageh*, 65:1, 2013.
- Nawaz M, Khan AA, Khan S, Sung K, Steele R: Isolation and characterization of tetracycline-resistant *Citrobacter* spp. from catfish. *Food Microbiol*, 25 (1): 85-91, 2008. DOI: 10.1016/j.fm.2007.07.008
- Jatobá A, Silva BC, Vieira FD, Mouriño JLP, Seiffert WQ: Isolation and characterization of hemolytic bacteria Fish disc and Neon Rainbow. *Semin Cienc Agrar*, 33 (2): 763-768, 2012. DOI: 10.5433/1679-0359.2012v33n2p763
- Mocerino R, Jolly J, Awerbuch E: *C. braakii* bacteremia of unclear source: A literature review and discussion. *Am J Respir Crit Care Med*, 197:A5298, 2018. DOI: 10.1164/ajrccm-conference.2018.197.1
- Pasquali F, Crippa C, Lucchi A, Francati S, Dindo ML, Manfreda G: *C. braakii* isolated from salami and soft cheese: An emerging food safety hazard. *Foods*, 14 (11):1887, 2025. DOI: 10.3390/foods14111887
- Vega-Manriquez DX, Davila-Arellano RP, Eslava-Campos CA, Salazar Jimenez E, Negrete-Philippe AC, Raigoza-Figueras R, Muñoz-Tenería FA: Identification of bacteria present in ulcerative stomatitis lesions

- of captive sea turtles (*Chelonia mydas*). *Vet Res Commun*, 42, 251-254, 2018. DOI: 10.1007/s11259-018-9728-y
20. Nowakiewicz A, Ziolkowska G, Zięba P, Dziedzic BM, Gnat S, Wójcik M, Dziedzic R, Kostruba A: Aerobic bacterial microbiota isolated from the cloaca of the European pond turtle (*Emys orbicularis*) in Poland. *J Wildl Dis*, 51 (1): 255-229, 2015. DOI: 10.7589/2013-07-157
 21. Hu SF, Yu GY, Li R, Xia XZ, Xiao XL, Li XF: Real-time TaqMan PCR for rapid detection and quantification of *Coliforms* in chilled meat. *Food Anal*, 9, 813-822, 2016. DOI: 10.1007/s12161-015-0271-y
 22. Wang GH, Clark CG, Liu CY, Pucknell C, Munro CK, Kruk T, Caldeira R, Woodward DL, Rodgers FG: Detection and characterization of the hemolysin genes in *Aeromonas hydrophila* and *Aeromonas sobria* by multiplex PCR. *J Clin Microbiol*, 41 (3): 1048-1054, 2003. DOI: 10.1128/jcm.41.3.1048-1054.2003
 23. Chen M, Qin Y, Lin YH, Ren SQ, Ye JZ, Zheng SJ: Genetic diversity analysis of *Cuora flavomarginata* based on COI genes in Zhejiang province. *Chinese J Wildl*, 45 (2): 367-377, 2024. DOI: 10.12375/ysdwxb.20240216
 24. Guo SL, Shao P: Breeding methods and tips for pet *Trachemys scripta elegans*. *Agric Technol*, 44 (21): 101-105, 2024. DOI: 10.19754/j.nyyjs.20241115021
 25. Zhao HX, Huang B: Anatomy of the digestive system and respiratory system of the yellow-margin box turtle. *Sichuan J Zool*, 29 (1): 59-62, 2010.
 26. Pedram S, Zehabvar O, Rostami A, Akbarein H, Zand S, Rezvani Y, Mahdi SM, Mollaei Z: Laparoscopic anatomy of the coelomic cavity organs in female red-eared slider (*Trachemys scripta elegans*). *Vet Med Int*, 2025:4041679, 2025. DOI: 10.1155/vmi/4041679
 27. Miyai N, Kozono T, Kuriki T, Todoroki M, Murakami T, Shinohara K, Yoshida T, Kigata T: Macro- and microscopic anatomy of the digestive tract in the red-eared slider (Emyidae: *Trachemys scripta elegans*). *PlosOne*, 19 (12): e0315737, 2024. DOI: 10.1371/journal.pone.0315737
 28. Wu CY, Ren SY: A brief analysis of the diagnosis, treatment, and prevention of respiratory disease in *Trachemys scripta elegans*. *Chinese J Anim Husb Vet Med*, 2023:3, 2023.
 29. Ye MH, Hu XC, Lv AJ, Sun JF, Liu XX, Song YJ: Isolation and identification of pathogens causing eye disease in *Trachemys scripta elegans* and histopathological study. *J Dalian Ocean Univ*, 2018:5, 2018.
 30. Bai J, Zhou MH, Hu XC, LV AJ, Ye MH, Sun JF: Isolation and identification of *Citrobacter freundii* and susceptibility characteristics of *Citrobacter freundii*. *J Dalian Ocean Univ*, 2029:6, 2019.
 31. CLSI (Clinical and Laboratory Standards Institute): Performance standards for antimicrobial susceptibility testing (34th ed.), Informational Supplement M100-ED34. Clinical and Laboratory Standards Institute, Wayne, PA, 2024.
 32. Chen QM: Studies on pathological conditions in hatchling and juvenile yellow pond turtles (*Mauremys mutica*) under aquaculture conditions. *Agric Technol*, 34 (10): 188, 2014.
 33. Liu YN, Zhang YS, Pan LD, Xu PP, Zheng JR: The sea turtle conservation and research progress of the disease. *J Aquac*, 36 (1): 35-40, 2015.
 34. Martinson SA, Greenwood SJ, Wadowska D, Martin K: Histopathological, ultrastructural and molecular phylogenetic analysis of a novel microsporidium in a loggerhead sea turtle (*Caretta caretta*). *Dis Aquat Org*, 129 (1): 31-39, 2018. DOI: 10.3354/dao03234
 35. Pasmans F, De Herdt P, Dewulf J, Haesebrouck F: Pathogenesis of infections with *Salmonella enterica subsp. enterica* serovar Muenchen in the turtle *Trachemys scripta scripta*. *Vet Microbiol*, 87 (4): 315-325, 2002. DOI: 10.1016/S0378-1135(02)00081-0
 36. Li Y, Hu QX, Li C, Qing B, Duan WB, Niu KS, Lv N, Zhang YJ, Guo RH, Wang XL: Isolation, identification and drug resistance analysis of *C. braakii* from night heron. *Anim Husb Vet Med*, 55 (7): 53-57, 2023.
 37. Zhu RL, Yang CQ, Jiang SD, Shen JJ, Zhang XH, Bao CH, Tang SS: Isolation, identification and antibiotic sensitivity analysis of *Citrobacter braakii* from *Procambarus clarkii*. *J Anhui Agric Univ*, 45 (4): 617-620, 2018.
 38. Zhu YM, Zhu HY, Wang YP, Feng XD, Zhao ZL, Liu J, Luo ZL, Liu X, Yang XW, Zhao GW: Pathogenic analysis and histopathological observation of multiple bacterial infections in cultured Chinese giant salamander (*Andrias davidianus*). *Chinese J Vet Sci*, 43 (6): 1304-1309, 2023. DOI: 10.16303/j.cnki.1005-4545.2023.06.28
 39. Wei Y: The effect and mechanism of gastric derived *C. braakii* induced inflammatory response in gastric epithelial cells. *MSc Thesis*, Qingdao University, 2024.
 40. Yu MC, Xie FY, Xu CZ, Yu T, Wang YX, Liang SZ, Dong QJ, Wang LL: Characterization of cytotoxic *C. braakii* isolated from human stomach. *Febs Open Bio*, 14 (3): 487-497, 2024. DOI: 10.1002/2211-5463.13770
 41. Huang YM, Li CL, Qin SJ, Lu W, Zhang BZ, Sun JY, Zhang WQ, Tong T, Zhang Q: Isolation, identification and drug resistance analysis of *C. braakii* from *Cherax quadricarinatus*. *Chinese J Vet Med*, 60 (1): 59-65, 2024.
 42. Feng YM, Ding PY, Shen JX, Xu YK, Zheng MX, Pan YS, Yuan L, Hu GZ, He DD: Detection of cfr in *C. braakii* and the characterization of two cfr-carrying plasmids from a chicken farm. *J Antimicrob Chemother*, 79 (8): 2071-2074, 2024. DOI: 10.1093/jac/dkac152
 43. Dong DD, Mi ZQ, Li DJ, Gao MM, Jia N, Li ML, Tong YG, Zhang XL, Zhu YQ: Novel IncR/IncP6 hybrid plasmid pCRE3-KPC recovered from a clinical KPC-2-producing *C. braakii* isolate. *mSphere*, 5 (2): e00891-19, 2025. DOI: 10.1128/mSphere.00891-19
 44. Liu JX, Yang YX, Li YX, Liu D, Tuo HM, Wang HN, Call DR, Davis M, Zhang A: Isolation of an IncP-1 plasmid harbouring mcr-1 from a chicken isolate of *C. braakii* in China. *Int J Antimicrob Agents*, 51 (6): 936-940, 2018. DOI: 10.1016/j.ijantimicag.2017.12.030.
 45. Pan LF, Yang YH, Peng YN, Li DJ, Khan TA, Chen P, Yan L, Hu SB, Ding XZ, Sun YJ, Xia LQ, Yi GF: The novel pathogenic *Citrobacter freundii* (CFC202) isolated from diseased crucian carp (*Carassius auratus*) and its ghost vaccine as a new prophylactic strategy against infection. *Aquaculture*, 533:736190, 2021. DOI: 10.1016/j.aquaculture.2020.736190
 46. Sharma PC, McCandless M, Sontakke SP, Varshney N, Brodell RT, Kyle PB, Daley W: Navigating viral gastroenteritis: Epidemiological trends, pathogen analysis, and histopathological findings. *Cureus*, 16 (5): e61197, 2024. DOI: 10.7759/cureus.61197
 47. Abreu REF, Magalhaes TC, Souza RC, Oliveira STL, Ibelli AMG, Demarqui FN, Gouveia JJS, Costa MM, Gouveia GV: Environmental factors on virulence of *Aeromonas hydrophila*. *Aquacult Int*, 26 (2): 495-507, 2018. DOI: 10.1007/s10499-017-0230-2
 48. Luo FL, Niu YC, Hu XC, Lv AJ, Ye MH, Sun JF: Clinical signs and histochemical observation of *Citrobacter freundii* disease in turtle (*Trachemys scripta elegans*). *J Tianjin Agric Univ*, 27 (2): 44-47, 2020. DOI: 10.19640/j.cnki.jtau.2020.02.010
 49. Huang CZ, Feng C, Liu X, Zhao RH, Wang ZJ, Xi HY, Ou HD, Han WY, Guo ZM, Gu JM, Zhang L: The bacteriophage vB-CbrM-HP1 protects Crucian carp against *C. braakii* infection. *Front Vet Sci*, 9:888561, 2022. DOI: 10.3389/fvets.2022.888561
 50. Lin DM, Koskella B, Lin HC: Phage therapy: An alternative to antibiotics in the age of multi-drug resistance. *World J Gastrointest Pharmacol Ther*, 8 (3): 162-173, 2017. DOI: 10.4292/wjgpt.v8.i3.162

RESEARCH ARTICLE

Evaluation of Microbiological Properties in Kefir Production with Fuzzy Logic-Based Decision Support System

Aslı AKILLI ^{1(*)}  Gizem KEZER ²  Ertuğrul KUL ³ 

¹ Department of Agricultural Economics, Faculty of Agriculture, Kırşehir Ahi Evran University, TR-40100 Kırşehir - TÜRKİYE

² Department of Agricultural Biotechnology, Faculty of Agriculture, Kırşehir Ahi Evran University, TR-40100 Kırşehir - TÜRKİYE

³ Department of Animal Science, Faculty of Agriculture, Kırşehir Ahi Evran University, TR-40100 Kırşehir - TÜRKİYE



(*) Corresponding author:

Aslı AKILLI
Phone: +90 386 280 4840
Cellular phone: +90 530 942 1421
Fax: +90 386 280 4677
E-mail: asliakilli@ahievran.edu.tr

How to cite this article?

Akıllı A, Kezer G, Kul E: Evaluation of microbiological properties in kefir production with fuzzy logic-based decision support system. *Kafkas Univ Vet Fak Derg*, 31 (5): 679-688, 2025.

DOI: 10.9775/kvfd.2025.34643

Article ID: KVFD-2025-34643

Received: 04.06.2025

Accepted: 09.09.2025

Published Online: 15.09.2025

Abstract

Parallel to rising consumer interest in functional foods, attention to probiotic and natural-content products such as kefir has significantly expanded in recent years. As in all instruments related to food production, the aim in the kefir production process is to obtain a high-quality product, and to ensure the sustainability of production in a healthy manner. In this study, the aim is to develop a fuzzy logic-based decision support system for the quality evaluation of kefir samples categorized into somatic cell and fat (low/high) measurement groups. For this purpose, the system inputs were determined as incubation temperature, incubation time, storage time, total bacterial count, and pH. In the model output, kefir quality indices were calculated for each observation, and quality classes were obtained. In the comparative quality evaluations between the system and expert decisions, the fuzzy logic-based decision support system was found to have achieved a success rate of 93.75%. In addition, the Chi-square statistic ($\chi^2 = 110.667$) and Kappa statistic ($Kappa = 0.901, s_x = 0.048$) regarding the decisions made by both the expert and the system were found to be statistically significant ($P < 0.05$). The results indicate that fuzzy logic can be effectively used as a decision support tool in the quality evaluation of kefir samples.

Keywords: Classification, Decision support system, Fuzzy logic, Kefir, Quality

INTRODUCTION

Kefir, a fermented milk beverage of Caucasian origin, has been gaining increasing importance in the food industry owing to its rich composition of probiotic microorganisms and its potential health benefits. It is known that various parameters are effective in the evaluation of kefir quality ^[1]. To obtain a high-quality kefir, the fermentation process must be carried out under optimal conditions, while maintaining the balance and diversity of microorganisms working in symbiosis ^[2].

In line with current technological advancements, literature show that in addition to classical methods, the use of artificial intelligence-based approaches in the quality evaluation of food products through various microbiological and physicochemical parameters has been increasingly adopted. The sole use of either subjective or objective methods in food quality evaluations may prove insufficient, particularly under conditions of uncertainty. In addition to measurable physical parameters, the

integration of linguistic data based on expert opinion into the decision-making process provides a contribution to quality assessment procedures ^[3,4]. At this point, the fuzzy logic approach, which contributes to the processing of both quantitative and qualitative data, is regarded as an effective and powerful tool for dealing with uncertainty in measurements and the lack of precision in expert evaluations ^[5].

Scientific studies employing fuzzy logic-based methods in food quality assessment have demonstrated that it is possible to integrate numerical measurements and expert judgments within a common decision-making framework under conditions characterized by uncertainty and measurement errors. In the dairy industry, microbiological test outputs obtained from bulk tank milk have been transformed into linguistic variables through membership functions, and compound indicators related to milking practices and herd quality have been derived by means of inference using rule bases (e.g., Mamdani or Takagi-Sugeno-Kang) ^[6]. In sensory evaluation, panel scores have



been integrated through fuzzification and rule-based/TSK modeling, allowing overall acceptability and product rankings to be calculated more consistently; this approach has been successfully applied to pistachio shell marmalade, various tea samples, and breads enriched with apple pomace [7-9]. In the context of packaging and storage, multi-criteria inputs such as modified atmospheric conditions, storage duration, and sensory descriptors have been synthesized within a fuzzy inference engine to perform suitability evaluations for various fruits [10]. In industrial quality control, product attributes that could not be precisely defined by sharp boundaries have been represented through knowledge-based fuzzy systems, enabling robust decision-making even in the absence of strict thresholds [11]. Furthermore, by means of hybrid designs that consider both subjective and objective criteria, the effects of different oil types and frying methods on the quality of potato slices have been evaluated through the integration of textual/sensory data and instrumental measurements within the same inference structure; similarly, the expression of expert cupping criteria for specialty coffee beans in fuzzy sets has provided consistent quality ratings [12,13].

The approaches and applied studies reported in the literature provide both a theoretical and practical foundation for the development of a fuzzy decision support system capable of performing holistic classification under uncertainty, specifically in the context of kefir. In the present study, measurable physical and microbiological indicators were integrated with expert opinions within a single inference architecture, and the suitability of the developed fuzzy logic-based system for reliably and consistently classifying kefir quality under uncertain conditions was examined. The hypothesis was tested that the classifications of the proposed fuzzy logic-based system after defuzzification would exhibit a statistically significant degree of agreement with expert evaluations. This study aimed to develop a fuzzy

logic-based decision support system to evaluate the quality of kefir samples produced from raw milk with varying somatic cell counts and fat content. The analyses conducted within the scope of this research were structured into two main phases. Throughout the study, a methodological workflow was employed that integrated both experimental procedures and fuzzy logic modeling, ensuring a systematic and comprehensive approach to quality assessment. This article is organized into four main sections following the introduction. In the second section, the materials and methods of the research are explained in detail; the data collection process, the design of the fuzzy system, and the technical details related to fuzzy rules are presented. The third section includes the application findings and results of the developed system. In the fourth section, the aforementioned results are discussed in comparison with expert evaluations, and the performance and limitations of the system are assessed.

MATERIAL AND METHODS

Ethical Statement

As no procedures were carried out on animals in this study, approval from the Local Ethics Committee for Animal Experiments was not required.

Study Design

Milk samples used in kefir production were obtained from a private dairy farm in Kırşehir province. Within the scope of the research, analyses related to the determination of milk components and somatic cell counts were conducted in the laboratories of the Department of Animal Science, Faculty of Agriculture, Kırşehir Ahi Evran University. Kefir production and microbiological analyses of the kefir samples were carried out in the Agricultural Biotechnology laboratories of the same faculty.

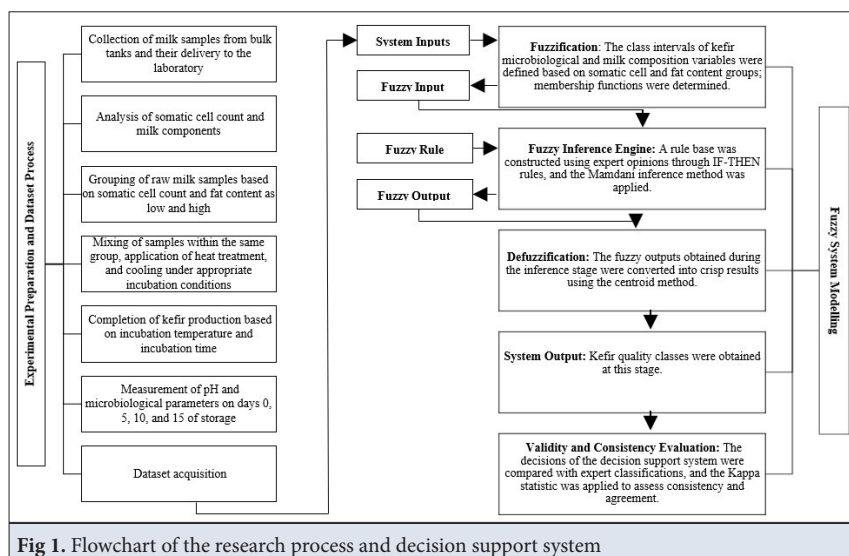


Fig 1. Flowchart of the research process and decision support system

The analyses conducted within the scope of this study were structured in two main phases. The methodological workflow applied throughout the research, including both experimental procedures and fuzzy logic modeling, is presented in [Fig. 1](#). During the first phase, milk samples were obtained and transferred to the laboratory under strictly controlled hygienic conditions. Subsequently, analyses pertaining to milk components and somatic cell counts were performed, alongside microbiological examinations of the kefir samples. In the second phase, applications related to fuzzy system modeling were carried out, and the design of the decision support system was optimized to enhance analytical robustness.

In the operational process of the fuzzy logic-based decision support system, milk samples were initially classified into two groups, low and high, based on somatic cell count and milk fat content. In the subsequent stage, the milk samples within each group were separately coded and converted into kefir in accordance with the procedures outlined in the methodology section. The measurement values related to the input variables were obtained through chemical and microbiological analyses. In the functioning of the fuzzy system, five input variables were considered, particularly for the formulation of “if-then” rules to ensure successful application. During the process of converting the input variables representing the kefir samples into fuzzy numbers, class boundaries were established based on the Turkish Codex on Raw Milk and Heat-Treated Drinking Milk (Communiqué No: 2019/12), expert opinions, and a detailed literature review. The data were restructured through rule base connections created in accordance with fuzzy logic terminology and the architecture of the decision support system. In this way, a fuzzy system was developed by using the microbiological characteristics of the kefir samples included in the dataset. The system inputs were defined as “Incubation Time,” “Incubation Temperature,” “Storage Time,” “pH,” and “Total Aerobic Mesophilic Bacteria Count (TBC).” The system output was designated as “Kefir Quality Class.”

Milk Sample Collection

Prior to sampling, milk in the bulk tanks was stirred to ensure homogeneity. Following this process, 1000 mL of milk was transferred into sterile tubes without the addition of any preservatives. Adhesive labels indicating the farm identification number and the sampling date were applied to each tube. The collected milk samples were placed between ice packs under hygienic conditions and transported in sealed containers to the laboratory of the Department of Animal Science, Faculty of Agriculture, Kırşehir Ahi Evran University. Upon arrival, the samples were stored at approximately +4°C, and all analyses were completed within five hours.

Milk Composition and Somatic Cell Count (SCC) Analyses

Within the scope of milk composition analysis, fat and solids-not-fat (SNF) contents were determined using a Funke Gerber LactoStar (3510) milk analyzer, which is located in the laboratory of the Department of Animal Science, Faculty of Agriculture, Kırşehir Ahi Evran University. For the determination of somatic cell count (SCC), milk samples were analyzed using a DeLaval brand cell counter in the same laboratory. Based on the results obtained, milk samples were classified into four groups according to somatic cell count (low/high) and fat content (low/high). The microbiological and chemical quality parameters of raw milk, as specified in the Turkish Food Codex Communiqué on Raw Milk and Heat-Treated Drinking Milk (Communiqué No: 2019/12), were used as a reference during the grouping of milk samples. The values used in the grouping stage are given in [Table 1](#) ^[14].

Table 1. Class limits for somatic cell count and fat measurements

Class Limits	Low	High
Somatic Cell Count (SCC) (cells/mL)	$x < 400.000$	$x \geq 400.000$
Fat (%)	$x < 3.5$	≥ 3.5

Kefir Production and Microbiological Analyses

Milk samples, previously grouped according to SCC and fat content levels (low/high), were homogenized within each group and subjected to heat treatment at 95°C for 3 min. After heat treatment, the milk samples were cooled to 25 degrees Celsius to be used for kefir production. Kefir production was carried out according to the traditional method, and each group was inoculated with 3% kefir grains. In accordance with the experimental design, two incubation temperatures “24°C and 28°C” were applied. For each temperature condition, two different incubation durations were implemented: the first group was incubated for 19 h, and the second group for 23 h. As a result of this grouping procedure, a total of 16 distinct kefir samples were obtained. PH values and total bacterial counts were measured on days 0, 5, 10, and 15 of storage. The enumeration of total aerobic mesophilic bacteria was performed using the pour plate method on Plate Count Agar (PCA; Darmstadt, Germany), followed by incubation at 30°C for 48 h. Colony-forming units were then counted ^[15]. pH measurements were conducted using a digital pH meter (Hanna HI 2211c pH/ORP Meter) with a sensitivity of 0.01 units ^[16].

Fuzzy Logic Based Decision Support System

The operation of fuzzy systems is based on interval mathematics and fuzzy logic, utilizing linguistic variables derived from membership functions as inputs in the

decision-making process^[17]. These input variables are matched through the antecedents of linguistic IF-THEN rules. The output of each rule is then converted into a numerical value by applying a defuzzification method based on the membership degrees of the relevant variables. The fuzzy inference system refers to the process of systematically mapping a comprehensive set of linguistic variables into output values through a rule-based framework. *Fig. 1* illustrates the operational structure of the fuzzy inference system. As shown in the diagram, the system architecture comprises four fundamental components: fuzzification, the fuzzy inference engine, the fuzzy rule base, and defuzzification.

In the fuzzification phase, converting crisp variables representing the quality evaluation of kefir samples into fuzzy inputs is carried out. During this process, the shape of the membership functions for the input variables, their positions on the x-axis, and the number of subsets is determined. By assigning a membership function ranging between 0 and 1 to each input variable, the transformation into linguistic variables is achieved^[18]. A membership function essentially consists of five conceptual components: the core (elements with a membership degree of 1), the support (elements with membership degrees greater than 0), the boundary regions (elements with membership degrees between 0 and 1 surrounding the core), the crossover point (elements with a membership degree of 0.5), and the height (the maximum membership degree attained by any element of the set). In this study, triangular, trapezoidal, and S-shaped functions were used by considering the structure of the input variables and the variation in quality class intervals. The triangular membership function is represented by three parameters: the interval between parameters a and c constitutes the support, and parameter b represents the core of the

membership function^[17]. Its mathematical representation is given in Equation 1.

$$\mu_A(x; a, b, c) = \begin{cases} a \leq x \leq b, & (x-a)/(b-a) \\ b \leq x \leq c, & (c-x)/(c-b) \\ x > c \text{ or } x < a, & 0 \end{cases} \quad [1]$$

The trapezoidal membership function is expressed by the function given in Equation 2, where the intervals between parameters $a-b$ and $c-d$ define the boundaries of the function, whereas the interval between parameters $b-c$ constitutes the core of the function^[19].

$$\mu_A(x; a, b, c, d) = \begin{cases} a \leq x \leq b, & (x-a)/(b-a) \\ b \leq x \leq c, & 1 \\ c \leq x \leq d, & (d-x)/(d-c) \\ x > d \text{ and } x < a, & 0 \end{cases} \quad [2]$$

The S-shaped membership function is represented by the mathematical expression given in Equation 3 for an increasing trend and in Equation 4 for a decreasing trend, through the parameters a_1 , a_2 , and a_3 ^[19].

$$\mu_A(x; a_1, a_2, a_3) = \begin{cases} -\infty < x < a_1 & 0 \\ a_1 \leq x \leq a_2 & 2[(x-a_1)/(a_3-a_1)]^2 \\ [(a_2 < x \leq a_3)] & 1 - 2[(x-a_2)/(a_3-a_1)]^2 \\ a_3 < x < +\infty & 1 \end{cases} \quad [3]$$

$$\mu_A(x; a_1, a_2, a_3) = \begin{cases} -\infty < x < a_1 & 1 \\ a_1 \leq x \leq a_2 & 1 - 2[(x-a_1)/(a_3-a_1)]^2 \\ (a_2 < x \leq a_3) & 2[(x-a_2)/(a_3-a_1)]^2 \\ a_3 < x < +\infty & 0 \end{cases} \quad [4]$$

In the inference phase, fuzzy information is expressed through IF-THEN rules using the logical connectors AND and OR. The process of deriving new information from the knowledge stored in the system's knowledge base is referred to as inference. In this process, the fuzzy sets in the knowledge base and the input and output variables in the model are defined, and the decision-making logic operates in conjunction. The rules were prepared based on expert knowledge and a detailed literature review, taking into account the number of subsets of the input

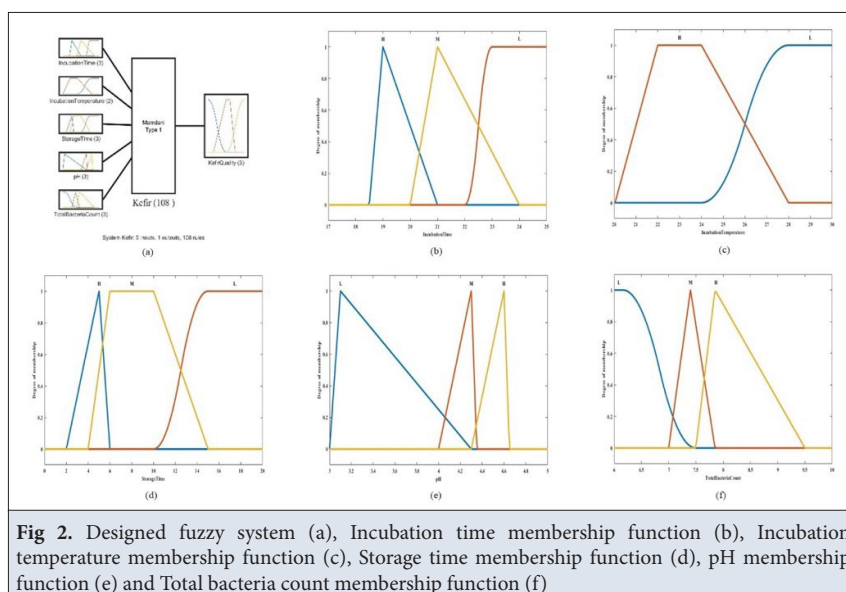


Fig 2. Designed fuzzy system (a), Incubation time membership function (b), Incubation temperature membership function (c), Storage time membership function (d), pH membership function (e) and Total bacteria count membership function (f)

variables. In this study, the ‘Mamdani’ inference method was used [20,21]. The rule structures of the Mamdani method are presented in Equation 5, where X_1 and X_2 represent input variables, and Z_1 and Z_2 represent output variables. A_1, B_1, A_2 , and B_2 denote membership functions, while C_1 and C_2 indicate the fuzzy result sets at the end of each rule [22].

$$\text{If } X_1 = A_1 \text{ and } X_2 = B_1 \text{ then } Z_1 = C_1 \quad [5]$$

$$\text{If } X_1 = A_2 \text{ or } X_2 = B_2 \text{ then } Z_2 = C_2$$

In the defuzzification phase, converting the fuzzy information obtained during the inference phase into precise output values is carried out. In this study, the ‘Centroid’ defuzzification method was used [23]. The mathematical representation of the Centroid method is provided in Equation 6, where y_i represents the defined output variable, $\mu_c(y_i)$ represents the membership degree of the output variable, and y represents the defuzzified value.

$$y^* = \frac{\sum_{i=1}^n y_i \mu_c(y_i)}{\sum_{i=1}^n \mu_c(y_i)} \quad [6]$$

In the output of the system designed within the scope of the study, kefir quality indices were calculated for each observation, and quality classes were obtained. The applications related to the fuzzy logic-based decision support system were carried out in the R2024b (Matrix Laboratory) environment. The quality classes of the kefir samples were also obtained through expert opinion provided by a subject-matter specialist. The quality evaluations of the fuzzy logic-based decision support system and those of the expert were compared. In addition, Kappa statistics and agreement test results were included to assess the consistency of the decisions.

RESULTS

In the design of the fuzzy system, the class intervals defined for the input variables are presented in Table 2. In this context, the classes were designed to be overlapping, in other words, to allow for partial intersection. According to the information provided in the table, in order to obtain high-quality kefir, the incubation time should be 19 h, and the incubation temperature must be maintained between 22-24°C. One of the significant indicators of high-quality kefir is the pH measurement, which is expected to be around 4.6. In the kefir production process, a total aerobic mesophilic bacteria count of 7.85 or a value close to it indicates that the kefir quality is high. Increases in the amount of total aerobic mesophilic bacteria within acceptable limits are interpreted as an indication that the kefir production has been carried out in a healthy manner and that the beneficial microorganisms within the structure of the kefir are functioning properly.

In the Matlab environment, to perform the fuzzification process, which is the first step of the fuzzy system design within the ‘fuzzy logic designer’, the membership functions of the selected parameters were defined. Additionally, the quality classes and class intervals were established based on the information presented in Table 2. The general structure of the fuzzy logic-based decision support system designed within the scope of this study is presented in Fig. 2-a. As can be seen in the toolbox, the system consists of five input variables and one output variable.

In the scope of this study, the membership functions of the input variables, are presented as follows: Incubation

Table 2. Quality class ranges of input variables

Class	Incubation Time (Hour)	Incubation Temperature (°C)	Storage Time (Days)	pH	Total Aerobic Mesophilic Bacteria Count (cfu/mL)
Low	$x \geq 22$	$x < 22$ or $24 > x$	$10 > x$	$3 < x < 4.3$	$x < 7.5$
Medium	$20 < x < 24$.	$6 < x < 10$	$4 < x < 4.35$	$7 < x < 7.85$
High	$18.5 < x < 21$	$22 < x < 24$	$2 < x < 6$	$4.3 < x < 4.65$	$7.85 \leq x \leq 9.5$

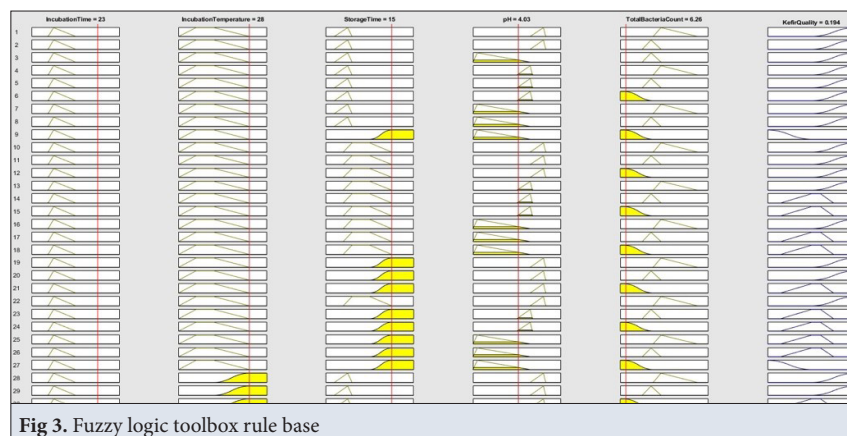


Fig 3. Fuzzy logic toolbox rule base

Table 3. Fuzzy rules

Rule No		Input 1	Class		Input 2	Class		Input 3	Class		Input 4	Class		Input 5	Class		Kefir Quality
1	If	IncTime	H	AND	Inc.Temp.	H	AND	Stor. Time	H	AND	pH	H	AND	TBC	H	THEN	H
4	If	IncTime	H	AND	Inc.Temp.	H	AND	Stor. Time	H	AND	pH	M	AND	TBC	H	THEN	H
5	If	IncTime	H	AND	Inc.Temp.	H	AND	Stor. Time	H	AND	pH	M	AND	TBC	M	THEN	H
14	If	IncTime	H	AND	Inc.Temp.	H	AND	Stor. Time	M	AND	pH	M	AND	TBC	M	THEN	M
15	If	IncTime	H	AND	Inc.Temp.	H	AND	Stor. Time	M	AND	pH	M	AND	TBC	L	THEN	M
18	If	IncTime	H	AND	Inc.Temp.	H	AND	Stor. Time	M	AND	pH	L	AND	TBC	L	THEN	M
19	If	IncTime	H	AND	Inc.Temp.	H	AND	Stor. Time	L	AND	pH	H	AND	TBC	H	THEN	H
27	If	IncTime	H	AND	Inc.Temp.	H	AND	Stor. Time	L	AND	pH	L	AND	TBC	L	THEN	L
28	If	IncTime	H	AND	Inc.Temp.	L	AND	Stor. Time	H	AND	pH	H	AND	TBC	H	THEN	H
29	If	IncTime	H	AND	Inc.Temp.	L	AND	Stor. Time	H	AND	pH	H	AND	TBC	O	THEN	H
83	If	IncTime	L	AND	Inc.Temp.	L	AND	Stor. Time	H	AND	pH	H	AND	TBC	O	THEN	M
84	If	IncTime	L	AND	Inc.Temp.	L	AND	Stor. Time	H	AND	pH	H	AND	TBC	L	THEN	M
85	If	IncTime	L	AND	Inc.Temp.	L	AND	Stor. Time	H	AND	pH	M	AND	TBC	H	THEN	M
86	If	IncTime	L	AND	Inc.Temp.	L	AND	Stor. Time	H	AND	pH	M	AND	TBC	M	THEN	M
87	If	IncTime	L	AND	Inc.Temp.	L	AND	Stor. Time	H	AND	pH	M	AND	TBC	L	THEN	L
98	If	IncTime	L	AND	Inc.Temp.	L	AND	Stor. Time	M	AND	pH	L	AND	TBC	M	THEN	L
99	If	IncTime	L	AND	Inc.Temp.	L	AND	Stor. Time	M	AND	pH	L	AND	TBC	L	THEN	L
100	If	IncTime	L	AND	Inc.Temp.	L	AND	Stor. Time	L	AND	pH	H	AND	TBC	H	THEN	H
104	If	IncTime	L	AND	Inc.Temp.	L	AND	Stor. Time	L	AND	pH	M	AND	TBC	M	THEN	L
105	If	IncTime	L	AND	Inc.Temp.	L	AND	Stor. Time	L	AND	pH	M	AND	TBC	L	THEN	L
107	If	IncTime	L	AND	Inc.Temp.	L	AND	Stor. Time	L	AND	pH	L	AND	TBC	M	THEN	L
108	If	IncTime	L	AND	Inc.Temp.	L	AND	Stor. Time	L	AND	pH	L	AND	TBC	L	THEN	L

time in *Fig. 2-b*, incubation temperature in *Fig. 2-c*, storage time in *Fig. 2-d*, pH in *Fig. 2-e*, and total bacterial count in *Fig. 2-f*. The selection of membership functions was carried out by considering the variation and structural characteristics of the input variables. For instance, when the incubation time exceeds 23 h, declines in kefir quality and structural deficiencies are encountered. Therefore, the S-shaped membership function was preferred. However, for the classes defined as high and medium, the boundaries related to the incubation time could, using triangular membership functions, be represented, thereby enabling the transformation into fuzzy numbers. Similar interpretations are valid for incubation temperature and storage time. When evaluating the membership function of another input variable, pH, it was determined that the fuzzification of the continuous data obtained using triangular membership functions led to better system performance than other methods. Considering the conditions under which kefir bacteria are cultivated, S, and triangular membership functions were used to represent the total bacterial count variable based on the variation in the data structure. In the inference stage, a rule base was created for the representation of knowledge. A section of the rule table created for the input variables used is presented in *Table 3*. According to the fuzzy

system structure, 108 “if-then” rules were formulated. The number of rules was obtained by the multiplication of the number of membership functions for each of the input variables. However, depending on the nature of the research, changes in the number of rules may occur in some cases. Here, “H” indicates high, “L” indicates low, and “M” indicates medium. The application of the rules indicates the decision’s quality.

In *Fig. 3*, the general view of the fuzzy rules created with the help of the ‘rule viewer’ in the fuzzy logic toolbox of the Matlab Program is presented. The views in the first five columns represent the input variables, while the views in the rightmost column represent the kefir quality classes. As can be seen in *Fig. 3*, when the incubation time of the kefir sample is 23 h; the incubation temperature is 28°C; the storage period is 15 days; the pH value is 4.03; and the total bacterial count is 6.26 cfu/mL, the output value obtained using the defuzzification method is 0.194. The quality class decision of the fuzzy system for the kefir sample is interpreted as “low.” When the figures were evaluated by an expert, it was confirmed that the fuzzy system produced realistic and accurate decisions.

As a result of the analyses conducted using the fuzzy logic-based decision support system, the changes in kefir

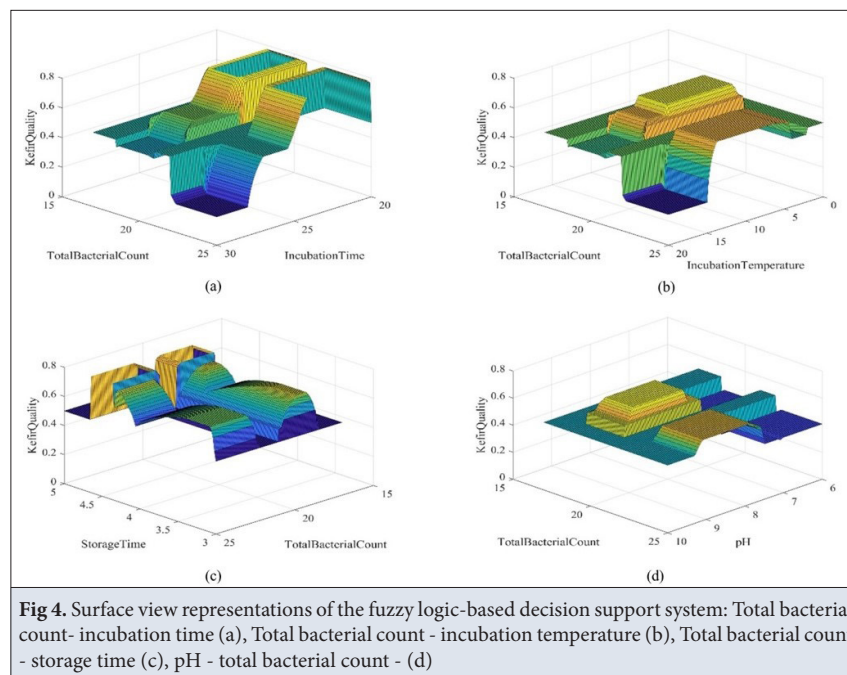


Table 4. Fuzzy system and expert decision results for somatic cell groups

Kefir Sample	SCC Group	Incubation Time (Hour)	Incubation Temperature (°C)	Storage Time (Days)	pH	TBC	System Decision	Expert Decision
1	Low	19	24	0	4.503	9.18	Medium	High
6	Low	19	28	0	4.480	9.22	Medium	High
18	Low	19	24	5	4.17	9.02	High	High
22	Low	19	28	5	4.14	9.18	High	High
28	High	23	24	5	4.13	8.95	High	High
35	Low	23	24	10	4.1	8.72	High	High
40	Low	23	28	10	4.09	8.38	Medium	Medium
48	High	23	28	10	4.11	8.76	Medium	Medium
57	High	19	24	15	4.077	6.37	Low	Low
64	High	23	28	15	4.009	6.49	Low	Low

quality were visualized in a three-dimensional graph. In *Fig. 4*, the surface view of the rules in the Matlab program is presented: total bacteria count-incubation time (a), total bacteria count-incubation temperature (b), total bacteria count-storage time (c), and pH-total bacteria count (d). As can be seen in *Fig. 4-a*, when the incubation time exceeds 20 h, significant decreases in kefir quality can be observed, especially under conditions of high bacterial load. The findings in *Fig. 4-a* indicate that exceeding a certain threshold of fermentation time negatively affects microbial viability and/or metabolic balance and leads to a decrease in product quality. In *Fig. 4-b*, when the incubation temperature exceeds 24°C, losses in kefir quality occur in parallel with decreases in bacterial count. At this point, it was determined that the increase in temperature negatively affected microbial

activity and reduced fermentation efficiency. Similarly, *Fig. 4-c* shows that increases in storage time caused decreases in total bacterial count and kefir quality. *Fig. 4-d* also shows that decreases in pH and total bacterial count lead to decreases in kefir quality. The findings of the research demonstrate that reductions in the kefir quality index occur with decreasing pH values and low microbial density. It was concluded that the reflection of laboratory-prepared conditions on kefir quality could be interpreted successfully through fuzzy numbers and the fuzzy rule base within the fuzzy logic-based decision support system.

In *Table 4*, a portion of the quality evaluation results of kefir samples produced from milk samples categorized as having low or high levels according to somatic cell count is presented. Based on the evaluations conducted on the kefir samples, it was determined that the low somatic

Table 5. Fuzzy system and expert decision results for milk fat groups

Kefir Sample	Fat Group	Incubation Time (Hour)	Incubation Temperature (°C)	Storage Time (Days)	pH	TBC	System Decision	Expert Decision
1	Low	19	24	0	4.582	7.9	Orta	High
6	Low	19	28	0	4.514	8.99	Orta	High
18	Low	19	24	5	4.18	8.85	High	High
22	Low	19	28	5	4.13	9.03	High	High
28	Low	23	24	5	4.17	9.27	High	High
35	Low	23	24	10	4.12	8.38	High	High
40	Low	23	28	10	4.09	7.42	Medium	Medium
48	Low	23	28	10	4.09	8.14	Medium	Medium
57	High	19	24	15	4.116	5.86	Medium	Medium
64	High	23	28	15	4.029	6.26	Low	Low

cell group kefir was of better quality compared to those in the high somatic cell group. In the evaluation of kefir samples classified according to somatic cell count (SCC), an increase in SCC level was found to be associated with a decrease in kefir quality classifications. As presented in Table 4, kefir samples in the low SCC group were observed to be classified predominantly as medium or high quality, whereas samples in the high SCC group were more frequently determined to be of lower quality. In Table 5 is presented a portion of the quality evaluation results, of kefir samples produced from milk samples categorized by milk fat content as low and high. Similar values were obtained regarding kefir quality across the milk fat profiles (Low/High). When the fuzzy logic-based decision support system and expert evaluations were compared within the scope of the SCC and fat groups, a correct classification rate of 93.75% and a high level of agreement were observed. Similarly, in the milk fat content groups, the system showed a 93.75% overlap with expert decisions, indicating consistent performance across different milk component groups. To evaluate the statistical agreement between the system and expert decisions, Cohen's Kappa coefficient and Chi-Square (χ^2) values were calculated. The results indicated that the Kappa statistic value reflected a very high level of agreement for both of somatic cell and fat groups (SCC group $Kappa = 0.901, s_x = 0.047$; Fat group $Kappa = 0.903, s_x = 0.048$). The designed fuzzy system could model expert decisions with high accuracy in accordance with multivariate quality parameters and demonstrated effective learning performance in samples characterized by uncertainty. The Chi-Square values (SCC group $\chi^2 = 110.667$; Fat Group $\chi^2 = 110.222$) calculated within the scope of the analyses proved statistically significant, demonstrating that the harmony between the fuzzy system and expert decisions was not coincidental but occurred through a strong relationship ($P < 0.05$).

DISCUSSION

A review of scientific studies in the literature addressing fuzzy logic-based decision support systems and quality classification problems has observed that features similar to those in the fuzzy system designed in this study are present. Moreover, the performance level of the findings is high. In the study conducted by Harris [24], the input variables were considered in terms of compositional (fat, dry matter) and hygienic aspects (SCC, total bacterial count). A system with a similar structure was designed, similar to our study. Kavdir and Guyer [25] designed a decision support system for apple quality grading using triangular and trapezoidal membership functions, along with the Centroid method, similar in structure to our study. Working with a much larger dataset than our research, the authors included input variables based on physical characteristics and reported a success rate of 89%. In the decision support system designed by Görgülü [19] for the quality classification of floral honey, triangular and trapezoidal membership functions and the Mamdani inference method were employed, similar to our study. A success rate of 94.28% was reported. Unlike our study, another study used a smaller number of samples and rules. In another study by the same author on fig fruit quality classification, a similar system operation and comparable success rate (94.26%) were observed [26]. Consistent with our study, a similar system operation was employed for agricultural product quality assessment by Baskar and Doraipandian [27]. Cha et al. [6] also designed a system incorporating triangular membership functions and the Mamdani inference method, similar to the structure of our study. In contrast to the current study, which used fewer samples, a different study used a larger number of samples, yet the system's success rate was reported as 77%. Akılı et al. [28] developed a fuzzy logic-based decision support system aiming to classify raw milk samples into

quality classes, utilizing the measured values of total bacterial count, somatic cell count, and protein content as input variables. Kefir production modeling was addressed similar to the present study, in the study conducted by Akgül et al.^[29]. In that study, incubation temperature, incubation time, and culture inoculum ratio were used as input variables. Unlike our study, where pH was reported as the output variable to be achieved at the end of kefir production. Additionally, due to the use of fewer input variables than in our study, fewer rules were employed. Akgül et al.^[30] modeled a similar dairy product, yogurt, using the Mamdani inference method. The researchers, who employed a system structure similar to our study, defined pH as the output variable. In contrast to our study, a different number of membership subsets and rules were used in this study, and a total of 343 yogurt samples were analyzed. As in our study, a high system success rate of 90.27% was obtained for the system in question. In the study by Ertekin and Kaya^[31], a similar structure was used with a fermented food product, and a comparable decision support system was designed. Similar to our study, microbiological analyses were used as input variables. As a result of their analysis, it was found that the decision support system which was established to determine the quality classes of samples showed a success rate of 85%. Unlike our research, the number of input variables in the study mentioned was three, and the number of rules was reported as 27. Upon reviewing fuzzy logic-based decision support systems designed for quality assessment of food and agricultural products in the literature, it has been determined that the number of input variables, membership functions, and subset counts vary depending on the nature of the product under investigation. System optimization is largely dependent on the accurate definition of the membership function. The subsequent stages of the system continue their operation through these functions. Therefore, a detailed literature review and system testing are of critical importance. Another crucial aspect is the accurate integration of expert knowledge into the system for the optimization of rules, as the performance of fuzzy systems largely depends on the knowledge-based consistency of the defined rules.

In this study, a decision support system was developed to assist in classifying the quality of kefir samples included in the dataset by evaluating their microbiological characteristics. By transforming numerical findings expressed as crisp values into fuzzy numbers, a large number of variables were simultaneously integrated into the system. Instead of binary definitions expressed only as “low-high,” a more flexible perspective was introduced for addressing the quality problem. An objective approach was presented for the quality evaluation of kefir, one of the fermented dairy products. The experimental validation

studies revealed that the system achieved a success rate of 93.75% in agreement with expert decisions. Furthermore, the statistical analyses of the system outputs indicated a highly significant level of consistency between the evaluations of human experts and the system results.

In conclusion, the developed fuzzy logic-based decision support system was able to classify kefir quality with high accuracy under conditions of uncertainty caused by measurements and environmental variables. In this regard, the fuzzy system contributed to the effective management of uncertainty in the quality control processes of dairy products and provided a flexible and reliable decision support approach. The study also examined the effects of grouping milk samples according to somatic cell count and milk fat content, on kefir quality. It was determined that increases in somatic cell count had a negative effect on kefir quality. It was also observed that increases in milk fat partially affected the kefir formation process. The total bacterial count was identified as the most important variable in kefir quality. The presence of probiotics, which enable the formation of kefir and are of great importance for human health, was identified as one of the most crucial factors determining kefir quality. When the effects of variations in the other input variables included in the system, on kefir quality were evaluated, it was observed that high-quality kefir was obtained with an incubation time of 19 h, an incubation temperature of 22-24°C, and a storage period of 5 days. In future studies, different perspectives may be developed by addressing different types of input variables, membership functions, inference, and defuzzification methods. It is also believed that the integration and optimization of different artificial intelligence methods will make a positive contribution to the quality assessment of fermented food products. The information presented in this study is expected to be beneficial to researchers working in the fields of food, agriculture, animal husbandry, and veterinary sciences in terms of decision-making, quality evaluation, and classification processes.

DECLARATIONS

Availability of Data and Materials: The datasets used and/or analyzed during the current study are available from the corresponding author (A. Akilli) on reasonable request.

Financial Support: This study was supported by the Scientific Research Projects Coordination Unit of Kırşehir Ahi Evran University within the scope of the project numbered ZRT.A4.21.013.

Acknowledgements: We express our gratitude to the Scientific Research Projects Coordination Unit of Kırşehir Ahi Evran University for providing facilities for the present study (No: ZRT.A4.21.013).

Conflict of Interest: The authors declare that there is no conflict of interest.

Declaration of Generative Artificial Intelligence (AI): The authors declare that the article, tables and figures were not written/created by AI and AI-assisted Technologies.

Author Contributions: Concept: A.A., GK., EK.; Design: A.A., GK., EK.; Supervision: A.A., GK., EK.; Resources: A.A., GK., EK.; Data Collection and/or Processing: A.A., GK., EK.; Analysis and/or Interpretation: A.A., GK., EK.; Literature Search: A.A.; Writing Manuscript: A.A. Critical Review: A.A., GK., EK.

REFERENCES

1. Szkolnicka K, Dmytrów I, Mituniewicz-Malek A, Bogusławska-Wąs E: Quality assessment of organic kefir made with kefir grains and freeze-dried starter cultures. *Appl Sci*, 14 (24):11746, 2024. DOI: 10.3390/app142411746
2. Azizi NF, Kumar MR, Yeap SK, Abdullah JO, Khalid M, Omar AR, Alitheen NB: Kefir and its biological activities. *Foods*, 10 (6):1210, 2021. DOI: 10.3390/foods10061210
3. Saleh M, Lee Y: Instrumental analysis or human evaluation to measure the appearance, smell, flavor, and physical properties of food. *Foods*, 12 (18):3453, 2023. DOI: 10.3390/foods12183453
4. De Pilli T: Application of fuzzy logic system for the pizza production processing optimisation. *J Food Eng*, 319:110906, 2022. DOI: 10.1016/j.jfoodeng.2021.110906
5. Vivek K, Subbarao KV, Routray W, Kamini NR, Dash KK: Application of fuzzy logic in sensory evaluation of food products: A comprehensive study. *Food Bioprocess Technol*, 13, 1-29, 2020. DOI: 10.1007/s11947-019-02337-4
6. Cha M, Park ST, Kim T, Jayarao BM: Evaluation of bulk tank milk quality based on fuzzy logic. In, *Proceedings of 2008 International Conference on Artificial Intelligence, ICAI 2008 and 2008 International Conference on Machine Learning: Models, Technologies and Applications*, July 14-17, 722-727, Las Vegas, USA, 2008.
7. Mohammadi MT, Salehi F, Razavi SM: Sensory acceptability modeling of pistachio green hull's marmalade using fuzzy approach. *Int J Nuts Relat Sci*, 2 (2): 48-55, 2011.
8. Sinija V, Mishra H: Fuzzy analysis of sensory data for quality evaluation and ranking of instant green tea powder and granules. *Food Bioprocess Technol*, 4 (3): 408-416, 2011. DOI: 10.1007/s11947-008-0163-x
9. Lu Q, Liu H, Wang Q, Liu J: Sensory and physical quality characteristics of bread fortified with apple pomace using fuzzy mathematical model. *Int J Food Sci Technol*, 52 (5): 1092-1100, 2017. DOI: 10.1111/ijfs.13280
10. Mangaraj S, Tripathi MK: Sensory quality evaluation of MA packaged fruits applying Fuzzy logic. *Trends Biosci*, 6 (2): 195-199, 2013.
11. Perrot N, Baudrit C: Intelligent quality control systems in food processing based on fuzzy logic. In, Maktouf S (Ed): *Robotics and Automation in the Food Industry*. 200-225, Woodhead Publishing, Cambridge, 2013.
12. Ghosh PK, Bhattacharjee P: Quality assessment of fried potato wedges by fuzzy logic and texture analyses. *Acta Aliment*, 44 (2): 178-184, 2015. DOI: 10.1556/aalim.2014.0002
13. Livio J, Hodhod R: AI Cupper: A fuzzy expert system for sensorial evaluation of coffee bean attributes to derive quality scoring. *IEEE Trans Fuzzy Syst*, 26 (6): 3418-3427, 2018. DOI: 10.1109/TFUZZ.2018.2832611
14. Ministry of Agriculture and Forestry: Turkish Food Codex Communiqué on Raw Milk and Heat-Treated Drinking Milk (Communiqué No: 2019/12). <https://www.resmigazete.gov.tr/eskiler/2019/02/20190216-6.htm>; Accessed: 13.06.2025.
15. Halkman AK: Gıda Mikrobiyolojisi Uygulamaları. Başak Matbaacılık Ltd. Şti., Ankara, 2005.
16. Dinç A: Kefirin bazı mikrobiyolojik ve kimyasal özelliklerinin belirlenmesi. *MSc Thesis*. Ankara University, Institute of Health Sciences, 2008.
17. Mazandarani M, Xiu L: Interval type-2 fractional fuzzy inference systems: Towards an evolution in fuzzy inference systems. *Expert Syst Appl*, 189:115947, 2022. DOI: 10.1016/j.eswa.2021.115947
18. Lima JF, Patiño-León A, Orellana M, Zambrano-Martinez JL: Evaluating the impact of membership functions and defuzzification methods in a fuzzy system: Case of air quality levels. *Appl Sci*, 15 (4):1934, 2025. DOI: 10.3390/app15041934
19. Görgülü Ö: Bulanık Mantık (Fuzzy Logic) Teorisi ve Tarımda Kullanım Olanakları Üzerine Bir Araştırma. *PhD Thesis*. Mustafa Kemal University, Institute of Natural and Applied Sciences, 2007.
20. Mamdani EH, Assilian S: An experiment in linguistic synthesis with a fuzzy logic controller. *Int J Man-Mach Stud*, 7 (1): 1-13, 1975. DOI: 10.1016/S0020-7373(75)80002-2
21. Mahapatra SS, Nanda SK, Panigrahy BK: A cascaded fuzzy inference system for Indian river water quality prediction. *Adv Eng Softw*, 42 (10): 787-796, 2011. DOI: 10.1016/j.advengsoft.2011.05.018
22. Elmas Ç: Bulanık Mantık Denetleyiciler. Seçkin Yayıncılık, 230 p., Ankara, 2003.
23. Baykal N, Beyan T: Bulanık Mantık İlke ve Temelleri. Bıçaklar Kitabevi, 406 p., Ankara, 2004.
24. Harris J: Raw milk grading using fuzzy logic. *Int J Dairy Technol*, 51 (2): 52-56, 1998. DOI: 10.1111/j.1471-0307.1998.tb02508.x
25. Kavdır İ, Guyer D: Apple grading using fuzzy logic. *Turk J Agric*, 27 (6): 375-382, 2003.
26. Görgülü O, Caliskan O: The development of a fuzzy decision support system for fig quality classification. *J Inf Technol Agric*, 4 (1): 1-9, 2011.
27. Baskar C, Doraipandian M: Fuzzy logic-based decision support for paddy quality estimation in food godown. In, Kumar D, Kumar A, Ram M (Eds): *Advances in Electrical and Computer Technologies: Select Proceedings of ICAECT 2019*. 279-286, Springer, Singapore, 2020.
28. Akıllı A, Atıl H, Kesenkaş H: Çiğ süt kalite değerlendirmesinde bulanık mantık yaklaşımı. *Kafkas Univ Vet Fak Derg*, 20 (2): 223-229, 2014. DOI: 10.9775/kvfd.2013.9894
29. Akgül HN, Yıldız Akgül F, Doğan T: Bulanık mantık ile kefir üretiminin modellenmesi. *Turk J Agric Food Sci Technol*, 2 (6): 251-255, 2014. DOI: 10.24925/turjaf.v2i6.251-255.75
30. Akgül HN, Yıldız-Akgül F, Karaman AD: Fuzzy logic modeling of yoghurt incubation. *Adnan Menderes Univ J Agric Fac*, 19 (1): 167-176, 2022. DOI: 10.25308/aduziraat.1119592
31. Ertekin Ö, Kaya SK: Determination of microbiological quality of fermented sausage samples by fuzzy logic approach. *Int J Pure Appl Sci*, 6 (2): 227-236, 2020. DOI: 10.29132/ijpas.784490

RESEARCH ARTICLE

Acute and Chronic Toxicity of the Coccidiostat Amprolium to *Daphnia magna* and Its Implications for Aquatic Contamination from Livestock Waste

Mehmet YARDIMCI ^{1(*)}  Çetin YAĞCILAR ²  Cemal POLAT ³ ¹ Tekirdağ Namık Kemal University, Faculty of Veterinary Medicine, Department of Animal Husbandry and Nutrition, TR-59030 Süleymanpaşa, Tekirdağ - TÜRKİYE² Tekirdağ Namık Kemal University, Faculty of Science and Literature, Department of Biology, TR-59030 Süleymanpaşa, Tekirdağ - TÜRKİYE³ Tekirdağ Namık Kemal University, Faculty of Agriculture, Department of Zootechny, TR-59030 Süleymanpaşa, Tekirdağ - TÜRKİYE**(*) Corresponding author:**

Mehmet Yardımcı

Cellular phone: +90 505 350 8215

E-mail: dr.yardimci@gmail.com

How to cite this article?

Yardımcı M, Yağcılar Ç, Polat C: Acute and chronic toxicity of the coccidiostat amprolium to *Daphnia magna* and its implications for aquatic contamination from livestock waste. *Kafkas Univ Vet Fak Derg*, 31 (5): 689-696, 2025.

DOI: 10.9775/kvfd.2025.34670

Article ID: KVFD-2025-34670

Received: 20.06.2025

Accepted: 27.09.2025

Published Online: 06.10.2025

Abstract

Pharmaceutical residues from livestock production are increasingly detected in aquatic systems where they may persist at low concentrations and affect non-target organisms. Among these, Amprolium is a coccidiostat extensively used in poultry farming with residues capable of reaching surface waters via runoff from manure-amended soils and wastewater effluents. Despite its widespread use, ecotoxicological data for freshwater invertebrates are limited, restricting reliable environmental risk assessment. This study aimed to evaluate both acute and chronic effects of Amprolium on *Daphnia magna*, a sensitive and widely used model organism in aquatic toxicology. Acute toxicity tests, performed according to OECD protocols, exposed neonates (<24 h old) to five concentrations (100–300 mg/L), producing a clear concentration- and time-dependent response, with a 48-h EC₅₀ of 48.71 mg/L. Chronic 21-day exposures at environmentally relevant concentrations (0.0625 and 0.125 mg/L) significantly reduced survival, heart rate and reproductive output relative to controls (P<0.05). Statistical analyses demonstrated that both exposure level and duration strongly influenced physiological and reproductive endpoints. These findings reveal that even trace levels of Amprolium may disturb population dynamics and ecosystem functioning. The results highlight the scientific and practical importance of incorporating ecotoxicity data into livestock waste management strategies and support the need for regulatory measures to limit pharmaceutical emissions to aquatic environments.

Keywords: Aquatic life, Amprolium, *Daphnia magna*, Micropollutant

INTRODUCTION

Pharmaceutical residues originating from human and veterinary use are increasingly recognized as micropollutants in aquatic environments ^[1]. These substances can persist at low concentrations in surface and ground waters, exerting biological activity on non-target organisms and potentially altering ecosystem functions ^[2,3]. The combined input from wastewater treatment plants, agricultural runoff and the application of animal manures create continuous exposure scenarios for aquatic biota ^[4,5].

An additional notable cause of drug contamination arises from utilizing fecal matter from animals like pigs, poultry, and humans as a source of nutrients. As highlighted by Suryanto et al. ^[6], some antibiotics may have a longer half-

life in water and can lead to adverse effects on the fish species. Reports have highlighted the adverse effects of antibiotics on aquatic organisms, including impacts on survival, growth, reproductive capabilities, and changes in biochemical indicators, potentially disrupting the entire aquatic food chain.

In large-scale animal farming, veterinary drugs such as coccidiostats and anthelmintics are commonly given to livestock. These chemicals can enter the aquatic environment through animal waste from outdoor animals or when contaminated liquid manure is applied to farmland. Through processes like surface runoff, leaching, and drift, these substances can lead to both acute and chronic toxicity in aquatic organisms, potentially disrupting biodiversity and affecting the functioning of ecosystems ^[7,8].



Amprolium is one of the widely used pharmaceuticals in poultry production as a coccidiostat, and residues have the potential to reach surface waters via runoff from manure-amended fields or direct discharges from intensive farms. The paucity of standardized acute and chronic ecotoxicity data for Amprolium constrains robust risk assessment for freshwater invertebrates^[9].

Daphnia magna, used in this study, is a widely recognized model organism in aquatic toxicology, frequently employed in both acute and chronic assays due to its high sensitivity to pollutants and practical advantages over vertebrate species. Its use facilitates pre-screening of chemicals, supports alternative testing strategies, and contributes to the development of more efficient and sustainable approaches in environmental risk assessment and toxicological research.

This study aims to fill that gap by quantifying both short-term (12-48 h EC₁₀-EC₅₀) and long-term (21-day reproductive and survival) effects of Amprolium on *Daphnia magna*, a standard model organism in aquatic toxicology. By coupling conventional endpoints (mortality, reproduction) with physiological measures we provide a more comprehensive toxicological profile and discuss the ecological implications for aquatic systems impacted by livestock waste.

MATERIAL AND METHODS

Ethical Statement

The study does not require approval from the Local Animal Experiments Ethics Committee.

Test Organism and Culture Conditions

Cultures of *Daphnia magna* were maintained in the laboratory before acute and chronic tests. For all toxicity tests, Daphnids (<24 h old) were obtained from these stock cultures and acclimated to test conditions. All toxicity tests were performed at 21°C±0.5°C in a temperature-controlled laboratory, consistent with standard *Daphnia* test conditions. Dissolved oxygen and pH were measured in all treatments and controls and were kept within acceptable ranges (dissolved oxygen ≥6 mg/L in stock; during tests, dissolved oxygen was maintained and reported for each group). The water temperature was maintained at 26°C±1°C in the laboratory where the research was conducted. Lighting was provided with a photoperiod providing 12 h of light and 12 h of darkness using fluorescent lamps placed on the water surface and automatically turning on and off. Each box contained an air stone that provided 8-10 ppm of oxygen. Test solutions were refreshed three times a week. *Daphnia* was fed with 0-100 µ size Inve Aquaculture brand feed daily. The feed was given in 0.1 g powder form by dissolving it in water.

Preparation of Amprolium

Ampronet oral solution, containing 250 mg/mL of Amprolium, was obtained from a local pharmaceutical warehouse in Tekirdağ, Türkiye. The solution, with Amprolium as its active ingredient, was then directly added to the experimental aquarium.

Acute Toxicity Tests

Acute toxicity tests expose *Daphnia magna* to elevated concentrations of a substance for a brief period, usually between 24 and 48 h. The acute toxicity test of Amprolium was conducted following standard OECD protocols for *D. magna* acute test^[10] under laboratory conditions that were consistent with the rearing procedures. Acute toxicity assays were conducted using Daphnids (<24 hrs old) to calculate EC₁₀ and EC₅₀ values. In addition to EC₅₀, EC₁₀ values were calculated to provide a more ecologically relevant threshold for sublethal effects. While EC₅₀ represents the concentration at which 50% of the organisms show a response, EC₁₀ is a more sensitive indicator of early physiological or behavioural changes that may occur at environmentally realistic concentrations. This parameter is frequently recommended in regulatory ecotoxicology as it better reflects no-effect or low-effect levels, which are critical for risk assessment and environmental protection standards.

Five test concentrations (100, 125, 200, 225 and 300 mg/L) plus a control were tested in triplicate, with 20 Daphnids per replicate (60 per concentration). The experiment employed 100 mL glass beakers as test containers; each filled with 25 mL of the test solution. The trial was conducted in the absence of aeration. Throughout the experiment, the test organisms did not receive any food to avoid affecting water quality. Immobility of *Daphnia* samples was assessed by gently shaking test tubes and the dead were observed to sink to the bottom motionless. pH and oxygen levels were assessed in the control and the test concentrations. Water change was done every 24 hours. Immobilization was recorded at 12, 24, 36 and 48 h by gently agitating the beakers and noting organisms that were unable to swim after agitation. No food was supplied during acute tests to avoid water-quality changes. pH and dissolved oxygen were monitored and reported for each sampling time.

Chronic Toxicity Tests

A total of 180 *Daphnia magna* were used for chronic toxicity tests consisting of three groups, one control and two trial groups, each containing 60 daphnids. Each group was kept in separate 9 boxes to consist of 3 replicate subgroups. The *Daphnia* divided into groups were obtained from the same aquarium and distributed according to the random sampling method. Chronic toxicity assays involve extended

exposure of *Daphnia magna* to lower concentrations of a substance, typically over several generations. The chronic assessments of *Daphnia magna* were conducted over 21 days, adhering to established OECD protocols [11] and maintaining the same temperature and photoperiod outlined in the rearing procedures. Daphnids, aged less than 24 hours at the start of the test, were exposed for 21 days to two different concentrations of Amprolium 0.0625 and 0.125 mg/L. These concentrations were determined considering concentrations likely to be present in practical wastewater conditions, with the European Food Safety Authority (EFSA) referring to predicted environmental concentrations of Amprolium in groundwater and surface water as 0.036 and 0.012 mg/L [12]. One group was kept in control and not exposed to Amprolium. The count of living offspring generated per animal per day was monitored from the initial offspring's first day. The Daphnids were transferred to freshly prepared pharmaceutical dilutions every alternate day and received daily feeding. Over the 21 days, the creatures were observed daily for mortality and reproductive status. Survival and offspring production were evaluated each time the solutions were refreshed, with pH and oxygen levels measured concurrently. The animals were not fed during the test times. The number of deaths and eggs were also recorded on the same test days.

The transparency of *Daphnia magna* enables clear observation of its internal structures and physiological processes under a microscope. On measurement days, individual test organisms were placed on a single-cavity microscope slide in a 50 µL droplet of aquarium water. One-minute video recordings of their movements under the microscope (Soif BK300-L) were taken and slowed down to 25% of the original speed using VLC Media Player. This approach was chosen because direct microscopic counting of heartbeats is often error-prone due to their rapid contractions. Video analysis provides more precise and reproducible results, reduces observer bias, allows post-experiment verification, and enables reliable detection of subtle physiological changes during long-term exposure.

Statistical Analysis

The software SPSS v27.0 was used for the statistical analyses. A one-way analysis of variance (ANOVA) followed by a Scheffe test was applied to assess the statistical differences between the different pharmaceutical concentrations and the control ($P < 0.05$) to determine if the applied concentration of the pollutants had a significant effect on the heartbeats.

The two-way Repeated Measures ANOVA, employing a Huynh-Feldt correction was used for mean heartbeat values across assessment stages.

The chi-square test was used to compare mortality rates

between groups, and the weekly egg production numbers were compared using the Kruskal-Wallis test due to non-normal distribution.

The acute EC_{10} (10% mortality) and EC_{50} (50% mortality) assays (measuring immobile organisms) were performed in triplicate for 100, 125, 200, 225 and 300 mg/L concentrations of Amprolium, each treatment containing 60 (20x3) Daphnids. The 95% confidence limits for these assays, as well as for the 12, 24, 36 and 48-h acute test was determined by calculating the effective concentration values and their 95% confidence limits using non-linear regression analysis through Probit analysis. Concentration factors were used as input data concentrations.

RESULTS

The mean of the heartbeat measurements was expressed in heartbeats per minute and averaged for the experimental and control test animals.

Acute Tests

Exposure of *D. magna* to Amprolium at different concentrations for 12, 24, 36 and 48 h resulted in a negative effect on its survival. During the acute tests with Daphnids, no mortality was observed in the control group. The oxygen content remained unaltered and there were no significant pH fluctuations throughout the testing process. *Table 1* presents the concentration levels examined, alongside the calculated EC_{10} and EC_{50} values for 12, 24, 36 and 48 h. A significant increase in deaths over time was observed due to the effect of the applied concentrations. Both EC_{50} and EC_{10} values were determined to provide insight into low effect levels that would occur at environmentally realistic concentrations. *Fig. 1* also demonstrates the concentration effect on survival over time.

Chronic Tests

Results showed that even low concentrations of Amprolium in water led to a decrease in heart rates, while simultaneously increasing death rates, egg numbers, and offspring production ($P < 0.05$). pH levels for control, 0.0625 and 0.125 mg/L groups were 7.04 (6.97-7.20), 6.58 (6.40-6.73) and 6.52 (6.40-6.75), respectively while O_2 levels for control, 0.0625 and 0.125 mg/L groups were 6.18 (6.00-6.40), 4.11 (4.00-4.20), 4.05 (4.00-4.20).

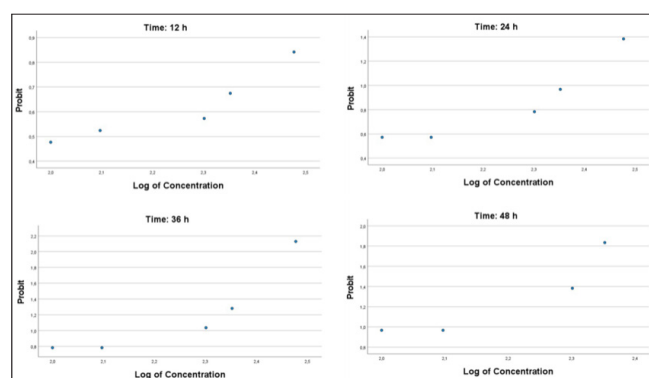
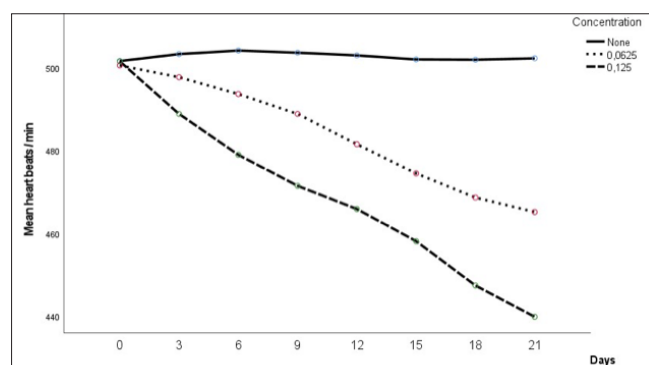
Changes in the Heartbeats

Over 21 days, differences in heart rates of *Daphnia magna* exposed to varying concentrations of Amprolium revealed a significant reduction in heart rates with increasing concentrations (*Table 2*, $P < 0.05$). The 0.125 g/mL group showed a significant difference from the control group within the first 3 days and differed from the 0.0625 g/mL group on day 6. By days 9 and 12, the trial groups were

Table 1. *Daphnia magna* acute EC values for Amprolium with confidence limits (95% probability)

Exposure Time (h)	n	Mortalities	EC	Concentration levels (100-300 mg/L)	LCI ^a	UCI ^b
12	60	43.8	EC ₁₀	0.28	NA	NA
			EC ₅₀	21.55	NA	NA
24	60	47.6	EC ₁₀	6.63	0.02	23.49
			EC ₅₀	47.77	5.24	80.45
36	60	51.6	EC ₁₀	10.55	0.39	27.83
			EC ₅₀	46.65	10.40	73.98
48	60	54.6	EC ₁₀	16.04	1.68	34.04
			EC ₅₀	48.71	15.60	72.24

a: Lower Confidence Interval, b: Upper Confidence Interval

**Fig 1.** Acute EC values for Amprolium with confidence limits (95% probability) for *Daphnia magna* at 12, 24, 36 and 48 h**Fig 2.** The course of the heart beats over time

significantly different from the control group, with all groups showing significant differences from each other on days 15, 18 and 21 ($P < 0.05$).

After the sixth day, the trial groups differed from the control group ($P < 0.05$), while the control group drew almost a stable curve throughout the entire study (Fig. 2).

The two-way repeated measures ANOVA test revealed that the difference between the repeated measurements depending on time and the interaction of the concentration with time was statistically significant ($P < 0.05$).

Table 2. One-way ANOVA test results for group comparisons of heartbeats by time (days)

Days	Concentration	n	\bar{x}	$S\bar{x}$	F	Sig.
0	None	60	500.40	3.62	0.637	.530
	0.0625	60	501.25	4.36		
	0.125	60	495.58	3.45		
3	None	60	503.87 ^a	4.47	5.36	.005
	0.0625	60	492.93 ^{ab}	5.98		
	0.125	60	479.08 ^b	5.52		
6	None	60	507.18 ^a	5.40	6.86	.001
	0.0625	60	498.25 ^a	5.97		
	0.125	59	478.59 ^b	5.31		
9	None	60	500.67 ^a	4.35	9.96	.000
	0.0625	60	474.00 ^b	5.30		
	0.125	57	472.68 ^b	5.37		
12	None	56	505.96 ^a	4.56	12.15	.000
	0.0625	60	483.98 ^b	5.59		
	0.125	50	470.24 ^b	4.86		
15	None	54	502.26 ^a	4.42	20.91	.000
	0.0625	52	475.19 ^b	5.30		
	0.125	44	458.20 ^c	4.91		
18	None	52	501.04 ^a	3.51	35.94	.000
	0.0625	48	470.60 ^b	4.97		
	0.125	42	452.62 ^c	3.56		
21	None	51	502.24 ^a	2.59	103.14	.000
	0.0625	35	465.14 ^b	3.36		
	0.125	29	439.83 ^c	3.72		

$P < 0.05$

The two-way Repeated Measures ANOVA, employing a Huynh-Feldt correction, revealed a statistically significant variance in the mean heartbeat values across assessment stages (0, 3rd, 6th, 9th, 12th, 15th, 18th, and 21st days) ($F(6.123, 685.723) = 13.023$, $P < 0.05$) (Table 3, Table 4.).

Table 3. The two-way repeated measures ANOVA - Mauchly's test of sphericity

Within Subjects Effect	Mauchly's W	Approx. Chi-Square	df	Sig.	Epsilon ^b		
					Greenhouse-Geisser	Huynh-Feldt	Lower-bound
Time	.442	89.298	27	.000	.811	.875	.143

b: A correction factor when the assumption of sphericity is violated

Table 4. Tests of within-subjects' effects on heartbeats

Source		Type III Sum of Squares	df	Mean Square	F	Sig.	Partial Eta Squared	Noncent. Parameter	Observed Power ^a
Time	Sphericity Assumed	99468.287	7	14209.755	13.023	.000	.104	91.161	1.000
	Greenhouse-Geisser	99468.287	5.678	17518.467	13.023	.000	.104	73.943	1.000
	Huynh-Feldt	99468.287	6.123	16246.283	13.023	.000	.104	79.734	1.000
	Lower-bound	99468.287	1.000	99468.287	13.023	.000	.104	13.023	.947
Time * Concentration	Sphericity Assumed	60561.686	14	4325.835	3.965	.000	.066	55.504	1.000
	Greenhouse-Geisser	60561.686	11.356	5333.096	3.965	.000	.066	45.021	.999
	Huynh-Feldt	60561.686	12.245	4945.809	3.965	.000	.066	48.546	.999
	Lower-bound	60561.686	2.000	30280.843	3.965	.022	.066	7.929	.701
Error (Time)	Sphericity Assumed	855444.657	784	1091.128					
	Greenhouse-Geisser	855444.657	635.926	1345.195					
	Huynh-Feldt	855444.657	685.723	1247.508					
	Lower-bound	855444.657	112.000	7637.899					

a: Computed using alpha = .05

Table 5. Survival * concentration crosstabulation

Survival		Concentration			Total
		None	0.0625	0.125	
Dead	Count	9	25	31	65
	Expected Count	21.7	21.7	21.7	65.0
Alive	Count	51	35	29	115
	Expected Count	38.3	38.3	38.3	115.0
Total	Count	60	60	60	180
	Expected Count	60.0	60.0	60.0	180.0

Table 6. Chi-square tests for survival * concentration

Test	Value	df	Asymptotic Significance (2-sided)
Pearson Chi-Square	18.686 ^a	2	.000
Likelihood Ratio	20.120	2	.000
Linear-by-Linear Association	17.385	1	.000
N of Valid Cases	180		

a. 0 cells (0.0%) have an expected count less than 5. The minimum expected count is 21.67

Additionally, time and concentration interactions were also found to be statistically significant ($P < 0.05$).

Survival

The survival and mortality data of test organisms throughout the 21-day exposure period are presented in [Table 5](#). According to these results, the highest mortality was recorded in the 0.125 g/L treatment group, whereas the lowest mortality occurred in the control group. The

statistical significance of the differences among groups was further evaluated using the chi-square test, the outcomes of which are summarized in [Table 6](#) ($P < 0.05$).

Egg Numbers

Fertility, as indicated by the number of eggs produced per week, was negatively affected over time in the trial groups exposed to different concentrations of Amprolium ([Table 7](#)).

Table 7. Kruskal-Wallis Test results for the comparison of the egg numbers

Time	Concentration	n	Mean	Mean Rank	Kruskal-Wallis H	df	P
Day 0	Control	60	2.92	86.33	1.442	2	.486
	0.625	60	3.37	96.92			
	1.25	60	2.82	88.25			
Day 3	Control	60	3.35	89.78	1.456	2	.483
	0.625	60	3.48	96.47			
	1.25	60	3.00	85.25			
Day 6	Control	60	2.25	116.12	28.486	2	.000
	0.625	60	1.40	86.31			
	1.25	59	.78	67.19			
Day 9	Control	60	2.07	115.40	32,103	2	.000
	0.625	60	1.02	80.01			
	1.25	57	.63	67.48			
Day 12	Control	56	1.70	96.03	9.398	2	.009
	0.625	60	.80	82.15			
	1.25	50	.52	71.09			
Day 15	Control	54	1.56	92.56	19.934	2	.000
	0.625	52	.42	66.82			
	1.25	44	.27	64.82			
Day 18	Control	52	1.58	90.36	24.189	2	.000
	0.625	48	.50	64.31			
	1.25	42	.21	56.37			
Day 21	Control	51	1.49	72.01	22.765	2	.000
	0.625	35	.43	49.20			
	1.25	29	.14	43.98			

P<0.05

DISCUSSION

This study utilized *Daphnia magna* as a sentinel species to examine the environmental and ecological consequences of pharmaceutical residues derived from animal waste. Findings revealed that even at trace concentrations, these contaminants present significant hazards to aquatic biota. In particular, changes in cardiac activity, survival rates, and reproductive output observed in *Daphnia* exposed to Amprolium emerged as highly sensitive biomarkers. Such endpoints can therefore serve as robust indicators for evaluating the ecological impacts of micropollutants and hold promise as early-warning metrics in aquatic environmental monitoring programs.

The acute toxicity tests conducted with *Daphnia magna* in the current study revealed a significant impact on their survival, demonstrating an increased sensitivity to Amprolium. The EC₅₀ value, which indicates the concentration of a chemical toxic to 50% of the test

organisms within a specific exposure period was determined to be 48.71 mg/L over 48 h. This finding underscores the heightened susceptibility of *D. magna* to Amprolium under laboratory conditions in a short-term exposure in this study.

Various studies report EC₅₀ values for antiparasitic and anticoccidial drugs with different values. Puckowski et al.^[13] reported 48-h EC₅₀ values for Flubendazole and Fenbendazole as 0.0448 mg/L and 0.0193 mg/L. Yoshimura and Endoh^[9] found 48-h EC₅₀ values for Amprolium hydrochloride, Levamisole hydrochloride, Pyrimethamine and Trichlorfon as 227 mg/L, 64.0 mg/L, 5.2 mg/L and 0.00026 mg/L, respectively. It is important to recognize that EC₅₀ values can vary significantly based on factors like strain, water hardness, pH, temperature, and other environmental conditions. As such, interpreting these values should be done carefully, considering the specific parameters of each study. Furthermore, the rate in surface waters and long-term exposure will lead to

significant changes in concentration values. When the effects of mixtures of different wastes are added to this, the table will change completely.

Chronic toxicity assessments provide a comprehensive understanding of potential ecological impacts and aid in determining acceptable long-term exposure levels. Different chemicals can have varying effects on *D. magna*, causing toxicity and affecting mortality and reproduction. In the current research, *D. magna* exposed to different concentrations of Amprolium with increased concentrations significantly reduced the heartbeat rates and this decrease became more pronounced over time ($P < 0.05$, Table 2). In an earlier study, the heartbeat rate proved to be the most sensitive toxicity endpoint [14]. Similar to this study, Vo et al. [15] examined the chronic effects of Ampicillin on *Daphnia magna* and found significant reductions in survival, reproduction, and growth. Several other researchers suggest that substances like herbicides, gasoline pollution, environmental hormones, and ethanol can impact the metabolism of *Daphnia magna* by reducing the heartbeat rate [16-18]. Taken together with literature information, our results indicate that the heart rate of *Daphnia magna* can provide a reliable basis for toxicological studies and testing of aquatic micropollutants.

The methodology applied in this study for calculating heart rate numbers led to different results from the numbers reported in the literature because the same precision was not applied in other similar studies. A remarkable change was seen in the numbers obtained by reducing the video recording speed to 25% in calculating the heartbeat numbers. This method offers the possibility of obtaining healthier values for fast repetitive movements at the microscopic level. In this study, it was determined that the control group had an average of 500 beats per minute, while values around 300 and below are reported in the literature [19]. It was observed that when attempting to count the heartbeats of *Daphnia* under a microscope by eye, accurate values could not be obtained.

Considering the aspect of repeated measurements, significant differences in each measurement period were noticed in the experimental groups, while a stable condition was observed in the control group (Fig. 1, Table 3, Table 4). Time concentration interaction was also found to be statistically significant; differences in values occurred not only depending on time but also depending on concentration.

There was a significant difference between the concentration groups in terms of the number of deaths ($P < 0.05$) during the chronic exposure. On a week-by-week basis, a significant increase in deaths has been observed in the last 3 weeks in the 0.125 and 0.0625 g/L concentration

groups in the last week. Considering both the mortality rates and the decreasing number of heartbeats, it can be concluded that a significant number of *Daphnia magna* exposed to Amprolium initially exhibit physiological resistance, but this resistance diminishes over time. This finding is also significant as it highlights the emergence of the resistance threshold.

Amprolium also had a negative impact on fertility in *Daphnia magna*, with a decrease in the number of eggs produced corresponding to the higher concentrations used. It is important to note that, while the presence of residual Amprolium in the water reduces heart rates and egg production in *Daphnia* over time, it also leads to an increase in mortality.

To mitigate potential risks to the aquatic environment, proper regulations are needed concerning the sale, use, and disposal of medications. Additionally, sanctions should be enforced against those who fail to comply with these regulations.

Since anticoccidials are commonly used in animal husbandry, their residues often end up in animal waste. These drugs are typically absorbed slowly and excreted through the feces. When animal waste is used as fertilizer, anticoccidials can leach into the environment, contaminating soil and water. This is particularly concerning in intensive farming systems, where large numbers of animals are confined and fed medicated feed pellets.

Pharmaceuticals and their metabolites, many of which are ionizable and whose ecotoxicological behavior varies with pH, represent an uncertain environmental risk; in marine aquaculture, their release via fish waste can contaminate coastal waters [20].

Building on the points discussed above, the following section highlights the key implications of our findings and their relevance to environmental risk assessment.

Daphnia studies are crucial for assessing the toxicity of aquatic substances, offering valuable insights into their ecological impacts. As sensitive water quality indicators, *Daphnia* help monitor environmental changes and evaluate ecosystem risks. The high responsiveness of *D. magna* to various stressors, including chemical pollutants, heavy metals, and pesticides, allows for detecting harmful effects even at low concentrations, making it a key model for evaluating environmental contaminants.

Utilizing both acute and chronic toxicity assays provides a comprehensive overview of a substance's toxicological profile. Acute tests detect immediate hazards, whereas chronic tests uncover subtle, long-term effects. Regulatory agencies often mandate data from both types of assessments for substance approval and classification, highlighting their critical role in environmental risk evaluation.

This study demonstrated that Amprolium had a significant effect on the survival and reproduction of *Daphnia magna*, highlighting its sensitivity as an indicator of micropollutant toxicity. Acute toxicity tests showed a clear increase in mortality over time, with statistically significant differences in repeated measurements and a notable interaction between concentration and time.

While pharmaceuticals are vital for treating infections, their responsible use is essential to minimize environmental damage from yearly pollutant releases into surface waters. Thus, standard laboratory ecotoxicity tests, as demonstrated by this study's findings, could effectively assess ecosystem quality and rank hazards in water bodies affected by urban runoff and wastewater.

In conclusion, the long-term effects of pollutants on aquatic organisms, including reproductive issues, physiological changes, and sensitive species extinction, can disrupt ecosystems and lead to broader community-level consequences. Therefore, we recommend that large-scale treatment plants integrate toxicity assessment with physicochemical parameter monitoring. This dual approach would refine animal waste management, reducing its potential impact on aquatic life before wastewater enters water systems.

DECLARATIONS

Availability of Data and Materials: Data will be offered by the corresponding author (MY) on demand.

Acknowledgements: The authors sincerely acknowledge the Aquatic Vertebrate Experimental Unit for their support and cooperation in the study.

Financial Support: This research was not supported by any specific grants from public, commercial, or non-profit funding agencies.

Conflicts of Interest: The authors have no conflicts of interest to declare.

Declaration of Generative Artificial Intelligence (AI): No AI tool is used in this research work write-up.

Author Contributions: MY and ÇY designed the study. MY, ÇY and CP helped in the methodology and work plan. MY and ÇY carried out the experiments. MY performed the statistical analysis. MY, ÇY and CP revised the paper.

REFERENCES

- O'Rourke K, Engelmann B, Altenburger R, Rolle-Kampczyk U, Grintzalis K: Molecular responses of daphnids to chronic exposures to pharmaceuticals. *Int J Mol Sci*, 24:4100, 2023. DOI: 10.3390/ijms24044100
- Caldas LL, Espíndola E, Moreira R, Novelli A: environmental risk assessment of drugs in tropical freshwaters using *Ceriodaphnia silvestrii* as test organism. *Bull Environ Contam Toxicol*, 110 (6):106, 2023. DOI: 10.1007/s00128-023-03739-z
- Distefano GG, Zangrando R, Basso M, Panzarin L, Gambaro A, Volpi Ghirardini A, Picone M: Assessing the exposure to human and veterinary pharmaceuticals in waterbirds: The use of feathers for monitoring antidepressants and nonsteroidal anti-inflammatory drugs. *Sci Total Environ*, 821:153473, 2022. DOI: 10.1016/j.scitotenv.2022.153473
- Oliveira LLD, Antunes SC, Gonçalves F, Rocha O, Nunes B: Acute and chronic ecotoxicological effects of four pharmaceutical drugs on cladoceran *Daphnia magna*. *Drug Chem Toxicol*, 39 (1): 13-21, 2016. DOI: 10.3109/01480545.2015.1029048
- Chyc M, Sawczak J, Wiąckowski K: Occurrence of pharmaceuticals in surface waters. *Sci Tech Innov*, 9 (2): 40-46, 2020. DOI: 10.5604/01.3001.0014.4578
- Suryanto ME, Yang CC, Audira G, Vasquez RD, Roldan MJM, Ger TR, Hsiao CD: Evaluation of locomotion complexity in zebrafish after exposure to twenty antibiotics by fractal dimension and entropy analysis. *Antibiotics*, 11 (8):1059, 2022. DOI: 10.3390/antibiotics11081059
- Goessens T, Baere SD, Troyer ND, Deknock A, Goethals P, Lens L, Pasmansd F, Croubels S: Highly sensitive multi-residue analysis of veterinary drugs including coccidiostats and anthelmintics in pond water using UHPLC-MS/MS: Application to freshwater ponds in Flanders, Belgium. *Environ Sci Process Impacts*, 22, 2117-2131, 2020. DOI: 10.1039/D0EM00215A
- Paíga P, Santos LHMLM, Ramos S, Jorge S, Silva J, Delerue-Matos C: Presence of pharmaceuticals in the Lis River (Portugal): Sources, fate and seasonal variation. *Sci Total Environ*, 573, 164-177, 2016. DOI: 10.1016/j.scitotenv.2016.08.089
- Yoshimura H, Endoh YS: Acute toxicity to freshwater organisms of antiparasitic drugs for veterinary use. *Environ Toxicol*, 20, 60-66, 2005. DOI: 10.1002/tox.20078
- Anonymous: OECD Guidelines for the testing of chemicals. Section 2 Effects on biotic systems test guideline No. 202 Acute Immobilisation Test, 2004. https://www.oecd.org/content/dam/oecd/en/publications/reports/2004/11/test-no-202-daphnia-sp-acute-immobilisation-test_g1gh28f3/9789264069947-en.pdf; Accessed: 20.03.2025.
- Anonymous: OECD Guidelines for the testing of chemicals. Section 2 Effects on biotic systems test guideline No. 211 *Daphnia magna* reproduction test, 2012. https://www.oecd.org/content/dam/oecd/en/publications/reports/2012/10/test-no-211-daphnia-magna-reproduction-test_g1g24069/9789264185203-en.pdf; Accessed: 20.03.2025.
- Rychen G, Aquilina G, Azimonti G, Bampidis V, Bastos ML, Bories G, Chesson A, Cocconcetti PS, Flachowsky G, Kolar B, Kouba M, Lopez-Alonso M, Lopez Puente S, Mantovani A, Mayo B, Ramos F, Saarela M, Villa RE, Wallace RJ, Wester P, Brantom P, Halle I, van Beelen P, Holczknecht O, Vettori MV, Gropp J: EFSA FEEDAP Panel, Scientific opinion on the safety and efficacy of COXAM® (amprolium hydrochloride) for chickens for fattening and chickens reared for laying. *EFSA J*, 16 (7):5338, 2018. DOI: 10.2903/j.efsa.2017.5021
- Puckowski A, Stolte S, Wagil M, Markiewicz M, Łukaszewicz P, Stepnowski P, Białk-Bielinska A: Mixture toxicity of flubendazole and fenbendazole to *Daphnia magna*. *Int J Hyg Environ Health*, 220 (3): 575-582, 2017. DOI: 10.1016/j.ijheh.2017.01.011
- Fekete-Kertész I, Kungléné-Nagy Z, Molnár M: Ecological impact of micropollutants on aquatic life determined by an innovative sublethal endpoint *Daphnia magna* heartbeat rate. *Carpas J Earth Environ Sci*, 11 (2): 345-354, 2016.
- Vo TMC, Pham NH, Nguyen TD, Bui MH, Dao TS: Development of *Daphnia magna* under exposure to ampicillin. *Archit Civ Eng Environ*, 3, 147-152, 2018. DOI: 10.21307/acee-2018-047
- Jeong E: Investigating the acute cardiac effects on aquatic organisms by gasoline pollution in lake-simulated beakers using *Daphnia magna*. *J Glob Ecol Environ*, 16 (4): 128-139, 2022. DOI: 10.56557/jogee/2022/v16i47903
- Karim A, Sanders A, Walker N, Zimmerman K, Wegener L: Blame it on the alcohol: An investigation on increasing ethanol concentrations lowering *Daphnia magna* heart rate. *JUBLI*, 1 (2): 1-4, 2018.
- Présing M, Véro M: A new method for determining the heartbeat rate of *Daphnia magna*. *Water Res*, 17 (10): 1245-1248, 1983. DOI: 10.1016/0043-1354(83)90248-8
- Kang J, Lee S, Park R, Kim J, Ha V, Lee J, Jang H: Analyzing the impact of residential chemicals upon the heartbeat of *Daphnia magna*. *J Glob Ecol Environ*, 20 (4): 29-42, 2024. DOI: 10.56557/jogee/2024/v20i48876
- Bethke K, Caba M: Effect of acidification on the chronic toxicity of diclofenac to *Daphnia magna*. *Aquat Toxicol*, 287:107497, 2025. DOI: 10.1016/j.aquatox.2025.107497

RESEARCH ARTICLE

Ecotoxicological Consequences of Heavy Metals on Emperor Fish (*Lethrinus*) Species in the Red Sea: Histopathology and Biochemistry

Soha A. ALSOLMY ¹  Raoum MOMINKHAN ²  Sahar J. MELEBARY ² (*) 

¹ Department of Environmental Sciences, College of Science, University of Jeddah, P.O. Box 80237, Jeddah 21589, SAUDI ARABIA

² Department of Biological Sciences, College of Science, University of Jeddah, P.O. Box 80237, Jeddah 21589, SAUDI ARABIA



(*) Corresponding author:

Sahar J. Melebary
Phone: +966 50 604 655
E-mail: sjmelebary@uj.edu.sa

How to cite this article?

Alsolmy SA, MominKhan R, Melebary SJ:
Ecotoxicological consequences of heavy metals on emperor fish (*Lethrinus*) species in the Red Sea: Histopathology and biochemistry. *Kafkas Univ Vet Fak Derg*, 31 (5): 697-708, 2025.
DOI: 10.9775/kvfd.2025.34770

Article ID: KVFD-2025-34770

Received: 12.07.2025

Accepted: 02.10.2025

Published Online: 07.10.2025

Abstract

Heavy metal (HMs) contamination in marine environments is a global concern, affecting fish health and seafood safety. This study examined the effects of HMs on 90 emperor fish from the Red Sea, focusing on metal levels in water and fish liver, blood parameters, and liver histopathology. Using inductively coupled plasma mass spectrometry, different levels of heavy metals were detected. While some metals, such as Pb, Cu, and Zn, were undetectable in seawater from both northern and southern regions, Ni, Fe, and Mn were higher in the north. As a result, compared to the South area, fish from the North showed a significant increase in serum hepatic enzymes, with ALT, AST, ALP, and GGT elevated by 27.3%, 36.9%, 11.6%, and 35.4%, respectively. Bilirubin levels were 20.5% higher in the North, indicating liver dysfunction. This matches liver histology findings, where the North area had a mean liver damage score of 2.0, indicating moderate hepatocellular degeneration, congestion, and prominent melanomacrophage centers. Conversely, the South area had a lower mean liver damage score of 0.5, reflecting mostly normal or mild changes and relatively intact liver structure. The study concludes that HMs poisoning significantly harms fish in the north, emphasizing the importance of biochemical and histopathological markers in assessing marine pollution and its risks to both environmental health and food safety.

Keywords: Biomarker's analysis, Fish, Food safety, Heavy metals, Environmental pollution, Histological techniques, Liver

INTRODUCTION

Food security, defined in numerous ways, is commonly understood as ensuring access to sufficient, quality food for all, through availability, accessibility, and sustainable practices and prevent hunger ^[1]. A strong food security system ensures access to safe, nutritious food for a country's population ^[2]. Aquatic animal production from fisheries and aquaculture worldwide reached 177.8 million tons in 2020 ^[3-5]. For many people, especially in coastal cities, fish is an important source of food because they are high in vitamins and minerals, low in fat, and have a considerable source of protein. For the prevention of chronic diseases linked to diet, public health guidelines often include 1-2 weekly servings of fish ^[6]. The internationally recognized definition of marine pollution encompasses the introduction of chemicals into the marine environment, either directly or indirectly through human activities, resulting in detrimental effects on biota and water quality ^[7]. Marine ecosystems face significant risk from industrial and domestic pollutant discharge ^[8,9]. The residence time

of pollutants in estuaries results in a significantly greater impact on the coastal zone compared to inland river systems ^[10]. The presence of heavy metals and organic pollutants within marine environments constitutes a significant ecological concern. Heavy metal deposition in fish organs is influenced by metal concentration, exposure time, absorption, environmental factors (temperature, hardness, pH salinity, water and sediment metal levels, ecological needs), and fishing period and the water's physical and chemical properties, and biological factors (age, feeding, size, gender). The primary organs of metal bioaccumulation are the gills, kidneys, and liver ^[11-13].

Heavy metal toxicity represents a major environmental and health concern, as exposure to these elements is associated with a wide range of adverse health effects. Although heavy metals have no essential biological role in the human body, their accumulation can impair physiological processes and disrupt normal biological functions. Prolonged retention of these toxic elements may result in chronic health conditions. The severity of



metal toxicity depends on the absorbed dose, the route of exposure, and the duration of contact ^[14]. Heavy metals exhibit several detrimental characteristics that make them particularly concerning from both environmental and biological perspectives. They possess long biological half-lives, allowing them to remain in organisms for extended periods without efficient metabolic elimination. Additionally, they have a high capacity for bioaccumulation and biomagnification, enabling them to concentrate in tissues and increase in abundance through the food chain. Their chemical stability contributes to strong environmental persistence, meaning they resist natural degradation processes and remain in ecosystems for decades or longer, posing sustained ecological and health risks ^[15].

The Red Sea represents a highly diverse and ecologically rich marine ecosystem, with more than 1,200 documented species of fish ^[16]. Sewage represents a significant environmental threat across the region. Coastal zones also host power and desalination plants, oil refineries, fertilizer production facilities, and chemical industries ^[17].

Fish and other seafood are frequently among the primary sources of metal exposure in the general population. When toxic metal concentrations in foods exceed permissible limits, they pose risks to human health and are prohibited from trade under many national and international regulations ^[18]. The experimental sites in Jeddah are subject to multiple contamination sources that significantly impact coastal water quality and marine ecosystems. The northern site (Dahaban) is near to Distillation Plant Dahaban which is a Water treatment plant. The southern site (Sarum) is close to the SAWACO seawater desalination plant and the Jeddah 2nd industrial city. These anthropogenic inputs may create distinct pollution gradients, making these locations ideal for comparative studies on heavy metal contamination and its effects on marine biota in the Red Sea ecosystem. This study investigates the effects of heavy metals on fish from the Red Sea, Jeddah. The research involves measuring the concentrations of selected heavy metals in seawater and fish liver, evaluating their impact on specific blood parameters, and examining histopathological alterations in fish liver tissue.

MATERIALS AND METHODS

Ethical Approval

The animal study has been reviewed and approved by ZU-IACUC committee. was performed in accordance with the guidelines of the Egyptian Research Ethics Committee and the guidelines specified in the Guide for the Care and Use of Laboratory Animals (2025). Ethical code number ZU-IACUC/3/F/284/2025.

Study Sites and Fish Sampling

This study was conducted from 2023 to 2024 in one of the major urban cities of the Kingdom of Saudi Arabia. Two sampling sites were selected, situated in the north and south of Jeddah. The northern site (Dahaban) is located about 50 km north of Jeddah city, at GPS coordinates 22°03'11.5"N and 38°55'16.5"E. It includes fishing areas and is close to the Distillation Plant Dahaban, which is a Water treatment plant. The southern site (Sarum) is located on the southern cornice of Jeddah, at GPS coordinates 21°07'32.5"N and 39°10'48.7"E, close to SAWACO seawater desalination plant and the Jeddah 2nd industrial city (Fig. 1).



Fig 1. Detailed map of Jeddah showing sampling locations

Eighteen water samples were collected from each site to ensure the collection of representative data. A map showing the geographic locations of these sampling stations in the northern and southern regions of Jeddah. The sites were selected based on their contrasting environmental conditions and pollution levels.

A total of 90 specimens of the emperor fish species, carset (*Lethrinus lentjan*, 21), Abu Bose (*Lethrinus microdon*, 12), Mohaysni (*Lethrinus mahsena*, 15), Abu Sirin (*Lethrinus obsoletus*, 9), khorrami (*Lethrinus nebulosus*, 8), Abu Nuqtah (*Lethrinus harak*, 7), saqa (*Lethrinus borbonicus*, 9), and abu Zahu - Kharmiya (*Lethrinus xanthochilus*, 9) were collected in a fish trap (cage) by local fishermen at each site. The species of fish were identified according to external features by Abu Shusha et al.^[19]. Fish samples were kept alive in clean tanks containing aerated seawater

and taken to the laboratory. For each fish, morphological measurements and blood drawn were taken. Then, all fish samples were dissected on the same day. The most abundant species of emperor fish were *Lethrinus lentjan* (Carset), *Lethrinus mahsena* (Mohaysni) and *Lethrinus microdon* (Abu Bose).

Water Analysis

The surface water samples from the north and south areas were collected in clean 1-L plastic bottles. All sample bottles were immediately transferred to a cool box to the National Water Company laboratory in Jeddah, where analyses were conducted on the same day of collection to avoid potential temporal effects on water quality parameters and heavy metal speciation.

Physicochemical Parameters

Each water sample was analyzed for water temperature (°C), pH, total dissolved solids (mg/L), and conductivity (µS/cm) using the multi meter (HACH, HQ40d, Loveland, CO, USA). Turbidity (NTU) was measured with the portable turbidimeter (HACH, 2100Q). Total hardness (mg/L), total alkalinity (mg/L), and chloride (mg/L) were determined using the AUTO Titration (Metrohm, 905 Titrando, potentiometric titration, Switzerland). Ammonia (mg/L), nitrate (mg/L), sulfate (mg/L), and iron (mg/L) were measured with the Laboratory Spectrophotometer (HACH, DR 5000™ UV-Vis).

Heavy Metal Analysis

The seawater samples were acidified to pH <2 with ultrapure nitric acid immediately upon arrival at the laboratory and then subjected to membrane filtration (0.45 µm) to remove particulates. Acidification and digestion were performed in the laboratory on the same day as collection, rather than in the field, to ensure sample integrity while allowing precise control of reagent purity and digestion conditions. Seawater samples were then diluted and analyzed for copper (Cu), zinc (Zn), lead (Pb), manganese (Mn), cadmium (Cd), and nickel (Ni) using a Perkin Elmer NexION 300X Inductively Coupled Plasma–Mass Spectrometer (ICP-MS). The ICP-MS was selected for seawater analysis due to its superior multi-element capability, very low detection limits (sub-µg/L), and high throughput, which are critical for trace-level determinations in complex saline matrices. The metals concentration was analyzed according to the American Public Health Association (APHA 3125) standard method. Metal concentrations in water samples are expressed as mg/L.

Morphological Parameters of Fish

In the laboratory, morphological measurements as conducted for all collected specimens. For each fish, the

total body length was measured to the nearest centimeter using a tape measure on a flat surface, and the total body weight was recorded to the nearest gram using digital balance (OHAUS, Scout pro balance). The condition factors of fish samples were calculated using the following equation ^[17]:

$$\text{Condition Factor (K)} = [\text{body weight (g)/body length}^3 (\text{cm}^3)] * 100.$$

In addition, other parameters (standard length, total length, fork length, head length, eye diameter, and body depth) of each fish were measured in (cm).

Biochemical and Hematological Parameters

The fish were anesthetized by adding 3-5 drops of clove oil to the water tank. Blood samples were withdrawn from the caudal vein using a heparinized syringe. Each blood sample was analyzed for the total cell count of red blood cells (RBCs), white blood cells (WBCs), neutrophils, lymphocytes, monocytes, eosinophils, basophils, hemoglobin (HGB), and platelets (PLT). A commercial kit for a complete blood count (CBC) from Bio-Lab Diagnostics Ltd. (Mumbai, India) was used to assess the blood cell count, following the manufacturer's recommendations. A hemocytometer was used in blood cell count, in which the blood diluting fluid was prepared as described by Svobodova et al.^[20]. The blood cells were counted on the counting chamber of a hemocytometer with the aid of a compound microscope.

In addition, blood samples were centrifuged at 2000 rpm for 20 min to obtain blood serum which was kept frozen at -20°C until being processed for various biochemical analyses: total protein [TP, Cat no 04810716, Roche Diagnostics (Switzerland)], albumin [ALB, OSR6102, Beckman Coulter (USA)], total bilirubin [BL, DF30, Siemens Healthineers (Germany)], aspartate aminotransferase [AST, 3L82, Abbott Diagnostics (USA)], alanine aminotransferase [ALT, 3L52, Abbott Diagnostics (USA)], gamma-glutamyl transferase [GGT, 3L72, Abbott Diagnostics (USA)], and alkaline phosphatase [ALP, 3L62, Abbott Diagnostics (USA)]. The biochemical analyses of blood samples were analyzed by Dynex Best 2000 automated microplate Immuno analyzer (DSX Automated Elisa System, Germany, Listing# 835485).

Collection of Liver Tissue for Heavy Metal Analysis

The dissected liver was removed and weighed to calculate the liver weight to body weight ratio then it was divided into liver tissue which will be fixed in 10% buffered formalin for histopathological examination. The other liver lobe will be frozen and kept at -20°C until biomarker analysis. Also, the concentrations of heavy metals iron (Fe, mg/kg), zinc (Zn, mg/kg), copper (Cu, mg/kg), manganese (Mn, mg/kg), nickel (Ni, mg/kg), lead (Pb, mg/kg), and cadmium (Cd, mg/kg) were measured in liver tissue using atomic absorption spectrophotometer (BIO RAD, SmartSpec Plus spectrophotometer). Liver digests were analyzed by

Atomic Absorption Spectrophotometry (AAS) because tissue matrices often require matrix-matched calibration, and AAS provides robust, cost-effective quantification for individual metals at higher concentration ranges. All metal determinations followed the APHA Method 3125 standard protocol, and results are reported as mg/L for water and mg/kg wet weight for liver samples. The liver tissues were transferred to an oven set at 80°C for 8 h until completely dried. Dry tissues were then digested in a mixture of concentrated nitric (HNO₃) and perchloric acids (HClO₄) according to the method described by Neugebauer et al.^[21]. The mixture in a flask was gently shaken and placed on a hot plate until the tissues were completely digested to clear solutions. Then, the concentration (mg/L) of heavy metals in the solution is measured using an atomic absorption spectrophotometer.

Collection of Liver Tissue for Histological Examination

Fixed liver in phosphate-buffered formal saline was dehydrated and embedded in paraffin as blocks. Then they were sectioned (8 µm thickness), spread on glass slides, and stained with haematoxylin and eosin (H & E)^[22].

Statistical Analysis

The statistical analyses for the data were conducted using the Statistical Package for the Social Sciences (SPSS). Significant differences between the north and south areas were tested using two-sample t-tests at a probability level of $P < 0.05$.

RESULTS

Physicochemical Parameters of Seawater

The physicochemical parameters of seawater at the north and south areas are presented in in *Table 1*. Surface water temperature and total hardness were relatively

consistent between the two sites. Electrical conductivity and total dissolved solids (TDS) were slightly higher in the northern area compared to the southern area. A notable difference in pH was observed, with the southern area showing a significantly higher pH than the northern area ($P < 0.01$). Additionally, turbidity was significantly higher in the north than in the south ($P < 0.01$). Total alkalinity was significantly greater in the southern site compared to the northern site ($P < 0.05$). The sulfate concentration was higher in the north than in the south ($P < 0.05$). No noticeable differences were observed in chloride and nitrate levels between the two locations, and ammonia concentrations remained below detectable levels (< 0.1 mg/L) across all samples.

Heavy Metals in Water

Table 2 displays the amounts of heavy metals in water samples taken from the north and south locations. All samples had cadmium (Cd), lead (Pb), copper (Cu), and zinc (Zn) levels below the limit of detection, which is less than 0.002 mg/L. The north had greater quantities of nickel (Ni) than the south. The northern samples had slightly higher concentrations of iron (Fe) than the southern ones. The north area had a higher concentration of Mn in water samples compared to the south area.

Morphological Parameters of Fish

Table 3 and *Table 4* display the data for each fish species from the north and south areas with respect to their total body weight, liver weight, standard length, fork length, body depth, head length, eye diameter, condition factor (K), and hepatosomatic index, which is the ratio of liver weight to body weight. The total body weight of *L. lentjan* was highest in the northern region, whereas that of *L. borbonicus* was lowest. When compared to other species in the south, *L. xanthochilus* had the highest total body

Table 1. Mean ± SE of physicochemical parameters in seawater from two areas			
Parameters	North	South	P Value
Temperature (°C)	22.143±0.15	22±0	0.9 NS
Electrical Conductivity (mS/cm)	62.09±0.93	61.84±0.05	0.89 NS
Total dissolved solids (mg/L)	41942.86±1046.96	39820±20	0.75 NS
pH	7.45±0.14	8.082±0.03**	<0.01
Turbidity (NTU)	9.14±1.08**	5.38±0.20	<0.01
Total Hardness(mg/L)	7862.43±55.64	7898.4±22.77	0.99 NS
Total Alkalinity(mg/L)	180±10.19	210.4±6.14*	<0.05
Ammonia(mg/L)	<0.1	<0.1	-
Chloride(mg/L)	34423.86±2408.54	29236.2±713.84	0.13 NS
Nitrate(mg/L)	1.02±0.31	1.19±0.08	0.89 NS
Sulfate(mg/L)	861.86±316.12*	349.4±48.55	<0.05
Two- sample t-test, * $P < 0.05$; ** $P < 0.01$, NS: Not significant			

Table 2. Mean \pm SE of some heavy metal concentrations in water from two areas

Heavy Metals	North	South	WHO (2011)	P Value
Cd(mg/L)	<0.002	<0.002	0.003	0.99 NS
Pb(mg/L)	<0.002	<0.002	0.01	0.95 NS
Cu(mg/L)	<0.002	<0.002	2.00	0.99 NS
Zn (mg/L)	<0.002	<0.002	3.00	0.99 NS
Ni (mg/L)	1.68 \pm 1.32*	0.18 \pm 0.05	0.05	<0.05
Fe (mg/L)	0.077 \pm 0.006	0.070 \pm 0.006	0.30	0.98 NS
Mn (mg/L)	1.04 \pm 0.22	0.67 \pm 0.19	0.50	0.045

Two- sample t-test; * P<0.05; ** P<0.01; NS: Not significant

weight while *L. obsoletus* had the lowest. The liver weights of the northern *L. lentjan* and *L. nebulosus* were higher than those of the other species, whereas the liver weights of the *L. microdon* were much lower. Liver weight was highest in *L. mahsena* and lowest in *L. obsoletus* in the southern region.

In the northern region, *L. lentjan* had the longest total body length, whilst *L. borbonicus* had the shortest. The total body length of *L. xanthochilus* was the longest in the southern region, whilst that of *L. obsoletus* was the shortest.

Similarly, in the northern region, *L. lentjan* had the longest forks and *L. borbonicus* the shortest. In the southern region, *L. xanthochilus* had the longest forks and *L. obsoletus* the

Table 3. Mean \pm SE of morphological parameters of fish from two areas

Area	Species	Total Body Weight (g)	Liver Weight (g)	Total Body Length (cm)	Condition Factor (K)	Hepatosomatic Index
North	<i>L. lentjan</i>	397.24 \pm 26.01	3.90 \pm 0.35	30.11 \pm 0.79	1.42 \pm 0.03	1.01 \pm 0.07
	<i>L. obsoletus</i>	240.25 \pm 0.25	2.60 \pm 0.2	25.7 \pm 0.10	1.46 \pm 0.025	1.05 \pm 0.05
	<i>L. nebulosus</i>	226.5 \pm 36.5	3.45 \pm 0.95	24.75 \pm 1.05	1.48 \pm 0.05	1.49 \pm 0.18
	<i>L. mahsena</i>	193.58 \pm 20.28	2.60 \pm 0.37	22.49 \pm 0.76	1.63 \pm 0.03	1.30 \pm 0.09
	<i>L. microdon</i>	165.29 \pm 37.80	1.68 \pm 0.44	22.60 \pm 1.55	1.30 \pm 0.05	1.02 \pm 0.11
	<i>L. borbonicus</i>	165.15 \pm 22.85	1.80 \pm 0	22.30 \pm 0.40	1.48 \pm 0.13	1.11 \pm 0.15
South	<i>L. xanthochilus</i>	221.25 \pm 68.75	1.85 \pm 0.55	25.40 \pm 2.10	1.30 \pm 0.09	0.84 \pm 0.01
	<i>L. mahsena</i>	218.67 \pm 45.20c	3.13 \pm 0.84	23.23 \pm 1.25	1.70 \pm 0.09	1.40 \pm 0.08
	<i>L. harak</i>	183.08 \pm 11.79	2.34 \pm 0.23	23.18 \pm 0.54	1.41 \pm 0.02	1.22 \pm 0.09
	<i>L. obsoletus</i>	126.4 \pm 0.2	1.15 \pm 0.15	21.25 \pm 0.5	1.31 \pm 0.12	0.80 \pm 0.01

Table 4. Mean \pm SE of morphological parameters of fish from two areas

Area	Species	Fork Length (cm)	Standard Length (cm)	Body Depth (cm)	Head Length (cm)	Eye Diameter (cm)
North	<i>L. lentjan</i>	28.23 \pm 0.71	25.70 \pm 0.65	10.08 \pm 0.28	8.44 \pm 0.25	1.65 \pm 0.04
	<i>L. obsoletus</i>	24.55 \pm 0.05	22.45 \pm 0.25	8.50 \pm 0.1	7.70 \pm 0.2	1.75 \pm 0.15
	<i>L. nebulosus</i>	23.30 \pm 0.70	20.95 \pm 0.55	8.35 \pm 0.45	6.95 \pm 0.25	1.60 \pm 0.1
	<i>L. mahsena</i>	21.12 \pm 0.70	19.71 \pm 0.85	8.67 \pm 0.25	6.52 \pm 0.21	1.65 \pm 0.07
	<i>L. microdon</i>	21.03 \pm 1.39	19.38 \pm 1.29	7.45 \pm 0.29	6.55 \pm 0.53	1.54 \pm 0.04
	<i>L. borbonicus</i>	20.70 \pm 0.20	19.65 \pm 0.15	8.10 \pm 0.80	6.20 \pm 0	1.45 \pm 0.15
South	<i>L. xanthochilus</i>	23.70 \pm 2.20	22.0 \pm 1.90	7.25 \pm 0.15	7.75 \pm 0.85	1.90 \pm 0.10
	<i>L. mahsena</i>	21.77 \pm 1.16	20.27 \pm 1.16	8.97 \pm 0.52	6.63 \pm 0.33	1.60 \pm 0
	<i>L. harak</i>	21.70 \pm 0.51	19.77 \pm 0.49	7.70 \pm 0.19	6.37 \pm 0.18	1.60 \pm 0.04
	<i>L. obsoletus</i>	19.75 \pm 0.5	18.1 \pm 0.1	7.15 \pm 0.05	6.05 \pm 0.15	1.45 \pm 0.05

shortest. Similar patterns emerged when looking at the standard length, with *L. lentjan* being the longest in the northern region and *L. borbonicus* and *L. microdon* were the shortest. Standard length was greatest for *L. xanthochilus* and lowest for *L. obsoletus* in the southern region. Among the northern species, the body depth in north area was the highest in *L. lentjan* and whereas was the lowest in *L. microdon*. The body depth in south area of *L. mahsena* was the highest, whereas *L. obsoletus* was the lowest among other fish species.

Head length was greatest in *L. lentjan* in the northern region and lowest in *L. borbonicus*. The southern region showed the greatest head length in *L. xanthochilus* and the shortest in *L. obsoletus*. In terms of eye diameter, the northern species of *L. obsoletus* had the largest measurement, while the southern species of *L. borbonicus* had the smallest. In the southern region, *L. obsoletus* had the smallest eyes and *L. xanthochilus* the biggest.

In the northern region, *L. mahsena* had the greatest condition factor (K) value, whilst *L. microdon* had the lowest. While *L. obsoletus* and *L. xanthochilus* displayed the lowest values in the southern area, and *L. mahsena* had the highest. In the northern region, *L. nebulosus* had the greatest hepatosomatic index, whilst *L. lentjan* and *L.*

obsoletus had the lowest. The hepatosomatic index was highest in *L. mahsena* and lowest in *L. xanthochilus* and *L. obsoletus* in the southern region.

Biochemical Blood Analysis

The biochemical analysis of fish serum from the North and South areas revealed significant differences across several liver function markers, protein metabolites (Table 5). Fish from the North area exhibited higher mean values for alanine aminotransferase (ALT), aspartate aminotransferase (AST), alkaline phosphatase (ALP), and gamma-glutamyl transferase (GGT) compared to those from the South area, suggesting increased hepatic enzyme activity and possible hepatocellular stress or damage in the North. In addition, albumin, bilirubin and total protein concentrations were slightly higher in the North area, further supporting altered liver function or protein metabolism in the North relative to the South.

Hematological Parameters of Blood

The values of WBCs, RBCs, platelets, hemoglobin, neutrophils, lymphocytes, monocytes, eosinophils, and basophils in blood fish samples are shown in Table 6. In this study, the average hematological parameters during the study period were higher in the northern

Table 5. Mean \pm SE of biochemical parameters in fish serum from two areas

Parameter		Unit	North Area	South Area	P Value
Liver Function Markers	ALT	U/L	30.48 \pm 4.32*	23.94 \pm 8.92	<0.05
	AST	U/L	41.29 \pm 5.91*	30.16 \pm 10.25	<0.05
	ALP	U/L	70.56 \pm 10.21*	63.20 \pm 13.80	<0.05
	GGT	U/L	35.89 \pm 6.87*	26.50 \pm 9.75	<0.05
Protein and Metabolites	Albumin	g/dL	4.60 \pm 0.52	3.86 \pm 0.78b	0.75 NS
	Bilirubin	mg/dL	1.06 \pm 0.18	0.88 \pm 0.14	0.62 NS
	Total Protein	g/dL	6.63 \pm 0.39	6.50 \pm 0.74	0.81 NS

Two- sample t-test; * P<0.05; ** P<0.01; NS: Not significant

Table 6. Mean \pm SE of hematological parameters in fish blood from two areas

Hematological Parameters	North	South	P Value
WBCs (cells/cubic millimetre)	12.26 \pm 0.97 $\times 10^3$	9.05 \pm 1.06 $\times 10^3$	0.67 NS
RBCs (cells/cubic millimetre)	4.67 \pm 0.60 $\times 10^6$	6.32 \pm 0.58 $\times 10^6$	0.58 NS
Platelets (cells/cubic millimetre)	783.42 \pm 76.71*	630.5 \pm 60.19	<0.05
Haemoglobin (g/dl)	10.7 \pm 0.53	12.23 \pm 0.59	0.15 NS
Neutrophil (%)	31.83 \pm 1.87	45.00 \pm 3.78*	<0.05
Lymphocyte (%)	53.17 \pm 2.50*	42.83 \pm 2.07	<0.05
Monocyte (%)	11.00 \pm 1.2	9.33 \pm 1.43	0.11 NS
Eosinophil (%)	3.52 \pm 0.61	2.17 \pm 0.60	0.23 NS
Basophil (%)	0.5 \pm 0.15	0.67 \pm 0.21	0.74 NS

Two- sample t-test; * P<0.05; ** P<0.01; NS: Not significant

area for some parameters. Conversely, levels of RBCs, hemoglobin, neutrophils, and basophils were higher in the southern area.

Although white blood cell counts were greater in the northern region than in the southern region, this difference did not reach statistical significance ($P>0.05$). Relative to this, there was no discernible difference between the north and the south in terms of RBC levels; nonetheless, southern levels were higher. Northern platelet counts were significantly greater than southern ones ($P<0.05$). While there was no statistically significant difference, northern regions had lower hemoglobin levels and southern regions had greater ones. In the south, there was a noticeable and statistically significant rise in neutrophil counts when contrasted with the north ($P<0.05$). On the other hand, there was a slight but noticeable increase in lymphocyte counts in the north. The north had somewhat higher numbers of monocytes and eosinophils, whereas the south had somewhat higher levels of basophils. But these variations did not reach a statistically significant level.

Heavy Metal Determination in Liver

Table 7 presents an analysis of heavy metal concentrations in the liver tissue. The accumulation pattern varied between the two areas: the North area showed higher concentrations of most metals, including Iron (Fe), Zinc (Zn), Manganese (Mn), Cadmium (Cd), and Nickel (Ni), may suggesting a broader and more intense source of industrial or multiple pollution sources in that region. Conversely, the South area had higher levels of Copper (Cu) and Lead (Pb), which could point to different contamination sources, such as agricultural practices (e.g., copper-based pesticides) or historical use of leaded fuel. The high levels of Cd are especially concerning because this metal has no biological role and is known to cause extensive cellular damage, impair neurological functions, and lead to organ failure. This data provides a clear and compelling explanation for the physiological changes previously observed in these fish. The significantly elevated liver enzymes (ALT, AST) are classic biomarkers

of liver cell damage and necrosis, directly linked to the toxic effects of these accumulated metals.

Histological Examination of Fish Liver

The liver of fish from south area: The largest portion of the liver consists of hepatic tissue, while a smaller portion includes pancreatic tissue, blood sinusoids, and bile ducts. In some specimens, vacuolated hepatocytes with deeply stained nuclei, exocrine pancreatic tissue surrounding the portal vein, and connected to blood sinusoids were observed (**Fig. 2-A**). Their cytoplasm is filled with lipids in the form of large lipid droplets. Additionally, histological examination revealed blood congestion in the blood sinusoids of most of the studied fish. Bile ducts, mostly located near the central vein in the liver tissue and close to exocrine pancreatic tissue (**Fig. 2-B,C**), were also observed. Furthermore, some specimens displayed exocrine pancreatic tissue surrounding the portal vein, separated from hepatocytes by wide spaces

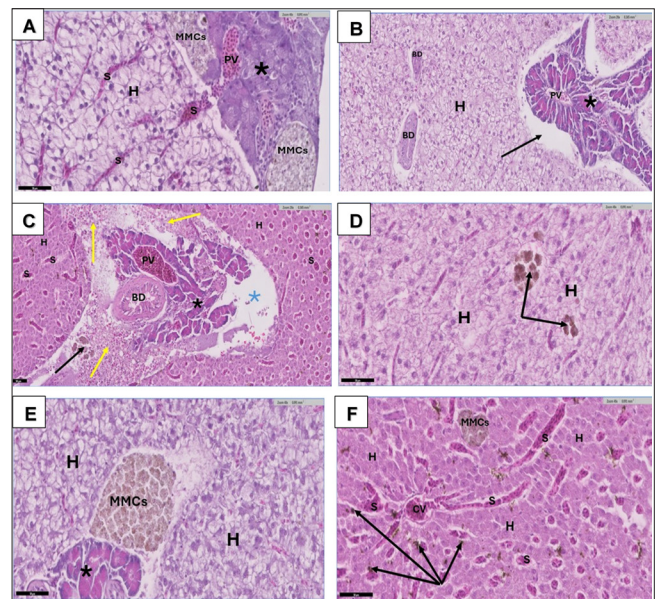


Fig 2. Histological sections of liver of south area showing: (A) Vacuolated hepatocytes (H) with deeply stained pyknotic nuclei, exocrine pancreatic tissue (*) surrounding portal vein (PV) and connected with blood sinusoids (S). Note: The melano-macrophage center (MMC) inside the exocrine pancreas (X 400 H&E). (B): Another liver section with numerous congested blood sinusoids (s) between deeply stained acidophilic hepatocytes (H), exocrine pancreatic tissue (*) surrounding portal vein (PV) and bile duct (BD). Note: The exocrine pancreatic tissue separated from hepatocytes by wide space (blue star), blood exudate (yellow arrows) and brown pigments (black arrow) (X 200 H&E). (C): numerous congested blood sinusoids (s) between deeply stained acidophilic hepatocytes (H), exocrine pancreatic tissue (*) surrounding portal vein (PV) and bile duct (BD). Note: The exocrine pancreatic tissue separated from hepatocytes by wide space (blue star), blood exudate (yellow arrows) and brown pigments (black arrow) (X 200 H&E). (D): accumulation of brown pigments (black arrows) between the vacuolated hepatocytes (H) (X 400 H&E). (E): vacuolated hepatocytes with deeply stained pyknotic nuclei (H), melano-macrophage center (MMC) and exocrine pancreas (X 400 H&E). (F): numerous congested blood sinusoids (s) between deeply stained acidophilic hepatocytes (H) and surrounding the central vein (CV). Note: the presence of brown pigments (black arrow) between the hepatocytes (X 400 H&E)

Table 7. Mean \pm SE of heavy metal concentrations (mg/kg wet weight) in liver tissue of fish from two areas

Heavy Metal	North Area	South Area	P Value
Fe (mg/kg)	2.31 \pm 0.30**	1.40 \pm 0.11	<0.01
Cu (mg/kg)	0.86 \pm 0.10	1.25 \pm 0.12*	<0.05
Zn (mg/kg)	2.79 \pm 0.15**	1.55 \pm 0.16	<0.01
Pb (mg/kg)	1.59 \pm 0.11	2.19 \pm 0.16*	<0.05
Mn (mg/kg)	2.01 \pm 0.12	1.68 \pm 0.10	0.88 NS
Cd (mg/kg)	4.26 \pm 0.22**	2.79 \pm 0.20	<0.01
Ni (mg/kg)	2.44 \pm 0.26**	1.29 \pm 0.11	<0.01

Two- sample t-test; * $P<0.05$; ** $P<0.01$; NS: Not significant

containing blood exudate and brown pigments (Fig. 2-C). The bile ducts are lined with cuboidal cells and are visible between the hepatocytes (Fig. 2-B). The presence of hemosiderin pigments was noted on hepatocytes, near blood sinusoids of fish from the southern area, and between the vacuolated hepatocytes (Fig. 2-D,F). Numerous congested blood sinusoids were observed between deeply stained acidophilic hepatocytes (Fig. 2F). The melano-macrophage center (MMC) is a special type of macrophage that contains various pigments, appears as a pigment cluster, and is surrounded by a capsule of simple squamous epithelium. Moreover, some MMCs were found surrounded by exocrine pancreatic tissue within the interstitial tissue, as well as located in the hepatic parenchyma (Fig. 2-A,E,F). These macrophages have small peripheral nuclei and contain various pigments in their cytoplasm, including brown melanin pigments.

The Liver of Fish From the Northern Area

The liver of fish from the northern area shows that the parenchymal hepatocytes are radially arranged around a central vein in cords of two cells thick. Narrow, straight blood sinusoids stemming from the central vein separate each cord. These sinusoids are covered by typical elongated endothelial cells with flattened nuclei (Fig. 3-A). The H&E-stained sections reveal hepatocytes with a normal appearance of vacuolar cytoplasm, likely due to numerous lipid droplets, with small amounts of cytoplasm and rounded, vesicular nuclei (Fig. 3-B). The pancreatic exocrine tissue is distributed within the liver as part of the hepatopancreas. Microscopic observations indicate that pancreatic cells are differentiated from hepatic tissue by their basophilic basal part and eosinophilic apical cytoplasm (Fig. 3-B,D). The epithelium of bile ducts is simple (Fig. 3-C). Hepatocytes that are highly vacuolated and degenerated, showing nuclear karyolysis, along with a dilated and congested central vein with a thick wall and clumps of brown pigments, were observed (Fig. 3-E). In some specimens, a C-shaped hyaline, acidophilic structure, possibly a worm, surrounded by a connective tissue capsule and located near the central vein, was seen (Fig. 3-F). Cells from the MMC aggregations are situated close to the hepatic blood vessels, bile ducts, and alongside the hepatopancreas (Fig. 3-A,D). Liver histology findings showed that the North area had a mean liver damage score of 2.0, indicating moderate hepatocellular degeneration, congestion, and prominent melanomacrophage centers. Conversely, the South area had a lower mean score of 0.5, reflecting mainly normal or mild changes and a relatively intact liver structure.

DISCUSSION

In this study, we measured physicochemical parameters and heavy metal concentrations in seawater and examined

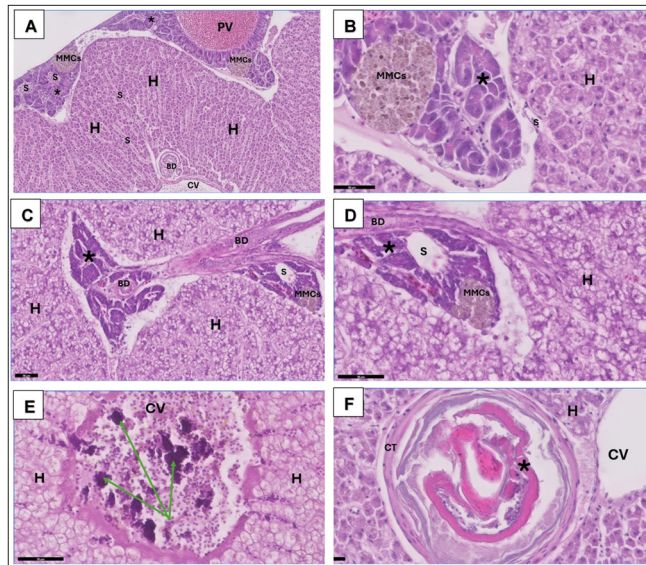


Fig 3. Histological sections of liver of north area showing: (A): Hepatic cell cords (H) radiating from the central vein (CV) and separated by blood sinusoids (S), exocrine pancreatic tissue (*) surrounding portal vein (PV) and blood sinusoids (S). Note: the melano-macrophage center (MMCs) and bile duct (BD) (X 100 H&E). (B): vacuolated hepatocytes (H) with vesicular nuclei and exocrine pancreatic tissue (*) surrounding the melano-macrophage center (MMCs). Note: the blood sinusoid (S) between the hepatocytes (X 400 H&E). (C): highly vacuolated hepatocytes (H) with nuclear karyolysis, degenerated exocrine pancreatic tissue (*) and bile ducts (BD). Note: the melano-macrophage center (MMCs) and the blood sinusoid (S) (X 200 H&E). (D): A higher magnification of the previous section shows highly vacuolated hepatocytes (H) with nuclear karyolysis, degenerated exocrine pancreatic tissue (*) and bile ducts (BD). Note: the melano-macrophage center (MMCs) and the blood sinusoid (S) (X 400 H&E). (E): highly vacuolated and degenerated hepatocytes (H) with nuclear karyolysis, dilated and congested central vein (CV) with thick wall and contained clumps of brown pigments (green arrows) (X 400 H&E). (F): vacuolated hepatocytes (H) with deeply stained pyknotic nuclei and appearance of C- shaped hyaline acidophilic structure (may be worm) (*) surrounded by connective tissue capsule (CT) located adjacent to the central vein (CV) (X 400 H&E)

the metabolic responses of emperor fish in northern and southern Jeddah, Red Sea. The results show that the northern area had higher average values for electrical conductivity (EC), total dissolved solids (TDS), chloride, sulfate, and turbidity, while the southern area had higher pH, total alkalinity, total hardness, and nitrate levels. Statistically significant differences were found for pH, turbidity, sulfate, and total alkalinity ($P < 0.05$).

All regions have mean pH values within the WHO-recommended 6.5-8.5 range. The north has lower pH levels (6.82-8.00) could be due to organic matter decomposition, whereas the south has higher pH values (up to 8.15) could be due to algal photosynthesis reducing CO_2 concentrations. CO_2 absorption from saltwater raises pH [23]. Many investigations in contaminated Al-Kumrah found pH levels of 6.62 and 7.00. In Jeddah city, various studies found pH of 7.84 in Rabigh and 8.31 in Al-Shoaibah [24]. The average TDS in two locations was greater than 30,000 mg/L, indicating that they were saline

water, which ranged from 30.000 to 40.000 mg/L. The Red Sea's high salinity and geographical location caused TDS concentrations to rise in the Shuaiba region to 38.600 to 48,400mg/L^[25]. In addition, EC analyzes water's dissolved ions and increased ion content from wastewater discharges drove EC similarly^[26]. The average EC at Safaga along the Egyptian red sea was 60.6 mS/cm. Elevated chloride, nitrate, and phosphate concentrations in sewage flow may explain the observed increases in electrical conductivity and temperature in these two regions^[27].

The low ammonia levels (<0.1 mg/L) in both regions may suggest minimal sewage impact. Rising nitrate levels in the south may indicate human-caused fertilizer loading, which may boost phytoplankton productivity. Younis et al.^[25] discovered minimum ammonia concentrations in Shuaibah, Red Sea water samples, ranging from 0.03 to 0.11 mg/L. Nitrogen forms, released effluents, phytoplankton uptake rate, and nitrification or denitrification in the research region may be affected by human activities. The north had turbidity levels above 5 NTU, which might be due to sedimentation and effluents, whereas the south met the clarity norms. Human impact appears to have decreased in the south. The northern spike may be due to more sewage and soil particles entering the sea^[27].

Natural geochemical characteristics and mineral-rich discharges may have created increased overall hardness and alkalinity in the north^[28]. Higher alkalinity in both places may raise carbonate concentrations, which buffer water. GoA's coastal waters have increased buffering ability due to the high concentration of calcium carbonates in the water column^[29].

Both regions have chloride and sulfate levels above the WHO recommendations, which are ≤ 250 and ≤ 500 mg/L, respectively. High chloride levels indicate environmental salinity and possibly industrial inputs, especially near desalination plants. Sulfate levels, however, are lower than in other studies, suggesting a lack of anthropogenic impacts. Al-Taani et al.^[29] found that Cl concentrations ranged from 13.500 to 35.000 mg/L and sulfate concentrations from 2.600 to 8.900 mg/L, indicating that desalination plant discharge may cause a significant concentration of chloride ions in the water, which is similar to the current study in the south.

In general, the north of Jeddah had the highest mean values for most metrics. The discharge of treated and untreated sewage and industrial effluents from enterprises and factories may cause these results. This is comparable to Red Sea areas affected similarly^[30]. In the present study, the means of Cd, Pb, Cu, and Zn were below the detection limit in two areas. In addition, Ni, Fe, and Mn were higher in the north area compared to the south area. The concentration of most heavy metals in seawater in

the north and south areas was below the WHO standards, except Mn and Ni. The concentrations of Mn, and Ni in the water of the south area were slightly higher than permitted ones, while those in the water of north area had greatly exceeded them.

The rise in heavy metal levels in seawater is directly linked to human activities. This correlation is supported by the findings of Al-HasawiHassanine^[24], which reported elevated levels of heavy metals in the Al-Khamra area of Jeddah, likely attributed to anthropogenic sources. The concentrations of Cd, Cu, Fe, Mn, Zn, Ni, and Pb collected from were significantly higher in this study compared to the current study. ICP-MS is selected for water analysis due to its ultra-trace sensitivity, which allows reliable measurement of elements at extremely low concentrations (down to parts per trillion), matching the low analyte content and simple matrix of water samples. In contrast, AAS is well-suited for biological samples like liver because it effectively manages moderate-to-high analyte concentrations and performs reliably in less complex organic matrices, while also being cost-effective for routine single-element quantification.

Fish morphological parameters varied widely. These variations in total length, body weight, and condition factor are normal and due to species, age, sex, and size. Fish size may fluctuate due to high water metal levels^[31]. *Lethrinus lentjan* in the north and *xanthochilus* in the south had the highest mean overall length and weight in this study. In *Lethrinus obsoletus*, overall length and weight averaged lowest. The current study matches GabrMal^[32], who found a link between length and weight for the top ten coral reef fish species from southern Jeddah. Shellem et al.^[33] showed an average total length of 27.2 cm for Jeddah *Lethrinus xanthochilus*, supporting the current study. *Lethrinus lentjan* averaged 27.31 cm in Egypt^[34], similar to the current study.

The condition factor K values indicate fish health, and greater K values reduced illnesses^[35]. A condition factor greater than one indicates fish fitness, which is supported by the current study's K value of 1.30-1.70, indicating healthy body weights. The hepatosomatic index (HSI) is the main metabolic indicator in animals. Varea et al.^[36] reported 1.42 and 0.47 condition factors and HSI in Viti Levu, Fiji's *Lethrinus harak* in the wet season.

The livers of emperor fish from two regions have higher ALT, AST, ALP, and GGT. The north region fish have higher liver enzymes than south area fish, may indicate persistent toxicity from ambient habitat toxicants. This contradicts Al-HasawiHassanine^[24] who analyzed liver enzymes in Jeddah-trapped emperor fish *Lethrinus harak*. Results indicate greater amounts of total protein, albumin, and bilirubin in the northern area, with no

significant difference ($P < 0.05$). Liver structural alterations that reduce aminotransferase and deamination may raise plasma protein levels. Total protein and albumin are essential fish metabolites. Fish total protein and albumin levels are important indicators for aquatic ecosystem toxicity^[37]. Serum biochemistry ranges vary by species and are regulated by seasonal changes, water temperature, nutrition, fish age, and sex^[38]. Thus, greater liver functions in the north may indicate higher pollution exposure than in the south.

Elevated liver enzymes, such as aspartate aminotransferase (AST), alanine aminotransferase (ALT), and gamma-glutamyl transferase (GGT), are commonly observed in individuals exposed to heavy metals like lead (Pb), cadmium (Cd), and mercury (Hg). These enzymes are released into the bloodstream when hepatocytes are injured or undergo necrosis, often as a result of cellular stress and the toxic effects of heavy metals. The primary mechanism behind this association is the induction of oxidative stress: heavy metals increase the production of reactive oxygen species (ROS), disrupt antioxidant defense systems, and damage cell membranes, leading to hepatocyte dysfunction and death. This oxidative stress induces the leakage of intracellular enzymes into the circulation, which serves as a sensitive indicator of liver injury and early hepatic toxicity in both epidemiological and experimental studies

Hematological parameters were selected based on their recognized sensitivity and importance in toxicological research. The results of this study are similar to those of El-Hamed et al.^[39] which they assessed many blood parameters (WBCs, hemoglobin, neutrophil, monocyte, and eosinophil) in *Lethrinus harak* fish from Safaga, Egypt. However, in contrast to this study, the RBCs values were lower, whereas the lymphocyte values were higher. In the current study, the means of WBCs, platelets, lymphocyte, monocyte, and eosinophil were higher in the north area. On the other hand, the means of RBCs, hemoglobin, neutrophil, and basophil were higher in the southern area. Stressful conditions often lead to decreased RBC counts and hemoglobin levels in fish. This stress-induced anemia serves as a valuable indicator for assessing environmental stress. This finding agrees with RBCs and hemoglobin levels in the current study where its level was less in the northern area. According to Javed et al.^[40] who observed increased WBC in *Channa punctatus* fish. Leukocytosis may be indicative of the extent of tissue damage and stress caused by heavy metals, potentially reflecting an activated immune response^[41]. So, this finding agrees with WBC levels in the current study where its level was high in the northern area.

Fish growth is negatively affected by contaminated food that contains high levels of heavy metals. A clear indicator

of metal toxicity in fish is the stunted growth^[42]. The mean concentrations of Fe, Zn, Mn, Cd, and Ni in liver tissue of fish from the north area were higher than fish from south area. On other hand, the mean of Cu and Pb were high in the south area. A significant difference was found in all concentrations of heavy metals in the emperor liver between the two areas at ($P < 0.05$) expect Mn. In the present study, the concentration of most heavy metals at two areas were below the FAO standards expect Cd and Mn in two areas and the Pb concentration on south area. Several studies have shown the effect of heavy metal pollution on liver tissue in emperor fish collected from the Red Sea, Jeddah Coast, Saudi Arabia^[43]. The liver is essential for detoxification and storage, serving as a key organ for both the accumulation and elimination of heavy metals from the body. The liver tissues tend to accumulate higher levels of heavy metals compared to muscle tissue, which is the primary edible portion and typically exhibits lower concentrations. This occurrence can happen even when the levels of heavy metals in water are low or not detectable^[44].

Thus, south-area emperor fish livers have better histological structure than north-area fish. This study found MMCs in the hepatic parenchyma of all fish species from two regions. MMCs aggregates contain Kupffer-like phagocytic cells. Al-Khumrah and Sudanese Red Sea investigations have found MMCs. Large MMC densities are usually linked to degenerative and necrotic liver diseases^[23,24]. Several northern specimens had extremely vacuolated and degraded hepatocytes with karyolytic nuclei. Many vacuolar structures and dark particles were found. Histological changes in fish liver tissue may be due to Kupffer cells, which detoxify contaminants or fat buildup in hepatocytes^[31]. Also, in Jeddah fish like *Lethrinus harak*^[23,24] and *Naso hexacanthus*^[45]. Lipid droplets were observed in both locations, but the southern area's cytoplasm had larger droplets, indicating more lipid buildup. Severe fatty infiltration caused hepatomegaly and pale liver tissue. Histologically, hepatocytes had extensive lipid droplets. In necrotic hepatocytes, these droplets showed as empty vacuoles as Mohammed et al.^[46]. Some current study specimens have blood sinusoids and central venous congestion. This study agrees with Jenjan et al.^[47], who found central venous congestion caused by larger hepatocytes with hydropic degeneration. Dilatation congests *Siganus rivulatus* hepatic blood sinusoids and arteries. Agree with Mohamed et al.^[48] in *S. rivulatus* and MahmoudAbd El Rahman^[49] in *Mugil capito* fish. Hepatocyte deterioration and blood sinusoidal congestion were found. Jasim Aldoghachi et al.^[50] also found liver deterioration and sinusoidal congestion in Pb and Cd-exposed fish. In conclusion, the results of this study show that *Lethrinus* fish, which were collected the northern

shore of Jeddah, are negatively affected by heavy metal pollution in terms of their liver function, blood parameters, and tissue structure. There may be dangers to human and environmental health from the elevated concentrations of Mn, Ni, Pb, and Cd, which surpassed international safety limits. The results highlight the critical need for monitoring and controlling coastal contamination and provide support for the idea that *Lethrinus* species can be useful bioindicators of marine pollution.

DECLARATIONS

Availability of Data and Materials: The datasets used and/or analyzed during the current study are available from the corresponding author (SAA) on reasonable request.

Competing Interests: The author declared that there is no conflict of interest.

Acknowledgment: This work was funded by the University of Jeddah, Jeddah, Saudi Arabia, under grant No. (UJ-24-FR-2222-1). Therefore, the authors thank the University of Jeddah for its technical and financial support.

Funding: This work was funded by the University of Jeddah, Jeddah, Saudi Arabia, under grant No. (UJ-24-FR-2222-1). Therefore, the authors thank the University of Jeddah for its technical and financial support.

Ethical Approval: The animal study has been reviewed and approved by ZU-IACUC committee. was performed in accordance with the guidelines of the Egyptian Research Ethics Committee and the guidelines specified in the Guide for the Care and Use of Laboratory Animals (2025). Ethical code number ZU-IACUC/3/F/284/2025.

Author Contributions: Sahar J. Melebary, and Soha A. Alsolmy: conceptualization, project administration, funding acquisition: Raoum MominKhan, writing the original draft, writing - review, and editing.

REFERENCES

1. Babayev FF: Food security in Azerbaijan in the context of global challenges. Role of business competitiveness. *Rev Univ Soci*, 15, 352-362, 2023.
2. Gupta A, Kaicker A: Food security and human health. *J Ecophysiol Occup*, 23 (3): 99-104, 2023. DOI: 10.18311/jeoh/2023/34445
3. ACTION B: The State of World Fisheries and Aquaculture. Food and Agriculture Organization (FAO), Rome, Italy, 2020. DOI: 10.4060/ca9229en
4. Dongyu Q: The State of World Fisheries and Aquaculture - Blue Transformation in Action. The State of World Fisheries and Aquaculture, Rome, Italy, R1-232, 2024. DOI: 10.4060/cd0683en
5. Van Anrooy R, Espinoza Córdova F, Japp D, Valderrama D, Gopal Karmakar K, Lengyel P, Parappurathu S, Upare S, Tietze U, Costelloe T, Zhang Z: World review of capture fisheries and aquaculture insurance - 2022. Food & Agriculture Org. 682, 2022. DOI: 10.4060/cb9491en
6. Organization WH: Population nutrient intake goals for preventing diet-related chronic diseases. <http://www.who.int/nutrition/topics/>, 2007.
7. Kuppusamy S, Maddela NR, Megharaj M, Venkateswarlu K, Kuppusamy S, Maddela NR, Megharaj M, Venkateswarlu K: Fate of total petroleum hydrocarbons in the environment. In, Total Petroleum Hydrocarbons: Environmental Fate, Toxicity, and Remediation, 57-77, 2020.
8. AbuQamar SF, El-Saadony MT, Alkafaas SS, Elsalahaty MI, Elkafas SS, Mathew BT, Aljasma AN, Alhammadi HS, Salem HM, Abd El-Mageed TA, Zaghloul RA, Mosa WFA, Ahmed AE, Elrys AS, Saad AM, Alsaed FA, El-Tarabily KA: Ecological impacts and management strategies of pesticide pollution on aquatic life and human beings. *Mar Pollut Bull*, 206:116613, 2024. DOI: 10.1016/j.marpolbul.2024.116613S
9. Saad AM, Sitohy MZ, Sultan-Alolama MI, El-Tarabily KA, El-Saadony MT: Green nanotechnology for controlling bacterial load and heavy metal accumulation in Nile tilapia fish using biological selenium nanoparticles biosynthesized by *Bacillus subtilis* AS12. *Front Microbiol*, 13:1015613, 2022. DOI: 10.3389/fmicb.2022.1015613
10. Saldarriaga-Hernandez S, Hernandez-Vargas G, Iqbal HM, Barceló D, Parra-Saldívar R: Bioremediation potential of *Sargassum* sp. biomass to tackle pollution in coastal ecosystems: Circular economy approach. *Sci Total Environ*, 715:136978, 2020. DOI: 10.1016/j.scitotenv.2020.136978
11. Alsulami MN, El-Saadony MT: The enhancing effect of bacterial zinc nanoparticles on performance, immune response, and microbial load of Nile tilapia (*Oreochromis niloticus*) by reducing the infection by *Trichodina heterodontata*. *Pak Vet J*, 44 (3): 599-610, 2024. DOI: 10.29261/pakvetj/2024.243
12. Mawed SA, Centoducati G, Farag MR, Alagawany M, Abou-Zeid SM, Elhady WM, El-Saadony MT, Di Cerbo A, Al-Zahaby SA: *Dunaliella salina* microalga restores the metabolic equilibrium and ameliorates the hepatic inflammatory response induced by zinc oxide nanoparticles (ZnO-NPs) in male zebrafish. *Biology*, 11:1447, 2022. DOI: 10.3390/biology11101447
13. Abd El-Hack ME, El-Saadony MT, Elbestawy AR, Ellakany HF, Abaza SS, Geneedy AM, Salem HM, Taha AE, Swelum AA, Omer F, AbuQamar SF, El-Tarabily KA: Undesirable odour substances (geosmin and 2-methylisoborneol) in water environment: Sources, impacts and removal strategies. *Mar Pollut Bull*, 178:113579, 2022. DOI: 10.1016/j.marpolbul.2022.113579
14. Shah AI: Heavy metal impact on aquatic life and human health - An over view. In, *Proceedings of the IAIA17 Conference Proceedings| IA's Contribution in Addressing Climate Change 37th Annual Conference of the International Association for Impact Assessment*, pp. 4-7, 2017.
15. Kotalova I, Calabkova K, Drabinova S, Heviankova S: Contribution to the study of selected heavy metals in urban wastewaters using ICP-MS method. In, *Proceedings of the IOP Conference Series: Earth and Environmental Science*, 012028, 2020.
16. Kotelevych V, Huralaska S, Honcharenko V: Veterinary and sanitary assessment of fish and seafood by quality and safety indicators. *Sci Prog Innovations*, 26, 103-112, 2023. DOI: 10.31210/spi2023.26.03.19
17. Younis EM, Abdel-Warith A-WA, Al-Asgah NA, Elthebite SA, Rahman MM: Nutritional value and bioaccumulation of heavy metals in muscle tissues of five commercially important marine fish species from the Red Sea. *Saudi J Biol Sci*, 28, 1860-1866, 2021. DOI: 10.1016/j.sjbs.2020.12.038
18. Djedjibegovic J, Marjanovic A, Tahirovic D, Caklovica K, Turalic A, Lugusic A, Omeragic E, Sober M, Caklovica F: Heavy metals in commercial fish and seafood products and risk assessment in adult population in Bosnia and Herzegovina. *Sci Rep*, 10:13238, 2020. DOI: 10.1038/s41598-020-70205-9
19. Abu Shusha T, Kalantan M, Al-Nazry H, Al-Ghamdi Y: Fishes from Territorial Saudi Arabian Red Sea Water. Marian Research Center-Jeddah 225, 2011.
20. Svobodova Z, Pravda D, Palackova J: Unified methods of haematological examination of fish; Research Institute of fish Culture and Hydrobiology, 1991.
21. Neugebauer E, Cartier GS, Wakeford B: Methods for the determination of metals in wildlife tissues using various atomic absorption spectrophotometry techniques. Canadian Wildlife Service.
22. Suvarna KS, Layton C, Bancroft JD: Bancroft's Theory and Practice of Histological Techniques. E-Book; Elsevier Health Sciences. 2018.
23. Al-Wesabi EO, Zinadah OAA, Zari TA, Al-Hasawi ZM: Comparative assessment of some heavy metals in water and sediment from the Red Sea coast, Jeddah, Saudi Arabia. *Int J Curr Microbiol Appl Sci*, 4, 840-855, 2015. DOI: 10.13140/RG.2.2.19628.82569
24. Al-Hasawi Z, Hassanine R: Effect of heavy metal pollution on the blood biochemical parameters and liver histology of the Lethrinid fish, *Lethrinus*

harak from the Red Sea. *Pak J Zool*, 55 (4): 1771-1783, 2022. DOI: 10.17582/journal.pjz/20220223170218

25. Younis AM, Elnaggar DH, El-Naggar M, Mohamedein LI: Assessment of heavy metal contamination and pollution indices in *Avicennia marina* of Nabq mangrove forest, the Red Sea, Egypt. *Egypt J Aquat Biol Fish*, 27, 361-385, 2023. DOI: 10.21608/ejabf.2023.329221

26. Alnashiri HM: Assessment of physicochemical parameters and heavy metal concentration in the effluents of sewage treatment plants in Jazan region, Saudi Arabia. *J King Saud Univ Sci*, 33:101600, 2021. DOI: 10.1016/j.jksus.2021.101600

27. Al-Alimi AQA, Saleh SM, Al-Mizgagi MA: Distribution of nutrients in surface seawater from Red Sea Coastal Area in Hodiedah Governorate, Yemen. *South Asian Res J Eng Tech*, 3 (6): 166-176, 2021.

28. Emarah DA, Seleem SA: Swelling soils treatment using lime and sea water for roads construction. *Alex Eng J*, 57, 2357-2365, 2018. DOI: 10.1016/j.aej.2017.08.009

29. Al-Taani AA, Rashdan M, Nazzal Y, Howari F, Iqbal J, Al-Rawabdeh A, Al Bsoul A, Khashashneh S: Evaluation of the Gulf of Aqaba coastal water, Jordan. *Water* 12:2125, 2020. DOI: 10.3390/w12082125

30. Zaghloul GY, El-Sawy MA, Kelany MS, Elgendy AR, Halim AMA, Sabrah MM, El-Din HME: A comprehensive evaluation of water quality and its potential health risks using physicochemical indices in coastal areas of the Gulf of Suez, Red Sea. *Ocean Coast Manag*, 243:106717, 2023. DOI: 10.1016/j.ocecoaman.2023.106717

31. Omar WA, Saleh YS, Marie MAS: Integrating multiple fish biomarkers and risk assessment as indicators of metal pollution along the Red Sea coast of Hodeida, Yemen Republic. *Ecotoxicol Environ Saf*, 110, 221-231, 2014. DOI: 10.1016/j.ecoenv.2014.09.004

32. Gabr MH, Mal AO: Trammel net fishing in Jeddah: species composition, relative importance, length-weight and length-girth relationships of major species. *Int J Fish Aquat Stud*, 6, 305-313, 2018.

33. Shellem CT, Ellis JI, Coker DJ, Berumen ML: Red Sea fish market assessments indicate high species diversity and potential overexploitation. *Fish Res*, 239:105922, 2021. DOI: 10.1016/j.fishres.2021.105922

34. Osman YA, Samy-Kamal M: Diversity and characteristics of commercial Red Sea fish species based on fish market survey: informing management to reduce the risk of overfishing. *J Fish Biol*, 102, 936-951, 2023. DOI: 10.1111/jfb.15339

35. Bakhraibah AO, Bin Dohaish AJA: Histopathological changes caused by parasites in carangoides bajad fish in the Red Sea, Jeddah. *Bulletin of the University of Agricultural Sciences & Veterinary Medicine Cluj-Napoca. Veterinary Medicine* 80, 2023.

36. Varea R, Paris A, Ferreira M, Piovano S: Multibiomarker responses to polycyclic aromatic hydrocarbons and microplastics in thumbprint emperor *Lethrinus harak* from a South Pacific locally managed marine area. *Sci Rep*, 11:17991, 2021. DOI: 10.1038/s41598-021-97448-4

37. Inyang IR, Obidiozo O, Izah S: Effects of *Lambda cyhalothrin* in protein and Albumin content in the kidney and liver of *Parapohiocephalus obscurus*. *Pharmacol Toxicol*, 2, 148-153, 2016.

38. Kavadias S, Castritsi-Catharios J, Dessypris A: Annual cycles of growth rate, feeding rate, food conversion, plasma glucose and plasma lipids in a

population of European sea bass (*Dicentrarchus labrax* L.) farmed in floating marine cages. *J Appl Ichthyol*, 19, 29-34, 2003. DOI: 10.1046/j.1439-0426.2003.00346.x

39. El-Hamed A, Hala A, El-Shaer WA: Study on clinicopathological and biochemical changes in some marine water fishes infested with internal parasites in Red Sea. *Egypt J Chem Environ Health*, 1, 1017-1031, 2015. DOI: 10.21608/ejceh.2015.253996

40. Javed M, Ahmad I, Ahmad A, Usmani N, Ahmad M: Studies on the alterations in haematological indices, micronuclei induction and pathological marker enzyme activities in *Channa punctatus* (spotted snakehead) perciformes, channidae exposed to thermal power plant effluent. *SpringerPlus*, 5 (1):761, 2016. DOI: 10.1186/s40064-016-2478-9

41. Witeska M, Kondera E, Bojarski B: Hematological and hematopoietic analysis in fish toxicology - A review. *Animals*, 13:2625, 2023. DOI: 10.3390/ani13162625

42. Zaynab M, Al-Yahyai R, Ameen A, Sharif Y, Ali L, Fatima M, Khan KA, Li S: Health and environmental effects of heavy metals. *J King Saud Univ Sci*, 34:101653, 2022. DOI:10.1016/j.jksus.2021.101653

43. Younis EM, Al-Asgah NA, Abdel-Warith A-WA, Al-Mutairi AA: Seasonal variations in the body composition and bioaccumulation of heavy metals in Nile tilapia collected from drainage canals in Al-Ahsa, Saudi Arabia. *Saudi J Biol Sci*, 22, 443-447, 2015. DOI: 10.1016/j.sjbs.2014.11.020

44. Younis AM, Mostafa AM, Elkady EM: Assessment of bioaccumulation and health risks of heavy metals in selected fish species from Red Sea coastal waters, Saudi Arabia. *Egypt J Aquat Res*, 50, 348-356, 2024. DOI: 10.1016/j.ejar.2024.07.007

45. Montaser M, Mahfouz ME, El-Shazly SA, Abdel-Rahman GH, Bakry S: Toxicity of heavy metals on fish at Jeddah coast KSA: Metallothionein expression as a biomarker and histopathological study on liver and gills. *World J Fish Mar Sci*, 2, 174-185, 2010.

46. Mohammed S, Idris OF, Sabahelkhiar M, El-Halim A, Musa MI: Hepatic enzymes and tissues responses of rabbit fish (*Siganus rivulatus*) against heavy metals Pb and Cd at Red Sea Coast, Sudan. *Red Sea Univ J Basic Appl Sci*, 2 (Special Issue-1): 425-442, 2017.

47. Jenjan HB, Efekrin SM, Alghamari AA, Eldurssi IS, Gheth EM, Elgabaroni AS: Histopathological changes induced by heavy metals (lead and cadmium) in *Siganus rivulatus* fish collected from the Benghazi Sea Port. *Al Qalam Med Appl Sci*, 6, 439-449, 2023.

48. Mohamed SA, Elshal ME, Kumosani TA, Mal AO, Ahmed YM, Almulaiky YQ, Asseri AH, Zamzami MA: Heavy metal accumulation is associated with molecular and pathological perturbations in liver of *Variola louti* from the Jeddah Coast of Red Sea. *Int J Environ Res Public Health*, 13:342, 2016. DOI: 10.3390/ijerph13030342

49. Mahmoud S, Abd El Rahman A: Eco-toxicological studies of water and their effect on fish in El Manzalah Lake. *Res J Pharm Biol Chem Sci*, 8, 2497-2511, 2017.

50. Jasim Aldoghachi MA, Abdullah AHJ, Hussein DA: Bioaccumulation, histological and structural changes in the gills of the Nile Tilapia (*Oreochromis niloticus*) exposed to heavy metals. *Egypt J Aquat Biol Fish*, 29 (2):2333, 2025. DOI: 10.21608/ejabf.2025.422694

ETHICAL PRINCIPLES AND PUBLICATION POLICY

Kafkas Universitesi Veteriner Fakültesi Dergisi follows and implements internationally accepted ethical standards to provide the necessary support to original scientific ideas and to publish high quality, reliable scientific articles in this direction. The journal's publication policy and ethical principles include the ethical standards of conduct that should be followed by author(s), journal editor(s), associate editors, subject editors, reviewers, and publishers who are the participants of this action.

The ethical statement of Kafkas Universitesi Veteriner Fakültesi Dergisi is based on the principles indicated in the "COPE Code of Conduct and Best Practice Guidelines for Journal Editors" (http://publicationethics.org/files/Code_of_conduct_for_journal_editors_Mar11.pdf) and "COPE Best Practice Guidelines for Journal Editors" (http://publicationethics.org/files/u2/Best_Practice.pdf).

GENERAL ETHICAL PRINCIPLES

• Objectivity and Independence

Editor-in-chief, editors, associate editors, and referees conduct the evaluation process of the manuscript sent to the journal objectively and in coordination within the framework of ethical principles. Editorial decisions are independent, and internal or external factors cannot influence these decisions. In accordance with the principle of impartiality, academics working in our institution are not deemed eligible to work as a section editor in Kafkas Universitesi Veteriner Fakültesi Dergisi, in order not to be effective in the evaluation of articles due to conflict of interest.

• Privacy

The content of the articles and the personal information of the authors such as name, e-mail address, and telephone numbers that are sent to Kafkas Universitesi Veteriner Fakültesi Dergisi are used only for the scientific purposes of the journal and not for other purposes, and cannot be shared with third parties. Article evaluation processes are also carried out confidentially.

• Authorship and Authors Rights

The authors of the manuscripts sent to Kafkas Universitesi Veteriner Fakültesi Dergisi must have contributed significantly to the design, execution or interpretation of the study. For example, in view of the research and publication ethics as well as authors rights, it is not acceptable to include those as authors who do not actively contribute to the research but just only help in writing or data collection processes, which may not require any scientific knowledge. All the authors in a publication should be in agreement of the names and the orders of the authors in the manuscript.

The competence of the authors to the subject of the study is evaluated by the editor within the framework of deontological rules and the professional fields of each author.

The corresponding author of the article should declare the contributions of the authors to the work under the title of "Author contributions". The corresponding author is primarily responsible for the problems that may arise in this regard.

In multidisciplinary studies, 2 authors who are from different disciplines can be "equivalent first name authors" and up to most 3 authors who are also from different disciplines can be "equivalent second name authors".

• Generative Artificial Intelligence (AI)

This declaration outlines the acceptable uses of generative AI technology in writing or editing manuscripts submitted to Kafkas Universitesi Veteriner Fakültesi Dergisi. During the writing process, AI and AI-assisted technologies are prohibited from writing or creating the article, tables, or figures. Authors should use AI and AI-assisted technologies solely to enhance the readability and language of the article. Authors should carefully review and edit the result of assisted parts of the manuscript by AI in term of reliability of the applying technologies.

When using generative AI and AI-assisted technologies in scientific writing, authors must declare this by including a statement in the cover letter when the article is first submitted. Once the article is accepted for publication, this statement should be included in the declarations section of the manuscript's final part.

If anything other than the declared conditions is detected, the articles in the evaluation stage will be rejected, and if it is detected in the published articles, the article will be retracted.

• Originality of Research Findings

The authors should declare that the article they presented contained the original research results, that the study data were analyzed correctly, and that they were prepared for publication using adequate and appropriate references, in the "cover letter" section of the on-line system at the submission stage. Using expressions such as "it is the first study done", "there has been no previous study on this subject" and "there is a limited number of studies" to add originality and importance to the article is not acceptable and may cause prevention of the scientific evaluation of the article by the editor.

• Similarity

Articles submitted to the journal are subjected to similarity analysis using appropriate software (iThenticate by CrossCheck) at the beginning and at every required stage. If unethical similarities are detected regardless of the rate of similarity, this situation is reported to the authors and corrections are requested or articles containing excessive similarities are rejected at the first evaluation stage without being evaluated.

• Plagiarism/Self-Plagiarism, Duplicate Publication

Kafkas Universitesi Veteriner Fakültesi Dergisi applies publication ethics and verifies the originality of content submitted before publication and checks all submitted manuscripts for plagiarism/self-plagiarism, similarity and duplication. All submitted manuscripts are meticulously screened by a similarity detection software (iThenticate by CrossCheck). Papers previously presented at scientific meetings and published only as an "abstract" should be indicated in the Title Page file as stated in the "Guidance for Authors". Authors do not have the right to use entire paragraphs from their previous publications into a new submission. These actions are also considered as a plagiarism. In any case, the manuscript should be original in terms of scientific contents and writing. In the event of alleged or suspected research misconduct, the Editorial Board will follow and act in accordance with "COPE Guidelines".

• Multi-part Publication (Piecemeal Publication)

Some authors may tend to divide study data into two or more articles and publish the results in different journals also having different authors names and orders. In principal, Kafkas Universitesi Veteriner Fakultesi Dergisi is against multi-part publication. When necessary, the ethical committee approval information of the study, project information, congress presentations, etc. are checked and such situations that will create an ethical problem are identified and reported to the authors.

Authors may think that their work should be published in multi parts that complement each other. For this, each part of the article should be titled "Part-I", "Part-II" and submitted to the journal "simultaneously". This issue can be evaluated by the editor-in-chief/subject editors/referees who may suggest that the article can be published in parts or as a whole. In addition, rejection of a submission presented in parts means that all parts will be rejected.

• Animal Rights and Ethics

The authors are responsible for conducting experimental and clinical studies on animal experiments within the framework of existing international legislation on animal rights. Authors must also obtain permission from the Animal Experiment Ethics Committees and provide relevant information in the Material and Method section to experiment with animals. In clinical studies, as well as the approval of the ethics committee, an "informed consent form" should be obtained from the animal owners and the information related to it should be declared in the Material and Method section. Declaration of "informed consent form" is sufficient for the articles in the "Case report" and "Letter to the Editor" category.

Ethics committee permission taken for a study can only be used in one article. It is unacceptable to use the same ethics committee approval number in articles with different names and contents. The editor/subject editors can request from the corresponding author, if necessary, to send a copy of the ethics committee approval form to the journal (electronically or by post).

In cases of violation ethical rules, the article is not taken into consideration or if it is in the evaluation stage, the procedure is terminated and the article is rejected.

• Conflicts of Interest/Competing Interests

The editor-in-chief pays attention to whether there is a conflict of interest or union of interest between editors, reviewers and author (s) for an objective and unbiased evaluation of the article. In addition, the authors should disclose any financial interests or links or any conditions that may raise the bias issue in research and article under the above heading.

• Copyright

Authors retain the copyright to their published work licensed under the Creative Commons Attribution-NonCommercial 4.0 International license (CC BY-NC 4.0) (<https://creativecommons.org/licenses/by-nc/4.0/>) and grant the Publisher non-exclusive right to publish the work. CC BY-NC 4.0 license permits unrestricted, non-commercial use, distribution, and reproduction in any medium, provided the original work is properly cited.

The authors must fill in the "Copyright Agreement Form" and sign it with a wet signature. Authors who submit articles from abroad should scan the signed form and send it to the editor via the system or by e-mail. Original forms that are wet signed for articles sent domestically should be submitted to the journal via mail or cargo. The works of the authors who do not submit the Copyright Agreement Form on time are not published.

• Withdrawal of a Submission

In case of if the authors detect a significant error or deficiency in their article under review or if this error is reported to them by the editor/subject editor/referees they can contact immediately to the editor-in-chief and ask the request to withdraw the article by stating the reason. The decision on this issue is up to the editorial board.

• Erratum

After an article has been published, the corresponding author may request the editor to publish "erratum" for any errors or inaccuracies noticed by the authors, editors or readers. In collaboration with the authors, the editor prepares and publishes the Erratum article in the first upcoming issue. These articles, like other publications, should contain the publication tag and DOI number.

• Retraction

If any ethical problem is detected about the article that cannot be compensated and cannot be eliminated with erratum after the article is published, the editor-in-chief and associate editors prepare a justification about the article and apply the retraction procedure to the article. The text file on the web page of a retracted article is blocked and the reason for retraction is added to the system as a file, ensuring that it is constantly in the archive.

• Advertising

Kafkas Universitesi Veteriner Fakultesi Dergisi do not accept advertising and sponsorships that are believed to create a potential conflict of interest. If the article sent to Kafkas Universitesi Veteriner Fakultesi Dergisi is for the promotion of a commercial product and/or the work carried out is directly supported by a company, it is rejected without consideration.

OPEN ACCESS STATEMENT

Kafkas Universitesi Veteriner Fakultesi Dergisi is an open access publication. The journal's publication model is based on Budapest Open Access Initiative (BOAI) declaration. Articles published in Kafkas Universitesi Veteriner Fakultesi Dergisi are available online, free of charge at <https://vetdergikafkas.org/archive.php>.

Except for commercial purposes, users are allowed to read, download, copy, print, search, or link to the full texts of the articles in this journal without asking prior permission from the publisher or the author. The open access articles in the journal are licensed under the terms of the Creative Commons Attribution-NonCommercial 4.0 International (CC BY-NC 4.0) licence.

ARTICLE EVALUATION AND PUBLICATION PROCESS**• Initial Evaluation Process**

Articles submitted to Kafkas Universitesi Veteriner Fakultesi Dergisi are primarily evaluated by the editors and associate editors. At this stage, articles not having suitable scope and aims, with low original research value, containing scientific and ethically important errors, having low potential to contribute to science and the journal, and having poor language and narration are rejected by the editor without peer-review process. Initial evaluation process takes up to most 2 weeks.

• Preliminary Evaluation Process

Articles that are deemed appropriate for editorial evaluation are sent to the subject editor related to the category of articles to be examined in terms of scientific competence and to the statistics editor for evaluation in terms of statistical methods. The subject editors examine the article in all aspects and report their decisions (rejection, revision or peer-review) to the chief editor. This stage takes about 1 month.

• Peer-review Process

Double-blind peer-review is applied to the articles that have completed preliminary evaluation process. Suggestions of subject editors are primarily considered in referee assignment. In addition, reviews can be requested from the referees registered in the journal's referee pool. At least 2 referees are assigned for peer-review. Opinion of more referees can be required depending on the evaluation process. At this stage, referees send their decision (reject, revision or accept) about the article to the editor-in-chief. If the rejection decision given by a referee reflects sufficient examination and evidence-based negativities or ethical problems about the scientific content and accuracy of the article, this decision is checked by the editor-in-chief and associate editors and submitted to the authors regardless of the other referees' decisions. The time given to referees to evaluate an article is ~4 weeks.

• Publication Process of an Article

Total evaluation period of an article, which is completed in the peer-review phase after completing the initial and preliminary evaluation process, takes 4-6 months. The articles that have completed the subject editorial and peer-review evaluation stages and accepted by the editorial are sent to the corresponding author for final checks and necessary final additions. After the acceptance, the article designed in the publication format of the journal is given an DOI number and published immediately on the Article in Press page. When it is time to publish the periodic edition of the journal, a selection is made from the articles kept on the Article in Press page, taking into account the submission date. The time it takes for the article to be published by taking the page number is 6-12 months.

NO PUBLICATION FEE

Processing and publication are free of charge with the journal. There is no article processing charges, submission fees or any other fees for any submitted or accepted articles.

RESPONSIBILITIES OF THE PUBLISHER, EDITORS AND ASSOCIATE EDITORS

The publisher (Dean of the Faculty of Veterinary Medicine of Kafkas University) contributes to the execution of the journal's routine processes such as printing, archiving, and mailing, in line with requests from the editor.

The publisher undertakes to carry out an independent and fair decision-making mechanism for its editors and assistants in the article evaluation process and decisions.

The publisher undertakes to carry out an independent and fair decision-making mechanism for its editors and associate editors in the article evaluation process and decisions.

Editor-in-chief/editors/associate editors of Kafkas Universitesi Veteriner Fakultesi Dergisi evaluate the articles submitted to the journal regardless of their race, gender, religious belief, ethnicity, citizenship or political views. In addition, it undertakes not to give any information about the article except for the authors, subject editors and referees.

Kafkas Universitesi Veteriner Fakultesi Dergisi follows internationally accepted principles and criteria and takes the necessary decisions to apply in the journal.

Editor-in-chief/editors/associate editors conduct the evaluation and decision process in the journal in coordination within the principles of confidentiality and have independent decision-making authority and responsibility without being affected by any internal or external factors.

Editor-in-chief/editors/associate editors make and implement all kinds of planning for the development of the journal and its international recognition. They also follow national and international meetings or events on the development of journals and article evaluation, and ensures that the journal is represented on these platforms.

The editor-in-chief/editors/associate editors make every effort to ensure that the journal's subject editors and referee pool have international qualifications. Likewise, it makes the necessary attempts to strengthen the author's profile.

Editor-in-chief/editors/associate editors make plans to improve the quality of the articles published in the journal and carry out the necessary process.

Editor-in-chief/editors/associate editors regularly conduct and control the initial evaluation, preliminary evaluation, peer review and acceptance-rejection decisions of articles submitted to the journal. While carrying out these procedures, features such as the suitability of the study for the aims and scope of the journal, its originality, the up-to-date and reliability of the scientific methods used, and the potential it will contribute to the development of the journal as well as its benefit to science/practice are taken into consideration.

Editor-in-chief/editors/associate editors systematically review, inspect and make decisions about the articles submitted to the journal in terms of features such as author rights, conflict of interest, observance and protection of animal rights, and compliance with research and publication ethics.

The editor-in-chief conducts the evaluation/revision process between the authors and subject editors and referees, and ensures that it is completed within the prescribed time.

ARCHIVE POLICY

The editorial office of the Kafkas Üniversitesi Veteriner Fakültesi Dergisi and the publisher (Dean's Office of the Faculty of Veterinary Medicine, Kafkas University) keep all the articles (electronic and printed) published in the journal in their archives. All articles and their attachment files sent to the journal are kept securely in the archive. In light of the technological developments, the editorial office of the Kafkas Üniversitesi Veteriner Fakültesi Dergisi regularly performs electronic processes for the development and updating of materials in digital environment and presents them to its readers on condition of keeping in safe the original documents and information regarding the articles.

Even if the journal ceases to be published for any reason, the publisher (Dean's Office of the Faculty of Veterinary Medicine, Kafkas University) will continue to protect the journal content in the long term and provide convenient access to users. Electronic services of Kafkas University Information Technologies Department will be used for the journal to maintain this responsibility.

RESPONSIBILITIES OF SUBJECT EDITORS

Subject editors do reviews and evaluations in accordance with the main publication goals and policies of the journal and in line with the criteria that will contribute to the development of the journal.

Author information is kept confidential in articles sent to the subject editor for preliminary evaluation by the editor.

Subject editors thoroughly examine the sections of the introduction, materials and methods, results, discussion and conclusion, in terms of journal publication policies, scope, originality and research ethics. Subject editor submits its decision (rejection, revision or peer-review) after evaluation to the chief editor in a reasoned report.

Subject editor may request additional information and documents related to the study from the authors, when necessary.

In multidisciplinary studies, the article can be submitted for the evaluation of multiple subject editors.

RESPONSIBILITIES OF REFEREES

Double-blinded peer-review procedure is applied in Kafkas Üniversitesi Veteriner Fakültesi Dergisi in order to evaluate the articles submitted to the journal in accordance with the principle of impartiality and in objective criteria; that is, referees and writers do not know about each other.

The referees submit their opinions and reports to the editor-in-chief to ensure the control and suitability of a submitted article, its scientific content, scientific consistency and compliance with the principles of the journal. When a referee makes a decision "reject" about an article, he/she prepares the reasons for the decision in accordance with the scientific norms and presents it to the editor.

The referee(s) also gives the authors the opportunity to improve the content of the article. Accordingly, the revisions requested from the authors should be of a quality that explains/questions specific issues rather than general statements.

Referees appointed for the evaluation of the articles agree that the articles are confidential documents and will not share any information about these documents with third parties, except for the editors participating in the evaluation.

Referees should place their criticism on scientific infrastructure and write their explanations based on scientific evidence. All comments made by the referees to improve the articles should be clear and direct, and should be written away from disturbing the feelings of the author. Insulting and derogatory statements should be avoided.

If a referee has an interest relationship with the author(s) on one or more issues, he/she must report the situation to the editor and ask his/her to withdraw from the referee position. The same is also applicable when the authors illegally obtain information about the referees of the article and try to influence them.

The editor-in-chief can share the comments and reports from the referees with the editors/associate editors and the relevant subject editor, as necessary, to ensure that the decision on the article is optimal. If necessary, the editor may share the critical decision and its grounds that a referee has sent about the article with the other referee(s) and present them to their attention.

Referee(s) may request revision many times for the article they evaluated.

The content of the referee reports is checked and evaluated by editor-in-chief/editors/associate editors. The final decision belongs to the editorial.

RESPONSIBILITIES OF AUTHOR(S)

It is not tolerable for the author (s) to send an article, which has been already sent to another journal, to Kafkas Üniversitesi Veteriner Fakültesi Dergisi within the scope of "which accepts" or "which publishes first" approach. If this is detected, the article is rejected at any stage of the evaluation. As a possible result of these actions, in the process following the previous acceptance of the article sent to another journal, the withdrawal request with this excuse that the authors submit for this article, the evaluation process of which is going on in our journal, is evaluated by the editors and associate editors of the journal and disciplinary action on the grounds of ethical violations about those responsible is started. This unethical action is also informed to the journal editor (if known) who accepted the article.

It is essential that the articles to be sent to Kafkas Üniversitesi Veteriner Fakültesi Dergisi include studies that have up-to-date, original and important clinical/practical results and prepared in accordance with the journal's writing rules.

Authors should choose the references they use during the writing of the article in accordance with the ethical principles and cite them according to the rules.

The authors are obliged to revise the article in line with the issues conveyed to them during the initial evaluation, preliminary evaluation and peer-review phases of the article and to explain the changes they made/did not make sequentially in the "response to editor" and "response to reviewer comments" sections.

If information, documents or data regarding to the study are requested during the evaluation process, the corresponding author is obliged to submit them to the editorial.

Authors should know and take into account the issues listed in the "General Ethical Principles" section regarding scientific research and authors.

The authors do not have the right to simultaneously submit multiple articles to Kafkas Üniversitesi Veteriner Fakültesi Dergisi. It is more appropriate to submit them with acceptable time intervals for the journal's policy.

INSTRUCTION FOR AUTHORS

1- Kafkas Universitesi Veteriner Fakultesi Dergisi (abbreviated title: Kafkas Univ Vet Fak Derg), published bi-monthly (E-ISSN: 1309-2251). We follow a double-blind peer-review process, and therefore the authors should remove their name and any acknowledgment from the manuscript before submission. Author names, affiliations, present/permanent address etc. should be given on the title page only.

The journal publishes full-length research papers, short communications, preliminary scientific reports, case reports, observations, letters to the editor, and reviews. The scope of the journal includes all aspects of veterinary medicine and animal science.

Kafkas Universitesi Veteriner Fakultesi Dergisi is an Open Access journal, which means that all content is freely available without charge to the user or his/her institution. Users are allowed to read, download, copy, distribute, print, search, or link to the full texts of the articles, or use them for any other lawful purpose, without asking prior permission from the publisher or the author. This is in accordance with the BOAI definition of Open Access.

2- The official language of our journal is English.

3- The manuscripts submitted for publication should be prepared in the format of Times New Roman style, font size 12, A4 paper size, 1.5 line spacing, and 2.5 cm margins of all edges. The legend or caption of all illustrations such as figure and table and their appropriate position should be indicated in the text. Refer to tables and figures in the main text by their numbers. Also figure legends explanations should be given at the end of the text.

The figures should be at least 300 dpi resolution.

The manuscript and other files (figure etc.) should be submitted by using online manuscript submission system at the address of <http://vetdergi.kafkas.edu.tr/>

During the submission process, the authors should upload the figures of the manuscript to the online manuscript submission system. If the manuscript is accepted for publication, the Copyright Agreement Form signed by all the authors should be sent to the editorial office.

4- The authors should indicate the name of the institute approves the necessary ethical commission report and the serial number of the approval in the material and methods section. If necessary, the editorial board may also request the official document of the ethical commission report. In case reports, a sentence stating that “informed consent” was received from the owner should be added to the main document. If an ethical problem is detected (not reporting project information, lack of ethical committee information, conflict of interest, etc.), the editorial board may reject the manuscript at any stage of the evaluation process.

5- Authors should know and take into account the “Generative Artificial Intelligence (AI)” and other matters listed in the “**Ethical Principles and Publication Policy**” section regarding scientific research and authors.

6- Types of Manuscripts

Original (full-length) manuscripts are original and proper scientific papers based on sufficient scientific investigations, observations and experiments.

Manuscripts consist of the title, abstract and keywords, introduction, material and methods, results, discussion, and references and it should not exceed 12 pages including text. The number of references should not exceed 50. The page limit does not include tables and illustrations. Abstract should contain 200±20 words.

Short communication manuscripts contain recent information and findings in the related topics; however, they are written with insufficient length to be a full-length original article. They should be prepared in the format of full-length original article but the abstract should not exceed 100 words, the reference numbers should not exceed 15 and the length of the text should be no longer than 6 pages in total. The page limit does not include tables and illustrations. Additionally, they should not contain more than 4 figures or tables.

Preliminary scientific reports are a short description of partially completed original research findings at an interpretable level. These should be prepared in the format of full-length original articles. The length of the text should be no longer than 4 pages in total.

Case reports describe rare significant findings encountered in the application, clinic, and laboratory of related fields. The title and abstract of these articles should be written in the format of full-length original articles (but the abstract should not exceed 100 words) and the remaining sections should be followed by the Introduction, Case History, Discussion and References. The reference numbers should not exceed 15 and the length of the text should be no longer than 4 pages in total. The page limit does not include tables and illustrations.

Letters to the editor are short and picture-documented presentations of subjects with scientific or practical benefits or interesting cases. The length of the text should be no longer than 3 pages in total. The page limit includes tables and illustrations.

Reviews are original manuscripts that gather the literature on the current and significant subject along with the commentary and findings of the author on a particular subject (It is essential that the author/s have international scientific publications on this subject). The title and summary of this manuscript should be prepared as described for the full-length original articles and the remaining sections should be followed by introduction, text (with appropriate titles), conclusion, and references.

“Invited review” articles requested from authors who have experience and recognition in international publishing in a particular field are primarily published in our journal.

Review articles submitted to our journal must be prepared in accordance with any of the three categories listed below.

Narrative reviews describe current published information on a scientific topic. However, it does not include a specific methodological process.

Systematic reviews include the search for original studies published in that field on a specific topic, the evaluation of validity, synthesis and interpretation within a systematic methodology.

Meta-analysis is a method of evaluating the results of many studies on a subject with the methods defined in this category and statistical analysis of the obtained findings.

7- The necessary descriptive information (thesis, projects, financial supports, etc.) scripted as an italic font style should be explained below the manuscript title after placing a superscript mark at the end of the title.

8- At least 30% of the references of any submitted manuscript (for all article categories) should include references published in the last five years.

References should be listed with numerical order as they appear in the text and the reference number should be indicated inside the parentheses at the cited text place. References should have the order of surnames and initial letters of the authors, title of the article, title of the journal (original abbreviated title), volume and issue numbers, page numbers and the year of publication and the text formatting should be performed as shown in the example below.

Example: Yang L, Liu B, Yan X, Zhang L, Gao F, Liu Z: Expression of ISG15 in bone marrow during early pregnancy in ewes. *Kafkas Univ Vet Fak Derg*, 23 (5): 767-772, 2017. DOI: 10.9775/kvfd.2017.17726

If the reference is a book, it should follow surnames and initial letters of the authors, title of the book, edition number, page numbers, name and location of publisher and year of publication. If a chapter in a book with an editor and several authors is used, names of chapter authors, name of chapter, editors, name of the book, edition number, page numbers, name and location of publisher and year of publication and the formatting should be performed as shown in the example below.

Example: McIlwraith CW: Disease of joints, tendons, ligaments, and related structures. **In,** Stashak TS (Ed): Adam's Lameness in Horses. 4th ed., 339-447, Lea and Febiger, Philadelphia, 1988.

DOI number should be added to the end of the reference.

In the references can be reached online only, the web address and connection date should be added at the end of the reference information. The generally accepted scientific writing instructions must comply with the other references. Abbreviations, such as “et al” and “and friends” should not be used in the list of the references.

Follow the link below for EndNote Style of Kafkas Universitesi Veteriner Fakultesi Dergisi;

<https://researchsoftware.com/downloads/journal-faculty-veterinary-medicine-kafkas-university>

9- Latin expression such as species names of bacteria, virus, parasite, and fungus and anatomical terms should be written in italic character, keeping their original forms.

10- The editorial board has the right to perform necessary modifications and a reduction in the manuscript submitted for publication and to express recommendations to the authors. The manuscripts sent to authors for correction should be returned to the editorial office within a month. After pre-evaluation and agreement of the submitted manuscripts by the editorial board, the article can only be published after the approval of the field editor and referee/s specialized in the particular field.

11- All responsibilities from published articles merely belong to the authors. According to the ethical policy of our journal, plagiarism/self-plagiarism will not be tolerated. All manuscripts received are checked by plagiarism checker software, which compares the content of the manuscript with a broad database of academic publications.

12- The editorship may request the language editing of the manuscript submitted to the journal. If the article is accepted, it will not be published without language editing. Before publication, a declaration and/or certificate stating that proofreading is done by a registered company will be requested from the corresponding author.

13- No fee is charged at any stage in Kafkas Üniversitesi Veteriner Fakültesi Dergisi (No APC/APF)

SUBMISSION CHECKLIST

Please use below list to carry out a final check of your submission before you send it to the journal for review. Ensure that the following items are present in your submission:

- Cover Letter

- Importance and acceptability of the submitted work for the journal have been discussed (Please avoid repeating information that is already present in the abstract and introduction).
- Other information has been added that should be known by the editorial board (e.g.; the manuscript or any part of it has not been published previously or is not under consideration for publication elsewhere).

- Title Page

- Title, Running Title (should be a brief version of the title of your paper, no exceed 50 characters)
- The author's name, institutional affiliation, Open Researcher and Contributor ID (ORCID)
- Congress-symposium, project, thesis etc. information of the manuscript (if any)
- Corresponding author's address, phone, fax, and e-mail information

- Manuscript

- Title, abstract, keywords and main text
- All figures (include relevant captions)
- All tables (including titles, description, footnotes)
- Ensure all figure and table citations in the text match the files provided

- Declarations

- Availability of Data and Materials
- Acknowledgements
- Funding Support
- Competing Interests
- Generative Artificial Intelligence (AI)
- Authors' Contributions

Further Considerations

- Journal policies detailed in this guide have been reviewed
- The manuscript has been "spell checked" and "grammar checked"
- Relevant declarations of interest have been made
- Statement of Author Contributions added to the text
- Acknowledgment and conflicts of interest statement provided

